IMPROVING RICE PHOTOSYNTHESIS IN SUBOPTIMAL CONDITIONS

TIARA HERMAN ABDULLAH

THESIS SUBMITTED TO THE UNIVERSITY OF NOTTINGHAM FOR THE DEGREE OF DOCTOR OF PHILOSOPHY

AUGUST 2019

ABSTRACT

For plants grown in agriculture, productivity and yield are two consequential factors which must be maintained to ensure a continued supply of food for a burgeoning population. Rice is consumed in many regions in the world. The high-yielding rice genotypes cultivated today are the result of decades of breeding for shorter stems and leaves with more erect canopies that maximises grain number and weight. As we approach the theoretical upper limits of yield capacity set by the environment and crop genetics, increasing pressure has been placed on identifying the traits and mechanisms that would improve photosynthetic efficiency, both at the leaf and canopy levels.

While rice is consumed in many locations of the world, it is mostly cultivated in tropical regions that are facing growing pressures both environmentally and economically. In Malaysia, rice is being cultivated in increasingly stressful environments, where the requirement for substantial amounts of nitrogen fertilisers is high. With the rising costs of fertiliser production and the increasing degradation of arable land, there is a need to select for more resilient rice varieties with improved photosynthetic efficiencies for cultivation in suboptimal conditions.

Canopy architecture plays an important role in determining overall plant productivity. As an essential nutrient, nitrogen is critical in determining the structure of a plant canopy and thus changes in nitrogen concentrations may have a large impact on plant productivity. This has been demonstrated in the study below, on two popular Malaysian cultivars, MR219 and MR253, and an IRRI cultivar, IR64. These rice cultivars were grown in different nitrogen treatments and analysed for changes in canopy architecture using in-depth physiology measurements coupled with canopy reconstructions using a novel 3-dimensional image-based technique with ray tracing. This

method allows for the capture of unique canopy traits and make predictions for whole plant canopy productivity, in terms of canopy photosynthesis and carbon gain. The IRRI cultivar, IR64, revealed the need for reevaluation while MR253 revealed the potential for increased photosynthetic efficiency in lower nitrogen conditions, with a lower susceptibility to nitrogen deficiency both in a controlled and field conditions.

ACKNOWLEDGEMENTS

Firstly, I would like to say thank you to my supervisors, Dr Erik Murchie and Professor Asgar Ali for giving me the opportunity to carry out this work, their academic support, enthusiasm and guidance during the course of my PhD. Special thanks to Dr Sean Mayes, my internal assessor for the guidance when I needed it.

Secondly, I would like to extend my thanks to my colleagues at Sutton Bonington in the Murchie lab group, Hayley Smith, Alexandra Burgess, Jamie Randall, Kannan Chinnathambi, and Umar Mohammad, who pitched in when I needed help, plus all the food and laughter! I would also like to thank my colleagues at the Nottingham Malaysia campus, Maysoun Mustafa, Azhane Ahmad, Paa Kwesi and Yeoh Wei Keat for their support. Special thanks to Afiq, GT and Vincent at CFFRC for helping out with the field trials.

Finally, I would like to thank my family, my partner Sam and my friends, in particular, Luke, for all the inspiration and unwavering support.

This research was funded by The Ministry of Education (MOE), Malaysia for the Long-term Research Grant Scheme LRGS (Food Security - Enhancing sustainable rice production) and Universiti Putra Malaysia for funding this research project.

ABBREVIATIONS

ϕPSII	Quantum yield of Photosystem II (or Fq'/Fm')
3-PGA	3-Phosphoglycerate
3-D	3-dimensional
A	Net carbon dioxide assimilation
A/Ci	Assimilation of carbon dioxide
ADP	Adenosine diphosphate
ANOVA	Analysis of variance
ATP	Adenosine triphosphate
C*a*	Atmospheric carbon dioxide concentration
C*c*	Chloroplastic carbon dioxide concentration
CFFRC	Crops for the Future Research Centre
Chl	Chlorophyll
C*i*	Substomatal carbon dioxide concentration
cLaI	Cumulative Leaf area index
CO_2	Carbon dioxide
DAS	Days after sowing
DAT	Days after transplanting
ETR	Electron transport rate
FAO	Food and Agriculture Organization
FI	Fractional interception
Fq'/Fm'	Quantum yield of Photosystem II (or ϕPSII)
Fv'/Fm'	Ratio of variable to maximum florescence
Fv/Fm	Dark-adapted quantum yield of Photosystem II
GA3P	glyceraldehyde 3-phosphate
gM	Mesophyll conductance
g_S	Stomatal conductance
GS	Growth stage
ha	Hectare
HI	Harvest index
HN	High nitrogen
IRGA	Infra-red gas analyser
IRRI	International Rice Research Institute
J_{max}	Maximum regeneration rate of Rubisco
k	Light extinction coefficient
LAI	Leaf area index
LN	Low nitrogen
MARDI	Malaysian Agricultural Research and Development Institute
N	Nitrogen
$NADP^+$	Nicotinamide adenine dinucleotide phosphate

NADPH	Nicotinamide adenine dinucleotide phosphate hydrogen
NPQ	Non-photochemical quenching
O_2	Oxygen
SBPase	Sedoheptulose-1,7-bisphosphate
P_{max}	Maximum net carbon dioxide assimilation
Pn	Primary production
PPFD	Photosynthetic photon flux density
ppm	Parts per million
PSI	Photosystem I
PSII	Photosystem II
Qy	Quantum yield of Photosystem II
qE	Fast relaxing form of NPQ
qI	PSII photoinhibitory damage
ROS	Reactive oxygen species
Rubisco	Ribulose 1,5-bisphosphate carboxylase oxygenase
RuBP	Ribulose 1,5-bisphosphate
RUE	Radiation use efficiency
t/ha	Tonnes per hectare
TPU	Triosphosphate utilisation
UPM	Universiti Putra Malaysia
Vc_{max}	Maximum carboxylation rate of Rubisco
Yp	Yield potential
εc	Efficiency by which intercepted solar radiation is converted into biomass
ε_i	Light interception efficiency
$[CO_2]$	Carbon dioxide concentrations

TABLE OF CONTENTS

ABSTRACT 2

ACKNOWLEDGEMENTS..... 4

ABBREVIATIONS 5

LIST OF FIGURES.....10

LIST OF TABLES.....18

Chapter 1 22

1.1 Introduction 22
1.1.1 Rice as a crop 23
1.1.2 Trends in rice production and yield 24
1.1.3 Rice growing systems 26
1.1.4 The production of rice in Malaysia..... 27

1.2 Increasing the production of rice.....31
1.2.1 Yield potential 31

1.3 The mechanism of photosynthesis.....34

1.4 Photosynthesis as a limiting factor 38

1.5 Plant responses to the environment 40
1.5.1 Photosynthesis and the light environment..... 42
1.5.2 Temperature..... 46
1.5.3 Nitrogen deficiency 47

1.6 Improving the mechanism of rice photosynthesis 50
1.6.1 Rubisco as a target of improvement..... 50
1.6.2 Introducing the C4 pathway into C3 rice..... 52
1.6.3 Reducing losses from photorespiration 54
1.6.4 Engineering optimum plant canopies..... 55
1.6.5 Photoprotection as an avenue to improve rice yield..... 57

1.7 Project aims and objectives.....61

Chapter 2 64

2.1 Introduction 64
2.1.1 Whole plant morphology..... 64
2.1.2 Leaf anatomy..... 66
2.1.3 Aims and objectives..... 68

2.2 Methods and materials.....69
2.2.1 Experimental set-up..... 69
2.2.2 Plant physiology measurements 73
2.2.3 Gas exchange analyses 77

2.3 Results 80
2.3.1 Plant physiology measurements 80
2.3.2 Gas exchange measurements..... 92

2.3.3 Chlorophyll 104
2.3.4 Correlations: N, gas exchange and anatomical parameters 104

2.4 Discussion 107
2.4.1 Light harvesting, Chl fluorescence and the Calvin cycle 107
2.4.2 The nitrogen profile on leaf anatomy and morphology 109

2.5 Conclusion 113

Chapter 3 116

3.1 Introduction 116
3.1.1 Solar radiation and canopy architecture..... 116
3.1.2 The light profile on photosynthesis..... 118
3.1.3 Modelling rice canopy architecture 119
3.1.4 Aims and objectives..... 120

3.2 Methods and materials 120
3.2.1 Plant growth and experimental design..... 120
3.2.2 Plant physiology measurements 124
3.3.1 Gas exchange measurements..... 127
3.3.2 High-resolution imaging and 3-dimensional canopy reconstruction 128
3.3.3 Data modelling..... 129

3.4 Results 132
3.4.1 Physiology measurements 132
3.5.1 Gas-exchange measurements 140
3.5.2 Canopy reconstructions and modelling 140

3.6 Discussion 153
3.6.1 Nitrogen on the photosynthesis of a canopy..... 154
3.6.2 N status effects on rice canopy architecture 154

3.7 Conclusion 157

Chapter 4 159

4.1 Introduction 159
4.1.1 Aims and objectives..... 160

4.2 Field Trial 1 161
4.2.1 Plant seeds and germination 161
4.2.2 Growth conditions and experimental design 163
4.2.3 Plant physiology and gas exchange measurements 168

4.3 Field Trial 2 170
4.3.1 Plant seeds and germination 170
4.3.2 Growth conditions and experimental design 171
4.3.3 Plant physiology and gas exchange measurements 175

4.4 Results 178
4.4.1 Mean temperature and relative humidity 178
4.4.2 Plant physiology measurements 181

1.1 186
4.4.3 Leaf and canopy morphology dynamics 193
4.4.4 Gas exchange measurements..... 199
4.4.5 Yield parameter..... 206
4.4.6 Correlation matrices 207

4.5 Discussion 210
4.5.1 Changes in rice phenology in low N rice 210
4.5.2 Nitrogen-mediated tillering 213
4.5.3 Relationship between photosynthesis and canopy responses to low N 215

4.6 Conclusion 220

Chapter 5 222

5.1 Introduction 222

5.2 Experimental Overview 222
5.2.1 Summary of findings of individual rice varieties 222
5.2.2 Wider impact of findings on breeding and farming practices 227
5.2.3 Future work 229

5.3 Final conclusions 231

References 232

LIST OF FIGURES

Figure 1.1: Global rice yields (t/ha) and harvested area (ha) from 1961 to 2015. (Source: FAOSTAT Database, January 28, 2016)... 25

Figure 1.2 : Malaysia's annual rice production from years 1980 to 2017 in terms of yield (t/ha), area harvested (ha) and N fertilisers (t/10ha) supplied to the agricultural system. (Source: FAOSTAT Database, June 13, 2019)..... 30

Figure 1.3: Schematic of pathways taken by an excited chlorophyll (1Chl*) to return to ground state (Chl) – 1) Chlorophyll a fluorescence, 2) photochemistry, 3) heat through NPQ and 4) reactive oxygen species (ROS). 36

Figure 1.4: (**a**) Light-dependent and (**b**) Calvin-Benson cycle reactions in the chloroplast. (Sources: (a) own collection and (b) Taiz and Zeiger, 2010. 37

Figure 1.5: Mean average solar irradiation at the surface of the earth in South East Asia (Source: solarGIS, February 23, 2015). . 43

Figure 1.6: Schematic of the (**a**) C3 photosynthetic pathway and (**b**) C4 photosynthetic pathway. In the C3 photosynthetic pathway, CO_2 is fixed by Rubisco in a single cell whereas two cells are required in C4 photosynthesis, where CO_2 is initially fixed in the mesophyll cell by PEP-C and then donated to the bundle sheath cell to Rubisco. (Source: Adapted from von Caemmerer *et al*., (2012). 53

Figure 1.7: Schematic of the rate of photosynthesis under increasing photosynthetic photon flux densities. Quantum yield of PSII, light compensation point, and dark respiration rate are shown. P_{max} is also indicated, and this is where photosynthesis saturates despite increasing light levels. 58

Figure 2.1: Rice leaves grow in an alternating fashion from the main stem. n represents the leaf number, and n+1 represents the subsequent leaf, which is growing on the opposite side. 65

Figure 2.2: A transverse section of the rice leaf (shown is the International Rice Research institute variety, IR64) Labelled are the major and minor veins (where the vascular bundles are located), the mesophyll (site of gas exchange) and bulliform cells (controls leaf rolling). Section was hand-cut and cleared using chloral hydrate to remove pigment for microscopy. (Source: own material) 67

Figure 2.3: Randomized complete block design within a container with split plot design between containers. (**a**) First growth room trial, with IR64 and Moroberekan. (**b**) Second growth room trial, with IR64, MR219 and MR253. 72

Figure 2.4: (**a**) Seedlings germinated in a Petri dish, (**b**) young plants in a bucket with hydroponic solution and (**c**) (from left to right) plants receiving 100% N, 50% N and 25% N treatments.... 73

Figure 2.5: A 40x magnification image of abaxial leaf surface of rice variety MR219 under the control treatment, with the red lines indicating to stomata. 75

Figure 2.6: Example curve-fitting of mean A/Ci for MR219 plants (n=3) under the control treatment. The black dots denote the values of A at different carbon dioxide concentrations with SEM. For some cases, the error bars are too small to be visible. Vc_{max} (green line) is the maximum rate of carboxylation of Rubisco, J_{max} (blue line) represents the RuBP regeneration rate while the red line represents triosphosphate utilisation. 79

Figure 2.7: Leaf extension rates following a variable sigmoidal slope response of the three varieties MR219, MR253 and IR64 under the 100% N, 50% N and 25% N treatments. Shown are the means and the standard errors of the means (SEM), n=5. For some cases, the error bars are too small to be visible. 82

Figure 2.8: Total number of leaves following a variable sigmoidal slope response, and the number of primary tillers at the end of Leaf 9 elongation. Shown are the means and the SEM. Same letters indicate no significant differences ($p>0.05$) between compared pairs, following a two-way ANOVA test and a Tukey's multiple comparisons test, n=5. For some cases, the error bars are too small to be visible. 85

Figure 2.9: Stomatal density of adaxial and abaxial surfaces and stomatal lengths of the three varieties under the three treatments. Shown are the means and SEM. For some cases, error bars are too small to be visible. Same letters indicate significant differences ($p<0.05$) between compared pairs from two-way ANOVA and Tukey's multiple comparisons test (n=6)..... 87

Figure 2.10: Hand-cut transverse sections of leaf 9 for each variety. Shown are the leaves under the control treatment (100% N). The red arrows in the IR64 denote the minor vein (minor vascular bundle) thickness. In the MR253 box, the red arrow highlights where the major vein (major vascular bundle) thickness is measured. Bulliform cells are shown in the MR219 box. Scale bar = 100 μm. (Source: own material)..... 89

Figure 2.11: Major and minor vein thickness for all varieties under the three nitrogen treatments. Shown are the means and the SEM. Same letters denote significant differences ($p<0.05$) between compared pairs (major and minor veins analysed separately) following a two-way ANOVA test and Tukey's multiple comparisons test, n=9. 90

Figure 2.12: Whole plant leaf area and leaf 9 area for the three varieties under the three treatments. Same letters indicate significant differences between compared pairs ($p<0.05$) from a two-way ANOVA test and Tukey's multiple comparisons test, n=4.91

Figure 2.13: Photosynthetic assimilation of CO_2 (μmol CO_2 m^{-2} s^{-1}) of (**a**) IR64 and (**b**) Moroberekan in the first trial, for plants under the three nutrient treatments, under increasing PPFD (μmol m^2 s^{-1}).

Data was fitted using the light response curve-fitting tool by Ye, (2007). Stomatal conductance (g_S, mol H_20 m^{-1} s^{-1}) is also shown for (**c**) IR64 and (**d**) Moroberekan. Shown are the means and SEM, n=4. For some mean data points, error bars are too small to be seen. 94

Figure 2.14: The assimilation of CO_2 (A) and stomatal conductance (g_S) of MR219, MR253 and IR64 at 100% N, 50% N and 25% N treatments in the second trial. Shown are the means and the standard errors of the means (SEM), n=4. For some cases, the error bars are too small to be visible. 95

Figure 2.15: Electron transport rate (μmol m^{-2} s^{-1}) of (**a**) IR64 and (**c**) Moroberekan as well as the ratio of variable to maximum fluorescence (Fv'/Fm') of (**b**) IR64 and (**d**) Moroberekan rice varieties under the three treatments. Shown are the means (n=4) and SEM indicated. For some cases, the error bars are too small to be visible. 97

Figure 2.16: Maximum quantum efficiency of PSII (ϕPSII) and relative electron transport rate (μmol m^{-2} s^{-1}) of MR219, MR253 and IR64 at 100% N, 50% N and 25% N treatments. Shown are the means and the standard errors of the means (SEM), n=6. For some cases, the error bars are too small to be visible. 98

Figure 2.17: The ratio of variable to maximum fluorescence (Fv'/Fm') of the three varieties under the three treatments in increasing PPFD (μmol m^2 s^{-1}). Shown are the means and the standard errors of the means (SEM), n=6. For some cases, the error bars are too small to be visible. 99

Figure 2.18: Maximum carboxylation rate of Rubisco (Vc_{max}), RuBP regeneration rate (J_{max}) and triosphosphate utilisation (TPU) of IR64, MR219, MR253 under the three treatments, in the second growth room trial. Values were obtained from curve-fitting A/Ci curves using the curve-fitting tool from Sharkey *et al*., (2007). Shown are the means and the standard errors of the means (SEM), n=4. For each bar, same letters (within each parameter e.g. Vc_{max}) indicate significant differences between compared pairs, following a two-way ANOVA ($p<0.05$) and Tukey's multiple comparison's test. 101

Figure 2.19: Non-photochemical quenching of MR219, MR253 and IR64 at 100% N, 50% N and 25% N treatments. Shown are the means and the standard errors of the means (SEM), n=4. For some cases, the error bars are too small to be visible. The asterisk (*) indicates significant differences between the 100% and 25% treatments within the varieties. 103

Figure 2.20: Chlorophyll content in SPAD value (greenness) of (**a**) IR64 and Moroberekan from the first trial, and of (**b**) IR64, MR219 and MR253 in the second trial. Shown are the means and SEM of leaf 9. Same letters indicate significant differences ($p<0.05$) between compared pairs, following a two-way ANOVA and Tukey's multiple comparisons test, n=4. 105

Figure 2.21: Pearson's correlation matrix with the correlation coefficients between chlorophyll (SPAD values), gas exchange parameters and leaf anatomical parameters in all varieties under all treatments ($n \geq 4$). P_{max} – light-saturated photosynthetic rate; Vc_{max} – maximum carboxylation capacity of Rubisco; ETR – electron transport rate; Fv/Fm – maximum quantum efficiency of PSII in dark-adapted state. Squares highlighted in pink represent significant correlation ($p<0.05$) and the squares highlighted in brown represent highly significant correlation ($p<0.0001$). 106

Figure 3.1: Rice seedlings growing in compost before transplanting in the FutureCrop glasshouse at The University of Nottingham... 121

Figure 3.2: (**a**) Watered soil bed with drip irrigation water pipes, (**b**) Rice plants in their individual microplots at leaf 5 developmental stage, (**c**) Line sensors at the top of the canopy to record incident PAR, and (**d**) Early flowering in IR64 plants. 123

Figure 3.3: (**a**) Plant height (cm) against number of days after transplanting for all varieties under the high N (HN) and low N treatments (LN). Data was fitted using a sigmoidal dose-response (variable slope), n=15. (**b**) The number of leaves on the main stem against the number of days after transplanting. Data was fitted using a linear regression, n=15. (**c**) Number of tillers against number of days. Data was fitted using a sigmoidal dose-response (variable slope), n=5. Shown are the means and the standard errors of the mean (SEM). For some, error bars are too small to be seen. 134

Figure 3.4: SPAD values (greenness/relative chlorophyll concentration) of the top of the canopy of rice varieties MR219, MR253 and IR64 under the high and low N treatments. Shown are the means and SEM. Bars indicate significant difference between the comparisons, ($p<0.05$), following a two-way ANOVA and Tukey's multiple comparisons test, where n=15. 136

Figure 3.5: Percentage leaf nitrogen (of dry weight) in the top layer of the canopy for the three varieties under the two treatments obtained from laboratory analyses. Shown are the means and SEM. Bars indicate significant difference ($p<0.05$) following a two-way ANOVA and Tukey's multiple comparisons test, where n=3. Leaf N analyses (Kjeldahl method) conducted by Lancrop Laboratories (Pocklington, York). 137

Figure 3.6: Major and minor vein thickness (μm) of the penultimate leaf on the main stem in all three varieties under the two treatments. Shown are the means and SEM. Bars indicate significant difference ($p<0.05$) following a two-way ANOVA and Tukey's multiple comparisons test, where n=12. 137

Figure 3.7: Penultimate leaf stomatal density and lengths for adaxial and abaxial leaf surfaces in all three varieties under both treatments. Shown are the means and SEM. Bars indicate significant differences ($p<0.05$), following a two-way ANOVA and Tukey's multiple comparisons test, where n=6. 138

Figure 3.8: Percentage of light intercepted by the plant canopy measured using canopy line sensors above and below the canopy. Shown are the means and SEM. Bars indicate significant difference, $p<0.05$, following a two-way ANOVA and Tukey's multiple comparisons test, where n=3. 138

Figure 3.9: Light response curves of plants at growth stages 1 (GS1), 2 (GS2) and 3 (GS3), for the top and bottom levels in the canopy. Shown are the mean photosynthetic assimilation rates, A, (μmol CO_2 m^{-2} s^{-1}) at increasing photosynthetic photon flux densities (PPFD in µmol m^2 s^{-1}) and SEM bars, where n=3. Data has been fitted using a light response curve-fitting tool (Ye, 2007). HN – high nitrogen, LN – low nitrogen..... 142

Figure 3.10: Detailed light response curves of plants at GS4 (65 DAT), for the top, middle and bottom levels of the rice canopy. Shown are the mean photosynthetic assimilation rates, A, (μmol CO_2 m^{-2} s^{-1}) at increasing photosynthetic photon flux densities (PPFD) and SEM bars, where n=3. Data has been fitted using a light response curve-fitting tool (Ye, 2007). HN – high nitrogen, LN – low nitrogen. 143

Figure 3.11: Maximum carboxylation rate of Rubisco (Vc_{max}), RuBP regeneration rate (J_{max}) and triosphosphate utilisation (TPU) of the rice varieties at 25°C, under the high and low N treatments, of the youngest fully extended leaf at growth stage 3. Values were calculated using the curve-fitting tool by Sharkey *et al*., (2007). Shown are the means and the SEM, n=3. For each bar, same letters indicate significant differences between comparisons following two-way ANOVA ($p<0.05$) and Tukey's multiple comparisons test. 147

Figure 3.12: Representations of the whole canopy constructions at the final growth stage, GS5. Some visual differences in density and leaf angle can be seen between the varieties with only minor differences observed between N treatments. (Acknowledgement: Alexandra Burgess) 148

Figure 3.13: Representations of the whole canopy constructions at each growth stage (GS) for IR64 HN (high N). GS1 – 18 DAT, GS2 – 25 DAT, GS3 – 49 DAT, GS4 – 65 DAT, GS5 – 77 DAT. (Acknowledgement: Alexandra Burgess) 149

Figure 3.14: (**a**) Modelled Leaf area index, (**b**) canopy extinction coefficient, k, values and (**c**) Predicted carbon gain per unit leaf and ground area over the five growth stages. (Acknowledgement: Alexandra Burgess) 150

Figure 3.15: (**a**) Modelled plant height and (**b**) Leaf inclination angles (°) from the bottom to the top of the plant canopy (with increasing depth in the canopy) for all treatments. The mean inclination angle was calculated (horizontal subsection with respect to the vertical subsection). Here, an angle approaching 0 indicates a more horizontal leaf while an angle approaching 90 degrees indicates an increasingly vertical leaf (Burgess *et al*., 2017). Data processed in Mathematica. (Acknowledgement: Alexandra Burgess) 151

Figure 3.16: Modelled cumulative leaf area index (cLAI) (the area of leaf material per unit ground as a function of depth) and fractional interception (FI) with increasing depth (mm) for all growth stages. Data processed in Mathematica. (Acknowledgement: Alexandra Burgess) 152

Figure 4.1: (**a**) Modules where seeds were germinated using compost. (**b**) Week-old seedlings with secondary leaf. (**c**) Prepared field with sprinklers for irrigation. (**d**) Rice plants at leaf 9. 162

Figure 4.2: Split-plot layout of Field Trial 1. Bold boxes represent control plots, and the un-bolded boxes are low N plots. Soil was sampled from two plots at four points each, as indicated by crosses. Red crosses represent sampling points in Plot 1, and blue for points in Plot 2. 164

Figure 4.3: Dimensions of the 7 by 6 micro-plot, where x represents a single rice plant. The length and breadth of the micro-plot is one meter and 1.2 meters respectively while the spacing between plants is 20 centimetres. 166

Figure 4.4: Split-plot layout of Field Trial 2. The bold box represents the control plot, and the non-bold box is the low N plot. In each plot, there are nine microplots. Within each microplot, a variety was grown (e.g. MR219) in a 8 by 7 configuration. 171

Figure 4.5: Dimensions of an 8 by 7 micro-plot in Field Trial 2, where x represents a single rice plant. The length and breadth of the micro-plot is 1.2 meters and 1.4 meters respectively while the spacing between plants is 20 centimetres. 172

Figure 4.6: Leaf inclination measurement. Dotted line with arrows represents the plane, which is perpendicular to the main stem. $\angle$ a is the inclination angle of the leaf, which is calculated from measuring angles $\angle$ b and $\angle$ c, using the equation above. 177

Figure 4.7: Daily mean temperature (°C) and relative humidity (%) across the two trials. The period between the black asterisks represent the time period for both trials. The table shows the mean temperatures and relative humidity (RH) during the trials and their standard deviation. 179

Figure 4.8: Daily mean solar radiation (MJ/m^2) across the two growth periods. The period between the black asterisks represent the time period for both trials. 180

Figure 4.9: Plant heights (cm) for all plants in both control and low N treatments in Field Trial 1 (**a**) and Field Trial 2 (**b**). Shown are the means (and SEM) plotted against thermal time (°Cd). Data was curve-fitted using a least squares Gaussian equation, n=6. 183

Figure 4.10: Leaf position (rank) and tiller numbers from Field Trial 2. Shown are the means and SEM, plotted against thermal time (°Cd), n=6. Data was fitted using a least squares non-linear regression (centered fourth order polynomial). Brackets represent significant differences between control and low N, following a two-way ANOVA and Tukey's multiple comparisons test. 184

Figure 4.11: Mean SPAD values for the three rice varieties in control and low N conditions in Field Trial 2. Shown are the means and the standard errors of the means (SEM), n=6. For some cases, the error bars are too small to be visible. The red bar indicates a significant difference following two-way ANOVA (p>0.05) and Tukey's multiple comparisons test. 189

Figure 4.12: (**a**) LAI for 48, 65 and 78 DAT in Field Trial 1. (**b**) LAI for plants in Field Trial 2 until heading. Shown are the means and SEM, n=15. For some cases, the error bars are too small to be visible. The letters indicate a significant difference (p<0.05) between compared pairs, following two-way ANOVA and Tukey's multiple comparison's test. The asterisks denote high significance (p<0.0001). 191

Figure 4.13: Comparison of LAI between both field trials at heading. Shown are the means and SEM, n=15. For some cases, the error bars are too small to be visible. The bars indicate a significant difference (p<0.05) between compared pairs following two-way ANOVA and Tukey's multiple comparison's test. 192

Figure 4.14: Mean leaf 9 and flag leaf lengths (cm) for the three rice varieties in control and low N conditions in Field Trial 2. Shown are the means and the standard errors of the means (SEM), n=6. Same letters indicate significant differences between compared pairs (analysed separately), following a two-way ANOVA (p<0.05) and Tukey's multiple comparison's test. 194

Figure 4.15: Mean leaf 9 and flag leaf widths (cm) for the three rice varieties in control and low N conditions. Shown are the means and the standard errors of the means (SEM), n=6. Same letters indicate significant differences between compared pairs (analysed separately), following a two-way ANOVA (p<0.05) and Tukey's multiple comparison's test. 194

Figure 4.16: Minimum and maximum values of leaf 9 inclination (°). Bars indicate significant differences between compared pairs, following a two-way ANOVA and Tukey's multiple comparisons test (n=6). 195

Figure 4.17: (**a**) Box and whiskers plot with minimum and maximum values of leaf area (cm^2) and (**b**) normalized difference vegetation index (NDVI). Same letters indicate significant differences (p<0.05) between compared pairs. following a two-way ANOVA and Tukey's multiple comparisons test (n=6). 197

Figure 4.18: Light intercepted (%) by canopy in control and stressed plants. Shown are the means and SEM. Same letters indicate significant differences (p<0.05) between compared pairs, from a two-way ANOVA and Tukey's multiple comparisons test (n=6). 198

Figure 4.19: Light response curves for top and bottom of the canopy in control and low N plants in Field Trial 1. Shown are the mean photosynthetic assimilation rates ($\mu mol\ CO_2\ m^{-2}\ s^{-1}$) at increasing photosynthetic photon flux densities (PPFD in $\mu mol\ m^2\ s^-$

^{1}) and SEM bars (n=3). Data has been fitted using a light response curve-fitting tool (Ye, 2007)..... 200

Figure 4.20: Mean and SEM of photosynthetic assimilation rates, P_{max} (μmol CO_2 m^{-2} s^{-1}) at the top and bottom canopy levels, in saturated light conditions obtained from curve-fitted data in Field Trial 1 (Ye, 2007). The bar denotes significant difference, following a two-way ANOVA and Tukey's multiple comparisons test (n=3). 201

Figure 4.21: Mean stomatal conductance, g_S (μmol CO_2 m^{-2} s^{-1}), at the top and bottom of the plant canopy in Field Trial 1, at increasing photosynthetic photon flux densities (PPFD in µmol m^2 s^{-1}) and SEM bars (n=3)..... 202

Figure 4.22: Light response curves for leaf 9 in control and low N plants in Field Trial 2. Shown are the mean photosynthetic assimilation rates (μmol CO_2 m^{-2} s^{-1}) at increasing photosynthetic photon flux densities (PPFD µmol m^2 s^{-1}) and SEM bars (n=3). Data has been fitted using a light response curve-fitting tool (Ye, 2007). 203

Figure 4.23: Mean and SEM of photosynthetic assimilation rates, P_{max} (μmol CO_2 m^{-2} s^{-1}), in saturated light conditions obtained from curve fitted data in Field Trial 2. No significant differences were found from a two-way ANOVA and Tukey's multiple comparisons test (n=3)..... 204

Figure 4.24: Light-adapted Fv'/Fm' in plants in Field Trial 1 at 48, 65 and 78 DAT. Shown are the means and SEM, n=3. Bars indicate level of significant differences between compared pairs from a two-way ANOVA and Tukey's multiple comparisons test..... 205

Figure 4.25: Maximum efficiency of Photosystem II in dark-adapted state or Fv/Fm values in Field Trial 2. Shown are means and SEM. Letters indicate significant differences ($p<0.05$) and asterisks indicate highly significant differences ($p<0.0001$) from a two-way ANOVA and Tukey's multiple comparisons test (n=6)... 206

LIST OF TABLES

Table 2.1: Final leaf lengths from curve-fitting for leaf 6, 7, 8 and 9 for all varieties under the three nitrogen treatments. Shown are the means and the SEM. Same letters indicated highly significant differences ($p<0.01$) between paired comparisons, following a two-way ANOVA test and a Tukey's multiple comparisons test, n=5. .. 83

Table 2.2: Number of days taken (from sow) to 50% full leaf extension (LE_{50}) in leaves 6,7,8 and 9 in the three varieties under the three N treatments. LE_{50} was obtained from the data in Figure 2.12. Same letters indicate highly significant differences between the means compared (within each leaf rank) following two-way ANOVA ($p<0.05$) and Tukey's multiple comparisons test. 84

Table 2.3: P_{max} (µmol CO_2 m^{-2} s^{-1}) for growth room trial 1, for IR64 and Moroberekan rice plants under the three nutrient regimes with their standard error of the means. Same letters indicate significant differences ($p<0.05$) between compared pairs (between varieties and between treatments), following a two-way ANOVA and Tukey's multiple comparisons test, n=4. 96

Table 2.4: P_{max} (µmol CO_2 m^{-2} s^{-1}) for growth room trial 2, for IR64, MR219 and MR253 rice plants under the three nutrient regimes with their standard error of the means. Same letters indicate significant differences ($p<0.05$) between compared pairs (between varieties and between treatments), following a two-way ANOVA and Tukey's multiple comparisons test, n=4. 96

Table 3.1: Final plant heights (cm) and number of tillers of the three varieties under the two nitrogen treatments. Shown are the means and SEM. Same letters denote significant difference ($p<0.05$) between compared pairs, following a two-way ANOVA and Tukey's multiple comparisons test, where n=15. 135

Table 3.2: Mean dry weights (g) of the three varieties at growth stages 2 (GS2), 3 (GS3), 4 (GS4), 5 (GS5) and at harvest with the SEM, n=3. Same letters indicate significant differences between compared pairs (both varieties and treatment), following two-way ANOVA ($p<0.05$) and Tukey's multiple comparison's test. 139

Table 3.3: The photosynthetic assimilation rates, P_{max}, (µmol CO_2 m^{-2} s^{-1}) for the rice varieties in both high and low nitrogen plots, at the top and bottom levels of the canopy, at growth stages 1 (GS1), 2 (GS2) and 3 (GS3). Shown are the means and their SEM, where n=3. Same letters indicate significant difference between the compared means ($p<0.05$) using a two-way ANOVA (comparing variety, treatment and level in canopy) and Tukey's multiple comparisons test. 144

Table 3.4: The photosynthetic assimilation rates, P_{max}, (µmol CO_2 m^{-2} s^{-1}), light compensation point (µmol photons m^{-2} s^{-1}), dark respiration, Rd, (µmol CO_2 m^{-2} s^{-1}) and maximum quantum yield (µmol CO_2 m^{-2} $s^{-}1$) for the rice varieties in both high and low

nitrogen plots, at the top, middle and bottom levels of the canopy, at growth stage 4. Shown are the means and their SEM, where n=3. Same letters indicate significant difference between the compared means ($p<0.05$) using a two-way ANOVA (comparing variety, treatment and level in canopy) and Tukey's multiple comparisons test. 145

Table 4.1: Soil analysis results for pH, N (%), K (m.e %), Na (m.e %), Fe (m.e %), P (ppm) and cation exchange capacity (m.e %). Soil was sampled from two plots. 163

Table 4.2: Control plot application at three application times. (T) is prior to transplanting, (AT) is at tillering and (PI) is panicle initiation. 166

Table 4.3: Lower-N plot application at three application times. (T) is prior to transplanting, (AT) is at tillering and (PI) is panicle initiation. 167

Table 4.4: Control plot application at split application times. (T) is prior to transplanting, (AT) is at tillering and (PI) is panicle initiation. 173

Table 4.5: Nitrogen stress plot application at split application times. (T) is prior to transplanting, (AT) is at tillering and (PI) is panicle initiation. 174

Table 4.6: List of parameters measured in Field Trial 2 that were similar to Field Trial 1, with minor changes. 175

Table 4.7: Growth characteristics prior to flowering at 1405 degree days (°Cd) for Field Trial 2. Included are the means and the standard deviations. Same letters represent significant differences ($p<0.05$) between compared pairs (plant height and tiller number analysed separately), from two-way ANOVA and Tukey's multiple comparisons test, n=6. 185

Table 4.8: Number of leaves on the main stem and estimated phyllochron (°Cd) for both field trials. Included are the means and the standard error of means. Same letters represent significant differences ($p<0.05$) between compared pairs within each trial (trials analysed separately), from two-way ANOVA and Tukey's multiple comparisons test, n=6. 186

Table 4.9: Mean SPAD values for the three rice varieties in control and low N conditions at two growth stages (maximum tillering - 21 DAT, heading – 65 DAT) in Field Trial 1. Also included are the SEM, n=12. Same letters represent significant differences ($p<0.05$) between compared means following a two-way ANOVA and Tukey's multiple comparisons test. 188

Table 4.10: Number of effective tillers from both field trials. Shown are means and standard error of means. Letters indicate significant differences ($p<0.05$) from a two-way ANOVA and Tukey's multiple comparisons test (n=6). 206

Table 4.11: Pearson's correlation matrix with correlation coefficients for growth parameters against the yield parameter, for

control plants in Field Trial 2 for control plants. PH – plant height; MS leaves – number of leaves on main stem; TN – tiller number; FLL – flag leaf length; FLW – flag leaf width; FLArea – flag leaf area; L9L – leaf 9 length; L9W – leaf 9 width; Cumul LAI – cumulative leaf area index; Eff. Tillers – number of effective tillers. Squares highlighted in pink represent significant correlation ($p<0.05$) and squares highlighted in brown represent highly significant correlation ($p<0.0001$). 208

Table 4.12: Pearson's correlation matrix with correlation coefficients for growth parameters against the yield parameter, for control plants in Field Trial 2 for low N plants. PH – plant height; MS leaves – number of leaves on main stem; TN – tiller number; FLL – flag leaf length; FLW – flag leaf width; FLArea – flag leaf area; L9L – leaf 9 length; L9W – leaf 9 width; Cumul LAI – cumulative leaf area index; Eff. Tillers – number of effective tillers. Squares highlighted represent significant correlation ($p<0.05$). 209

Chapter 1: Introduction

Chapter 1

1.1 Introduction

Food prices have risen over the past decade and addressing the global food security problem is crucial. Rice (*Oryza sativa)* is one of the most commercially important crops in the world. It is believed to have been first domesticated from its wild ancestor *Oryza rufipogon* in East Asia approximately 9000 years ago (Callaway, 2014). Since then, it has been a major source of nutrition for a large percentage of the world's population, accounting for more than 40% of the global food production. Unfortunately, the production of rice is not rising fast enough to sustain the increase in global population, which is expected to reach almost 10 billion by 2050 (UN DESA, 2019).

Rice is produced in at least 95 countries across the world (IRRI, 2002). The two main regions of rice production are Asia and Africa, and it has been predicted that most of the extra demand for food will originate from the developing countries in these regions - where poverty is most concentrated (Murchie *et al*., 2009; Sheehy and Mitchell, 2013). Rice is the staple for a majority of the countries in Asia (Makino, 2011), as people depend on it as a source of nutrition and calories. The Rice Market Monitor by the Food and Agriculture Organization in 2012 stated that the current rice production has shown to outpace consumption. Nevertheless, an increase in supply of rice would be required to meet the future demands of a rise in world population. In the context of Asia, an estimated 50% increase in rice yield would be necessary to sustain population growth by 2050 (Sheehy *et al*., 2000). Yet currently, regions predominantly involved in agriculture are being driven to confront the inevitable prospect of growing under increasingly unfavourable circumstances due to changing patterns of land use and fluctuating environmental conditions.

1.1.1 Rice as a crop

Since domestication rice cultivation was largely done in standing water, in river deltas and low-lying areas. European settlers introduced rice cultivation to the New World prior to 1685 and spread to west continental America (GRiSP, 2013). Rice is presently cultivated under a range of climatic conditions – from the dry deserts of Saudi Arabia to the wettest areas in the state of Meghalaya in Northeast India. While the majority of rice famers across the world currently practice intensive agriculture, subsistence farming still exists in some areas in South Asia, where human labour is still the largest cost of crop production (Ye and Pan, 2016).

O. sativa and *O. glaberrima* are the two species of rice that are most cultivated across the world. While *O. sativa* is the more widely grown species, *O. glaberrima* is confined to the African continent. Three widely cultivated ecological varieties exists within the *O. sativa* species itself: the long-grained indica variety that is mostly grown in the tropical and sub-tropical regions of Asia, the medium-grained javanica rice that is grown in the Philippines, and the short/medium grained japonica variety which is cultivated in the more temperate regions of Northern China and Japan (Huang *et al*., 2012; GRiSP, 2013). Tropical and sub-tropical rice growing regions mainly practice irrigated or rain-fed lowland farming systems under two to three crop rotations. These systems produce about three-quarters of the rice in the world. Upland rice is grown in more temperate areas and produces up to 4% of rice in the world (GRiSP, 2013).

Rice is a semiaquatic annual cereal, with two morphological phases of growth. The first is the vegetative phase, which is in itself divided into germination, seedling and tillering stages. The second phase is the reproductive phase, which includes panicle initiation and heading. The duration of growth is genotype and climate dependent – lasting between 3-6 months (Toriyama *et al*., 2005; GRiSP, 2013).

During the vegetative phase, plant height increases, and leaves emerge at regular intervals. At the emergence of the fifth leaf, the tillering stage commences. Tillers can grow from the main stem, primary tillers and secondary tillers. The number of panicles is determined from the number of productive tillers formed. Tillering itself is genotype dependent, and the formation of productive tillers can be affected by factors such as planting density, nutrients and solar irradiation. Unfavourable conditions can result in the eventual loss of panicles. The reproductive phase is characterised by the emergence of the final leaf on the main stem – the flag leaf. Prior to heading is the panicle initiation stage, where the panicle grows to about 1 mm in length. Flowering occurs at heading (anthesis). Field anthesis normally occurs over the span of a couple weeks. Ripening occurs after fertilization and can occur over a period of 15 to 40 days (variety dependent) (Yoshida, 1981; Fageria, 2007). Most tropical varieties in South East Asia take an average of 120 days to complete the growth cycle. These varieties spend half of that in the vegetative stage, 30 days in reproduction and the last 30 in the ripening phase.

1.1.2 Trends in rice production and yield

Technologies of the Green Revolution in the 1960s have allowed huge gains in yield across the world through better management techniques, crop nutrition and protection, giving rise to elite cereal cultivars which now dominate the rice growing world. Elite rice varieties are semi-dwarf plants with shorter maturation periods and have been bred to produce a larger harvestable aboveground biomass (a high harvest index) with improved carbon partitioning (Gifford and Evans, 1981; Evans, 2013) as compared to ancestral varieties. In the two decades after the Green Revolution, food supply more than doubled in Asia notwithstanding the small increase in harvest area of only 4%. However, the technologies from the Green Revolution caused the rise of intense monoculture systems, an overreliance of nitrogenous fertilisers and destructive highly mechanised farming practices (Walsh, 2009).

Figure 1.1 shows the trend in global rice production from 1961 to 2015 (FAOSTAT Database, accessed January 28, 2015). Rice yields have increased, partly due to the increase in the amount of available land dedicated to rice cultivation. However, the amount of land for cultivation is declining and will continue to decline, due to continued urbanization and industrialization. How much of an increase in rice production required will be ultimately determined by factors such as the rates of population growth, dietary shifts and socio-economic transitions (Smil, 2005).

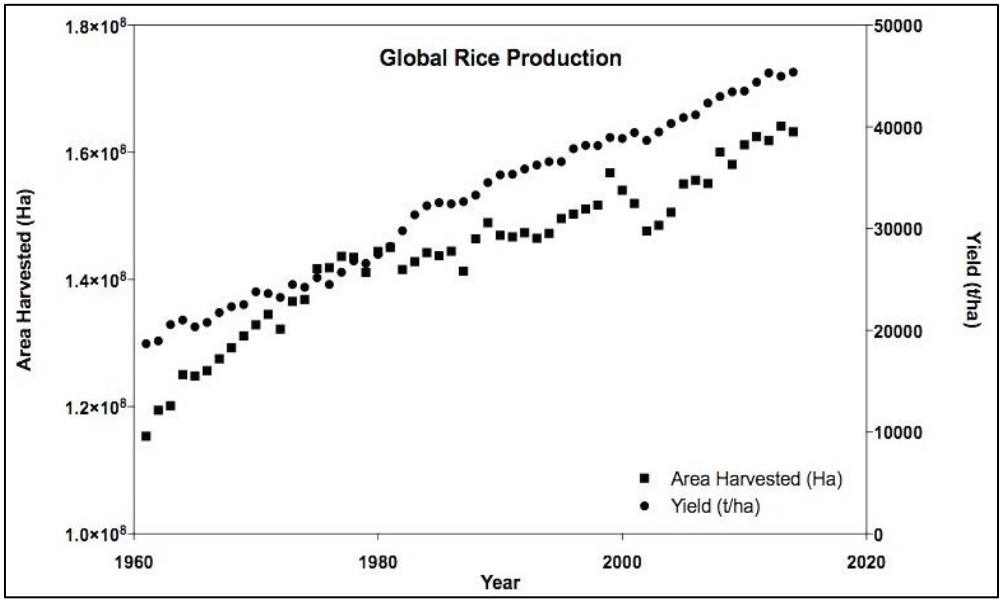


Figure 1.1: Global rice yields (t/ha) and harvested area (ha) from 1961 to 2015. (Source: FAOSTAT Database, January 28, 2016)

It is becoming more evident that the increase in yield is approaching a theoretical upper limit, indicating that Green Revolution related yield progressions are stagnating. The rising population and increasing affluence in the world's cereal crop producing regions are experiencing this stagnation in yield progress. This theoretical upper limit comes in the form of a barrier set by the efficiency of resource capture and energy conversion in photosynthesis (Sheehy *et al*., 2007; Sheehy and Mitchell, 2011). Furthermore, shifts in climate are becoming more unpredictable,

potentially introducing abiotic stresses to agricultural systems. Environmental conditions such as solar irradiance, seasons and soil fertility have an effect on the protein and starch content of rice (Chen *et al*., 2012; Patindol *et al*., 2015; Li *et al*., 2018).

This is a key concern for economically and environmentally vulnerable regions where agriculture is the main source of income, livelihood and diet. There is a need to look at other avenues for increasing yield on less arable land, as food is becoming increasingly expensive. Concerns and the uncertainties over the availability of resources, the erratic fluctuations in climate and other emerging constraints have led to major investments in plant and crop science research and the development of cross-disciplinary tools. Specifically, it is becoming more recognized and pertinent that capacity for photosynthesis needs to be improved in order to provide the extra biomass needed to support further potential yield increases (Furbank *et al*., 2009a; Parry *et al*., 2011; Acevedo-Siaca *et al.,* 2020). There are two major ways that this can be achieved; through improvements to light capture through increased erectness of the plant canopy and increasing the efficiency of the photosynthetic machinery. Details on how these mechanisms play a role in overall yield production are discussed in section 1.2.1 below.

1.1.3 Rice growing systems

Rice grows in a wide variety of environments across the world. The main environments that persists across cropping systems are rainfed and irrigated or direct seeding in either wet or dry soil in lowlands. Upland rice is usually grown in dry soil with or without irrigation (rainfed). Flooded (deep water) and floating rice are normally lowland and grown in places like India and Bangladesh, where annual rainfall is high, and flooding occurs due to a rise in the water table.

It is estimated that a significant 93 million hectares of irrigated lowland rice makes up 75% of the global production of rice (Maclean

et al., 2002; GRISP, 2013). Rainfed cropping systems supply 19% while the remaining are the combination of flood and floating rice. In irrigated cropping systems, water is provided fully during the dry season and as a supplement during the wet season. Here, rice is grown as a monoculture and generally grown twice a year. Rice farmers typically do rotate with other crops (with short growth cycles) during the non-rice growing seasons of the year. Rainfed environments are constrained by the geography and topology of the land and more so dependent on a constant supply of water from rain. This unpredictable resource often creates a less than optimal environment not only for the growth of rice, but the management of the cropping system (Nguyen, 2002; Peng *et al*., 2004; Fitzgerald and Resurreccion, 2009; IRRI, 2012; Redfern *et al*., 2012).

1.1.4 The production of rice in Malaysia

Rice is the staple food and the second most cultivated crop in Malaysia, with the majority of its cultivation occurring in the northern parts of Peninsular Malaysia and Eastern Malaysia. States such as Kedah, Perak and Kelantan control more than 50% of the country's harvested area (Nguyen, 2002). Yield has been averaging between 3.39 tonnes per hectare (t/ha) in 2006 and 3.81 t/ha in 2013 – one of the lowest in the Southeast Asian region (GRiSP, 2013). Out of 656.4 million tonnes of rice produced in Asia, only 2.7 million tonnes are from Peninsular and Eastern Malaysia - approximately 0.4% of Asia's rice production as reported by the FAO in 2011. To meet the demand for rice that overwhelms the supply, Malaysia has to import increasingly more from neighbouring Thailand and Vietnam. In 2008, 1120 kilo tonnes of rice were imported – approximately three times more than that imported in 1995 (FAOSTAT Database, accessed January 28, 2016). Malaysia's self-sufficiency in rice production currently stands at 70% according to the Malaysian Agriculture Research and Development Institute (MARDI), and its aim to reach 100% self-sufficiency in rice production by 2015 has proven challenging (Alam

et al., 2012; Siwar *et al*., 2013; Vaghefi *et al*., 2013). These challenges, however, are not unlike those faced by other countries involved in rice cultivation. Rice production is declining or stagnating across the world, due to increasing soil degradation and an excessive utilisation of agrochemicals with decreased use efficiency (Siwar *et al*., 2014).

Both Peninsular and Western Malaysia have natural geographical disadvantages. A majority of the country is covered in tropical rainforest, which limits rice cultivation to coastal regions. These regions, however, are facing severe soil degradation and an increase in salinity, which will reduce the land available for cultivation. Siwar *et al*., (2009) revealed that changes in the rice production would be affected by a reduction in the water available for irrigation due to an increase in salinity as well as a rise in sea levels. A crop simulation model used by Vaghefi *et al*., (2015) predicted that significant changes in rainfall and fluctuating temperatures could reduce the yield of Malaysian rice until 2030 by 12% and 31.3% respectively.

Nevertheless, rice yields within the country are seeing a rise. The usage of N fertilisers shows a decrease after 2010 according to FAOSTAT (Figure 1.2) (FAOSTAT Database, accessed June 13, 2019). This may be due to unreported figures in the FAOSTAT data, since application data of P and K do not show a similar pattern (data not shown). Alternatively, it has been suggested that the recent increases in rice production per unit area have been attributed to innovations in farming operations, government support and increased mechanisation (Shamshiri, 2018). To fulfil the demand of a rising population in the current climate, the country has to be able to sustain rice production and at the same time sustainably increase productivity of the crop per unit hectare, without having to expand granary areas (Najim *et al*., 2007; Herman *et al*., 2015). On the socio-economic side, there are more than 300,000 paddy farmers, growing rice on approximately 675,000 hectares of land (Rabu and

Shah, 2013) and many of them still marginalised. Cultivating rice in Malaysia is not as cost effective as its rice growing counterparts such as Thailand and Vietnam, where rice is still imported from to meet Malaysia's consumption needs. At present, Malaysia is capable of producing 70% of its consumption requirements, with the remaining 30% being imported from Thailand, Vietnam and Pakistan (Fatah & Cramon-Taubadel, 2017). It has been argued that the lack of economic competitive advantage of Malaysian farmers is due to the abundance of inefficiently managed small farms compared with industrial scale production prominent in neighbouring countries (Shamsudin, 2014). In fact, at the level of production, Malaysia had a slightly higher production per unit area compared with Thailand and Pakistan between 2008 and 2018 (FAOSTAT Database, accessed May 8, 2020). Given that there is still scope for significant improvement, The Minister of Agriculture and the Agro-Based Industry in Malaysia have committed to increasing rice production to meet 100% self-sufficiency by 2020 (Fatah & Cramon-Taubadel, 2017). Nevertheless, even if economic policy changes and improved farm management can reduce Malaysia's reliance on imports, continual increases in production must still be achieved to satisfy the ever-increasing demand from national consumption.

Breeding programmes have been focusing on high yielding hybrid rice varieties, with high abiotic stress tolerance. Varieties MR219 (released in 2001) and MR220 (released in 2003) are the two most widely cultivated indica rice varieties in Peninsular Malaysia – more than 90% of rice growing regions in Malaysia have grown these two varieties over at least 20 seasons. Recently however, farmers have found reductions in yield which they have attributed to an increased frequency of pest and disease attacks. MARDI released two new varieties as alternatives, MR253 and MR263 in December 2010. According to MARDI, growing these varieties not only overcomes the yield reduction seen in the older cultivars, but are better suited to the changing environments. The new varieties also boast improved

resistance to pest and diseases as well as the ability to thrive in marginal soil conditions (Mahmood *et al*., 2014).

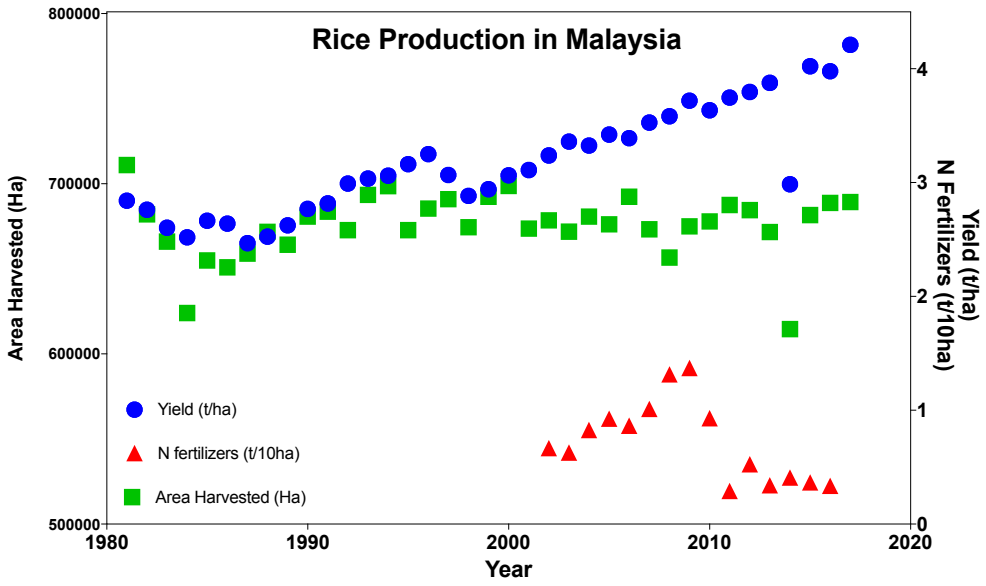


Figure 1.2 : Malaysia's annual rice production from years 1980 to 2017 in terms of yield (t/ha), area harvested (ha) and N fertilisers (t/10ha) supplied to the agricultural system. (Source: FAOSTAT Database, June 13, 2019)

1.2 **Increasing the production of rice**

While better crop management has played a vital role in the increase of rice production in the past, there is a growing need to look at other avenues to push past the yield stagnations. This need has included making the crop more efficient in its usage of primary resources (light, water, nutrients), e.g. through the reengineering of photosynthesis. Efficient rice production should maximise the conversion of incoming solar energy into chemical energy, with the least amount of resources spent (Sheehy *et al*., 2007). Meeting the challenge of increasing rice production in light of the increasing constraints would necessitate the development and utilisation of new and more sustainable technologies. Current developing technologies have included breeding varieties with higher yield potential and increased yield stability via conventional hybridization techniques (Khush, 2005). Genetic engineering approaches are equally useful in developing rice genotypes that are capable of withstanding abiotic stresses but not accepted universally, e.g. within the European Union.

1.2.1 Yield potential

Yield potential (Y_p) is defined as 'the yield of a cultivar when grown in environments to which it is adapted, with nutrients and water non-limiting, and with pests, diseases, weeds, lodging and other stresses effectively controlled' (Evans and Fischer, 1999). Thus far, high yielding varieties have optimized Y_p at 10 t ha^{-1} with a harvest index of 0.5 in tropical conditions (Peng, 2000). Harvest index (HI) is also known as the partitioning efficiency, which is defined as the total biomass energy partitioned into the harvested region of the crop. Over the past 50 years, Y_p increase has been largely achieved through the increase in HI (Long *et al*., 2006b).

Increased harvest index (HI) until now has resulted through the shortening of stem (dwarfing), and the increase in the potential number of seeds set (Zhu *et al*., 2010). Dwarfing the stem has also

improved the ability of the plant to withstand unfavourable weather conditions such as heavy rain and wind. Nevertheless, the HI of rice is reaching a plateau (thought to be set by a theoretical limit to this parameter); hence further increases in yield would require an increase in productive biomass and therefore an increase in photosynthesis (Parry *et al*., 2011). Crop biomass is considered as a function of intercepted radiation and both properties have been observed to share a linear relationship (Monteith, 1972; Monteith, 1977; Sinclair and Muchow, 1999; Quero *et al*., 2019). More than 90% of crop biomass is derived from photosynthetic products.

Radiation use efficiency (RUE) describes the relationship between radiation intercepted and the rate of production of biomass (kg of dry weight/MJ radiation intercepted) where an increase in RUE would result in the increase in plant biomass. In principle, RUE can be increased through altering improving leaf and canopy photosynthetic rate. This could be achieved, for example, by altering the biochemical properties of the enzyme Rubisco (ribulose 1,5-bisphosphate carboxylase oxygenase) to promote carboxylation and minimizing photorespiration, introducing the C4 photosynthetic pathway into the C3 rice pathway (in warm regions), up-regulating the enzymes in the Calvin cycle, improving the capacity for photoprotection, the recovery rate from photoprotection and reducing photoinhibition (Zhu *et al*., 2008; Murchie *et al*., 2009; Zhu *et al*., 2010; Ort *et al*., 2015; Kromdjik *et al*., 2016).

Efforts in maximising the function of the Calvin cycle has gained traction in the past decade, with particular interest in the enzyme that has a significant control over the rate of carbon fixation, sedoheptulose-1,7-bisphosphatase (SBPase) (Raines, 2003, 2011). Research on transgenic tobacco (Lefebvre *et al*., 2005; Lawson *et al*., 2006), tomato (Ding *et al*., 2016, 2017), rice under different abiotic stress (Feng *et al*., 2007a, 2007b, 2009) and wheat (Driever *et al*., 2017). Increasing photosynthetic potential will therefore necessitate

the improving of photosynthetic efficiency through substantial research at a leaf, cellular and subcellular level.

To provide more detail: Y_p of a crop and total crop biomass (in MJ m^{-2}) can be explained by the Monteith (1977) equation,

Total Biomass or Primary Production (P_n) = $\frac{S_t \cdot \varepsilon_i \cdot \varepsilon_c}{Ce}$

Yield Potential (Y_p) = $HI \cdot P_n$

where S_t is the total incident solar radiation over the duration of the growing season; ε_i is the light interception efficiency by the crop; εc is the efficiency by which intercepted solar radiation is converted into biomass; *Ce* the energy content of the harvested material, which is dependent on the lipid:carbohydrate:protein ratio of the harvested material. When computing the Y_p, it is necessary to include the HI.

1.3 **The mechanism of photosynthesis**

Photosynthesis is a physio-chemical process by which plants and other autotrophic organisms convert light energy to chemical energy by fixing carbon dioxide into sugars. The region of wavelengths between 400 and 700 nanometres (McCree 1981; Zhen & Bugbee, 2020) is considered to be photosynthetically active, which drives carbon assimilation. Nevertheless, recent research has demonstrated that far-red wavelengths of 700 – 750 nm are also efficient at driving canopy photosynthesis (McCree 1981; Zhen & Bugbee, 2020).

The most photosynthetically active regions of plants are leaf mesophyll cells. These cells receive high light levels and contain high concentrations of chloroplasts, which contain chlorophyll, a pigment that is involved in light capture. These pigments are found in the light harvesting complexes in Photosystem II (PSII) and Photosystem I (PSI) embedded within the thylakoid membrane first intercept light (Taiz and Zeiger, 2010). After absorbing light, chlorophyll rises from its ground state to an excited state. Figure 1.3 shows how an excited chlorophyll returns to its original ground state – 1) through chlorophyll *a* fluorescence 2); by fuelling photosynthetic reactions (photochemistry); 3) by dissipating heat in non-photochemical quenching (NPQ) and 4) formation of a reactive oxygen species (ROS).

The interception of light creates resonance energy, which is then transferred from neighbouring chlorophyll molecules to the reaction centres of PSII and PSI (Figure 1.4a). Photolysis, the splitting of water molecules that generates electrons and protons, occurs in the oxygen evolving complex (Barber, 2017). Electrons are then transferred from PSII to PSI via the redox reactions within the electron transport chain and this is coupled with the transfer of H^+ across the thylakoid membrane. In the stroma of the chloroplast, $NADP^+$ (nicotinamide adenine dinucleotide phosphate) is reduced to NADPH, and at the same time, the electrochemical proton gradient generated from the electron transport redox reactions drives the

formation of ATP (adenosine triphosphate) using ATP synthase (Taiz and Zeiger, 2010). Both NADPH and ATP are used in the Calvin-Benson cycle or the inaccurately-named 'light-independent' reactions to fix CO_2 (Figure 1.4b) (Buchanan, 2016).

The Calvin-Benson cycle takes place in the stroma of the chloroplast. It is made up of three main phases – 1) carbon fixation of CO_2, 2) reduction of 3-phosphoglycerate (3-PGA) and 3) regeneration of ribulose 1,5-bisphosphate (RuBP). In carbon fixation (Figure 1.4b), the enzyme Rubisco (ribulose bisphosphate carboxylase oxygenase), catalyses the reaction between the substrate RuBP and CO_2. For each molecule of CO_2 fixed, two molecules of 3-PGA are formed. In the reduction phase, ATP and NADPH from the light reactions are used to convert six molecules of 3-PGA to six molecules glyceraldehyde 3-phosphate (GA3P). This is a reduction reaction as it involves the gain of electrons by 3-PGA. ATP is broken down into ADP (adenosine diphosphate) and inorganic phosphate (P_i), releasing energy, while NADPH is converted to $NADP^+$ through the loss of an H atom. These two molecules are recycled back into the light reactions. In the final phase, only one molecule of GA3P leaves the Calvin cycle to be used in the formation of large carbon compounds that are primarily sugars. The remaining five molecules of GA3P remain in the Calvin cycle and are utilised in the regeneration of RuBP (Taiz and Zeiger, 2010).

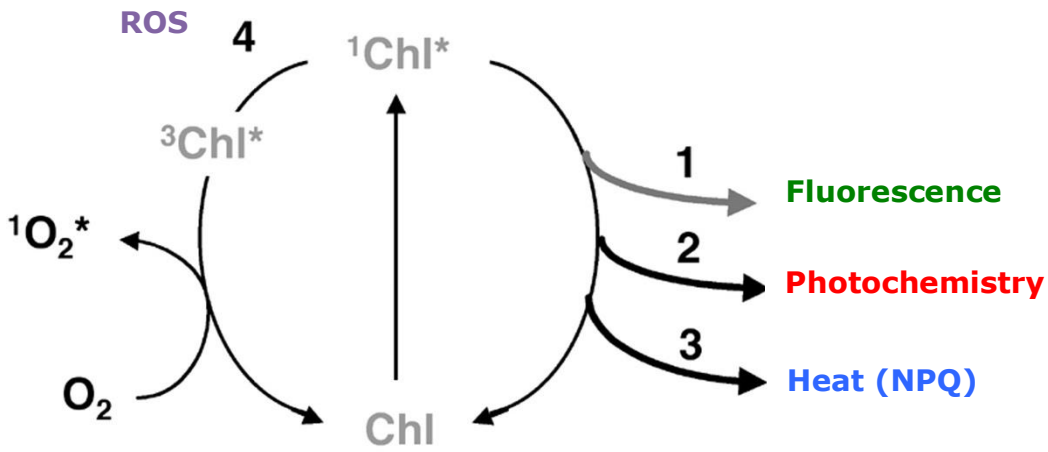


Figure 1.3: Schematic of pathways taken by an excited chlorophyll (1Chl*) to return to ground state (Chl) – 1) Chlorophyll a fluorescence, 2) photochemistry, 3) heat through NPQ and 4) reactive oxygen species (ROS).

a **b**

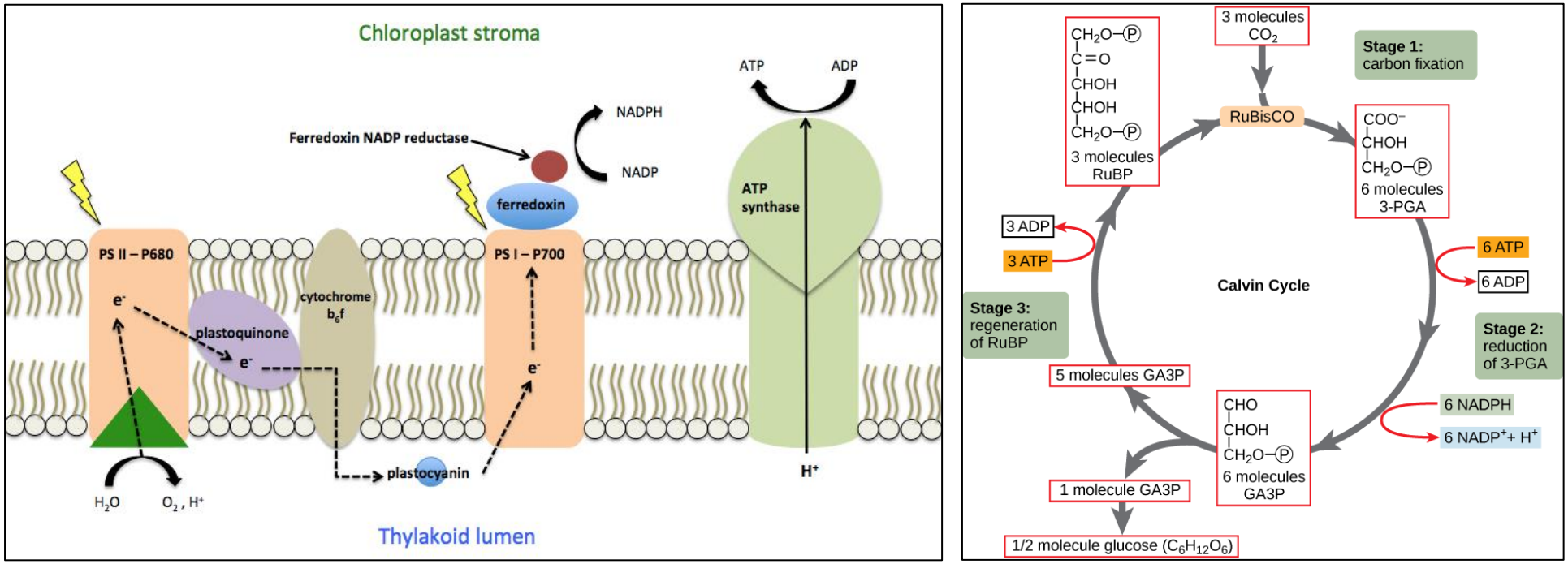


Figure 1.4: (**a**) Light-dependent and (**b**) Calvin-Benson cycle reactions in the chloroplast. (Sources: (a) own collection and (b) Taiz and Zeiger, 2010.

1.4 **Photosynthesis as a limiting factor**

Photosynthetic research has picked up speed in the past three decades, leaving behind traditional breeding techniques from the Green Revolution in the ultimate goal of increasing yield potential. However, before considering the prospects of increasing net photosynthesis, there is a need to establish whether an increase in photosynthesis (and subsequently biomass) in fact results in increased crop yield.

There are many limiting factors within the photosynthetic machinery, which in itself determine the rate of photosynthesis at the leaf level and more variables involved when looking at photosynthesis at the canopy level under different environmental conditions. However, multiple studies have shown that the rate of photosynthesis does not necessitate an increase in grain yield (Yamori *et al.,* 2016). This is because the production of plant biomass also depends on factors that influence the scaling of leaf processes to whole canopy productivity such as the allocation of the products of photosynthesis (photosynthates), sink capacity of assimilates (capacity to use the these photosynthates) as well as coping with environmental stress (Zivcak *et al*, 2017). It is also possible to point to many studies that show a correlation between photosynthesis and yield occurs, the most convincing of which are the array of Free Air CO_2 enrichment studies (Long *et al*, 2006a; Ainsworth and Long, 2005).

The diversity of conversion efficiencies (of photosynthetic assimilates into biomass) between different crop species has been found to be significant, for example, due to the use of the C3 and C4 mechanism. Studies suggest that photosynthetic rate at a leaf level can be poorly correlated with crop yield at genotypic level, with a few earlier studies even reporting a negative correlation between photosynthetic rate and grain yield (Reynolds *et al*., 2000; Richards, 2000). Evans and Dunstone (1970) observed leaf photosynthetic rate to be lower in modern bread cultivars as compared to their wild

ancestors. More recently, Reynolds *et al*., (2005) concluded in their study with spring wheat that yield was affected largely by radiation use efficiency (RUE), which can be improved by increasing sink strength, ultimately showing that yield in this case was sink limited.

Source-sink relationships within plants are maintained to ensure that source outputs are consistent with the requirements of the sink organs. Source outputs are often limited by environmental factors such as light and N availability, leading to a forced reduction in the sink organs biomass. Alternatively, excessive supply by source organs can also be downregulated by sink organs (Asseng *et al*, 2017). In the case of photosynthate production, a lower or reduced sink capacity (when grown in either optimal or stressed conditions) leads to the eventual down-regulation of photosynthetic capacity (Peet and Kramer, 1980; Zivcak *et al*., 2017), which seems to have more of a limitation on biomass production than the rate of photosynthesis itself. A recent study on the electron transport component, cytochrome b_6/f complex, have shown that a lower amount of this protein can severely curtail the rate of electron transport linked to Photosystem II (Yamori *et al*., 2016). The transgenic rice exhibited lower CO_2 assimilation rates, similar to that in tobacco (Yamori and von Caemmerer, 2009). Therefore, breaking down the different components of mechanism of photosynthesis is necessary to identify key rate-limiting factors. Down and up-regulating various components in the light-dependent and light-independent reactions and seeing the effect on CO_2 assimilation rate are useful in determining if photosynthesis is indeed the main limitation for plant productivity and yield. However, the lack of correlation between increased photosynthetic activity and yield discussed previously, in many cases, is also likely to be due to the strategy for measurement of photosynthesis in terms of which leaves are measured, at what point during the life cycle and what parameter of photosynthesis (light saturated rates are common). Several studies have demonstrated a clear link between crop yield and biomass, and photosynthetic rate. The dynamics of photosynthesis i.e. its response to environmental change, are now considered to be

critical when making the link between leaf photosynthesis and yield (See Murchie *et al*., 2009, Murchie *et al*., 2017, Kromdjik *et al*., 2016, Nehe *et al*., 2018, Hubbart *et al*., 2018).

The link between the photosynthesis and yield has been shown clearly with experiments using elevated concentrations of CO_2. An increase in the concentration of CO_2 [CO_2] gives rise to two major effects: 1) a rise in leaf photosynthesis and 2) a decrease in diffusion of water vapour via stomatal conductance (Long *et al*., 2006a). The elevated [CO_2] inhibits the oxygenase activity of Rubisco and thus reduces photorespiration. This promotes the carboxylation activity of Rubisco due to the freeing up of the binding site on the enzyme, which would in turn lead to an increase in yield. This is reflected in two studies conducted by Morgan *et al* (2005) and Dermody *et al* (2008) compared the yield of soybean under ambient and artificially elevated [CO_2]. Under ambient [CO_2] (380 ppm), yield was found to be 10.6 MJ m^{-2} whereas under the higher [CO_2] (550 ppm), yield increased to 12.2 MJ m^{-2}; a 15% increase in yield (Zhu *et al*., 2010). This is provided that other factors do not become limiting.

While more recent work has shown an increase in yield in plants grown in elevated CO_2 environments (Ainsworth, 2008), the link between direct improvements on photosynthesis, at both the genetic and whole-plant levels, productivity and crop yield has only been shown in a few studies in the field (Kromdjik *et al*, 2016).

1.5 **Plant responses to the environment**

Photosynthesis has often been studied and measured in controlled environments. It can be typically estimated by enclosing a part of the leaf in a chamber, where the exchange of CO_2 between the air outside the leaf and intercellular air spaces within the leaf is measured. Plant and crop science have depended heavily on mathematical models to predict the effect of physiological and environmental parameters on C3 photosynthesis. Existing models of photosynthesis (for review see

Farquhar & von Caemmerer, 1982; von Caemmerer 2000; von Caemmerer, Farquhar & Berry, 2009) have been helpful in predicting steady-state photosynthesis (CO_2 assimilation), taking into account light intensity, CO_2 and O_2 partial pressures as well as temperature (von Caemmerer, 2013).

In the field, photosynthesis is frequently limited by environmental factors and fluctuations. Stressful environments can cause extensive losses in production and yield in agricultural systems. Drought, salinity, high heat, strong sunlight and heavy metals are just a few abiotic stresses plants are routinely exposed to in nature, even when grown under optimal conditions. Being sessile organisms, plants are required to adapt and develop effective strategies that will allow them to avoid and tolerate the stressful environment around them (Takahashi and Shinozaki, 2019). Research work and studies on stress have often focused on a single stress condition, which is more often than not, unrepresentative of actual field conditions where plants could be subjected to a combination of stresses (Choudhury *et al*., 2017). In the tropics, rice plants often encounter fleeting periods of high light stress in conjunction with heat stress; while in drier climates, the combination of heat and drought stress is more common.

The responses of the plant to a combination of stresses are unique and it cannot be extrapolated from single stress studies (Mittler, 2006). In fact, the responses of plants simultaneously subjected to multiple stresses can sometimes be antagonistic and contradictory. For example, plants growing under drought and high heat conditions would not be able to cool down by opening stomata due to a need to conserve water, resulting in an increase in leaf temperature, as shown in tobacco plants and *Arabidopsis* (Rizhsky *et al*., 2002, 2004). Nutrient deficiency can further exacerbate the situation by preventing the synthesis and function of compounds necessary for acclimation. The period (stages of growth) of stress occurrence has to also be taken into account. With climate change

leading to more temperature extremes in many areas, stress arising in the early stages of growth in the field is becoming less uncommon.

1.5.1 Photosynthesis and the light environment

Light varies spatially and temporally in plant canopies. Incident solar radiation at the surface of the earth has a major effect on the diurnal and seasonal temperature variations (Wild *et al*., 2004) and governs the productivity of both terrestrial and aquatic plants by providing energy for the assimilation of carbon by plant canopies. The main driving variable in photosynthesis is incident PAR (photosynthetically active radiation) on the crop, and this is on average 1673 μmol m^{-2} s^{-1} at midday in the tropical regions (Sheehy and Mitchell, 2013). The capacity of photosynthesis to utilise sunlight is limited however, with rice photosynthesis found to generally saturate at irradiance levels only just above 1000 μmol m^{-2} s^{-1} despite many places in the rice growing regions receiving a mean average light intensity of higher than 1500 μmol m^{-2} s^{-1} (shown in Figure 1.5). The exchange of CO_2 is chiefly controlled by PAR and the efficiency at which the energy harvested is used for photosynthesis, or RUE (Murchie *et al*., 2009).

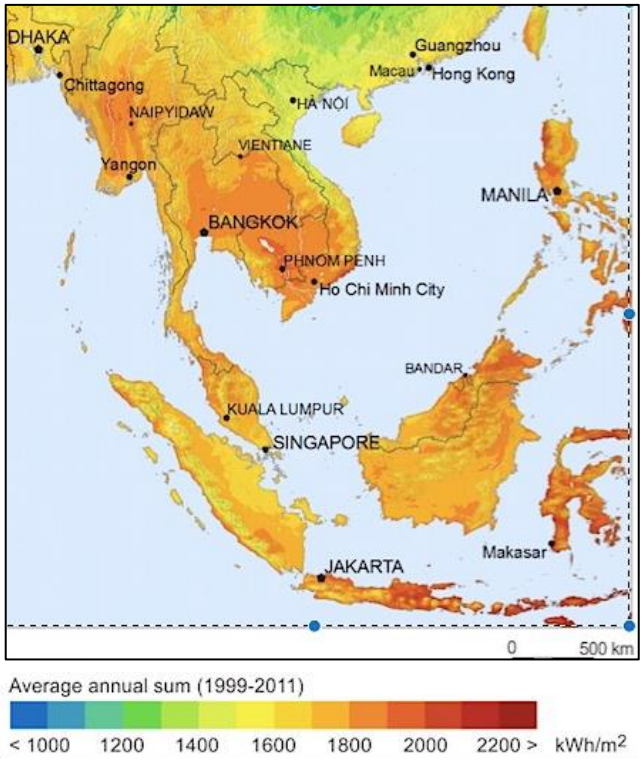


Figure 1.5: Mean average solar irradiation at the surface of the earth in South East Asia (Source: solarGIS, February 23, 2015).

Leaf photosynthesis is influenced by the intensity of light under which plants are grown. The relationship between light and photosynthesis has been widely studied in many different species of plants. A majority of these studies have shown that generally, plants growing under high irradiance show high rates of photosynthesis under elevated light intensities. Light levels also affect the morphology of whole-plant growth (Makino *et al*., 1997). Plants growing under lower intensities of light generally show increased plant height, with a smaller number of leaves from decreased tillering (Inada and Nishiyama, 1987; Makino *et al*., 1997). These plants generally have thinner and wider leaves, an adaptive strategy employed to capture more light at lower light levels.

Rice is primarily grown in the tropic and sub-tropic regions of the world. Prolonged exposure to high light intensities beyond saturation can result in a significant light-dependent decline in

quantum yield and subsequently a reduction in the photosynthetic capacity of the plant – a state known as photoinhibition. Although plants growing in marginal habitats would generally experience more substantial photosynthetic losses through photoinhibition, it is fairly common in crop plants growing under optimal conditions due to high and fluctuating light intensities (Murchie *et al*., 1999). At these fleeting points of excess light, the rate of photoinhibition of PSII balances the rate of repair (Davis and Hangarter, 2012). Under sustained high light conditions however, the rate of damage can exceed the rate of repair of PSII. This could have a severe impact on the assimilation rate of CO_2, resulting in a sustained and irreversible decline in photosynthesis. A substantial reduction in maximum photosynthetic capacity can be observed in some severe cases. The result of photoinhibition is a non-functional PSII, where the core protein, D1, has been damaged and disassembled (Kyle *et al*., 1984). D1 is the reaction centre-binding protein that is the most prone to light stress, as compared to other intrinsic and extrinsic protein subunits (Yamamoto *et al*., 2008). A new D1 protein has to be synthesized and co-translationally and post-translationally incorporated into the PSII core complex (Zhang *et al*., 2000) for PSII to regain functionality.

High light stress can induce modifications in plant morphology and eventually irreversible changes in the biochemical composition of the leaves and alter the plant's photosynthetic competence (Murchie *et al*., 1999). The inclusion of other abiotic and biotic stress factors will lower the light saturated capacity of photosynthesis of the plant and increase the amount of excess excitation energy in the pigment bed. To avoid and combat this, plants have evolved a range of protective mechanisms at both cellular and canopy levels that prevent over-excitation as well as the production of damaging oxygen radicals. These mechanisms include – 1) the avoidance of excess light absorption, by the repositioning of chloroplasts within the mesophyll cells and changing the angle of incidence; 2) photoacclimation, where the amount of photosynthetic machinery is regulated to match the

existing light intensity; 3) NPQ and; 4) alternative electron transport pathways (Zhou *et al*., 2007; Murchie *et al*., 2009; Murchie *et al*., 2015; Hubbart *et al*., 2018; Malnoë, 2018).

Chronic photoinhibition occurs under light intensities higher than the saturation point as well as under an amalgamation of environmental stresses, causing a decrease in both ΦPSII and Pmax and is associated with the damage and replacement of the D1 protein in the PSII reaction centre. This type of photoinhibition can persist for days to months. Photoinhibition is thought to be an energy control mechanism (Horton and Ruban, 2005) where excess energy dissipated in PSII restricts linear electron flow, avoiding more serious downstream oxidative damage to PSI (Keren and Krieger-Liszkay, 2011; Iseki *et al*., 2013).

1.5.2 Temperature

Temperature has a direct effect on the rate of growth and development. Within each plant species, there exists a specific range of temperatures in which the plant grows optimally as well as a maximum and a minimum (Hatfield and Prueger, 2015). The temperature at which cultivated plants are grown in is a challenge to maintain, especially with major fluctuations in the climate and weather patterns. It is difficult to control and hence raises the potential of dramatic changes in the growth patterns and productivity of cultivated plants in an agricultural setting. The rising unpredictability and probability of the occurrence of extreme temperature events have a dramatic effect on the productivity of plants, regardless of how short-lived these occurrences are (Challinor *et al*., 2005; Jagadish *et al*., 2007; Wassmann *et al*., 2009). For producers, consistency in crop yield is most important, and significant changes in temperature associated with climate change pose a threat to this stability.

Temperature stress is itself a complex phenomenon. It is a function of intensity, in the form of temperature degrees, duration and the rate of increase or decrease in temperature (Hall, 2001). Changes in growth temperature induce morphological responses and alternations in biomass allocation (Boese and Huner 1990; Equiza and Tognetti, 2002; Nagai and Makino, 2009). Such changes cause intrinsic differences in the reliance of the relative growth rate on temperature in different plant species. The response of plant growth to temperature is still not very well known, but there have been studies that attempt to explain how relative growth rate is temperature dependent by using growth parameters and indices such as specific leaf area, leaf area ratio, leaf weight ratio and net assimilation rate (Nagai and Makino, 2009). This is because there are many variations between species and subspecies, where the role of the different parameters on relative growth rate as a temperature response appear to differ.

High temperatures can increase the rate of reproductive development, and consequently reduces the time for fruiting or seeding. Generally, the rate of growth of a plant decreases as temperature increases, and halts after reaching the maximum permissible temperature. A few stages of the plants' phenology are more susceptible to changes in temperature. The viability of cereal pollen during the pollination stage, for example, decreases when temperatures exceed 35 °C. Viability is a function of moisture content, which is strongly reliant on vapour pressure deficit. As such, at higher temperatures, the viability of pollen decreases (Hatfield and Prueger, 2015). Sensitivity in other factors such as grain yield, seed harvest index and grain filling to higher temperatures (exceeding 33 °C) have been displayed in rice and other cereals such as sorghum and maize. At temperatures beyond 40 °C, viability reaches zero (Prasad *et al*., 2006a, b). Rice, particularly, has been shown that photosynthesis can function safely up to 40 °C (Zhu *et al*., 2018).

1.5.3 Nitrogen deficiency

Nutrients are essential for the growth of a plant. Research in mineral nutrition have shown that high crop yields depend heavily on fertilization; on nitrogen, phosphorus and potassium-based fertilization in particular. While plants can obtain these elements in their inorganic forms from the soil, ensuring dependable yields in an agricultural system requires the external application of these essential elements in the form of fertilisers.

Out of the macronutrients, N is required in the greatest amount. It is a constituent of numerous cell components; primarily nucleic acids and amino acids. Plants grown in soil with sufficient N would grow rapidly, with leaves of a healthy green colour. Ammonium is taken up by the roots and assimilated into amino acids in the roots, while nitrate is mainly assimilated in the shoots of the plants (Taiz

and Zeiger, 2010). Unlike most of other crops, rice uses mostly ammonium as a source of N. This is due to ammonium being the major form of N in waterlogged soils. Roots and shoots of plants are physiological sinks for the assimilation of inorganic nitrogen during the vegetative phase of growth (Hirel *et al*., 2007). Generally, after the onset of flowering, the remobilization of N occurs; previously sink structures now behave as sources of N by supplying amino acids to reproductive and storage organs such as seeds (Hirel *et al*., 2007; Pilbeam, 2015).

A large part of N in the rice plant is distributed to leaves throughout the lifecycle of the plant. Between 65 and 70% of N in the shoots of the plant is spent in the production of leaf blades for dry matter production through photosynthesis (Mae and Ohira, 1981). The amount of nitrogen affects leaf area index (LAI) as well as the amount of N per unit leaf area, which is known as the specific leaf N (SLN) (Mae, 1997). The photosynthetic activity per unit leaf area is largely affected by the amount of N in the leaf and could at times be the limiting factor in photosynthesis, due to allocation to the synthesis of Rubisco. Rubisco accounts for up to 35% of leaf N in higher plants (Evans, 1989; Kumar *et al*., 2002; Makino *et al*., 2003).

With the other yield components reaching their upper limit, rice is increasingly dependent on direct improvements in biomass production, which requires more nitrogen fertilization in the face of climate change (Peng *et al*., 2000; Murchie *et al*., 2009). Combined with better crop management and breeding, the production and application of N fertilisers in the last 60 years have resulted in a substantial increase in food production globally (Good *et al*., 2004; Xu *et al*., 2012). Following the trends in fertiliser usage, it is predicted that the use of nitrogenous fertilisers worldwide will reach approximately 240 million metric tonnes by 2050. Unfortunately for many farmers and producers, the economic cost of nitrogenous fertilisers has been on an increase and will continue to increase as resources dwindle. Large amounts of nitrogenous fertilisers are used

in developed countries to prevent fluctuating levels of N from affecting yield (Kant *et al*., 2011), but this comes with an environmental cost.

1.6 **Improving the mechanism of rice photosynthesis**

Further increases in harvest index may lead to a decrease in yield, as plants require a substantial number of aboveground components for growth and support. Increasing the yield potential would necessitate the increase in total biomass by improving photosynthesis (Evans, 2013).

1.6.1 Rubisco as a target of improvement

Rubisco (ribulose 1,5-bisphosphate carboxylase oxygenase) is the enzyme responsible for fixing CO_2 with RuBP in the Calvin-Benson cycle in C3 photosynthesis, producing glyceraldehyde-3-phosphate. In ambient concentrations however, Rubisco has two functions – oxygenation and carboxylation, where O_2 and CO_2 are both substrates competing for the same active site (Murchie *et al*., 2009). The process of oxygenation results in the formation of 2-phosphoglycolate (2-PG), which is subsequently metabolized in photorespiration at the cost of energy thereby reducing the efficiency of photosynthesis. Rubisco has a slow catalytic rate, and a large amount of the enzyme is required to maintain high rates of photosynthesis at ambient CO_2 (Galmés *et al*., 2019). This dual specificity of the enzyme has a serious impact on plant water use. This inefficiency explains why the enzyme is one of the most abundant protein in the leaves of plants – accounting for approximately 25% of leaf nitrogen and constitutes about 50% of the soluble protein in leaves (Parry *et al*., 2003).

The rate of carbon fixation is largely determined by the kinetic properties and function of Rubisco (Reynolds *et al*., 2012). The concentration and *in vivo* activity of Rubisco are observed to be a rate-limiting factor in carbon fixation, under saturating light conditions. It has been long recognized that C3 photosynthesis could potentially improve by controlling the activity of Rubisco through genetic modification. One theoretically feasible approach to increase the rate of carboxylation is by increasing the content Rubisco in the

chloroplast. This is particularly advantageous in saturating light and high temperatures, when the concentration of CO_2 is low. A higher amount of photosynthetic machinery should correspondingly increase the rate of light-saturated photosynthesis per unit leaf area (Murchie *et al*., 2009). This would require a significant 'top-up' of the enzyme, which would consequently mean investing in more nitrogen. On top of nitrogen being a limited and costly resource in agronomic systems (Parry *et al*., 2011), cereals have generally low nitrogen use efficiencies of approximately 33%. Without the input of nitrogen, the plant is forced to redistribute the internal nitrogen, causing a cascade of problems for CO_2 fixation. Suzuki *et al*., (2007) found in their study that rice with the sense rbcS did not show an increase in the photosynthetic rate even at lower CO_2 concentrations. The overproduction of Rubisco in rice may have led to lower N investment for other components, limiting photosynthesis. Nevertheless, more recent studies suggest that overexpression of Rubisco in transgenic *RBCS*-sense rice leads to higher grain yields through an increase in nitrogen use efficiency (NUE) when sufficient N is available (Yoon *et al.,* 2020).

Another strategy would be to enhance the specificity for CO_2 relative to O_2 (τ) of the Rubisco through genetic modification, via a higher catalytic rate, a higher affinity for CO_2 and/or lower affinity for O_2. It has been observed that the Rubisco forms with higher τ showed lower maximum catalytic rates of carboxylation per active site (Bainbridge *et al*., 1995). This inverse relationship also suggests that increased τ might only be achieved with at the expense of the maximum catalytic rate of Rubisco (Zhu *et al*., 2010). Zhu *et al*. (2004) found that the average τ found in C3 crops currently surpasses the optimal level for the present atmospheric [CO_2] of 400 ppm but would be optimal for approximately 220 ppm of CO_2, which coincides with the average 400,000 years ago.

1.6.2 Introducing the C4 pathway into C3 rice

Unlike C3 plants (Figure 1.6a), C4 plants have the advantage of concentrating CO_2 - allowing Rubisco to function in a CO_2-rich space (Figure 1.6b). This increase in carboxylation relative to oxygenation of Rubisco results in more CO_2 being fixed per photon of light absorbed by the plant. The C4 photosynthetic pathway was initially proposed in the early 1960s; through $^{14}CO_2$ labelling experiments in maize (*Zea mays*) and sugarcane (*Saccharum officinarum*) that discovered the presence of malate and Asp, both four-carbon (4C) compounds, early on in the photosynthetic pathway (Kortachak *et al*., 1965; Langdale 2011). The model was finally elucidated in 1966 by Hatch and Slack (1966) by examining the radioactive products formed from $^{14}CO_2$ labelling in sugarcane, where they found CO_2 to be initially fixed into a 4-carbon compound. The C4 pathway involves the spatial separation of atmospheric CO_2 fixation. It is subdivided between two distinct cell types – the bundle sheath and the mesophyll cells, which is known as the Kranz anatomy. CO_2 is fixed in the mesophyll cells by phosphoenol pyruvate (PEP) to form malate. This reaction is catalysed by PEP-carboxylase. Malate is then pumped across the mesophyll cell membrane through interconnecting plasmodesmata (Danila *et al*., 2016) into the bundle sheath cell at the expense of ATP, where it is then separated into CO_2 and a 3C compound. CO_2 enters the Calvin Cycle in the bundle sheath cell. The concentration of CO_2 in the bundle sheath cell is 10-20 times the concentration in the mesophyll cells in C3 plants. One of the advantages of this efficient photosynthetic pathway is the reduction in photorespiration. Oxygen cannot compete effectively for Rubisco due to the high availability of CO_2 as a substrate for the enzyme.

The development of C4 rice should be feasible by engineering C4 genes into rice and replicating strong selection pressure for C4 traits. Historically, evolution of C3 to C4 photosynthesis has occurred in at least 60 plant taxa (Sage *et al*., 2011; Sage *et al*., 2012; Christin and Osborne, 2013). A combination of vital information is needed to

engineer a complex biochemical pathway into C3 plants. C4 regulatory genes are first identified, and the combination of identified genes with screens of mutagenized C4 *Sorghum bicolor* and *Setaria virids* with activation-tagged rice will eventually reveal candidate genes for transgenic rice. The ability of C4 plants to carry out net photosynthesis at very low carbon dioxide concentrations allows for the testing of the activation of the C4 pathway in transgenic rice. This gain of function test would allow us to screen for successful integration of the C4 pathway in mutants.

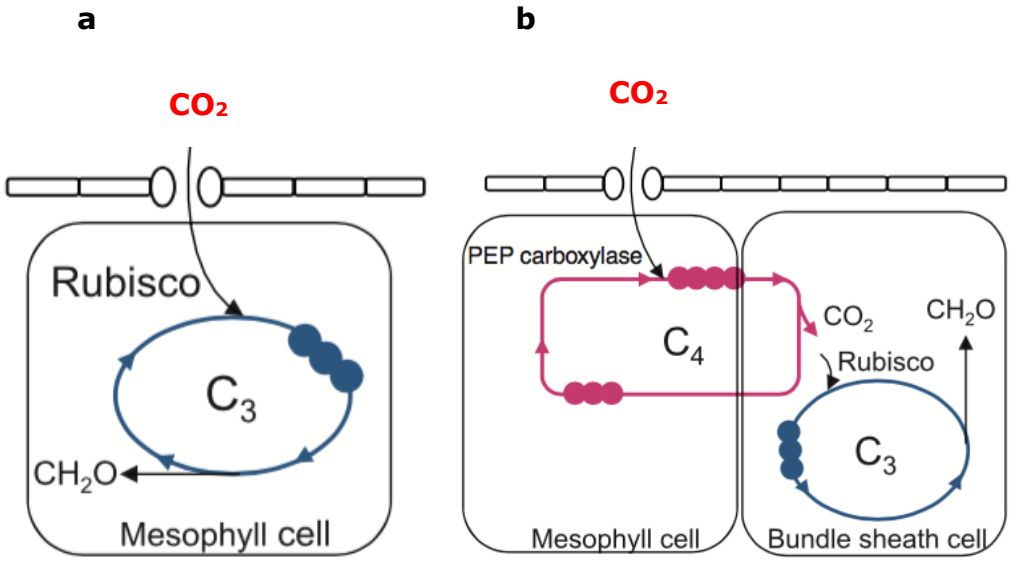


Figure 1.6: Schematic of the (**a**) C3 photosynthetic pathway and (**b**) C4 photosynthetic pathway. In the C3 photosynthetic pathway, CO_2 is fixed by Rubisco in a single cell whereas two cells are required in C4 photosynthesis, where CO_2 is initially fixed in the mesophyll cell by PEP-C and then donated to the bundle sheath cell to Rubisco. (Source: Adapted from von Caemmerer *et al*., (2012).

1.6.3 Reducing losses from photorespiration

Under higher temperatures, the affinity of Rubisco to carboxylation decreases, and an increasing amount of carbohydrate formed from C3 photosynthesis is lost to photorespiration. It has been established that photorespiration causes a 20% loss of net-photosynthesis in C3 plants and can be even higher in warmer and dryer environments (Cegelski and Schaefer 2006; Liu *et al*., 2013). Photorespiration is of particular interest in tropical climate due to the higher temperatures. The strategy of most interest would be engineering the C4 photosynthetic pathway into C3 plants. In terms of εc, the C4 pathway performs better under current [CO_2] conditions as compared to the C3 pathway. This is due to the CO_2 concentrating mechanisms present that concentrates CO_2 around Rubisco (Hatch 1987; von Caemmerer 2003), but at the same time would require more energy to operate, typically 2 ATP molecules per CO_2 molecule assimilated. Nevertheless, this added energy required for the fixation of CO_2 in the C4 photosynthesis is still lower than the amount of light energy diverted to photorespiration in C3 photosynthesis when temperatures exceed 25°C.

Blocking the photorespiratory metabolism downstream of Rubisco via down regulation or deletion of an enzyme in the pathway would result in the carbon entering a dead-end metabolic pathway (Long *et al*., 2006b; Zhu *et al*., 2010). It has been observed that mutants without any one of the enzymes involved in the photorespiratory pathway would not survive unless grown under very high [CO_2] or low O_2 concentration to prevent RuBP oxygenation.

1.6.4 Engineering optimum plant canopies

Plant architecture in cereal crops has contributed significantly to the success of the Green Revolution in the last century. This has been associated with the improvements in the harvest index and the increase in seed set number (Zhu *et al*., 2010). One of the major breakthroughs from the Green Revolution was the selection and breeding of elite cultivars with more erect canopies, allowing a better penetration of light to lower levels of the canopy. The possibilities of improving cumulative radiation interception in leaves over the crop cycle are growing. Such possibilities include promoting fast early-leaf area growth to more rapidly reach highest radiation interception, and by extending the duration of green leaf area as the crop matures. Extended leaf area duration has been implicated as an important component of yield potential gains under high-input conditions in the UK (Shearman *et al*., 2005).

In terms of leaf angle, a canopy with a gradual decreased leaf angle can increase the daily uptake of carbon as much as 40% on a sunny day mid-latitude, as compared to a canopy with horizontal leaves (Long *et al*., 2006b; Mantilla-Perez and Fernandez, 2017). An improvement of εc over the duration of the crop season by 20% by manipulating canopy architecture could result from the avoidance of severe light saturation at the top regions of the crop canopy and as such, severe light limitation within the canopy. It is key, however, to consider not just the leaf in isolation, but to consider the entire crop and the resources available to it (Reynolds *et al*, 2009; Parry *et al*., 2011).

Engineering the optimum canopy architecture to avoid light saturation for maximum plant productivity in the changing climate is becoming increasingly important (Long *et al*., 2006b; Zhu *et al*., 2008; Murchie and Niyogi, 2011)This challenging task has for a long time, involved the estimation of canopy photosynthesis of crops in the field. Recently, canopy photosynthesis models have been

developed to estimate the assimilation rate instead. These models exist on a variety of scales, under three particular categories – the big-leaf model, the sunlit-shaded model as well as the multi-layer model. The big-leaf model used the amount of nitrogen in the leaves of the plant as a proxy to describe the light environment inside the canopy (Running and Coughlan, 1988; Llyod *et al*., 1995; Song *et al*., 2013). This assumption of a proportional relationship between the capacity for photosynthesis of chloroplasts and radiation capture fails to take into account the heterogeneity of the light environment within the canopy both spatially and temporally.

The multi-layer models utilise the Beer-Lambert Law, which predicts that the capture of light reduces exponentially down the canopy (Monsi and Saeki, 1953; Monsi and Saeki, 2005) and that the light travelling down the canopy can be divided into two distinct categories – diffuse and direct light. While these models are the most accurate amongst the three, one of the major disadvantages of it is being time consuming and often complex. The sunlit-shade model works on a similar level as the multi-layer model, except that is simplifies the canopy into either sunlit or shaded portions (Sinclair *et al*., 1976; Zhu *et al*., 2004; Ort *et al*., 2011; Song *et al*., 2013). The reproducibility of the model relies on the ability to identify the proportion of the canopy that is sunlit and shaded in terms of area, as well as the amount of light in these portions.

1.6.5 Photoprotection as an avenue to improve rice yield

Incident solar radiation at the surface of the planet controls the macroclimate, weather, diurnal and temperature variations (Wild *et al*., 2004; Kambezidis *et al*., 2012) and is important for all life on earth. A critical resource in yield formation is the amount of solar radiation available to the plant, and how efficiently it is used in the production of plant biomass (Murchie *et al*., 2009).

The intensity of light and spectral quality varies greatly at the surface of the earth, both spatially and temporally. The capture of solar radiation at the leaf surface is dependent on the capacity of photosynthesis to use sunlight and is very much species and genotype dependent. Light fluctuates in various environments and is affected by the seasons and the position of the earth at different times of the year. As such, plants are exposed to different light intensities, experiencing a sudden rise or fall in light levels within a short period of time and as such rarely photosynthesising at maximum capacity (Sheehy and Mitchell, 2013; Murchie *et al*., 2015; Hubbart *et al*., 2018). To cope with these sudden changes in light intensities, plant have evolved various forms of 'photoprotective' mechanisms that prevent over-excitation that causes the formation of damaging oxygen radicals and ultimately irreversible photoinhibition.

It is generally accepted that the principle limitation to leaf photosynthesis at high light intensities is the concentration availability of carbon dioxide for the primary reactions of photosynthesis, and at lower photon flux densities (approximately at 30% full sunlight), photosynthesis becomes light limited (Long *et al*., 2006b). Due to the multi-layered architecture of most plant canopies, radiation decreases exponentially as it penetrates the layers of leaves. Even at high light, photosynthesis at lower layers of the canopy is light limited and thus any decrease in solar radiation could be expected to reduce productivity.

It is essential to first examine the relationship between light and photosynthesis, using a light response curve. As light intensity increases in the initial part of the curve, the compensation point is reached. This is when the uptake of CO_2 is equal to the rate of CO_2 evolved. As light intensity increased beyond the compensation point, the rate of photosynthesis (assimilation rate of CO_2) increases proportionally until it saturates at Pmax as shown in Figure 1.7. The initial linear portion of the curve (dotted line) denotes the efficiency (maximum quantum yield) of photosynthetic CO_2 uptake, or oxygen evolution. As light intensity increases beyond a certain photo flux density, the rate of CO_2 assimilation plateaus. In this region of the curve, photosynthesis is light saturated. At periods of sustained high light intensities (past the point of light saturation), photoinhibition and photooxidative responses could occur.

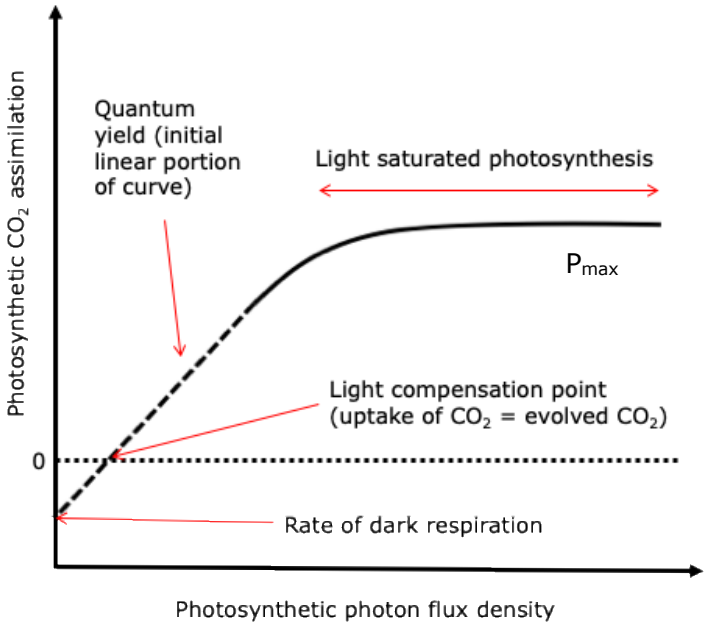


Figure 1.7: Schematic of the rate of photosynthesis under increasing photosynthetic photon flux densities. Quantum yield of PSII, light compensation point, and dark respiration rate are shown. P_{max} is also indicated, and this is where photosynthesis saturates despite increasing light levels.

As mentioned above, photoinhibition denotes the inactivation of the PSII photosynthetic apparatus. Photoinhibition is a state describing the light-dependent decline in quantum yield and if high light is maintained a reduction in the photosynthetic capacity of photosynthetic organisms. Although plants growing in marginal and stressful habitats would generally experience more substantial photosynthetic losses through photoinhibition, it is also fairly common in crop plants growing under optimal conditions due to high and fluctuating light intensities (Murchie *et al*., 1999).

Dynamic photoprotection in the field exists under moderate excess and fluctuating light intensities and can form and relax within minutes. In this case the excess energy in PSII can be quenched by pH-dependent quenching (qE) which is regulated by the protein PsbS (Horton and Ruban, 2005; Belgio *et al*., 2014) and the xanthophyll cycle which determines the kinetic capacity for qE as well facilitates the dissipation of excess energy through a de-epoxidation sequence of oxygenated carotenoids (Demmig-Adams, 1990; Demmig-Adams and Adams III, 1992; Horton *et al*., 1996; Hubbart *et al*., 2018). This has the same effect as photoinhibition i.e. it causes a brief reduction in photosynthesis quantum yield, but it is not associated with long term damage to PSII and in fact will help to reduce the occurrence of photoinhibition.

Photosynthesis in rice is found to generally saturate at irradiance levels only just above 1000 μmol m^{-2} s^{-1} (Murchie *et al*., 1999; Wang *et al*., 2005; Murchie *et al*., 2015). It is important to realise that chronic photoinhibition in tropical rice (exemplified by a slow but reversible loss of PSII function) can exist even under optimal conditions in the field, as displayed by a significant decline in the quantum yield of carbon fixation at midday. The plants may have been initially experiencing dynamic photoprotection only to shift to a more chronic form under increasing exposure to higher solar irradiances and/or other abiotic stresses. This midday depression has been estimated to result in an estimated loss of 30% of

photosynthesis and is suggested to arise as a result of decreased stomatal conductance from high leaf temperatures, an accumulation of carbohydrates and a decrease in the efficiency of PSII (ΦPSII) (Murchie *et al*., 1999). However, it has recently been reported that the midday depression in photosynthesis is mostly associated with the reversible inactivation of PSII as found in rice (Horton and Murchie, 2000; Wang *et al*., 2005), and soybean (Huang *et al*., 2006).

Despite being a rain-fed and irrigated crop, rice (and its yield) can be significantly affected by periodic drought in lowland plantations in South and Southeast Asia (Redfern *et al*., 2012), caused by climate-related events such as El Niños. Drought, combined with high light conditions, enhances the production of ROS by the photosynthetic apparatus of the rice leaf. To mitigate photoinhibition, electron dissipation processes such as photorespiration and the water-water cycle are up-regulated. Rice cultivars exhibit varying degrees of susceptibility to photoinhibition and thermal dissipation – a result of a long history of evolution across different geological regions (Demao and Xia, 2001). Rice genotypes that are highly productive have been shown to exhibit less photoinhibition and more tolerance under stressed conditions. The Japanese cultivar Akenohoshi, for example, develops more symmetrical (erect) leaves under low N than under sufficient N (Kumagai *et al*., 2014).

1.7 **Project aims and objectives**

Responsiveness and adaptability to the changing environment, through improved photosynthetic efficiency, are key traits that have become major breeding targets (Parry *et al*., 2011; Foulkes *et al*., 2011; Furbank *et al*., 2019). While a lot of work has been carried out surrounding photosynthesis involving a number of model rice varieties, a very limited number of physiological studies on Malaysian rice cultivars have been done to properly discern plant performance of these varieties in suboptimal conditions. As the environmental conditions are constantly changing, rice productivity (and the accompanying economic impact) (Vaghefi *et al*., 2011) is continually threatened and the ability to adapt to stressful environments would be highly beneficial. This study focuses on nitrogen primarily, as the efficient use and application of nitrogen to agricultural soils remains a challenge, particularly in suboptimal soil conditions (Choudhury and Kennedy, 2005). Increasing rice productivity in the changing climate (Masud *et al*., 2014) poses a wider and pertinent problem – can we increase yields to meet the increasing human dietary demands sustainably, and if so, how? Currently, it appears that an increase in productivity will be largely depended on at least maintaining, if not increasing the current levels of N fertiliser application to agricultural soils (Gilland, 2006; Sylvester-Bradley and Kindred, 2009).

The objectives of the thesis are to:

1. Investigate the behaviour of Malaysian rice cultivars in different nitrogen conditions by using in depth knowledge on plant physiology as well as model plant growth using new imaging techniques.
2. Investigate the role of canopy architecture at different nitrogen treatments in Malaysian cultivars.

The data and information gained from this project could then be used in line with breeding programs to create new and more resilient rice cultivars in the changing climate. Chapter 2 studies the effects of nitrogen deficiency in the early physiological development of Malaysian rice plants in a controlled environment. In Chapter 3, the effects of different nitrogen treatments on canopy architecture, gas exchange and carbon gain are investigated using a novel 3-dimensional canopy reconstruction technique coupled with ray tracing. Finally, Chapter 4 examines the changes in canopy architecture and gas exchange in field-grown Malaysian rice under reduced nitrogen fertilization.

Each chapter has been written as individual manuscripts to be submitted to scientific journals. The final chapter, Chapter 5, ties the three working chapters together via a general discussion.

Chapter 2:
The effect of nitrogen deficiency on leaf extension rates and photosynthesis in rice varieties in a controlled environment

Chapter 2

This chapter provides an analysis of key morphological and photosynthetic parameters in rice under nutrient-deficient (suboptimal) conditions in a controlled environment. The aims are firstly to test the hypothesis that low to deficient levels of nitrogen do not alter the rate of appearance of leaves (thermal time, phyllochron) secondly to confirm the effect of controlled nitrogen deficiency on photosynthesis and growth in key Malaysian cultivars and lastly to provide a standard baseline under controlled conditions for the remaining chapters that are based in glasshouses and the field.

2.1 Introduction

2.1.1 Whole plant morphology

Leaves in higher plants are the primary location of photosynthesis. In monocotyledons (cereals and grasses), the leaves are generally long and narrow. Along the main stem are a series of nodes and internodes arranged in an alternating order. A node is a point on the main stem that bears a leaf, which corresponds to the joint between sections of the stem while the section between the nodes is called the internode (Moldenhauer *et al*., 2001; Moldenhauer *et al*., 2003). In some types of rice, such as deep-water rice, internodes are able to elongate in deep water environments to ensure that the photosynthetic parts of the plant remain above the surface of the water.

The alternating presence of nodes gives rise to the alternating emergence of leaves; a new leaf emerges above a fully elongated leaf from the node on the opposite side of the main stem (Figure 2.1). In the figure, n represents the older leaf and n+1 represents the subsequent leaf after n. The leaf blade is connected to the main stem of the plant via the leaf sheath, which covers the internode. The base of the leaf blade is a triangular membrane structure called the ligule,

and directly below the ligule are small ear-like hinges called auricles. Rice plants have a ligule at every internode. The vegetative stage of growth ends when the uppermost leaf on the main stem, the flag leaf, fully extends. The flag leaf is generally the most photosynthetically active leaf of all the leaves on the main stem (Hudson and Jeffree, 2001).

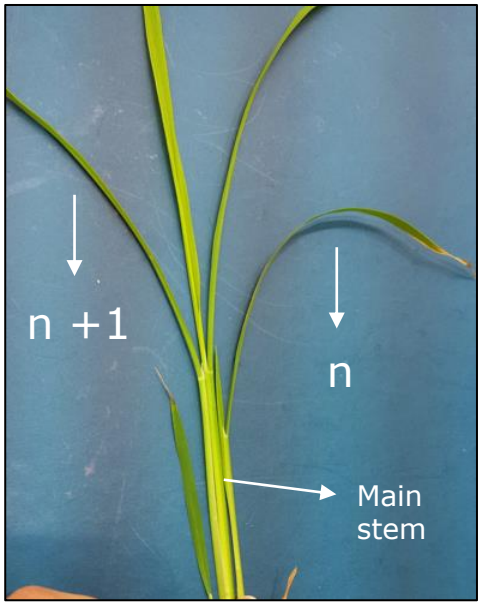


Figure 2.1: Rice leaves grow in an alternating fashion from the main stem. n represents the leaf number, and n+1 represents the subsequent leaf, which is growing on the opposite side.

Right above the flag leaf is the panicle, which comprises the reproductive organs of the rice plant. In some rice cultivars, the panicles can drop below the exposed part of the flag leaf, especially after grain filling. The branches on the panicle bear spikelets, which eventually fill up and develop into grains. Each spikelet consists of the reproductive parts contained by the lemma and palea. The rice flower is made up of a pistil (containing the stigma, style and ovary) and six stamens (made up of six anthers on slender filaments). During the process of reproduction, pollen drop from the stamens

(male part) onto the stigma (female part) and bury into the ovary, where fertilization occurs with the ovule. The fertilized ovule (embryo) grows and ripens, while the endosperm (starchy part of the grain that consists of the materials needed to germinate to produce a new rice plant. The endosperm is the part of the rice grain that is edible (Moldenhauer *et al*., 2003).

2.1.2 Leaf anatomy

Figure 2.2 shows a vertical cross-section of the rice leaf. Highlighted are the mesophyll cells, minor and major veins as well as bulliform cells. In rice leaves, the mesophyll cells are normally lobed (Ouyang *et al*., 2017), but in a monocotyledonous plant like rice, there is no distinction between the palisade and spongy mesophyll unlike dicotyledons (Kinsman and Pyke, 1998; Sakaguchi and Fukuda, 2008; Sage and Sage, 2009). Between the mesophyll structure of cells (mesophyll layer) within the leaf are intercellular air spaces, which are important for the diffusion of gases and water internally (Smilie *et al*., 2012). These cells have been found to be smaller than other species of crops (Burundukova *et al*., 2003).

Pore-like structures (stomata) on the leaf surface manage the exchange of gases and water from the external environment. These organs are essential in regulating gas exchange including photosynthesis, water use efficiency and leaf temperature and can affect photosynthesis under stress (Farquhar and Sharkey, 1982; Jones, 1998). Bulliform cells are a group of parenchyma motor cells on the adaxial (top) surface of the leaf that control the movement of the rice blade. During water loss in drought conditions and high light conditions, the bulliform cells enlarge which in turn cause the leaf to roll and fold. Moderate leaf rolling helps prevent excessive water loss and improve photosynthetic efficiency (Li *et al*., 2016). Extended periods of leaf rolling under extreme conditions, however, can significantly reduce crop yield (Turner *et al*., 1986; Nguyen *et al*.,

1997). The veins of the leaf are the sites of vascular bundles and they are arranged parallel to one another along the leaf blade. Vascular bundles contain an arrangement of xylem, an extensive vessel that transports water and minerals, as well as the phloem, which is responsible for the transport of sugars (Ueno *et al*., 2006; Taiz and Zeiger, 2010). Surrounding the vascular bundle is a group of bundle sheath cells, which serve as temporary storage vessels and facilitate the movement of transported molecules (sugars, water and minerals) between the vascular bundle to the necessary parts of the leaf (Hopkins, 1999; Taiz and Zeiger, 2010).

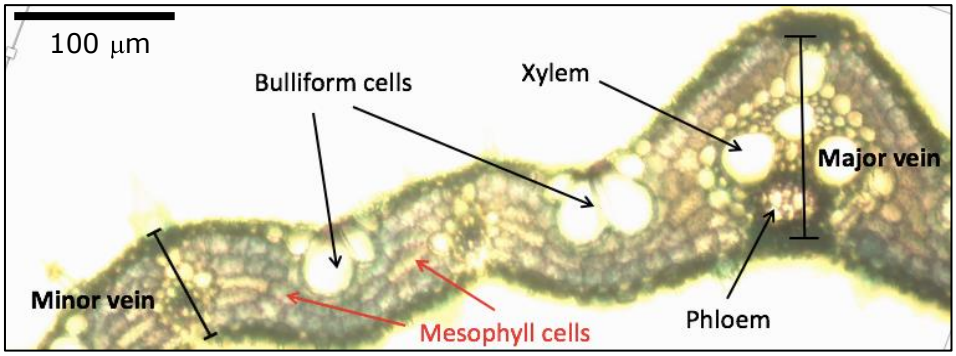


Figure 2.2: A transverse section of the rice leaf (shown is the International Rice Research institute variety, IR64) Labelled are the major and minor veins (where the vascular bundles are located), the mesophyll (site of gas exchange) and bulliform cells (controls leaf rolling). Section was hand-cut and cleared using chloral hydrate to remove pigment for microscopy. (Source: own material)

2.1.3 Aims and objectives

Understanding the effect of abiotic stress on photosynthesis is vital in identifying ways to improve plant productivity and subsequently yield. The primary objective of the work described in this chapter was to investigate the effect of nitrogen deficiency on photosynthesis and development in the vegetative phase in model rice varieties in controlled environments (see above). The results from this chapter will support the work in later chapters. Two growth room studies were conducted to investigate varietal differences in stress response and establishing baseline physiology measurements. The first experiment was carried out using a model lowland indica cultivar, IR64 and an upland African variety, Moroberekan. In the second trial, IR64 and two Malaysian rice varieties, MR219 and MR253, were used. The experimental design and growth conditions were similar for both trials with slight differences in the methodology of analysis. The second trial included more in-depth physiology and biochemistry measurements. Any differences in methodology will be highlighted.

2.2 **Methods and materials**

Experiments were conducted in a dedicated tropical rice growth room at the Sutton Bonington campus at The University of Nottingham, UK.

2.2.1 Experimental set-up

Growth conditions

The growth room was environmentally controlled and maintained at 30/25°C (day/night) (average day temperature 28.3°C ±0.760), 50-60% relative humidity with a 12h photoperiod (08:00 to 20:00 h). For the duration of these growth room-based experiments, Metal halide lamps (400 Watts) were used as the light source. Light intensity at plant height was approximately 500 μmol m^{-2} s^{-1}.

Plant seeds and germination

The first experiment was conducted using IR64, a Philippine indica rice cultivar from IRRI (International Rice Research Institute) and the African variety, Moroberekan (Khush, 2005). IR64 is a medium-stature high yield plant, and over the last 3 decades it has been one of the most widely grown rice varieties in the world. Moroberekan is a tropical japonica rice variety from Guinea, that has a long stature and is deeply rooted. This variety is usually used in regions prone to drought.

In the second experiment, Malaysian rice varieties MR219 and MR253 were used. These rice seeds were from MARDI (Malaysian Agricultural Research and Development Institute) in Penang, Malaysia as well as University Putra Malaysia (UPM) in Serdang, Malaysia. Philippine cultivar IR64 (IRRI) was also used as a model variety for comparison. The Malaysian and Philippine rice varieties were imported and treated with an anti-fungal dressing before arriving in Nottingham, UK.

To remove any residue from treatment or storage, seeds were rinsed in distilled water. For some slightly infected seeds, mild detergent was used for rinsing. For germination, seeds were placed in round Petri dishes on damp filter paper and sealed using paraffin film to retain moisture surrounding the seeds as well as to avoid fungal contamination.

Plant nutrition

Plant nutrition were exactly the same in both growth room trials. When the seedling hypocotyl was around 2-3 cm (Figure 2.4a), the seedlings were first transferred to a 20-litre rectangular light proof plastic 'bucket' (dimensions: 30cmx20cmx20cm) containing hydroponic solution (full nutrient complement, i.e. 100% N). The full hydroponic medium, adapted from Makino *et al*., (1985) contained: 1.4 mM NH_4NO_3, 0.6 mM $NaH_2PO_4.H_2O$, 0.5 mM K_2SO_4, 0.8 mM $MgSO_4$, 0.2 mM $CaCl_2$, 0.009 mM $MnCl_2.4H_2O$, 0.001 mM $(NH_4)_6Mo_7O_{24}.4H_2O$, 0.037 mM H_3BO_3, 0.003 mM $CuSO_4.5H_2O$, 0.000138 mM NH_4VO_3, 0.00075 mM $ZnSO_4.7H_2O$, 0.07 mM Fe-EDTA. The pH was adjusted to around 5.5 with 3 M HCl. This recipe is comparable to the ratio of N:P:K applied in Chapter 4, where the ratio of N:P:K is 7:3:3. In this bucket, every seedling was suspended in a hollow 1.5 millilitre micro-centrifuge tube on the surface of the nutrient solution (held by a polystyrene rack). This support allowed the roots of the seedlings to establish. The full method can be found in Murchie *et al*., (2005).

At the emergence of leaf 3 or at the establishment of a substantial root system, the young plants were then moved into three separate nutrient solutions with 3 concentrations of N – 100% of the NH_4NO_3 component (at 1.4 mM NH_4NO_3), 50% of the NH_4NO_3 component (at 0.7 mM NH_4NO_3) and 25% of the NH_4NO_3 component (at 0.35 mM NH_4NO_3). The buckets (dimensions as above) were watered daily as necessary with tap water. For the duration of the experiment, there was no observable nutrient deficiency symptoms other than the experimented nitrogen deficiency. The containers were

not given altered nutrients to avoid variation in nutrient application according to different rates of uptake. The plants were held in place on the buckets by lightproof plastic boards, as shown in Figure 2.4b. Holes of 3 cm in diameter were drilled into the plastic boards, and the plants were inserted through the holes and held in place with sponge. This allowed the roots to be completely immersed in nutrient solution. The containers were topped up with water when needed. Measurements were taken up till leaf 9, when the rice plants were subsequently harvested. The growth room was kept pest and disease free as much as possible by the use of biological controls and by keeping human movement in and out of the room to a minimum.

Figure 2.3 is the experimental design for both growth room trials, where each rectangle represents a container with 10 plants in a randomized complete block design.

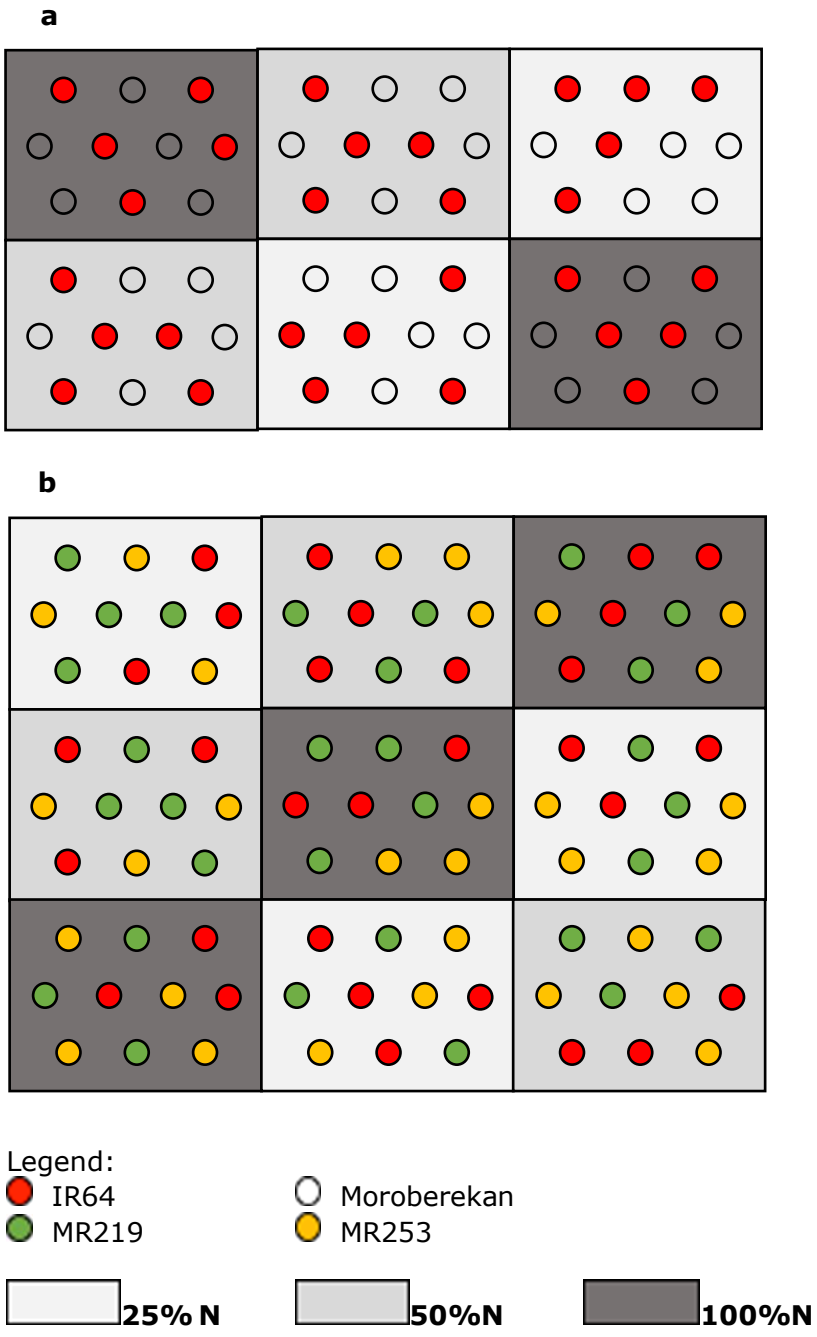


Figure 2.3: Randomized complete block design within a container with split plot design between containers. (**a**) First growth room trial, with IR64 and Moroberekan. (**b**) Second growth room trial, with IR64, MR219 and MR253.

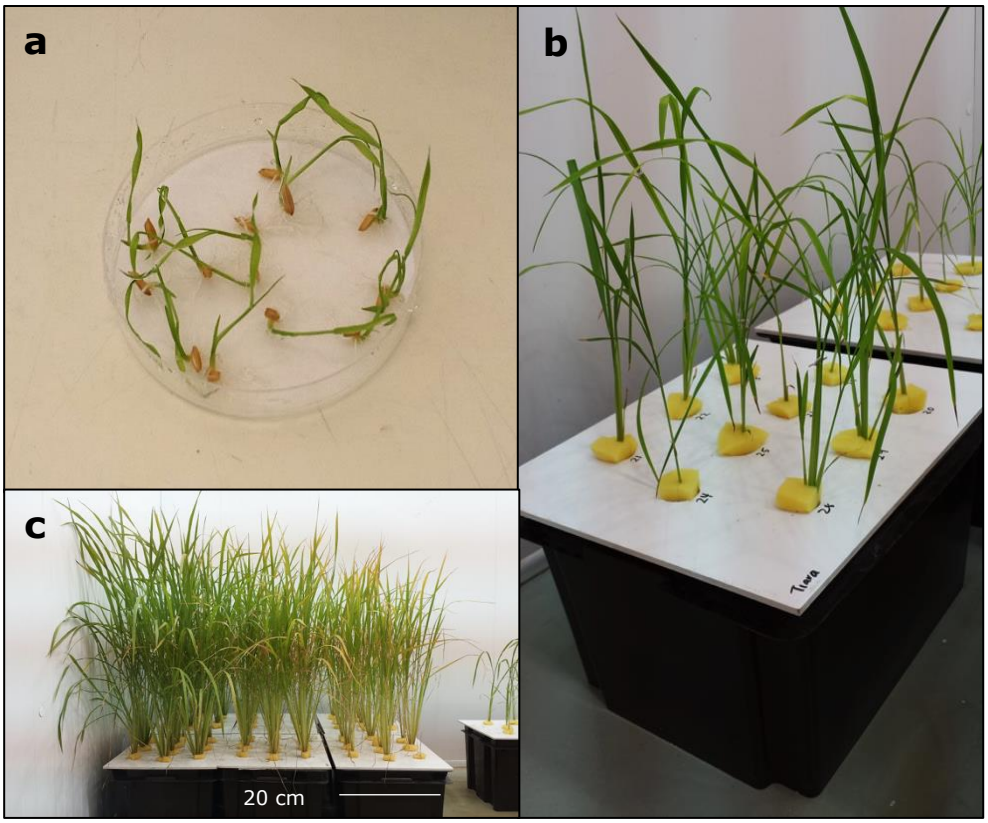


Figure 2.4: (**a**) Seedlings germinated in a Petri dish, (**b**) young plants in a bucket with hydroponic solution and (**c**) (from left to right) plants receiving 100% N, 50% N and 25% N treatments.

2.2.2 Plant physiology measurements

In both trials, photosynthetic light response and assimilation of CO_2 in increasing CO_2 concentrations via an infrared gas analyser (IRGA), and chlorophyll content (handheld Minolta SPAD device), were measured.

Leaf lengths and development

Leaf lengths were measured daily in the second trial. This was done from the emergence of leaf 6, between 10:00 and 15:00 hours. Using a ruler, maximum leaf length was measured from the ligule to the tip of the emerging leaf until full extension was reached. Full extension was achieved when elongation was less than 0.5 cm daily. Leaf extension rates were measured from leaf 6 until the complete elongation of leaf 9 for the purpose of this study. Maximum leaf lengths were obtained from curve-fitting leaf extension data. Primary tillers were counted at the end of the elongation of leaf 9. Number of leaves (minus the leaves on the main stem) were also recorded until harvest. At harvest, whole plant leaf area was measured using the benchtop leaf area meter LI-3100C (Lincoln, Nebraska). There was a total of five replicates per variety per treatment.

Stomatal density

Stomatal number was obtained using leaf impressions of both the adaxial and abaxial surfaces on the widest part of leaf 9 in the second growth room trial (Weyers and Johansen, 1985; Hubbart *et al*., 2013). Leaf surface impressions were made using Coltène® PRESIDENT Plus silicone-based dental putty (Coltène Whaledent, Switzerland). The putty had two components; both were mixed and applied using a teaspoon to the adaxial and abaxial surfaces of the leaf. The putty hardened (approximately 8 to 10 minutes) and was peeled off and stored in a dry place for extraction at a later date.

To extract the layer for view under the microscope, clear nail varnish (Sally Hansen, USA) was applied to the hardened putty and then later peeled off and mounted on microscope glass slides. A 20x-magnification confocal light microscope (Nikon, UK) was used to view the slides and images of two fields of view were captured for each plant under each treatment using an attached digital camera (Leica Microsystems, Germany). The number of stomata on adaxial (top) and abaxial (bottom) leaf 9 surfaces was counted per field of view

(Figure 2.5) with an area of 520 by 389 microns. A total of 6 images were taken per variety per treatment.

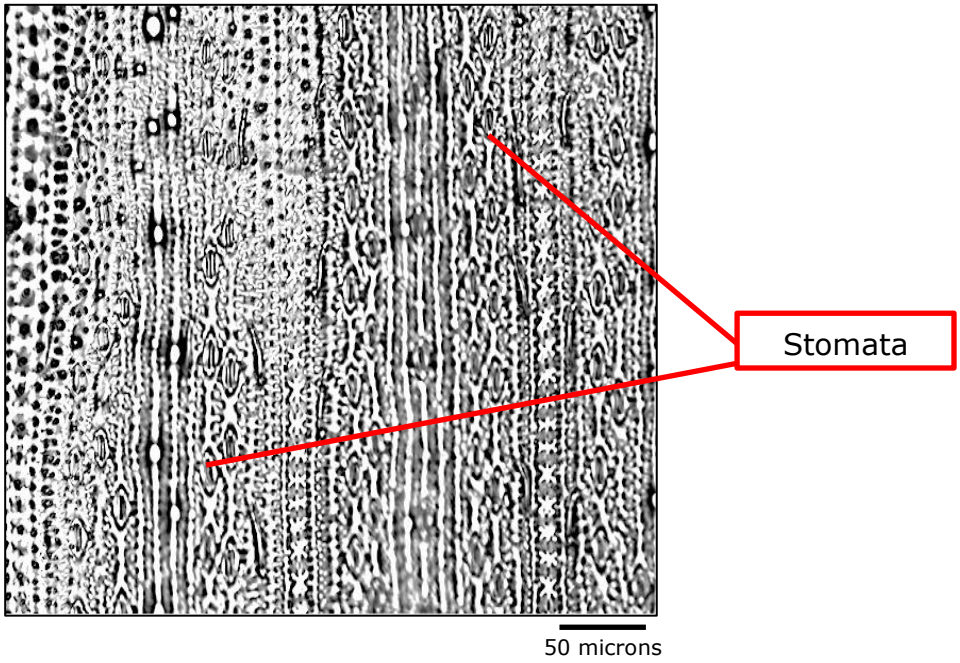


Figure 2.5: A 40x magnification image of abaxial leaf surface of rice variety MR219 under the control treatment, with the red lines indicating to stomata.

Leaf thickness and morphology

Rice leaves were hand cut using a sharp razor blade to produce a traverse cross-section of the widest part of the leaf. As hand cut cross-sections need to as thin as possible for clear view under microscope, the razor blades were frequently replaced. The samples were the placed on microscope glass slides and a few drops of distilled water added to prevent the leaf samples from rolling (Hubbart *et al*., (2013).

Leaf thickness can be measured via microscope without clearing and subsequent staining (Hubbart *et al*., 2013) but for a more detailed leaf structure, samples here were cleared of pigments (Smillie *et al*., 2012). To remove the pigment present in the sample, a solution of 85% lactic acid that had been saturated with chloral

hydrate was added to samples on the glass slides. Slides were placed in Petri dishes and covered and subsequently placed in a water bath and heated at 70°C for at least 45 minutes. This was performed in a fume hood so the fumes from the chloral hydrate could dissipate. When the pigments in the leaf appear to be have been cleared, the slides were removed from the water bath. The remaining chloral hydrate on the slides was washed off with distilled water using a plastic pipette. This was done a few times to make sure all the clearing solution was removed thoroughly.

Immediately after the wash, the samples were stained for 15 seconds using 1% toluidine blue in 1% sodium tetraborate ($Na_2B_4O_7 \cdot 10H_2O$) and the leftover solution washed off with distilled water. A glass slip was placed on each sample slide and view under a 20x magnification confocal light microscope (Nikon, UK) and images of sections were taken using an attached digital camera (Leica Microsystems, Germany). Images were stored in a hard drive and analysed using the software Image J.

Chlorophyll content

Leaf greenness was measured on leaf 9 in both trials, after complete elongation, using the SPAD (Soil Plant Analysis Development) 502 Chlorophyll Meter (Minolta, Spectrum Technologies). This non-invasive and non-destructive technique allows for the in-situ instant estimation of leaf N content (a proxy) by its close association and correlation with leaf chlorophyll absorbance at specific wavelengths.

2.2.3 Gas exchange analyses

Light response curves

Light response curves of gas exchange and chlorophyll fluorescence were carried out using the LiCor-6400XT (Lincoln, Nebraska), a portable infrared gas analyser system with a fluorometer attached (6400-40 unit). The fluorometer provided irradiance using red and blue LEDs (approximately 10% blue). Throughout all gas exchange measurements, the cuvette air temperature was set to 28°C, relative humidity maintained at approximately 50%, and flow rate at 500 µmol s^{-1}. The internal temperature and relative humidity in both growing systems were measured daily using Tiny Tag Ultra 2 Devices (Gemini Data Loggers, Chichester, UK) suspended above the plants. For the preliminary study, all photosynthesis measurements were carried out on a fully expanded leaf 9, to avoid leaf-ageing effects and severe N-deficiency. The width of the leaf was measured to adjust for the area of the leaf within the IRGA cuvette. Measurements were taken in-situ, between 10:00 hours and 15:00 hours each day to allow plants to reach maximum photosynthesis and avoid any beginning or end of day effects such as carbohydrate accumulation. Four plants were measured per variety under the three nutrient complements (see experimental design).

Chlorophyll fluorescent light response curves were taken as follows. For this measurement, the reference chamber CO_2 concentration was kept at 400 µl l^{-1} (to simulate the concentration of CO_2 in the atmosphere). Leaves were inserted into the chamber and exposed to different light intensities. The rate of photosynthesis (P) was recorded once the values of P remained stable for at least two minutes.

In the first trial, plants were exposed to nine levels of light intensity – 1500, 1000, 800, 600, 400, 300, 200, 100 and 0 µmol m^{-2} s^{-1} of light. There was a slight variation in the second growth room trial, where 300 µmol m^{-2} s^{-1} was replaced with 50 µmol m^{-2} s^{-1}. This

was for a more detailed measurement of the initial (quantum yield) part of the slope in the light response curve. In both trials, data was fitted using a light response curve-fitting tool (Ye, 2007), to obtain the maximum photosynthetic assimilation rate (Pmax) in light-saturated conditions (Tables 2.3 and 2.4).

CO_2 assimilation (A/Ci)

The rates of assimilation of CO_2 on leaf 9 were also recorded in the second growth room trial. The conditions are similar to the fluorescent light response, apart from the light level, which was set to 1000 μmol m^{-2} s^{-1} throughout the measurement. The concentrations of CO_2 ppm (parts per million) used here were 400, 400, 50, 60, 80, 100, 150, 250, 350, 500, 650, 800, 1200. Values were obtained from curve-fitted A/Ci data using the curve-fitting tool by Sharkey *et al*., (2007) based on the biochemical model of photosynthesis developed by von Caemerer and Farquhar (1981).

Non-photochemical quenching (NPQ)

In the second growth room trial, non-photochemical quenching (NPQ) induction was also recorded. A section on the widest part of leaf 9 was dark-adapted using foil for a duration of an hour and 30 minutes. The dark-adapted section was then exposed to actinic light at 1000 μmol m^{-2} s^{-1} for a period of 900 s (15 minutes) to elicit a transient of the Kautsky effect (chlorophyll a fluorescence induction).

Statistical analyses and curve fitting

GraphPad Prism (GraphPad, California, USA) was used to carry out the statistical analyses for both trials. Two-way analysis of variance (ANOVA) was the primary analysis carried out, and P values were obtained for the identification of significant differences between means. Tukey's test was utilised to correct for multiple comparisons.

Light response data was fitted using the curve-fitting tool from Ye, (2007), and A/Ci curves were fitted using the tool by Sharkey *et al*., (2007). Three components (Vc_{max}, J_{max} and TPU) were calculated

from the curve-fitted A/Ci, denoted in Figure 2.6. The correlations between chlorophyll, gas exchange parameters and leaf anatomical parameters were determined using Pearson's correlation analysis.

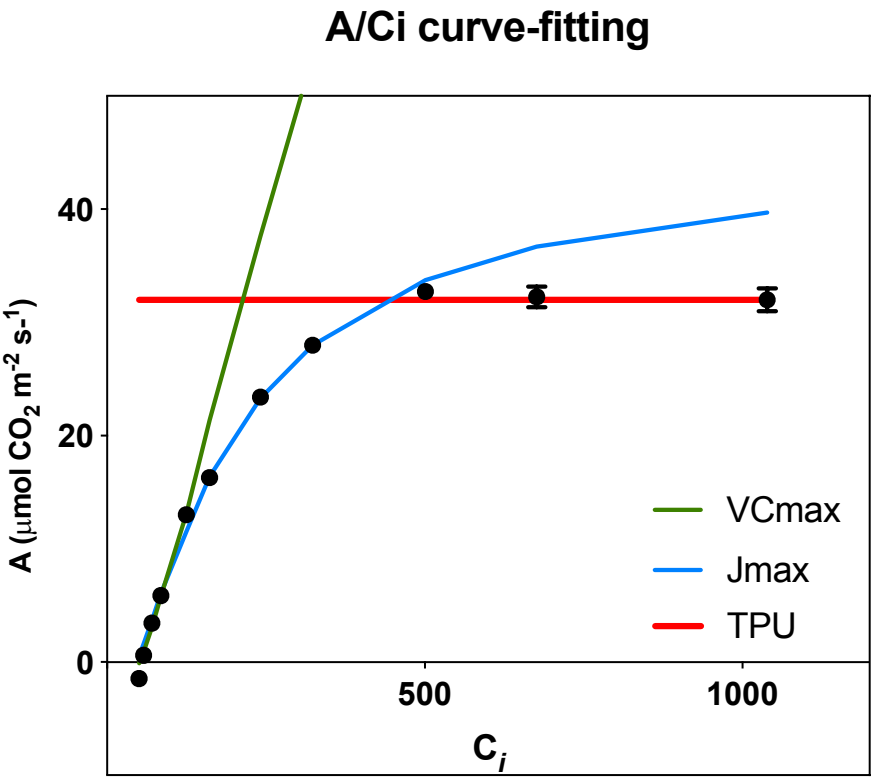


Figure 2.6: Example curve-fitting of mean A/Ci for MR219 plants (n=3) under the control treatment. The black dots denote the values of A at different carbon dioxide concentrations with SEM. For some cases, the error bars are too small to be visible. Vc_{max} (green line) is the maximum rate of carboxylation of Rubisco, J_{max} (blue line) represents the RuBP regeneration rate while the red line represents triosphosphate utilisation.

2.3 **Results**

For clarification, control plants will be referred to as 100% N while plants that received half and a quarter of the full nutrient complement will be referred to as 50% N and 25% N respectively.

2.3.1 Plant physiology measurements

Leaf lengths and development

Individual leaf lengths (means and SEM) were plotted against days after transplanting (DAT) into their respective treatment hydroponic system. To calculate the rate of leaf extension, a sigmoidal dose-response (variable slope) equation was used for curve fitting, as shown in Figure 2.7. As leaf elongation does not follow a linear or exponential growth pattern, data for each leaf fitted well to the variable sigmoidal response slope with a four–parameter logistic equation. From every curve fit, leaf lengths (Table 2.1) and the LE_{50} (time taken for the leaf to reach 50% full extension) (Table 2.2) were extracted and tabulated, together with their standard errors. The total number of leaves as well as the number of primary tillers are shown in Figure 2.8.

From Figure 2.7, it can be seen that there is a visible difference in leaf lengths in all plants according to age – leaf 6 was the shortest while leaf 9 was generally the longest. MR219 leaf lengths were completely unaffected by the different nitrogen treatments ($p>0.01$), while IR64 showed marginally more sensitivity to the lower N status. A majority of the differences observed (Table 2.1) were varietal, rather than as a result of nitrogen concentrations. The effect of nitrogen deficiency on leaf extension rates in this study did not follow a consistent pattern. Nitrogen treatment had a minimal impact on the time taken for each leaf to achieve 50% full leaf extension (Table 2.2). Moreover, LE_{50} for all MR253 plants was completely unaffected by nitrogen concentration ($p>0.05$). Similar to final leaf lengths, most

differences observed in LE_{50} were varietal differences, and only between lower N plants. It can be concluded that at the individual leaf level, Malaysia rice varieties appear less susceptible to lower N concentrations.

At the plant level however, differences were clear across all varieties. Generally, plants grown in the full nutrient compliment had the highest number of leaves (Figure 2.8). IR64 had the highest number of leaves, under all treatments. In all varieties, 50% N plants had a lower number of leaves compared to the 100% N plants, with 25% N plants having the lowest number of leaves ($p<0.05$). This was also consistent in the number of primary tillers (Figure 2.8). Comparing tiller number and number of leaves, it is evident that IR64 tillers more profusely than the Malaysian varieties.

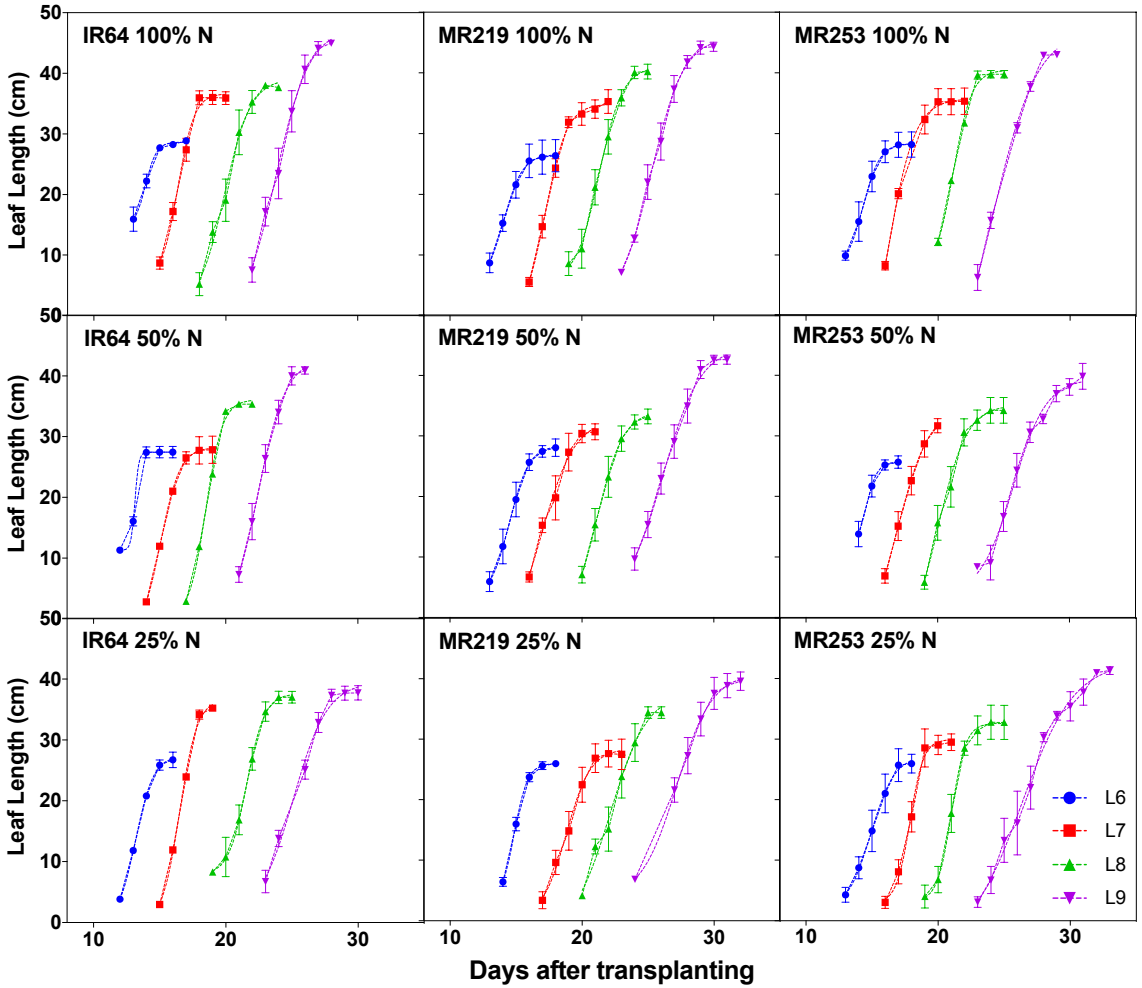


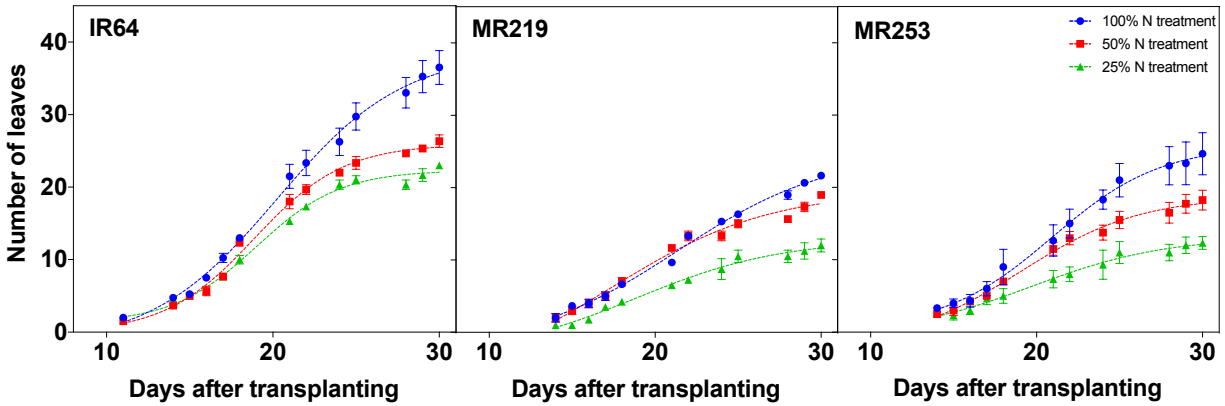
Figure 2.7: Leaf extension rates following a variable sigmoidal slope response of the three varieties MR219, MR253 and IR64 under the 100% N, 50% N and 25% N treatments. Shown are the means and the standard errors of the means (SEM), n=5. For some cases, the error bars are too small to be visible.

Table 2.1: Final leaf lengths from curve-fitting for leaf 6, 7, 8 and 9 for all varieties under the three nitrogen treatments. Shown are the means and the SEM. Same letters indicated highly significant differences ($p<0.01$) between paired comparisons, following a two-way ANOVA test and a Tukey's multiple comparisons test, n=5.

100% N	**Leaf 6**		**Leaf 7**		**Leaf 8**		**Leaf 9**	
	Mean	**SEM**	**Mean**	**SEM**	**Mean**	**SEM**	**Mean**	**SEM**
IR64	28.6*f*	0.304	36.6*c*	1.09	39.1	1.94	47.3*e*	2.39
MR219	26.6*f*	0.303	34.9	0.544	41.0	1.14	45.9	1.08
MR253	28.4	0.108	35.8	0.571	40.5*a*	1.13	47.2*b*	3.83
50% N	**Leaf 6**		**Leaf 7**		**Leaf 8**		**Leaf 9**	
	Mean	**SEM**	**Mean**	**SEM**	**Mean**	**SEM**	**Mean**	**SEM**
IR64	27.5	0.00	28.3*cdhi*	0.365	36.1	1.05	42.8	1.24
MR219	28.4*g*	0.298	32.8*h*	3.51	34.1	0.501	44.8*n*	1.44
MR253	25.7*g*	0.00	34.8*i*	1.30	35.1	1.47	39.5*bn*	1.31
25% N	**Leaf 6**		**Leaf 7**		**Leaf 8**		**Leaf 9**	
	Mean	**SEM**	**Mean**	**SEM**	**Mean**	**SEM**	**Mean**	**SEM**
IR64	27.4	0.516	36.8*djk*	2.11	37.6*l*	0.356	39.5*e*	2.05
MR219	26.0	0.0292	28.4*j*	1.03	37.7*m*	4.35	40.9	0.828
MR253	27.2	1.08	29.9*k*	1.15	32.6*alm*	0.237	42.9	1.71

Table 2.2: Number of days taken (from sow) to 50% full leaf extension (LE_{50}) in leaves 6,7,8 and 9 in the three varieties under the three N treatments. LE_{50} was obtained from the data in Figure 2.12. Same letters indicate highly significant differences between the means compared (within each leaf rank) following two-way ANOVA ($p<0.05$) and Tukey's multiple comparisons test.

	Leaf 6		**Leaf 7**		**Leaf 8**		**Leaf 9**	
100% N	**Mean**	**SEM**	**Mean**	**SEM**	**Mean**	**SEM**	**Mean**	**SEM**
IR64	13.9	0.0983	16.4	0.198	19.9	0.345	23.8	0.412
MR219	14.1	0.134	17.2	0.177	21.3	0.147	25.3*g*	0.192
MR253	14.3	0.0320	16.2	0.600	21.2	0.271	24.2	1.17
	Leaf 6		**Leaf 7**		**Leaf 8**		**Leaf 9**	
50% N	**Mean**	**SEM**	**Mean**	**SEM**	**Mean**	**SEM**	**Mean**	**SEM**
IR64	13.1	0.00	15.1*ab*	0.112	18.5*ef*	0.149	22.5*hij*	0.208
MR219	14.5	0.0680	16.9*ac*	1.36	21.1*e*	0.156	26.1*h*	0.314
MR253	14.5	0.00	16.9b	0.290	20.1	0.664	25.7*i*	0.284
	Leaf 6		**Leaf 7**		**Leaf 8**		**Leaf 9**	
25% N	**Mean**	**SEM**	**Mean**	**SEM**	**Mean**	**SEM**	**Mean**	**SEM**
IR64	13.2	0.0966	16.5*d*	0.194	21.6*f*	0.0442	25.1*jk*	0.631
MR219	14.9	0.00870	18.8*cd*	0.260	22.1	0.649	27.2*gk*	0.137
MR253	14.9	0.172	17.9	0.145	21.0	0.0326	26.3	0.404



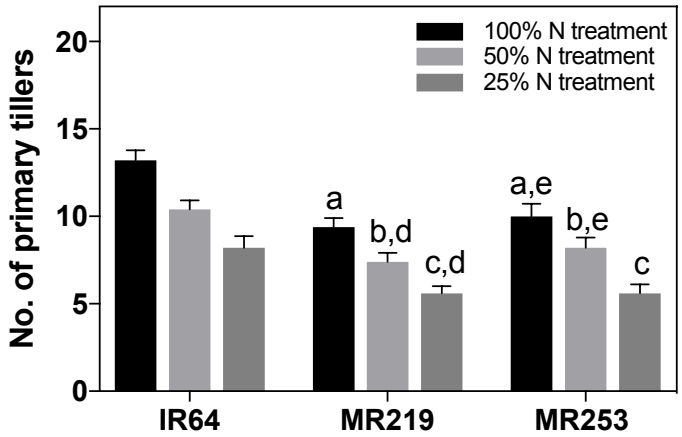


Figure 2.8: Total number of leaves following a variable sigmoidal slope response, and the number of primary tillers at the end of Leaf 9 elongation. Shown are the means and the SEM. Same letters indicate no significant differences ($p>0.05$) between compared pairs, following a two-way ANOVA test and a Tukey's multiple comparisons test, n=5. For some cases, the error bars are too small to be visible.

Stomatal density and length

The relationship between N treatment and stomatal morphology in rice has not been widely studied. The number of stomata on both surfaces was counted per field of view with an area of 520 by 389 microns and calculated to obtain the number of stomata per mm^2 (Figure 2.9). Stomatal lengths (μm), were measured from tip to tip and means are also shown in Figure 2.9. It can be seen that the abaxial surface of the leaves (underside of the leaves) generally had a higher stomatal density as compared to the adaxial surface. MR253 appears to have a significantly lower ($p<0.05$) stomatal density for both adaxial and abaxial leaf surfaces under all three treatments compared to the other two varieties. Treatment and variety did not have a significant effect on the stomatal lengths on either side of the leaves ($p>0.05$). The number of stomata decreased with decreasing N, and this was observed more particularly on the abaxial surface of the leaves. It is noted that the 50% N and 25% N leaves had a smaller area indicating that the difference in stomatal density was not caused by a co-alteration of cell size (no changes in stomatal lengths noted) and leaf area.

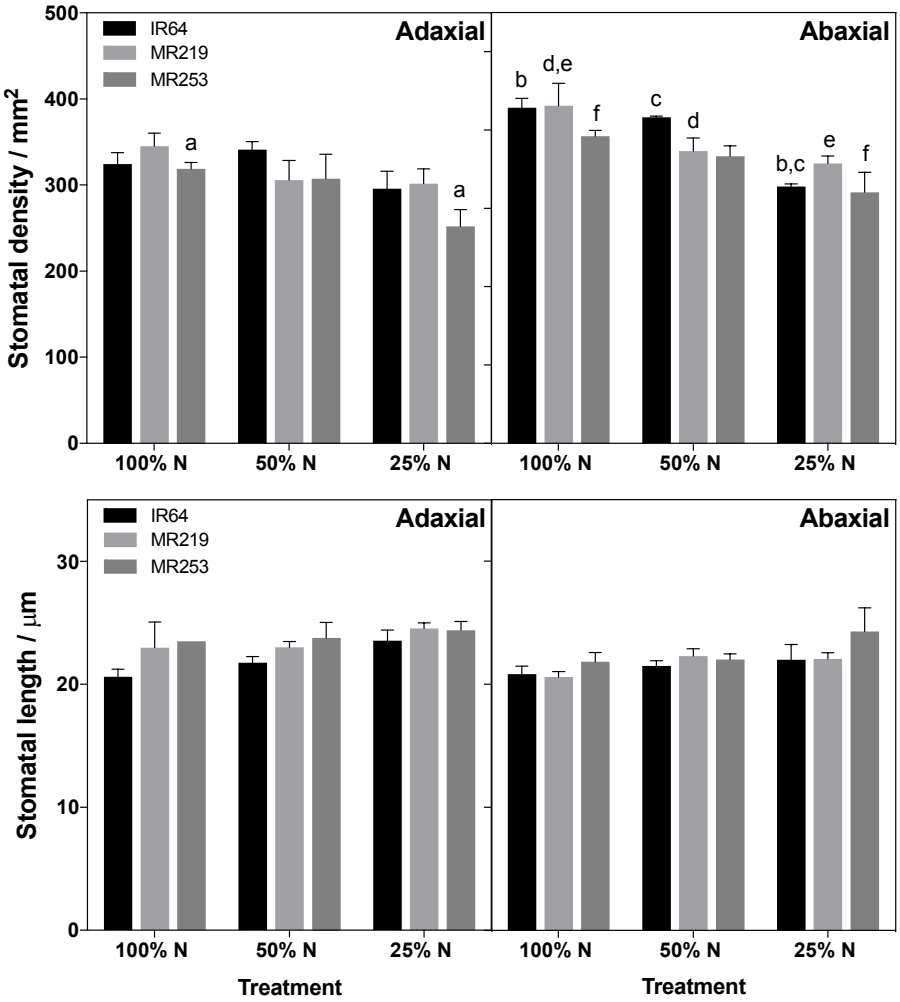


Figure 2.9: Stomatal density of adaxial and abaxial surfaces and stomatal lengths of the three varieties under the three treatments. Shown are the means and SEM. For some cases, error bars are too small to be visible. Same letters indicate significant differences ($p<0.05$) between compared pairs from two-way ANOVA and Tukey's multiple comparisons test (n=6).

Leaf thickness

Examples of major and minor veins as well as bulliform cells for the three varieties are shown in Figure 2.10. The red arrows indicate leaf thickness measurements, which was done perpendicular to the abaxial and adaxial surfaces of the rice leaf. Two measurements, major and minor vein lengths, were taken as the rice leaf does not have a flat surface. As expected in most cases, the low N treatment resulted in thinner leaves consistent with the lower photosynthetic capacity. Under the control treatment, the Malaysian varieties had significantly thicker major and minor veins ($p<0.05$) than IR64, as shown in Figure 2.11. In fact, the multiple comparisons test highlighted larger significant differences in major vein lengths between the Malaysian varieties and IR64 ($p<0.01$). Major vein lengths averaged at 163.72 μm for MR219, and 161.64 μm for MR253, while IR64 leaves had a mean major vein thickness of 137.85 μm. MR219 and MR253 both have large vascular bundles in their major vein. The vascular bundles transport nutrients and water to the leaves. In minor vein thickness, the difference was less significant but present ($p<0.05$). The quality of the sections was not sufficient to provide data on cell size, number or arrangement.

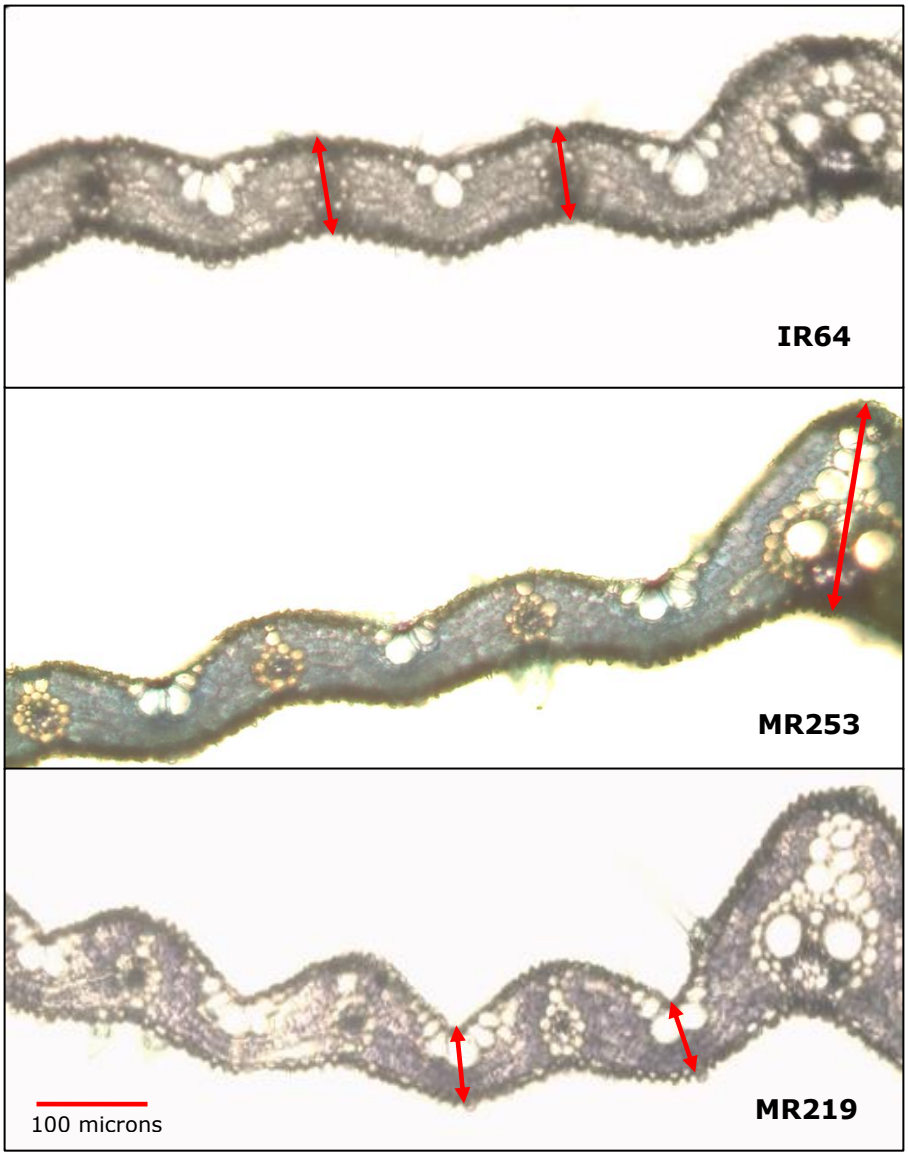


Figure 2.10: Hand-cut transverse sections of leaf 9 for each variety. Shown are the leaves under the control treatment (100% N). The red arrows in the IR64 denote the minor vein (minor vascular bundle) thickness. In the MR253 box, the red arrow highlights where the major vein (major vascular bundle) thickness is measured. Bulliform cells are shown in the MR219 box. Scale bar = 100 μm. (Source: own material)

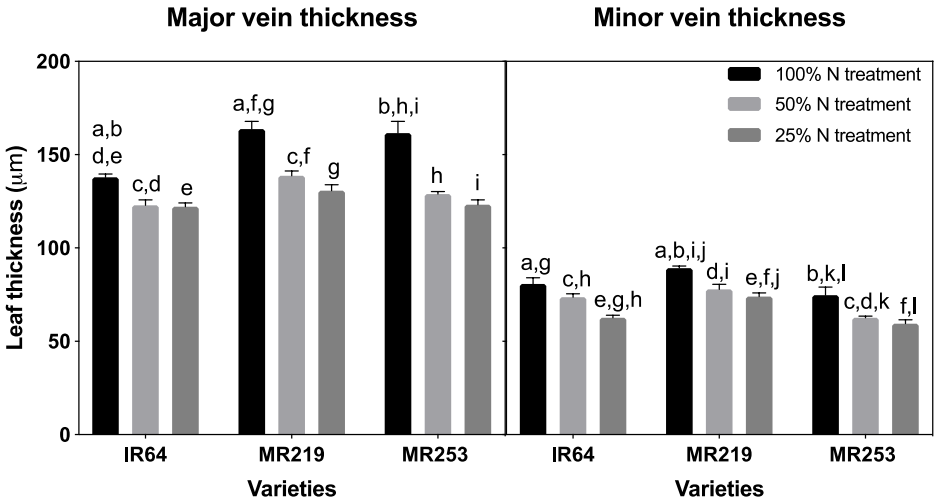


Figure 2.11: Major and minor vein thickness for all varieties under the three nitrogen treatments. Shown are the means and the SEM. Same letters denote significant differences ($p<0.05$) between compared pairs (major and minor veins analysed separately) following a two-way ANOVA test and Tukey's multiple comparisons test, n=9.

Leaf area

It is interesting to note that while the number of leaves (Figure 2.8) for the Malaysian varieties were significantly lower than the IR64 variety, there were no varietal differences found in the accumulated leaf area (Figure 2.12). This corroborates with physical observation throughout the study, wherein IR64 had shorter leaves (primary, secondary and tertiary tillers) than the Malaysian varieties.

There is a progressive and significant decline in whole plant leaf area from control to 50% to 25% (Figure 2.12) indicating that although leaf lengths were similar (Table 2.1), a difference in area resulted from a change in leaf width.

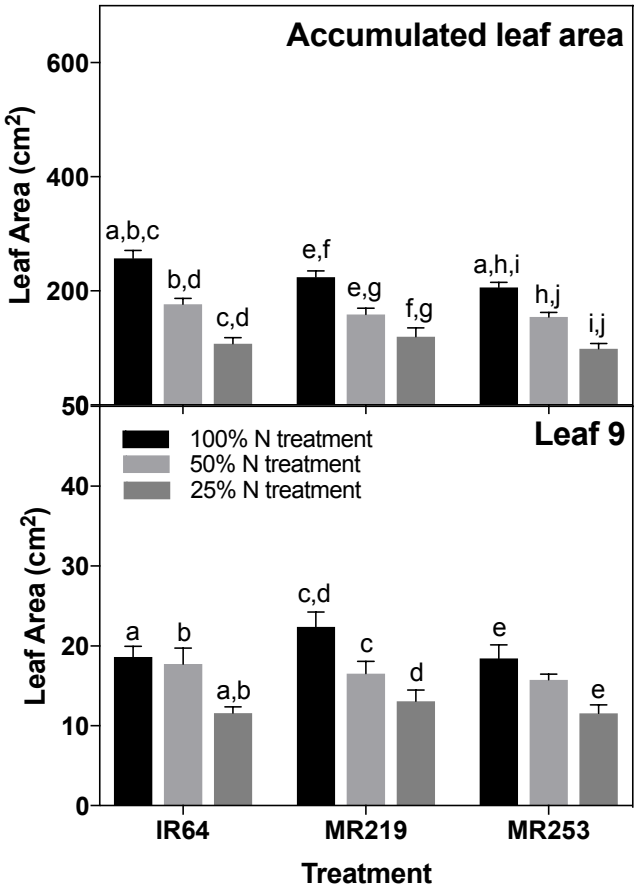


Figure 2.12: Whole plant leaf area and leaf 9 area for the three varieties under the three treatments. Same letters indicate significant differences between compared pairs ($p<0.05$) from a two-way ANOVA test and Tukey's multiple comparisons test, n=4.

2.3.2 Gas exchange measurements

Fluorescent light response

Photosynthetic assimilation (A) and stomatal conductance (g_S) under increasing photosynthetic photon flux densities (PPFD) for IR64 and Moroberekan plants in the first trial is shown in Figure 2.13. A and g_S for IR64, MR219 and MR253 in the second trial are shown in Figure 2.14.

Following a two-way ANOVA and Tukey's multiple comparisons test and in both trials and all plants, no varietal differences within treatments were found ($p>0.05$). Within each variety however, significant reductions in Pmax between control (100% N) and 25% N plants were observed for all varieties, apart from Moroberekan. This considerable decline in Pmax was not mirrored in g_S however, and no significant differences ($p>0.05$) were found between treatments in each variety. This may indicate minimal direct stomatal limitation on Pmax. The electron transport rates (ETR) of Photosystem II (calculated as ϕPSII x PPFD x 0.84 x 0.5) (Murchie and Lawson, 2013) however, were found to saturate at lower levels of PPFD ($p<0.05$), as shown in Figure 2.15. This suggests that the lowered nitrogen status of the plant in 25% N plants severely limited CO_2 assimilation and limited electron transport at higher PPFD (Long *et al*., 2015).

Interestingly, in the first trial, Moroberekan exhibited similar Pmax in 100% N and 25% N plants at higher PPFD with the highest value being reached by 50% N. g_S was not found to be significantly different between treatments in Moroberekan plants but were different in their rates of electron transport at higher light levels. ETR followed the same trend as P_{max}. In addition to this, light adapted proportion of variable to maximum fluorescence (Fv'/Fm') at higher PPFD was significantly lower in control Moroberekan plants than in the other two treatments. Fv'/Fm' describes the maximum efficiency of PSII photochemistry in light-adapted conditions and often correlates with (and a useful proxy for) the level of non-

photochemical quenching (NPQ) which is a measurement of protective chlorophyll energy dissipation. P_{max} correlates well with leaf N content (Peng *et al*., 1995a, 1995b; Makino *et al*., 2003; Li *et al*., 2009).

IR64 behaved differently between the trials in terms of N response. In the first trial, there was a significant two-fold decline ($p<0.05$) in P_{max} between control and 25% N IR64 plants, but no differences ($p>0.05$) were observed between control and 50% N IR64 plants, as well as between 50% N and 25% N IR64 plants. The amount of nitrogen fertilization had a more significant effect on P_{max} in the second experiment (Table 2.4). Stomatal conductance was observed to be statistically similar across the treatments. This is expected in hydroponically grown plants as humidity was not a limiting factor.

The Malaysian varieties in the second growth room trial were found to have significantly lower P_{max} in 50% and 25% N treated plants than in control plants ($p<0.05$). There were small or no differences between 25% N and 50% N. Under the 25% N treatment, MR219 plants exhibited lower stomatal conductance ($p<0.05$) at lower PPFD but was seen to achieve similar stomatal conductance as the other two treatments at higher PPFD. This did not however, associate with an increase in P_{max}. ETR was significantly lower in 25% N plants (Figure 2.16), but unlike IR64 and Moroberekan, 25% N MR219 plants exhibited a significantly lower ϕPSII ($p<0.05$) at higher PPFD. It is evident that the patterns of P_{max} here are more associated with PSII ETR rather than stomatal conductance in 25% N. MR253 behaved in a similar way to MR219, apart from the lack of significant differences between treatments for ϕPSII (Figure 2.16). All varieties showed a reduction of between 30-40% in Fv'/Fm' in the second trial (Figure 2.17).

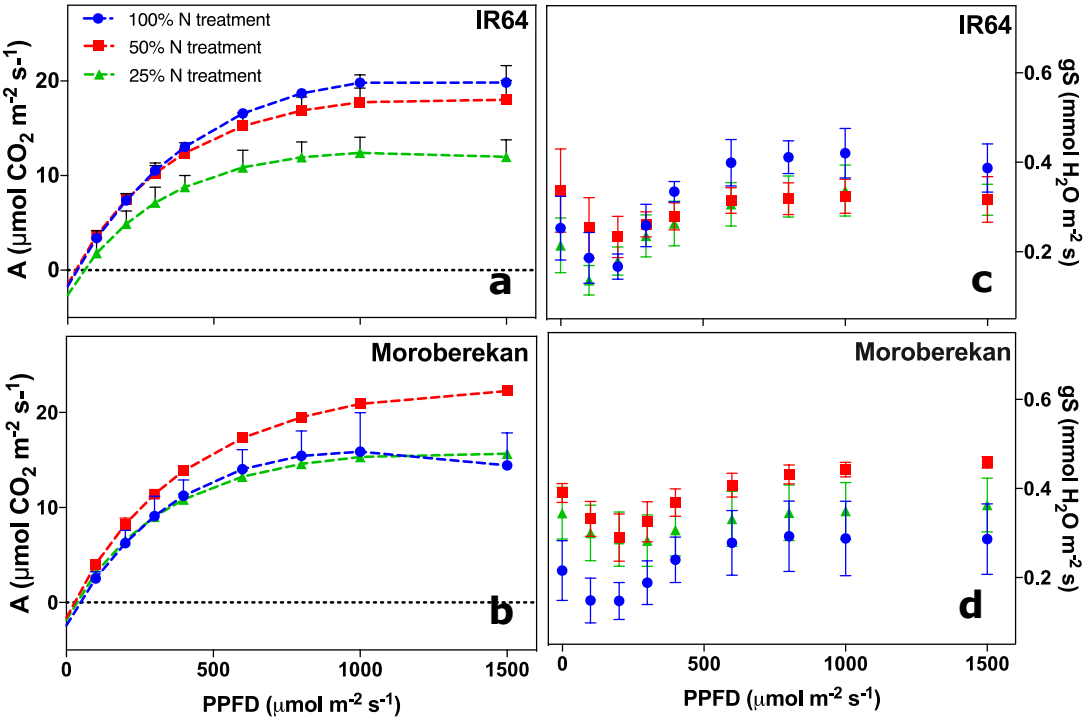


Figure 2.13: Photosynthetic assimilation of CO_2 (µmol CO_2 m^{-2} s^{-1}) of (**a**) IR64 and (**b**) Moroberekan in the first trial, for plants under the three nutrient treatments, under increasing PPFD (µmol m^2 s^{-1}). Data was fitted using the light response curve-fitting tool by Ye, (2007). Stomatal conductance (g_S, mol H_20 m^{-1} s^{-1}) is also shown for (**c**) IR64 and (**d**) Moroberekan. Shown are the means and SEM, n=4. For some mean data points, error bars are too small to be seen.

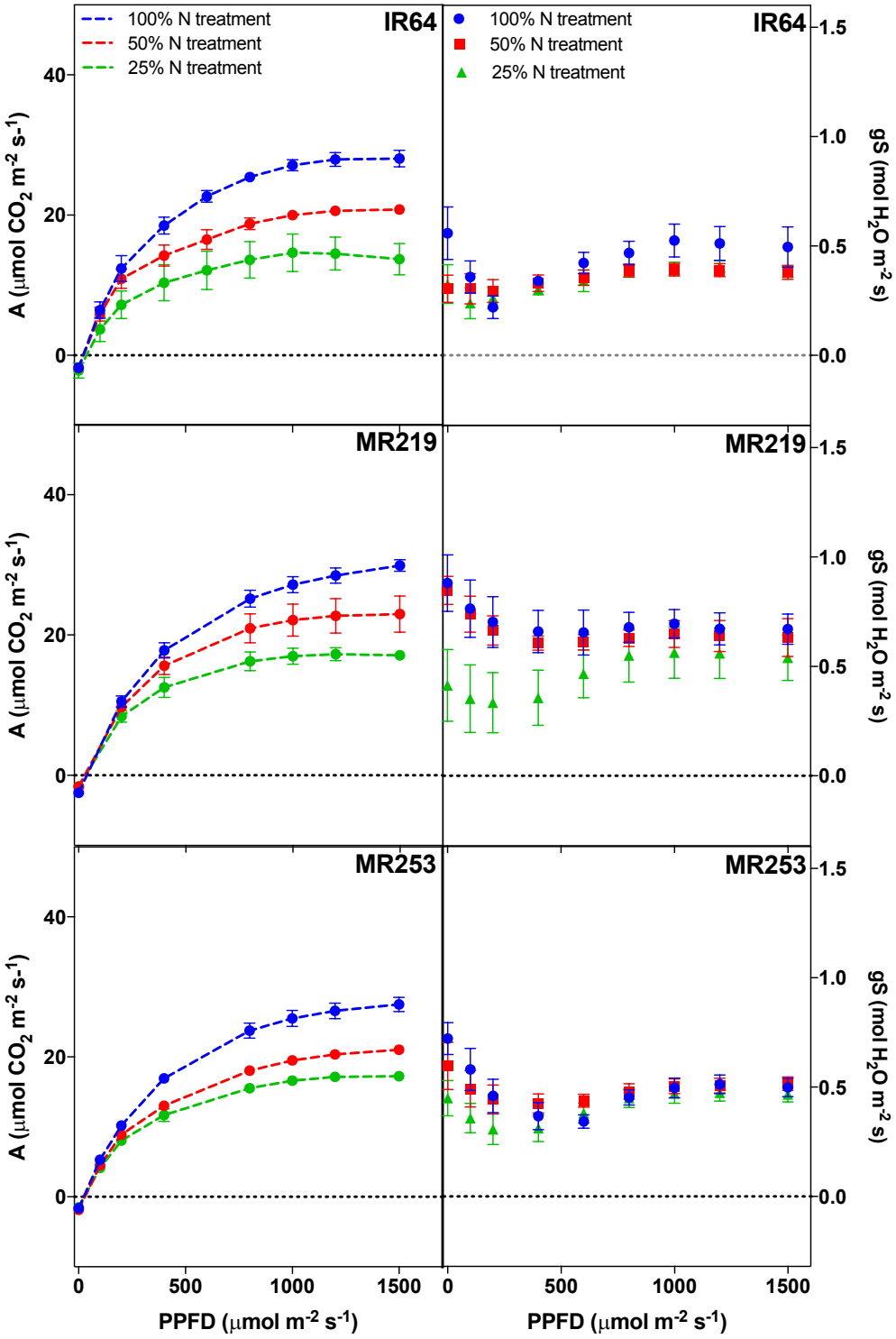


Figure 2.14: The assimilation of CO_2 (A) and stomatal conductance (g_S) of MR219, MR253 and IR64 at 100% N, 50% N and 25% N treatments in the second trial. Shown are the means and the standard errors of the means (SEM), n=4. For some cases, the error bars are too small to be visible.

Table 2.3: P_{max} (µmol CO_2 m^{-2} s^{-1}) for growth room trial 1, for IR64 and Moroberekan rice plants under the three nutrient regimes with their standard error of the means. Same letters indicate significant differences ($p<0.05$) between compared pairs (between varieties and between treatments), following a two-way ANOVA and Tukey's multiple comparisons test, n=4.

	IR64		**Moroberekan**	
N treatment	Mean	SEM	Mean	SEM
100%	19.3*a*	1.80	15.2*b*	2.06
50%	17.0	2.05	21.9*bc*	0.523
25%	11.3*a*	1.79	14.5*c*	0.462

Table 2.4: P_{max} (µmol CO_2 m^{-2} s^{-1}) for growth room trial 2, for IR64, MR219 and MR253 rice plants under the three nutrient regimes with their standard error of the means. Same letters indicate significant differences ($p<0.05$) between compared pairs (between varieties and between treatments), following a two-way ANOVA and Tukey's multiple comparisons test, n=4.

	IR64		**MR219**		**MR253**	
N treatment	Mean	SEM	Mean	SEM	Mean	SEM
100%	28.9*ab*	1.26	26.6*de*	2.63	28.4f*g*	1.26
50%	20.3*ac*	0.585	16.3*d*	1.31	21.1*f*	0.433
25%	14.1*bc*	2.64	16.2*e*	0.917	17.0*g*	0.512

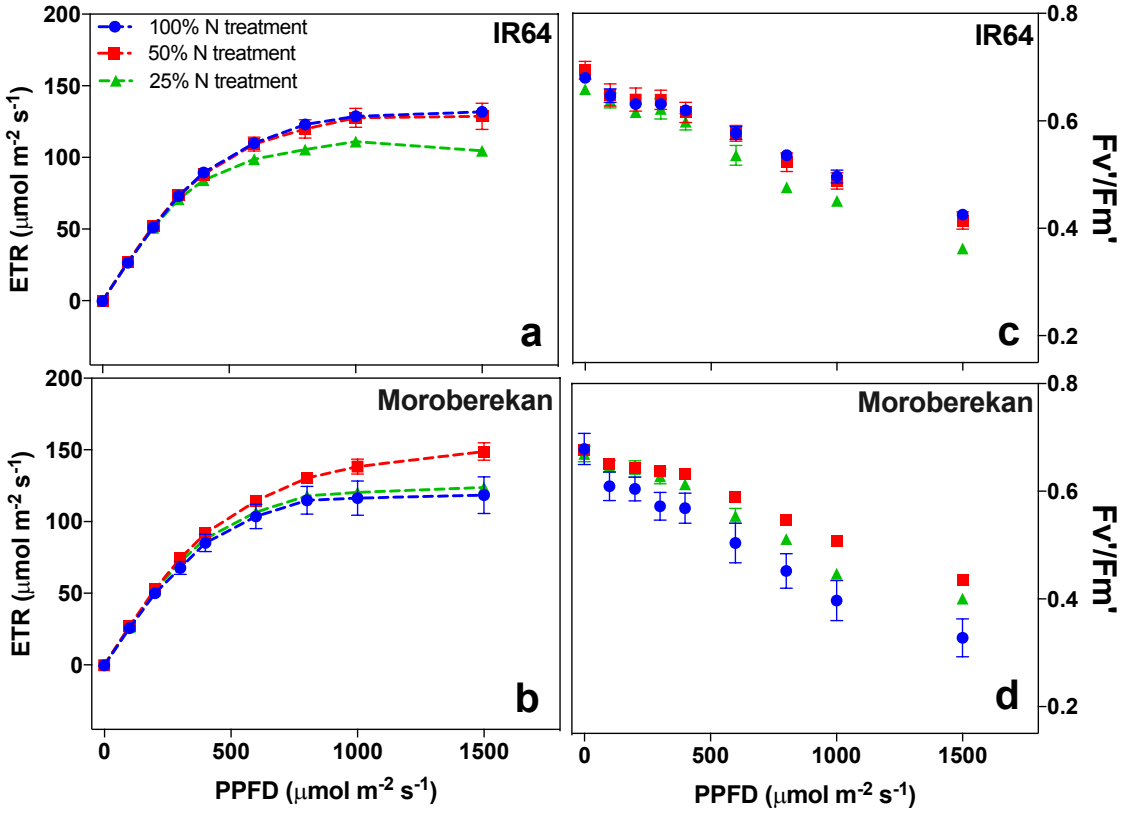


Figure 2.15: Electron transport rate (μmol m^{-2} s^{-1}) of (**a**) IR64 and (**c**) Moroberekan as well as the ratio of variable to maximum fluorescence (Fv'/Fm') of (**b**) IR64 and (**d**) Moroberekan rice varieties under the three treatments. Shown are the means (n=4) and SEM indicated. For some cases, the error bars are too small to be visible.

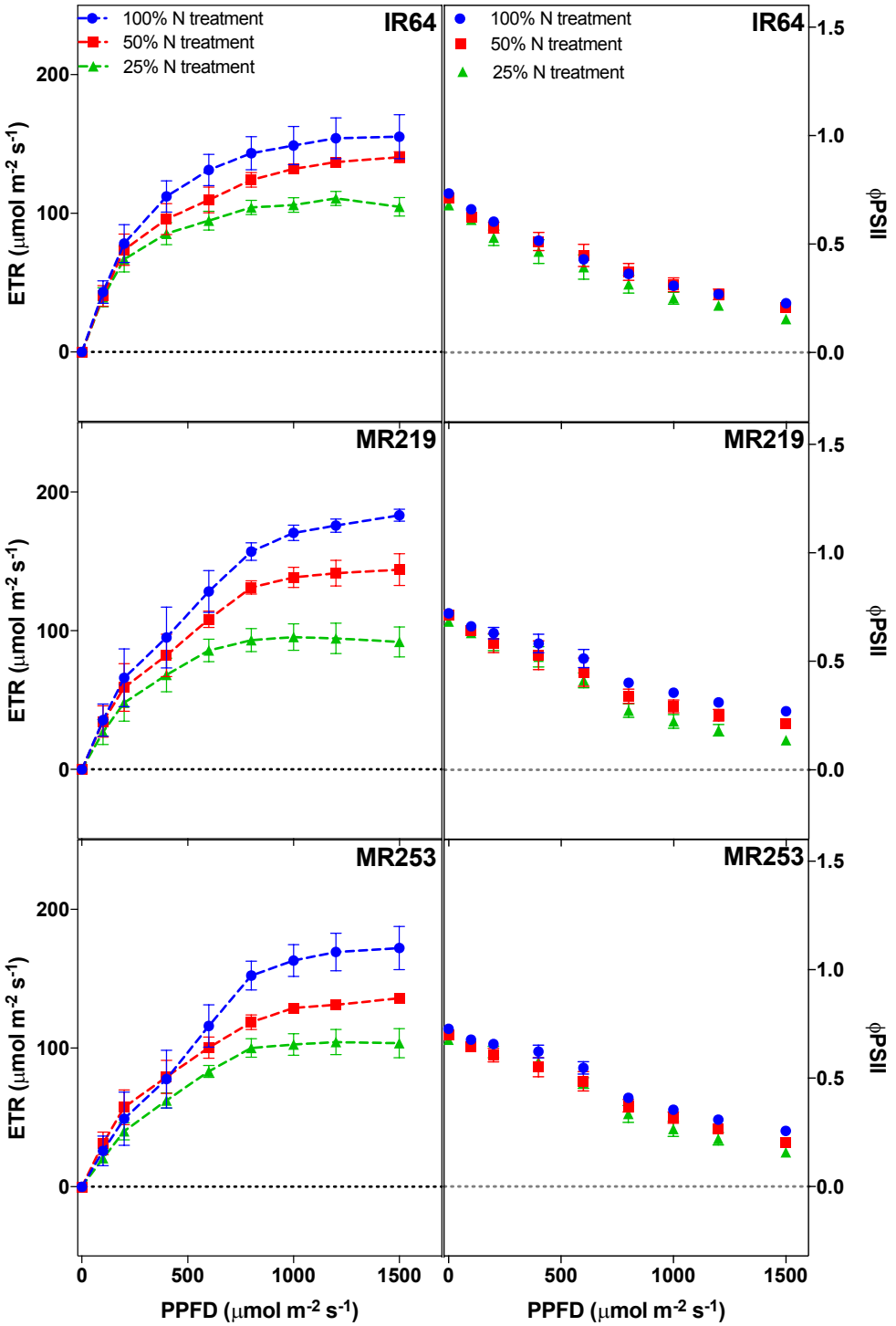


Figure 2.16: Maximum quantum efficiency of PSII (ϕPSII) and relative electron transport rate (μmol m^{-2} s^{-1}) of MR219, MR253 and IR64 at 100% N, 50% N and 25% N treatments. Shown are the means and the standard errors of the means (SEM), n=6. For some cases, the error bars are too small to be visible.

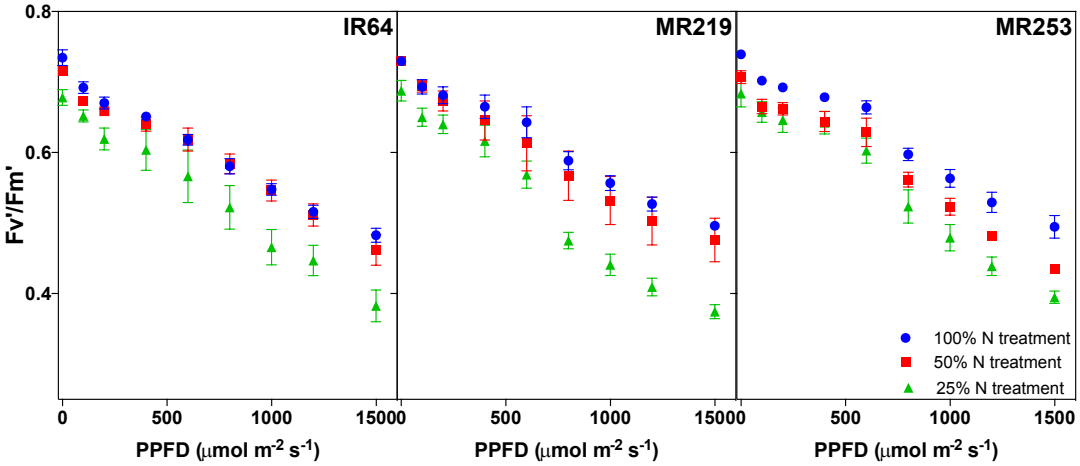


Figure 2.17: The ratio of variable to maximum fluorescence (Fv'/Fm') of the three varieties under the three treatments in increasing PPFD (µmol m^2 s^{-1}). Shown are the means and the standard errors of the means (SEM), n=6. For some cases, the error bars are too small to be visible.

Photosynthetic assimilation to increasing CO_2 (A/Ci)

In the second growth room trial, plants were tested for the net rate of CO_2 assimilation in increasing CO_2 conditions at a fixed light level (A/Ci analysis). This is done to separate the components of photosynthesis that can exert control over rate: notably Rubisco carboxylation and electron transport. Figure 2.18 shows the maximum carboxylation rate of the enzyme Rubisco (Vc_{max}) and the maximum rate of regeneration of ribulose-bisphosphate (RuBP), known as J_{max}. J_{max} is maximum rate of electron transport and indicates the capacity for regeneration of the substrate RuBP in light saturated conditions.

IR64, MR219 and MR253 exhibited similar rates of Vc_{max} at the same treatment levels ($p>0.05$), but within each variety, differences were observed between treatments. For all varieties, 50% N plants showed a significant decline of at least 25% from control plants, while Vc_{max} for 25% N plants decreased by almost half ($p<0.05$) following a two-way ANOVA and Tukey's multiple comparisons test. Between

50% and 25% N plants however, there were no significant differences detected ($p>0.05$). It is evident that a decrease in the N-status of the plant had a substantial negative effect on the activity of the enzyme Rubisco and this effect was almost parallel. Vc_{max} values showed a similar pattern of response to P_{max}, indicating that Rubisco activity was largely determining the rate of P_{max} measured.

There was a varietal difference observed in J_{max} in control plants; the Malaysian varieties exhibited higher electron transport rates than IR64 ($p<0.05$). However, at the 50% N and 25% N treatment levels, no varietal differences were seen ($p>0.05$). The decline in J_{max} between control and 25% N plants were more significant in the Malaysian varieties. While IR64 control plants had a substantially lower J_{max} than the Malaysian varieties, the relative decline between control and 25% N IR64 plants was less severe. Triosphosphate utilisation decreased with decreasing N in the Malaysian varieties but this was absent in IR64 plants. TPU offers a form of end product feedback (Sharkey, 2019), as most of the carbon exiting the Calvin cycle leaves as triosphosphate.

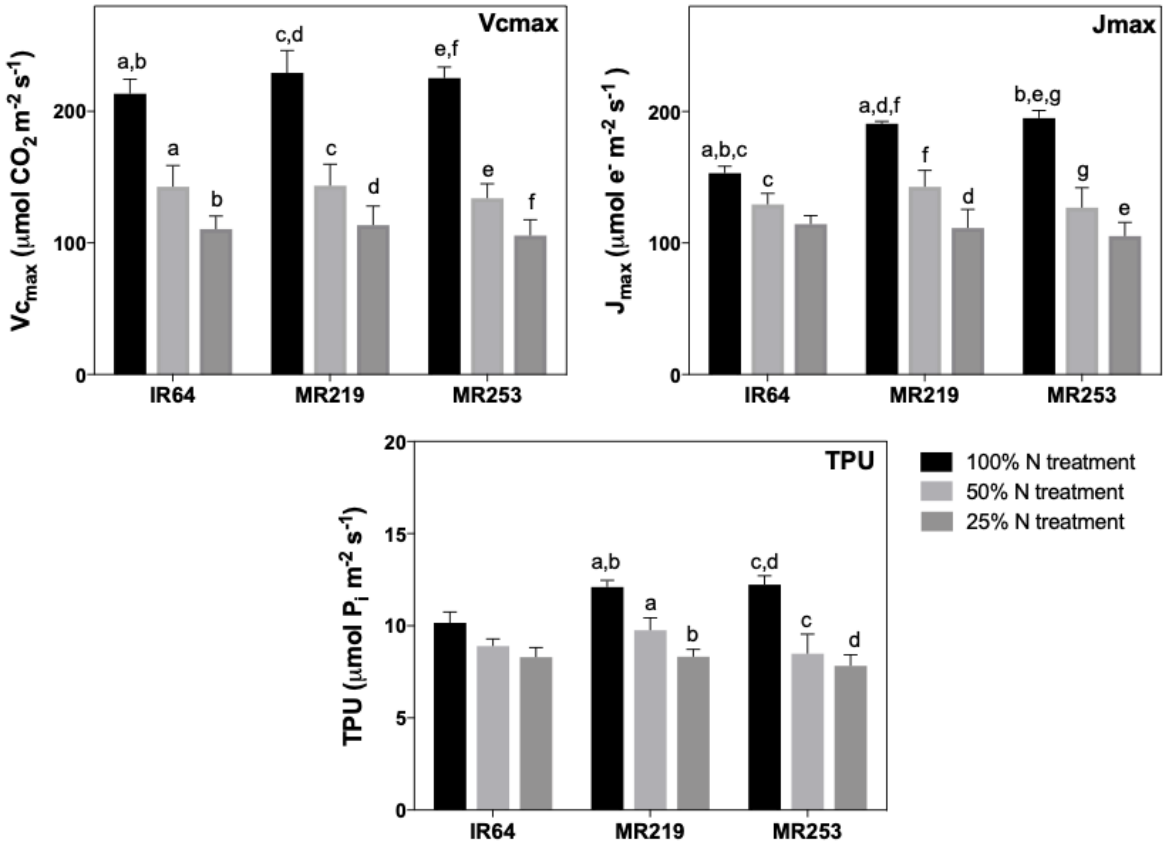


Figure 2.18: Maximum carboxylation rate of Rubisco (Vc_{max}), RuBP regeneration rate (J_{max}) and triosphosphate utilisation (TPU) of IR64, MR219, MR253 under the three treatments, in the second growth room trial. Values were obtained from curve-fitting A/Ci curves using the curve-fitting tool from Sharkey *et al*., (2007). Shown are the means and the standard errors of the means (SEM), n=4. For each bar, same letters (within each parameter e.g. Vc_{max}) indicate significant differences between compared pairs, following a two-way ANOVA ($p<0.05$) and Tukey's multiple comparison's test.

Non-photochemical quenching (NPQ)

In the second growth room trial, IR64, MR219 and MR253 were dark-adapted and subsequently exposed to actinic light (red light) at 1000 micromoles m^{-2} s^{-1} for one minute, and this induction assay is shown in Figure 2.19. The objective of this assay was to reveal any differences in NPQ. There were no statistical differences found between varieties, but this was present between treatments within the varieties. The letters denote significant differences between control and 25% N plants, in all varieties ($p<0.05$). In addition to this, significant differences were found between control and 50% N IR64 plants, but this was absent in the Malaysian varieties. In summary, 25% N plants had significantly higher NPQ in comparison to control plants ($p<0.05$). Non-photochemical quenching is a protective mechanism that plants under photooxidative stress utilise to mitigate excess excitation energy (Murchie *et al*., 2013). This is to help prevent photodamage, which can be irreversible, and long-term decline in the quantum yield of PSII and subsequently, the photosynthetic capacity of the plant (Murchie *et al*., 1999; Zhang *et al*., 2000; Kramer *et al*., 2004; Murata *et al*., 2007; Takahashi and Murata, 2008). It is observed here that there was increased photoprotection for severely (25%) N-deficient plants, in high light conditions. Interesting to note, 50% N IR64 plants exhibited a significant increase in NPQ compared to control plants, indicating a heightened sensitivity to the prevention of the plant to light-induced damage. The lowered photosynthetic capacity can lead to an increase in absorbed light energy that is in excess of photosynthetic requirements which leads to an enhanced level of energy dissipation (Murchie and Niyogi, 2011).

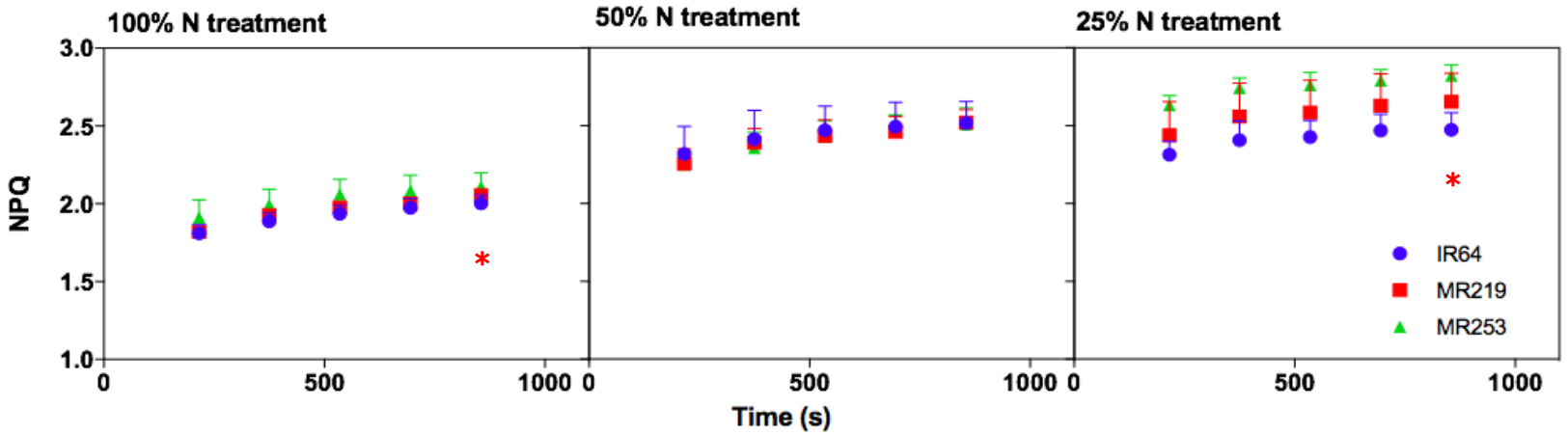


Figure 2.19: Non-photochemical quenching of MR219, MR253 and IR64 at 100% N, 50% N and 25% N treatments. Shown are the means and the standard errors of the means (SEM), n=4. For some cases, the error bars are too small to be visible. The asterisk (*) indicates significant differences between the 100% and 25% treatments within the varieties.

2.3.3 Chlorophyll

Chlorophyll content often correlates with leaf N content (Peng *et al*., 1995a). Here a handheld chlorophyll meter was used to analyse differences between treatment. The greenness (SPAD value) of leaf 9 was recorded in both growth room trials, and the means and standard error of means are shown in Figure 2.20a (trial 1) and Figure 2.20b (trial 2). In the first trial, no differences were found between the treatments in IR64. In Moroberekan however, there were significant differences between control and 50% N plants, and well as between 50% N and 25% N plants.

In the second trial, more significant differences were observed, but again, these were not varietal. Unlike in the first trial, IR64 exhibited differences in SPAD value between control and nitrogen deficient plants ($p<0.05$), which were also present within the Malaysian varieties. The device measures leaf absorbance at key wavelengths for chlorophyll but is dependent on variety–specific properties which can affect the slope of the relationship between chlorophyll content and SPAD value. Hence it gives a good indication of chlorophyll content for a given variety but comparisons between variety requires further calibration. Hence a higher SPAD value indicates the presence of a higher concentration of chlorophyll. Here, control plants generally had higher greenness, which corresponds to a higher chlorophyll concentration in the leaf blade.

2.3.4 Correlations: N, gas exchange and anatomical parameters

Highlighted in Figure 2.21 are correlation coefficients larger than 0.75, which indicate high positive correlations. No negative correlations were found. SPAD values were highly correlated with Vc_{max}, as expected as chlorophyll is largely correlated with the

enzyme Rubisco, and its corresponding maximum carboxylation capacity, Vc_{max}.

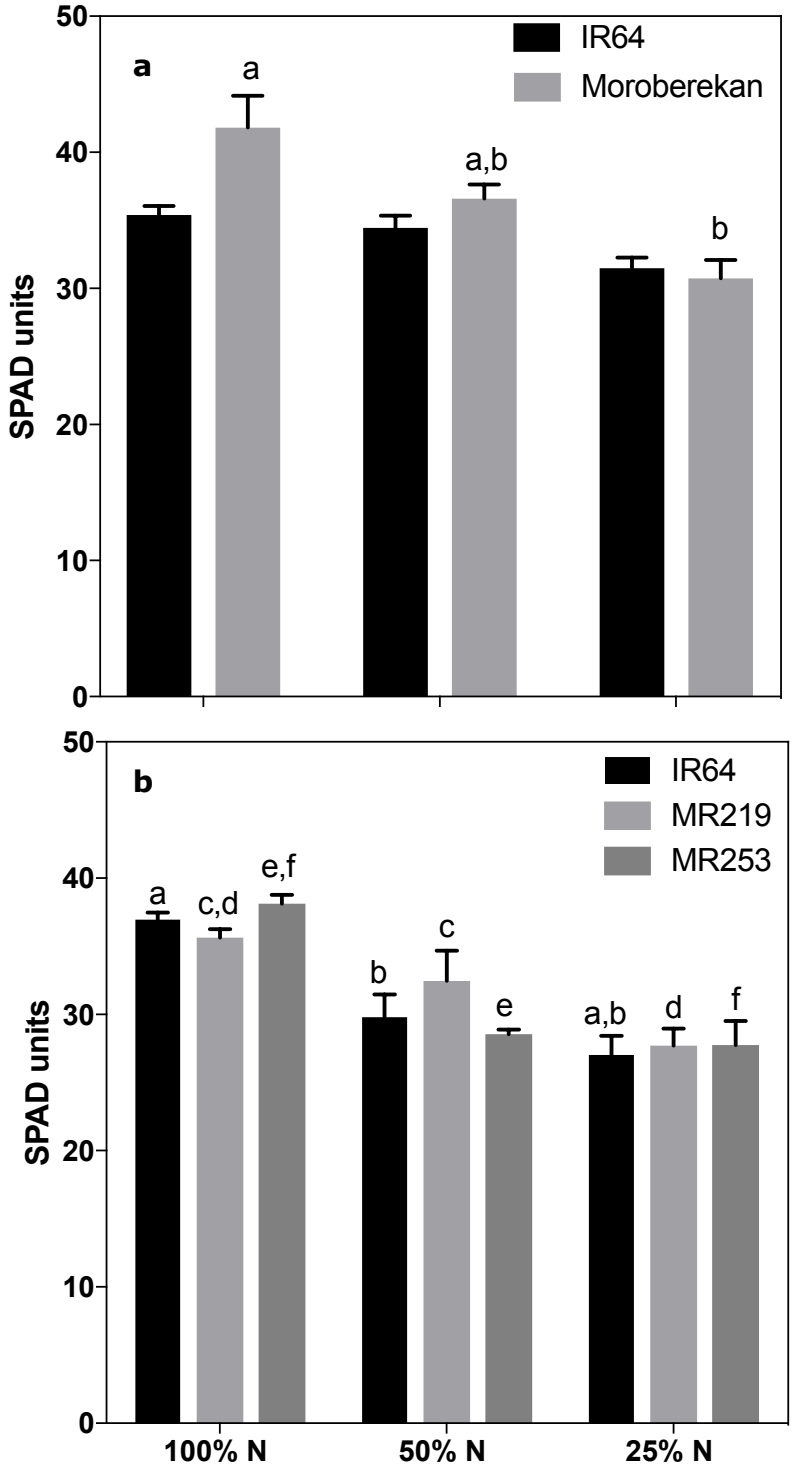


Figure 2.20: Chlorophyll content in SPAD value (greenness) of (**a**) IR64 and Moroberekan from the first trial, and of (**b**) IR64, MR219 and MR253 in the second trial. Shown are the means and SEM of leaf 9. Same letters indicate significant differences ($p<0.05$) between compared pairs, following a two-way ANOVA and Tukey's multiple comparisons test, n=4.

Figure 2.21: Pearson's correlation matrix with the correlation coefficients between chlorophyll (SPAD values), gas exchange parameters and leaf anatomical parameters in all varieties under all treatments ($n \geq 4$). P_{max} – light-saturated photosynthetic rate; Vc_{max} – maximum carboxylation capacity of Rubisco; ETR – electron transport rate; Fv/Fm – maximum quantum efficiency of PSII in dark-adapted state. Squares highlighted in pink represent significant correlation ($p<0.05$) and the squares highlighted in brown represent highly significant correlation ($p<0.0001$).

	SPAD	**P_{max}**	**Vc_{max}**	**ETR**	**Fv/Fm**	**No. of stomata (abaxial)**	**No. of stomata (adaxial)**	**No. of stomata (abaxial)**	**Stomatal Length (adaxial)**	**Leaf thickness (major vein)**	**Leaf thickness (minor vein)**
SPAD											
P_{max}	0.715										
Vc_{max}	0.849	0.695									
ETR	0.709	0.644	0.758								
Fv/Fm	0.393	0.161	0.165	0.145							
No. of stomata (abaxial)	0.553	0.474	0.663	0.600	0.072						
No. of stomata (adaxial)	0.398	0.307	0.505	0.565	-0.099	0.741					
Stomatal Length (abaxial)	-0.241	0.337	-0.425	0.279	0.068	-0.678	-0.400				
Stomatal Length (adaxial)	-0.344	0.386	-0.411	-0.390	-0.101	-0.724	-0.633	0.428			
Leaf thickness (major vein)	0.749	0.539	0.775	0.761	0.062	0.523	0.412	-0.307	-0.267		
Leaf thickness (minor vein)	0.517	0.486	0.654	0.544	-0.141	0.580	0.458	-0.393	-0.228	0.560	

2.4 **Discussion**

Nitrogen is a key macronutrient in plant growth. Rice plants use nitrogen in early development to produce leaves that are the indispensable light harvesting photosynthetic organs required for growth. The greatest requirement for this macronutrient is during the vegetative stage of development, where the plant undergoes rapid tillering. During the reproductive stage (panicle initiation to flowering), nitrogen is necessary for the growth of the flag leaf, which is the main producer of photosynthates for the rest of the growth cycle. At ripening, high leaf nitrogen delays leaf senescence, and contributes to grain filling (Dobermann, 2000). The deficiency of this nutrient can have a drastic effect on the morphology and productivity of the plant. The level of effect varies across genotypes and cultivars, and the co-existing abiotic and biotic stress factors. In this study, the changes in leaf anatomy and its impact on gas exchange were investigated to study genotypic variation, notably in Malaysian rice cultivars, and identify mechanisms employed by the rice plants to circumvent nitrogen deficiency.

2.4.1 Light harvesting, Chl fluorescence and the Calvin cycle

Gas exchange measurements can uncover valuable information on the behaviour of the photosynthetic machinery in response to changing exogenous factors (Long *et al*., 2015; Zivcak *et al*., 2017). Light response curves revealed that the rate of maximum photosynthesis for deficient plants saturated at light levels significantly lower than control plants. This decline was not a result of a stomatal limitation, but rather a downregulation caused by the reduced rate of electron transport. ETR is a calculated from the quantum yield of PSII and light intensity, as such is able to reflect the behaviour of electron acceptors downstream of PSII in light conditions. In the first growth room trial, IR64 and Moroberekan grown in 25% N were exhibiting lower Fv'/Fm' under increasing PPFD, but the operating efficiency of PSII in photochemistry (ϕPSII or

Fq'/Fm') was found to be unaffected by the decrease in nitrogen supply ($p<0.05$). In increasing PPFD, ϕPSII generally decreases but the quantum yield of PSI remains relatively constant (Dau, 1994). While the true quantum yield of PSII photochemistry decreases in increasing PPFD while PSI stays fairly constant, the value of ϕPSII fails to remain a good representation of the actual quantum yield of PSII photochemistry. This could be the reason behind the lack of a decline in ϕPSII when Fv'/Fm' decreased in the nitrogen deficient plants in this study (Pfundel, 1998).

Lower Fv'/Fm' values in stressed plants indicates an increase in non-photochemical quenching, as a response to excess excitation energy. While plants growing in optimum environments also utilise NPQ during periods of high light for photoprotection, NPQ has been found to increase in stressed plants (Maxwell and Johnson., 2000; Chen *et al*., 2003; Cha-um *et al*., 2007; Baker, 2008; Yin *et al*., 2010; Vaz and Sharma, 2011; Shrestha *et al*., 2012). The supply of excitation energy increasingly outweighs the demand from the photosynthetic apparatus in increasing PPFD. As a large proportion of nitrogen is invested in photosynthetic apparatus (thylakoid proteins and enzymes in the stroma).

Greenness (measured by SPAD) is an index used to predict the total extractable chlorophyll in plants and has been found to positively correlate with leaf N status (Argenta *et al*., 2004; Uddling *et al*., 2007). Both growth room trials in this study found that while there were no varietal differences in the greenness at the treatment levels, a majority of the varieties exhibited differences in greenness between control and N-deficient plants. 75% of leaf N is distributed to chloroplasts to sustain high rates of photosynthesis (Sun *et al*., 2016). This reduction in chlorophyll may have directly contributed to a decrease in the plant's light harvesting capacity, which conferred a decrease in Pmax and an increase in NPQ in N-deficient plants.

The carboxylation capacity of Rubisco has been found to be the rate-limiting factor of photosynthesis in ambient CO_2 concentrations under light saturated conditions (Sage, 1990; Makino *et al*., 1997; Vicente *et al*., 2011; Vicente *et al*., 2015; Carmo-Silva *et al*., 2015). Nitrogen influx has a substantial impact on the amount of Rubisco in photosynthetic organs (Imai *et al*., 2008). Rubisco is the most abundant protein in plants, accounting for almost 35% of leaf nitrogen in C3 cereal crops (Evans 1989, Makino *et al*., 2003). Its abundance is the compensatory result of the carboxylation inefficiency of the enzyme, even in ambient CO_2 concentrations (Carmo-Silva *et al*., 2015). As such, Vc_{max} is highly sensitive to stress, as was observed in this study. Interestingly, the rate of electron transport for RuBP regeneration (J_{max}) in control plants was significantly lower in IR64 than the Malaysian varieties.

2.4.2 The nitrogen profile on leaf anatomy and morphology

While differences in leaf mechanics (leaf extension rates and leaf lengths) were more profound in IR64 plants under all treatments as compared to the Malaysian rice, they followed no conclusive pattern. While there is still much unknown on the precise nature of N limitation on the mechanics of leaf development in rice, a study by Vos *et al*., 2005 similarly concluded that the supply of nitrogen had no effect on the rate of leaf appearance (i.e LE_{50}) and leaf expansion rate in maize (*Zea mays* L.). This response has been examined in other species part of the Gramineae family.

A related study on potato (*Solanum tuberosum* L.) showed a contrasting response; leaf size was found to vary by three to four folds in response to the status of N (Vos and Van der Putten, 1998). The photosynthetic capacity is the result of the lowering of leaf nitrogen per unit leaf area in response to the availability of N, which in turn lowers key parameters such as cell number, chloroplast number, Rubisco amount and chlorophyll amount in the leaves as reflected in SPAD values.

Understanding the relationships between the structure of the photosynthetic machinery and the physiological impact it confers at canopy level under different environmental conditions can shed light on characteristics and features that can potentially enhance plant productivity (Niinemets and Anten 2009). In this study, leaf morphology and anatomy were affected by the nitrogen status in all the plants, but a greater sensitivity was noted within the Malaysian varieties.

The Malaysian rice leaves had thicker major and minor veins, as compared to IR64 in control plants (refer to Figure 2.10 for a visual example, and Figure 2.11 for means and SEM), that was observed to decrease significantly in vein thickness with decreasing prevailing nitrogen concentrations ($p<0.05$). MR219 and MR253 also exhibited significant changes to stomatal density under the different nitrogen regimes. Leaf morphology and anatomy is genetically predisposed, but it has been shown that plasticity allows for the plant to adjust to less than optimum N concentrations, as seen in certain grasses (Siebenkas *et al*., 2015). Thicker veins are in part the result of larger dimensions of vascular cells (the xylem and phloem), allowing for the larger transport potential of water and sugars (Sack and Scoffoni, 2013). Thick leaves generally have high leaf N content per unit area, and this positively correlates with the amount of photosynthetic apparatus (light harvesting complexes, proteins etc.) within the leaf (Murchie *et al*., 2002). Leaf mesophyll architecture have significant implications on light attenuation within the leaf lamina (Vogelmann *et al*., 1989; Evans, 1999; Terashima *et al*., 2011; Giuliani *et al*., 2013). The combination of mesophyll architecture and stomatal size and density greatly determines the gas exchange capacity from the external environment, to the intercellular air spaces and subsequently the stroma of the chloroplast (Flexas *et al*., 2008).

While stomatal conductance to gas diffusion (Figure 2.14) did not vary largely between treatments in general, there were decreases

observed in stomatal density (abaxial surface) between the 100% N and 25% N plants across all varieties (Figure 2.9). Stomata are key players in the gas exchange between the leaf and while the mechanisms are still relatively unknown, stomatal population of newer and developing leaves may be regulated by older leaves (Lake *et al*., 2001; Terashima *et al*., 2011). The structure to function relationship, however, is realized where the rate of photosynthesis increases with increased stomatal conductance (from a general increase in stomatal density). Stomatal conductance measures the rate at which gas diffuses from the atmosphere into leaf intercellular air space within leaf mesophyll cells through the stomata (Nobel, 2009), or the inverse of stomatal resistance to CO_2 diffusion (Evans *et al*., 2009; Nobel, 2009; Giuliani *et al*., 2013). In the liquid phase (diffusion to chloroplasts), the resistance to CO_2 diffusion is stronger, which accounts for the lower concentration of CO_2 within chloroplasts (C_c) as compared to intercellular CO_2 (C_i). This have been found to greatly limit Pmax. This overall resistance is a combination of resistances exerted by various leaf organelles (cell wall, cytoplasm, etc.) and Rubisco-limited carboxylation (Evans *et al*., 2009; Tholen and Zhu, 2011; Tholen *et al*., 2012). The significant decline in Pmax was not a result of a reduced stomatal conductance, but possibly mesophyll conductance (diffusion capacity of CO_2 inside mesophyll cells). Mesophyll conductance could be estimated using three methods – (1) simultaneous chlorophyll fluorescence and gas exchange, (2) the curvature of the A/Ci curve that is Rubisco-limiting and (3) the oxygen sensitivity of photosynthesis (Pons *et al*., 2009; Bunce, 2018; Zhu *et al*., 2019). Here there is a possible exertion (although not the only reason) from limitations in structural mechanics on net photosynthesis, which was caused by the decrease in the nitrogen pool and allocation to the manufacture of leaf material.

The area of leaf 9 was found to be largely similar between varieties, even under different nitrogen treatments. Leaf area did not have a direct relationship with major and minor vein thickness, as seen from this study. However, large variations could be seen

between the accumulated leaf area, particularly in the accumulated leaf area between the control and N-deficient plants within each variety ($p<0.0001$). Leaf thickness, accumulated leaf area and photosynthetic capacity were generally correlated here. As nitrogen alters the morphology of leaves, it also has a compounding impact on the 'sun-shade' behaviour of the canopy. Sun leaves (high light) in plants under the full nutrient complement were generally thicker from the additional mesophyll layer, or longer layers of palisade mesophyll (Xu *et al*., 2009).

2.5 **Conclusion**

This controlled environment study has revealed that the effects of nitrogen deficiency on rice plants can be multi-fold and have shown to vary at the individual leaf and whole plant levels. IR64 plants evaluated in this study have shown a higher sensitivity to N deficiency in terms of leaf phenology and photosynthetic gas exchange than the Malaysian varieties. The Malaysian varieties were less affected by N treatments with respect to leaf development. Nevertheless, overall canopy size reduced with decreasing N status as the number of tillers was reduced. These findings suggest that the link between increasing N application and increasing plant productivity operates on both the micro and macro-physiological level.

Chapter 3: Analysis of the effect of nitrogen nutrition on rice canopy architecture using 3-dimensional reconstruction techniques in field-simulated conditions

Tiara Herman, Alexandra J. Burgess, Asgar A. Ali, Erik H. Murchie

TH AAA and EHM conceived and designed the experiment, while experimental work was performed by TH and AJB. TH performed gas exchange, morphology and light interception. AJB and TH performed imaging of the canopy plants. AJB performed in silico reconstruction and modelling. TH wrote the chapter with assistance from AJB, EHM and AAA.

This chapter has been written into a manuscript due to be submitted to AoB plants or Physiologia Plantarum in September 2020.

Chapter 3

3.1 Introduction

Climate change is likely to place constraints on productivity on plants both in specific natural and agricultural ecosystems, including tropical cereals (Wassmann *et al*., 2009; Seneweera *et al*., 2018). New challenges have emerged with regards to increasing yield to meet the demand of a rising global population. This has placed emphasis on farming systems that are able to adapt to and mitigate climate shocks (Sheehy and Mitchell, 2015). One of the key determinants of the changes in temperature during the seasons and climate is solar radiation. On the biomass level, sunlight contributes significantly to the productivity of photosynthetically active aquatic and terrestrial organisms (Murchie *et al*., 2015; Zhu *et al*., Kambezidis *et al*., 2012), and can have a substantial impact on the behaviour of plant canopies during periods of high light.

3.1.1 Solar radiation and canopy architecture

The maximum productivity of a plant canopy results from a combination of factors. At the leaf and individual plant level, productivity is affected by the arrangement, internal structure, dimensions and morphology of individual organs. At the community level planting density and cropping patterns emerge as key factors in productivity. Both levels or scales determine canopy architecture which is the 3-dimensional orientation of plant organs in space and can be described with varying degrees of complexity.

Canopy architecture greatly determines the 'behaviour' of light spatially and temporally on the internal and external surfaces of the plant and is dynamic due to frequent shifts between high and low light, which directly affects the carbon gain capacity of plants (Sinclair

and Horie, 1989; Kromdjik *et al*., 2016). The characteristics of leaves in the upper levels of the canopy greatly differs from lower in the canopy, in both biochemistry and morphology. These leaves receive the highest amounts of solar radiation, and as such would generally be the most photosynthetically active or the most photoinhibited portion of the plant. In canopies that are denser, such as broadleaf species and plants that tiller profusely, lower parts of the canopy are often shaded by the upper layers. Although this mechanism serves as a protection for the lower parts of the plant from high light, it is thought to be at the expense of overall plant productivity, due to a reduction in yield from the lack of light penetration to lower in the canopy, or the reduction in yield from irreversible photoinhibition (Murchie and Niyogi, 2011; Murchie *et al*., 2015; Retkute *et al*., 2015).

The modern elite varieties of cereals grown around the world currently originate from the selection of high-yielding short stature plants with shorter maturation periods during the Green Revolution in the 1960s. These plants are also generally more erect in nature, allowing light to penetrate deeper into the canopy, to maximise the leaf area index and maximise photosynthesis across a larger area of photosynthetically active organs (Sheehy and Mitchell, 2011; Furbank *et al*., 2015). In addition to this, there is also a decline in light saturated photosynthesis in the upper leaves (due to the erect nature of the canopy, more light is able to pass through to lower layers) (Evans, 1973) and thus reduces photoinhibition that is directed at only one part of the canopy (Murchie *et al*., 1999; Murchie *et al*., 2015). The spreading or distribution of light across canopy levels is key in plant response to high and low light stress, and it remains that a more erect canopy is highly desirable and that this trait should be exploited to maximise plant productivity by improving daily carbon gain, regional carbon balance as well as water use efficiency (Long *et al*., 2006b; Kwon *et al*., 2010; Song *et al*., 2013; Zhu *et al*., 2015; Burgess *et al*., 2015; Murchie *et al*., 2015; Burgess *et al*., 2017).

3.1.2 The light profile on photosynthesis

During light harvesting reactions in photosynthesis, light on the surface of photosynthetic organs is first absorbed by chlorophyll molecules. This occurs in the light harvesting complexes of Photosystem II (PSII), creating resonance energy within the thylakoid membrane. An excited electron follows one of four major pathways to return to ground state – chlorophyll fluorescence, thermal dissipation, formation of a reactive oxygen species or photochemistry. There is a complex interplay of signals and transduction pathways when it comes to how a plant behaves under different light profiles, and it is quite challenging to completely isolate a component of the response to stress. More often than not, there is an overlap of more than one stress factor, especially when plants are grown in agricultural settings where conditions are less controlled than a glasshouse for example. In response to a single photosynthetically limiting stress, the plant evokes different degrees of response, which often varies with time.

Rice is cultivated in many tropical and subtropical regions across the world, and many of these places often receive high levels of solar radiation (Murchie *et al*., 2015). Plants often experience fluctuating light levels in the field, as a result of cloud cover, wind, biotic and anthropogenic influences. In high light conditions, plants employ a plethora of photoprotective mechanisms (Demmig-Adams and Adams, 2006) in response to photoinhibition, which is the downregulation of photosynthesis through the reduction of the quantum yield of PSII, often the result of damage. In the case of sustained high solar radiation levels, severe photoinhibition can result, which confers a long-term downregulation of photosynthesis through lowered ϕPSII, which is the operating efficiency of PSII (Anderson *et al*., 1995; Murchie and Horton., 1997; Walters, 2005; Athanasiou *et al*., 2010; Retkute *et al*., 2015). High light and photoinhibition in field conditions is not uncommon (Murchie *et al*., 1999; Zhu *et al*., 2004), and plants have developed methods to overcome these fluctuating

periods of high light intensities through varying levels of photoprotection.

3.1.3 Modelling rice canopy architecture

Improving canopy architecture has shown much potential in increasing overall carbon gain of an individual plant and as a plant community (Hedden, 2003; Peng et la., 2008; Zhu *et al*., 2012; Song *et al*., 2013; Burgess *et al*., 2015). Estimating canopy photosynthesis in field grown plants is challenging and has to take into account a variety of factors derived from the extrapolation of empirical data (Burgess *et al.,* 2017). As it is common for multiple factors to limit plant photosynthesis and growth in field conditions, it is particularly useful to model the canopy architecture of plants within different environments to ascertain the canopy that maximises carbon gain. Recent studies have tried to isolate traits of ideal plant architecture and simulate plant productivity at a community scale with emergent properties (Song *et al*., 2013) using high resolution 3-dimensional imaging and mathematical modelling of crop canopies. Empirical data and further photosynthesis modelling work are needed to substantiate the framework for the design of ideal plant architecture for enhanced productivity and increased carbon gain through increased canopy photosynthesis (Long *et al*., 2006b; Zhu *et al*., 2010; Song *et al*., 2013; Burgess *et al*., 2015).

There is surprisingly little information on the alterations of 3-D canopy architecture resulting from suboptimal N conditions. For example, low nitrogen in cereal plants is known to limit tillering and leaf area (Chen *et al*., 2003). Therefore, the light distribution, light extinction and light dynamics are likely to be strongly affected. Recent developments in methodology allow us to produce realistic 3-D reconstructions of crop plants and predict detailed light distribution and dynamics in a way that is not possible using traditional manual methodology (e.g. Burgess *et al* 2015, 2017).

3.1.4 Aims and objectives

The aim of this chapter is, for the first time, to generate detailed 3-D reconstructions of Malaysian rice canopies grown with two different nitrogen application regimes in field-simulated conditions. In addition, detailed analyses of light distribution and patterns and comparisons to observed rates of photosynthesis and indicators of productivity are performed.

3.2 Methods and materials

We investigated the impact of different nitrogen regimes on three Asian rice cultivars. Two are Malaysian indica cultivars, MR219 and MR253, and the third one is the high-yielding Philippine variety, IR64. These rice lines were selected for their contrasting canopies and cultivated in a glasshouse setting. Plant physiology measurements were taken throughout the glasshouse trial, with gas exchange measurements at four key growth stages. In addition to these measurements, the development of the canopies over the growing season were imaged and reconstructed digitally using a PMVS (Patch-based Multi-view Stereo) software (Furukawa and Ponce, 2010; Wu, 2011).

3.2.1 Plant growth and experimental design

The Malaysian rice varieties, MR219 and MR253, are both from the Ministry of Agriculture Research and Development Institute (MARDI) located in Seberang Prai, Penang, Malaysia. The Philippine variety, IR64, is a high yielding cultivar from the International Rice Research Institute (IRRI). The facility used for this trial was a tropical glasshouse, FutureCrop, at The University of Nottingham, Sutton Bonington campus. This facility permits the growth of rice crop canopies in plots within beds 5 m x 5 m x 1.5 m (w x b x d). Seeds were germinted in module trays (Figure 3.1) using a mixture of

compost and sand (Levington Module compost) on the 8th of May, 2015.



Figure 3.1: Rice seedlings growing in compost before transplanting in the FutureCrop glasshouse at The University of Nottingham.

The experimental plots containing sieved sandy loam extracted from local fields were prepared (Figure 3.2a) and watered before application of fertiliser, and were divided into high nitrogen (contained 350 kg N ha^{-1}) and low nitrogen (250 kg N ha^{-1}) plots. It is important to note that both nitrogen levels are high in comparison to field conditions due to the high residual nitrogen availability in the plot. As such, no additional nitrogen was added to the soil prior to planting. Other macro (potassium and phosphorus) and micronutrients were supplied to the soil before transplanting. Water was supplied to the experimental plots through drip irrigation for 15 minutes, at 7 am and at 7 pm each day. The duration was determined by the type of soil (sandy loam) and the amount of time that was need to saturate the soil. To maintain a 12 hour photoperiod (from 7 am to 7pm), supplemental lighting was provided by metal halide lamps, which was connected to an external light sensor that detected when radiation fell below 250 $\mu mol\ m^{-2}\ s^{-1}$. Blackout blinds were activated at the end of the day to maintain a constant temperature and photoperiod, as well as a relative humidity of between 50-60%.

Seedlings were transplanted into the prepared beds of soil at the appearance of the third true leaf. The experimental plot was divided into a total of 18 plots – nine high N and nine low N microplots. Each microplot contained 42 plants in a 7 by 6 configuration (Figure 3.2b). For each variety, three high N and three low N replicates were arranged in a complete randomised block design. Line sensor PAR line quantum sensor, Skye instruments, Llandrindod Wales) was fixed into the soil at canopy level and the height were adjusted accordingly to the height of the growing canopy, to measure incident light at just above plant canopy level allowing (Figure 3.2c). Use of a ceptometer (Accupar LP-80, Decagon evices, USA) at the base of each plot canopy permitted the calculation of fractional interception. Plant growth was monitored to see varietal differences in key developmental stages (Figure 3.2d). Plants on the border of the microplots were not used for any of the measurements to avoid the border effect. At the end of the growing season, remaining plants were subsequently harvested for dry weights. During the growth cycle, pesticides and herbicides were used to minimize the proliferation of insect pests and weeds.

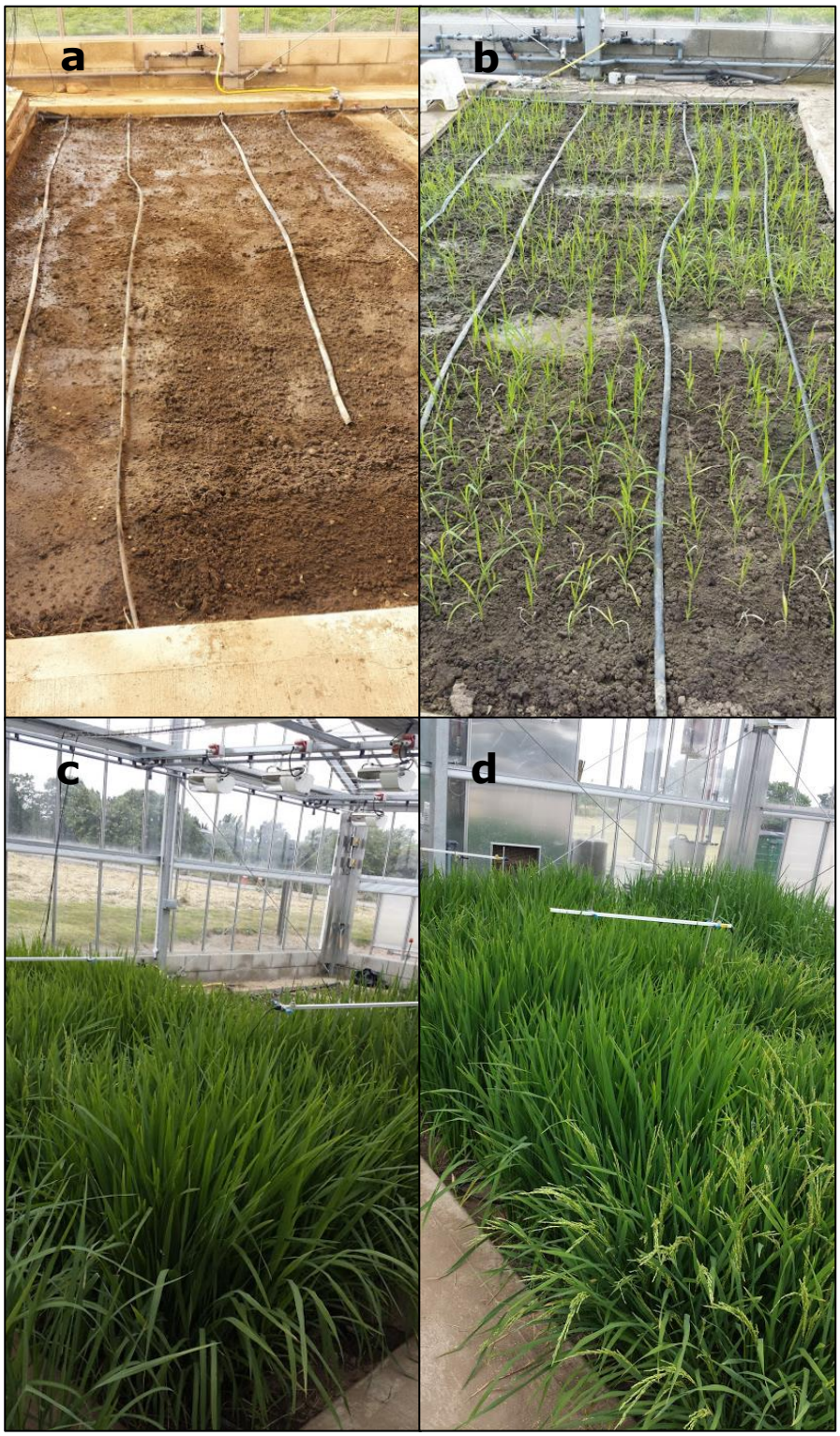


Figure 3.2: (**a**) Watered soil bed with drip irrigation water pipes, (**b**) Rice plants in their individual microplots at leaf 5 developmental stage, (**c**) Line sensors at the top of the canopy to record incident PAR, and (**d**) Early flowering in IR64 plants.

Plant physiology, gas exchange measurements and modelling were carried out over five growth stages – growth stage 1 (GS1) at 18 DAT, growth stage 2 (GS2) at 35 DAT, growth stage 3 (GS3) at 49 DAT, growth stage 4 (GS4) at 65 DAT and growth stage 5 (GS5) at 77 DAT.

3.2.2 Plant physiology measurements

Plant heights and leaf rank

Plant heights and leaf number on the main stem (leaf rank) were obtained from 15 days after transplanting (DAT), until 100 DAT, at the start of the flowering stage. For plant height, a ruler was used to measure from the base of the plant (the botom of the ruler placed on the surface of the soil) to the tip of the highest and longest leaf on the top of the plant canopy. Leaf number was noted from true leaf 6 until the emergence of the flag leaf.

Chlorophyll

Soil-plant analyses development (SPAD) measurements were taken using the Minolta 502 Plus Chlorophyll Meter (Spectrum Technologies, USA), to obtain the total available chlorophyll within a specified leaf area. Measurements were taken on the widest part of the third and fourth fully expanded leaf from the top of the canopy.

PAR within the canopy and leaf area index

The interception of photosynthetically active radiation (PAR) was measured at two canopy levels (bottom and top) using the AccuPAR LP-80 ceptometer (Decagon Devices, USA). Five measurements were taken per microplot at random positions, at both parallel and diagonal points of planting line. The leaf area index (LAI) was calculated using the in built sofware in the ceptometer and the values recorded. Care

was taken to maintain uniformity in measurements especially during particularly cloudy days where light levels fluctuate more frequently.

Leaf thickness

Leaf thickness was measured at the major and minor veins using leaf sectioning. Sections of the penultimate leaf on the main stem were cut from the widest part of the leaf using a sharp razor blade, for mounting on microscope slides. After mounting, the leaf sections were cleared using 85% (w/v) lactic acid saturated with chloral hydrate. The slides were heated in a hot water bath (70°C) for an hour. After clearing, the leaf sections were washed with distilled water and stained using 1% toluidine blue dye in 1% (w/v) disodium tetraborate. A few drops of glycerol were added to the leaf sections to preserve the samples before being viewed under a calibrated light microscope and images captured using a digital camera (Nikon DXM 1200). All images were analysed using the analytical software ImageJ.

Stomatal density

All images were analysed using the analytical software ImageJ. The stomatal density and length were determined using leaf impressions of both the adaxial and abaxial surfaces on the widest part of the flag leaf using the same method for stomatal density and length in Chapter 2. Impressions were made using Coltène® PRESIDENT Plus silicone-based impression putty. Clear nail varnish was then applied to the hardened putty and later peeled and mounted on microscope glass slides for view under a 40x-magnification confocal light microscope. Images of six fields of view were taken for each variety under each treatment for analysis (Sampson, 1961; Bakker, 1991; Hubbart *et al*., 2013).

Leaf nitrogen

Leaf nitrogen analysis was carried out by Lancrop Laboratories, York, United Kingdom. Three plants per plot were chosen at random for this analysis. For each plant, leaves were clipped at the top portion of the canopy (including the flag leaf, at 10 cm height) to make up 200

grams of fresh plant material. Samples were labeled and couriered to the laboratory on the same day.

Fresh and dry weights

The fresh and dry weights of the plants were taken at each growth stage – GS2: 35 DAT, GS3: 49 DAT, GS4: 63 DAT and GS5: 77 DAT. For fresh weights, the plants were harvested and immediately weighed (minus the roots). The plants were then transferred to an oven set to 60°C. After 48 hours, the plants were removed from the oven and weighed.

3.3.1 Gas exchange measurements

All gas exchange measurements were carried out using the Licor-6400XT (Lincoln, Nebraska) infrared gas-exchange analyser.

Light response curves

Methods employed here are similar to Chapter 2. Light response curves were obtained at four growth stages - growth stage 1 (GS1) at 18 DAT, growth stage 2 (GS2) at 35 DAT, growth stage 3 (GS3) at 49 DAT, growth stage 4 (GS4) at 65 DAT. The block temperature was maintained at 30°C using a flow rate of 500 ml min^{-1}. Reference CO_2 was maintained at 400 µl l^{-1} to simulate ambient CO_2 concentration. A stability period of between 2 and 3 minutes was programmed to allow for the leaf to adjust to the light level which contained 10% of blue light. Light was supplied through a combination of built-in red and blue light emitting diodes (LEDs). Leaf width was noted to adjust the calculations for the leaf area within the cuvette. At GS1, 2 and 3, light response curves were obtained at seven light intensities – 0, 100, 300, 600, 1000, 1500 and 2000 µmol m^{-2} s^{-1}, at two heights (top and bottom of the canopy). For the last growth stage, after flowering, more in-depth light response curves were obtained using 13 light intesities – 0, 50, 100, 150, 200, 400, 600, 800, 1000, 1200, 1500, 1800 and 2000 µmol m^{-2} s^{-1}. Measurements were taken at three heights (top, middle and bottom of the canopy). The penultimate fully extended leaf was measured at the top of the canopy. Middle of the canopy measurement was taken at the midpoint of the plant height (i.e. if the plant was 80 cm in height, measurements were taken on the leaf on the main stem at 40 cm from soil surface). All gas exchange measurements were taken on the leaves on the main stem (not tillers).

CO_2 assimilation (A/Ci)

Performed as described in chapter 2. Leaves were exposed to a light intensity of 1000 µmol m^{-2} s^{-1} throughout the measurements. The leaves were inserted in the chamber with a CO_2 concentration of 400

ppm initially for a maximum of two minutes, to stabilise the internal chamber environment around the leaf. The leaf was then exposed to different concentrations of CO_2 – 400, 400, 40, 80, 120, 200, 400, 800, 1000, 1200, 1500 μmol m^{-2} s^{-1}. A waiting time of between 60 - 200 seconds at each CO_2 concentration is used to ensure stability before a measurement is recorded (Evans and Santiago, 2014).

3.3.2 High-resolution imaging and 3-dimensional canopy reconstruction

The imaging and reconstruction of the rice canopies followed the protocol of Pound *et al*., (2014). At the four growth stages, plants were imaged using three digital single-lens reflex (DSLR) cameras (Canon 650D with a 35-mm lens) at three fixed heights using a calibration reference target of width 397mm. This allowed the imaging of the plant at a variety of angles around the plant and also from above, while the reference target helped the automatic calibration of the camera. Prior to imaging, rice plants were dug up from the soil (with roots still attached) and transferring them into pots, before moving them into the imaging area. Care was taken to prevent wilting, by supplying the root zone with water. A minimum of 40 images were taken per single plant with a revolving turntable, within 15 minutes of transfer to the pot.

An initial point cloud was acquired using the PMVS software, where the photometric consistency threshold was set to 0.45 to optimise the amount of plant material that is recognised in the point cloud (Equation 2 in Fukurawa and Ponce, 2010). The same default parameters were chosen as in Burgess *et al*., (2015) (see Image and Ray Tracing section in paper). One plant per plot was extracted at each growth stage, which resulted in a total of three replicates per variety. The resulting canopies were reconstructed by duplicating and rotating each plant at random to form a 3 by 3 grid with a 10 cm radius (within and between rows) (Burgess *et al*., 2015). Reconstructed canopies are made up of a number of triangles (*n*) that

exist within a mesh, with coordinates of the *i*th triangle given by the vector $\{x_i^1, y_i^1, z_i^1, x_i^2, y_i^2, z_i^2, x_i^3, y_i^3, z_i^3\}$. The *x* and *y* coordinates correspond to ground coordinates while *z* corresponds to the height above ground surface. Total light per unit leaf area for the *i*th triangle at time *t*, $L_i(t)$, was predicted using a forward ray-tracing algorithm applied in fastTracer (fastTracer, version 3; PICB; Song *et al*., 2013). On the ray-tracer, the latitude was set to 3, for Kuala Lumpur in Malaysia, light refelctance at 7.5%, light transmittance at 7.5%, and atmospheric transmittance at 0.5 on the day of the imaging. Over the course of the day, the light intensities over a whole rice canopy were recorded at 30 minute intervals. The software fires rays through a box with defined boundaries: when they exit one boundary (i.e. the side) they enter again from the opposite side.

3.3.3 Data modelling

All modelling was performed in Mathematica (Wolfram), by Alexandra Burgess. Cumulative leaf area index (cLAI; leaf area per unit ground area as a function of depth) was calculated from each of the canopy reconstructions. For each depth (*d*; distance from the highest point of the canopy), we found all triangles with centres lying above *d* (Equation 1).

$$d_i = \max_{j=1,2,3;1\le i\le n} z_i^j - \left(z_i^1 + z_i^2 + z_i^3\right)/3 \qquad \text{(Equation 1)}$$

We then calculated the sum of the areas of these triangles and then divided this sum by ground area. The cumulative LAI as a function of depth through the canopy was calculated using Equation 2.

$$cLAI(d) = \frac{\sum_{i=1}^{n} I(d_i \le d) S_i}{\left(\max_{1\le i\le n} x_i - \min_{1\le i\le n} x_i\right)\left(\max_{1\le i\le n} y_i - \min_{1\le i\le n} y_i\right)}, \qquad \text{(Equation 2)}$$

where *I(A)=1* if condition *A* is satisfied and S_i is the area of a triangle *i*.

The light extinction coefficient of the canopy was calculated using the 3D structural data and the light distribution obtained from ray tracing. In order to calculate fractional interception within a canopy as a function of depth at time *t*, we first identified all triangles lying above depth, *d* (Equation 1). We then calculated their contribution to intercepted light by multiplying PPFD received per unit surface area (ray tracing output) by the area of triangle. The light intercepted was summed for all triangles above the set *d,* and divided by light intercepted by ground area according to Equation 3.

$$F(d,t) = \frac{\sum_{i=1}^{n} I(d_i \le d)\, S_i L_i(t)}{L_0(t) * ground\ area}, \qquad \text{(Equation 3)}$$

where $L_0(t)$ is light received on a horizontal surface with a ground area $\left(\max_{1\le i\le n} x_i - \min_{1\le i\le n} x_i\right)\left(\max_{1\le i\le n} y_i - \min_{1\le i\le n} y_i\right)$, and $L_i(t)$ is light intercepted by a triangle *i*.

The light extinction coefficient, *k*, was calculated by fitting (by least squares) the function,

$$f(x) = a\left(1 - e^{-k\,x}\right) \qquad \text{(Equation 4)}$$

to the set of points $\{cLAI(d), F(d,t)\}$ calculated by varying depth from 0 to the height at total c*LAI* with step Δd = 1 mm, *a* in Equation 4 is a fitted parameter.

The response of photosynthesis to light irradiance, *L*, was calculated using a nonrectangular hyperbola given by Equation 5:

$$F_{NRH}(L,\phi,\theta,P_{max},\alpha) = \frac{\phi\, L + (1+\alpha)P_{max} - \sqrt{(\phi L + (1+\alpha)P_{max})^2 - 4\theta\phi L(1+\alpha)P_{max}}}{2\theta} - \alpha P_{max} \qquad \text{(Equation 5)}$$

The nonrectangular hyperbola is defined by four parameters: the quantum use efficiency, ϕ; the convexity, θ; the maximum photosynthetic capacity; *Pmax*, and the rate of dark respiration, R_d. We assumed that the rate of dark respiration is proportional to the maximum photosynthetic capacity, according to the relationship $R_d = \alpha\ Pmax$ (Givnish, 1998; Niinemets and Tenhunen, 1997; Retkute *et al*., 2015), where $\alpha = 0.1$.

Values for *Pmax* were determined from leaf gas exchange measurements. Curve fitting was carried out using the Mathematica command **FindFit** with a minimum constraint on dark respiration at 0.05 and convexity at 0.7.

As each canopy was divided into 2 layers, each triangle from the digital plant reconstruction was assigned to a particular layer *m* according to the triangle centre (i.e. with triangle centre between upper and lower limit of a layer depth). Carbon gain per unit canopy area was calculated as daily carbon assimilation over a whole canopy divided by the total surface area of the canopy according to Equation 6.

$$C = \frac{\sum_{i=1}^{n} P_i}{\sum_{i=1}^{n} S_i}. \qquad \text{(Equation 6)}$$

3.4 **Results**

3.4.1 Physiology measurements

Plant heights, leaf rank and tillers

Plant heights for high and low N plants for all three varieties are shown in Figure 3.3a, where means are plotted with standard error of means (SEM). The data was best fitted using a sigmoidal dose-response (variable slope) curve, where $R^2 > 0.850$. Maximum plant height means with SEM are denoted in Table 3.1. Same letters denote significant differences between compared pairs following a two-way ANOVA and Tukey's multiple comparisons test. Generally, IR64 plants were observed to be significantly shorter than the Malaysian varieties, in both high N and low N plants. In both Malaysian varieties, significant differences were observed between high N and low N plants ($p<0.05$), where low N plants were at least 25% shorter than high N plants. Within the IR64 variety however, no significant differences were found between the two treatments ($p>0.05$). No significant diffences were found in the rate of appearance of leaves on the main stem (leaf rank), however, as shown in Figure 3.3b. Leaf rank data was fitted using a linear regression, where $R^2 > 0.995$. Tiller number data was fitted using sigmoidal dose-response (variable slope) curve, where $R^2 > 0.940$. There were both varietal and treatment differences in the number of tillers (Figure 3.3c), as seen in the final tiller number in Table 3.1. IR64 HN plants produced the highest number of tillers ($p<0.0001$) relative to the rest of the varieities and treatments.

Chlorophyll

Spad readings (Figure 3.4) revealed similar patterns in cholorophyll content in both high N and low N plants – greenness fell sharply at 44 and 79 days after transplanting in a majority of the plants. Significant differences between high N and low N plants were observed in all three varieties ($p<0.05$), and while this was more obvious later in development, lower N MR219 plants were consistently

lower in greenness as compared to high N plants. Low N MR253 plants contained significantly higher percentage leaf N in the top layer of the canopy than low N MR219 and IR64 plants (Figure 3.5). No varietal differences were observed in high N plants. Within varieties, no differences in percentage leaf nitrogen were seen between treatments. The SPAD meter measures the difference between the transmittance of red (650 nm) and infrared (940 nm) light through the leaf

Leaf thickness

Leaf thickness at the major and minor veins (Figure 3.6) was greater in high N compared to low N MR219 plants ($p<0.0001$), whereas no significant changes were seen between high and low N 1R64 and MR253 plants. Similarly, there were significant differences in abaxial stomatal density (Figure 3.7) between low and high N MR219 plants. The abaxial and adaxial stomatal densities of the other two varieties were unaffected by the different nitrogen treatments. There were no significant differences observed in abaxial and adaxial stomatal lengths in all varieties ($p>0.05$) (Figure 3.7).

Biomass

Biomass (dry weights) (Table 3.2) between varieties and treatments were observed to be not statistically different from GS1 to GS4. In GS5, all varieties in the low N treatment had lower biomass than the high N treatments ($p<0.05$). The only varietal difference was between IR64 and MR253 under the low N treatment. Similarly, harvest biomass was observed to be significantly different between treatments, with MR253 showing substantially lower biomass in low N plants relative to high N plants ($p<0.0001$).

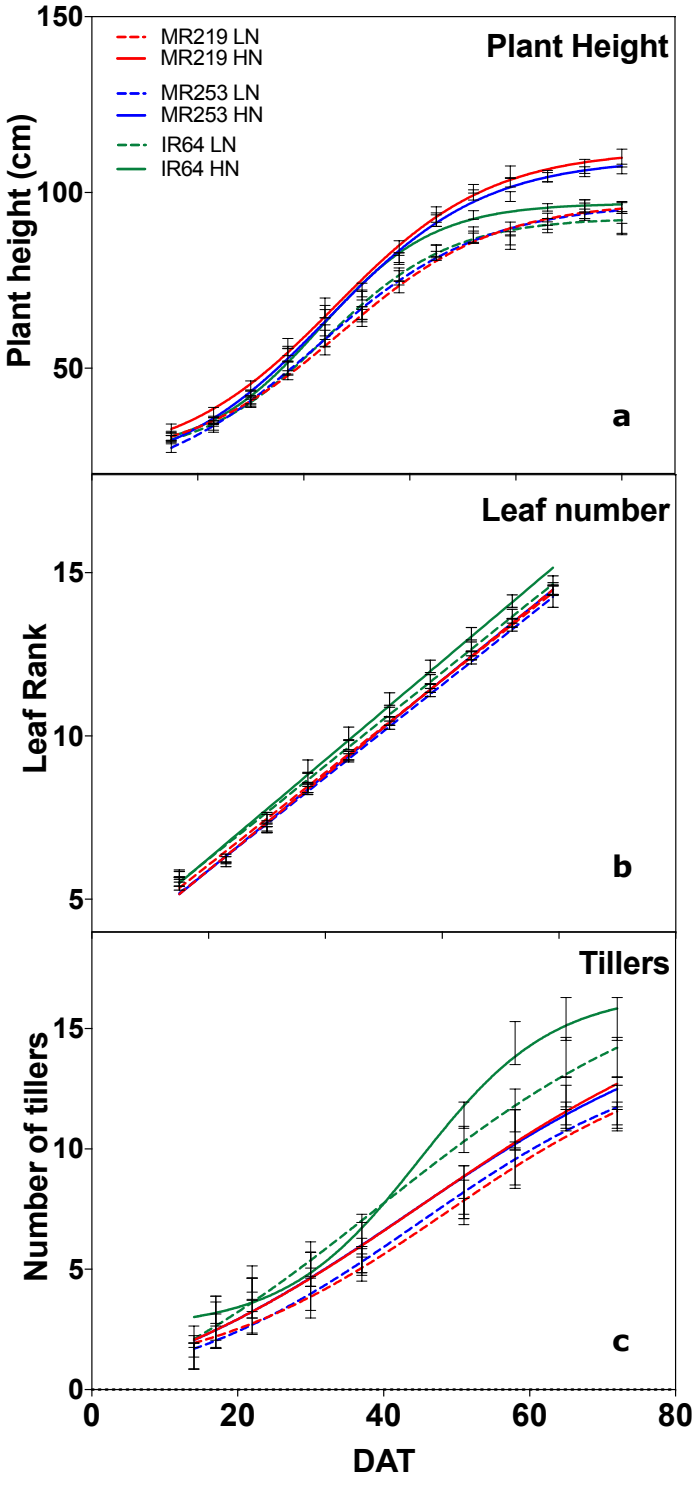


Figure 3.3: (**a**) Plant height (cm) against number of days after transplanting for all varieties under the high N (HN) and low N treatments (LN). Data was fitted using a sigmoidal dose-response (variable slope), n=15. (**b**) The number of leaves on the main stem against the number of days after transplanting. Data was fitted using a linear regression, n=15. (**c**) Number of tillers against number of days. Data was fitted using a sigmoidal dose-response (variable slope), n=5. Shown are the means and the standard errors of the mean (SEM). For some, error bars are too small to be seen.

	MR219				**MR253**				**IR64**			
	High N		**Low N**		**High N**		**Low N**		**High N**		**Low N**	
	Mean	SEM	Mean	SEM	Mean	SEM	Mean	SEM	Mean	SEM	Mean	SEM
Final plant height (cm)	110*acde*	2.15	95.7*ab*	1.70	106*bfgh*	1.01	95.6*cf*	1.53	91.5*eg*	3.08	89.6*dh*	1.63

	MR219				**MR253**				**IR64**			
	High N		**Low N**		**High N**		**Low N**		**High N**		**Low N**	
	Mean	SEM	Mean	SEM	Mean	SEM	Mean	SEM	Mean	SEM	Mean	SEM
Final tiller number	12.2*b*	0.200	11.2*a*	0.200	12.0*d*	0.447	11.4*c*	0.245	15.4*bde*	0.400	13.8*ace*	0.374

Table 3.1: Final plant heights (cm) and number of tillers of the three varieties under the two nitrogen treatments. Shown are the means and SEM. Same letters denote significant difference ($p<0.05$) between compared pairs, following a two-way ANOVA and Tukey's multiple comparisons test, where n=15.

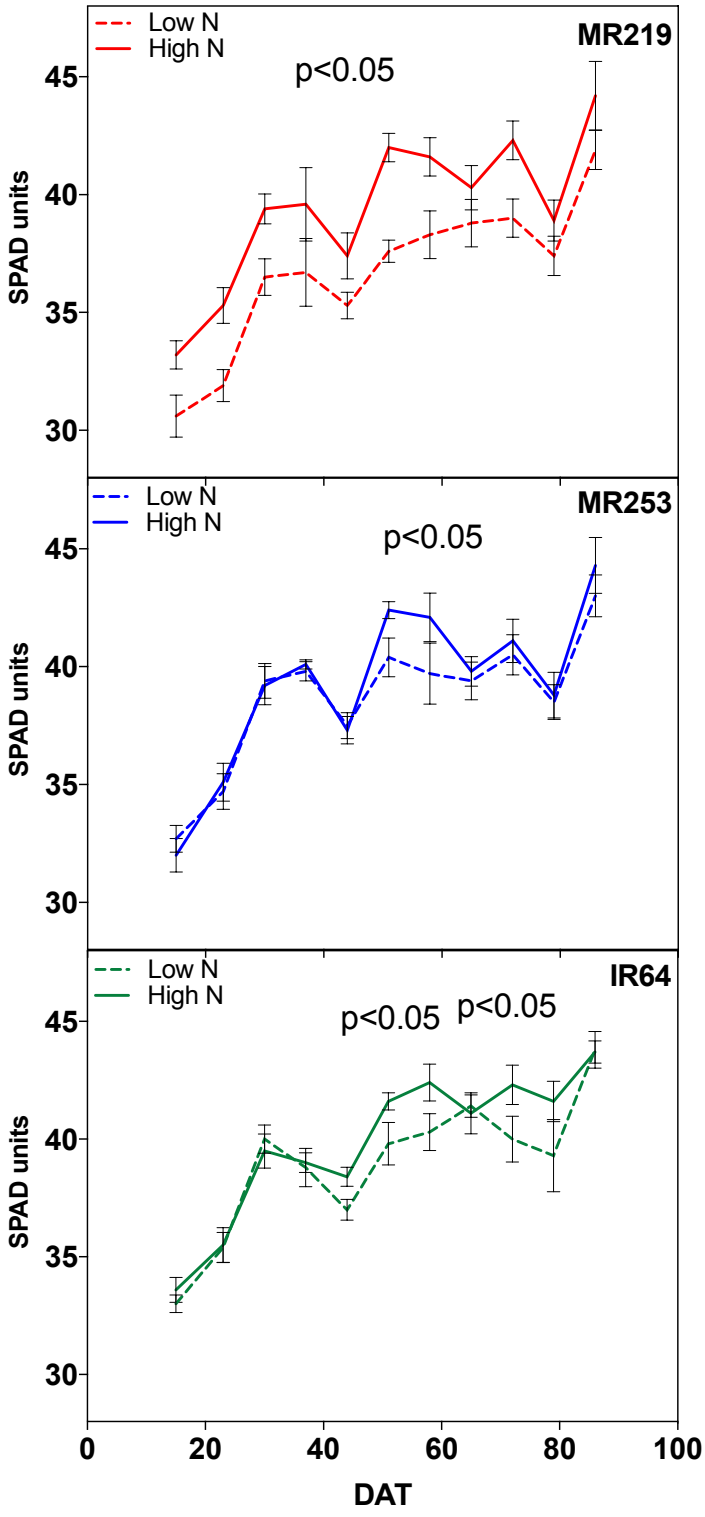


Figure 3.4: SPAD values (greenness/relative chlorophyll concentration) of the top of the canopy of rice varieties MR219, MR253 and IR64 under the high and low N treatments. Shown are the means and SEM. Bars indicate significant difference between the comparisons, ($p<0.05$), following a two-way ANOVA and Tukey's multiple comparisons test, where $n=15$.

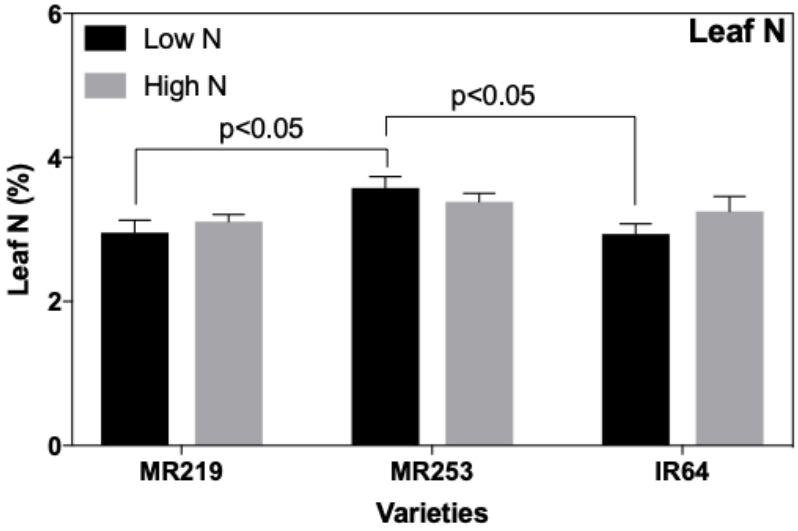


Figure 3.5: Percentage leaf nitrogen (of dry weight) in the top layer of the canopy for the three varieties under the two treatments obtained from laboratory analyses. Shown are the means and SEM. Bars indicate significant difference ($p<0.05$) following a two-way ANOVA and Tukey's multiple comparisons test, where n=3. Leaf N analyses (Kjeldahl method) conducted by Lancrop Laboratories (Pocklington, York).

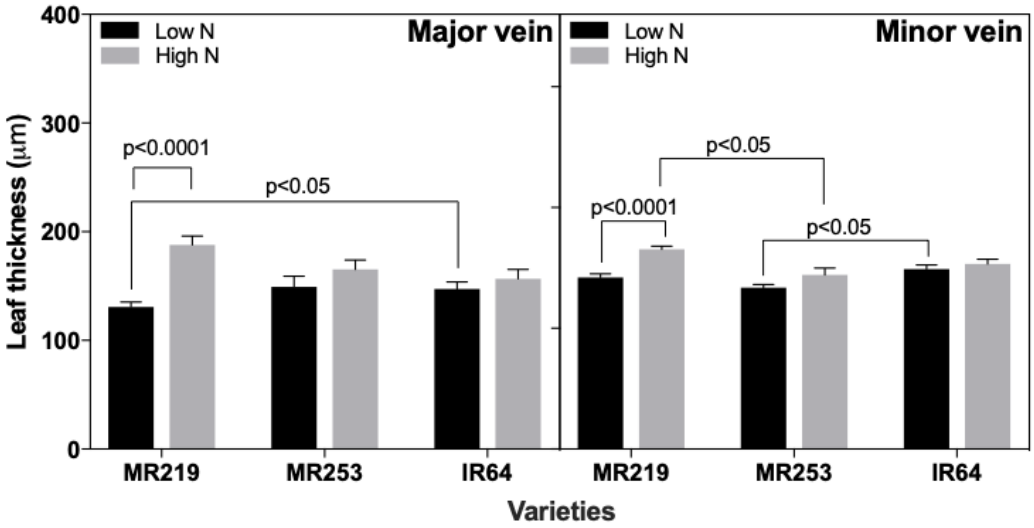


Figure 3.6: Major and minor vein thickness (μm) of the penultimate leaf on the main stem in all three varieties under the two treatments. Shown are the means and SEM. Bars indicate significant difference ($p<0.05$) following a two-way ANOVA and Tukey's multiple comparisons test, where n=12.

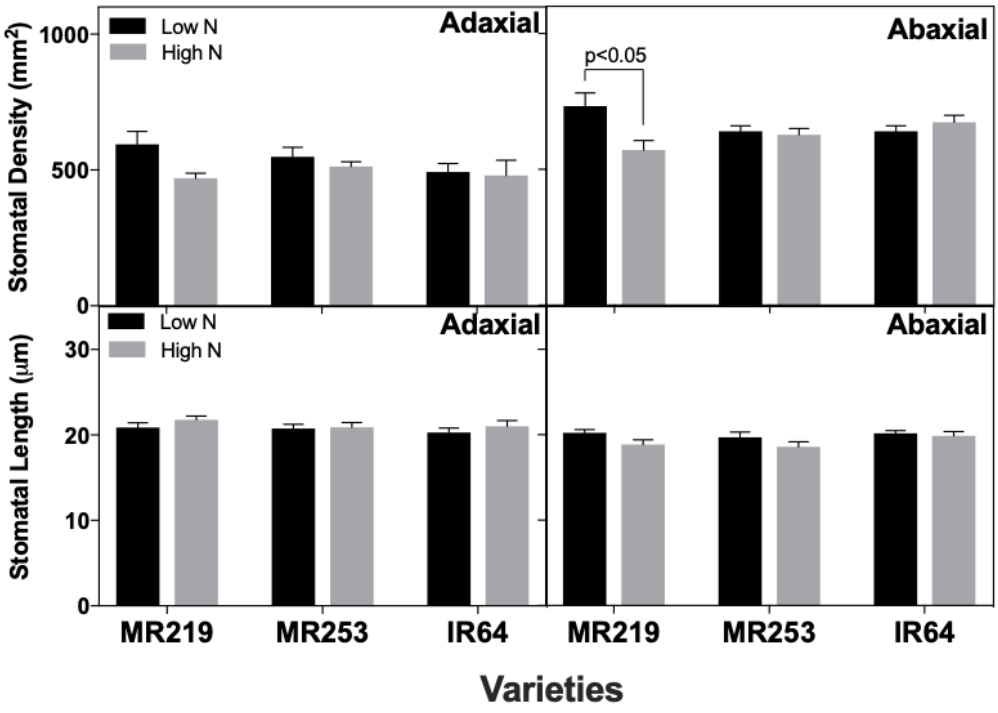


Figure 3.7: Penultimate leaf stomatal density and lengths for adaxial and abaxial leaf surfaces in all three varieties under both treatments. Shown are the means and SEM. Bars indicate significant differences ($p<0.05$), following a two-way ANOVA and Tukey's multiple comparisons test, where n=6.

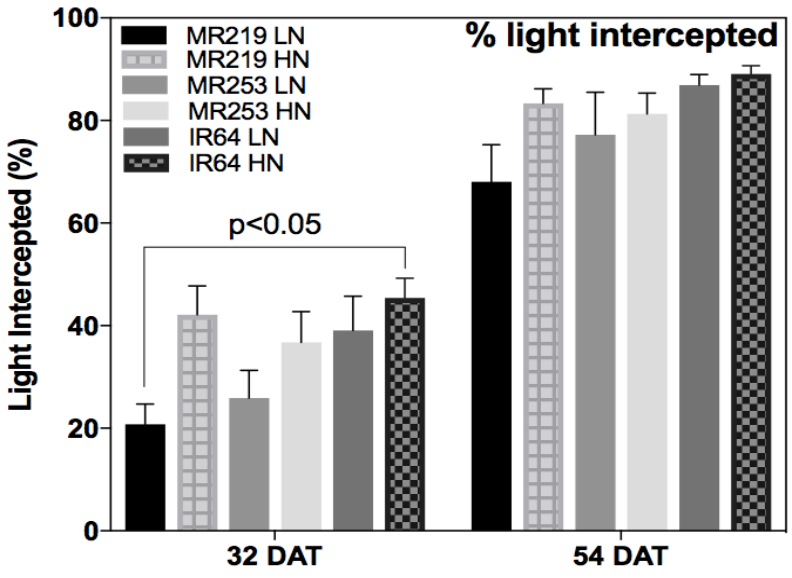


Figure 3.8: Percentage of light intercepted by the plant canopy measured using canopy line sensors above and below the canopy. Shown are the means and SEM. Bars indicate significant difference, $p<0.05$, following a two-way ANOVA and Tukey's multiple comparisons test, where n=3.

Low N										
Growth Stage	*GS2*		*GS3*		*GS4*		*GS5*		*Harvest*	
Dry Weight (g)	Mean	SEM	Mean	SEM	Mean	SEM	Mean	SEM	Mean	SEM
IR64	2.40	0.204	8.94	1.46	16.3	4.15	18.6*cd*	2.07	18.6	1.14
MR219	2.57	0.241	13.1	2.10	14.9	1.94	16.7*a*	2.50	15.1*e*	0.866
MR253	2.06	0.284	6.13	0.729	11.4	0.201	9.99*bc*	0.863	17.5*g*	1.07

High N										
Growth Stage	*GS2*		*GS3*		*GS4*		*GS5*		*Harvest*	
Dry Weight (g)	Mean	SEM	Mean	SEM	Mean	SEM	Mean	SEM	Mean	SEM
IR64	2.41	0.237	10.8	0.653	10.6	0.693	27.1*d*	4.43	19.4*f*	1.07
MR219	3.27	0.476	8.50	1.63	15.0	0.516	25.8*a*	4.95	27.2*ef*	1.86
MR253	2.19	0.396	11.8	0.497	13.6	1.34	18.5*b*	1.72	30.0*g*	1.86

Table 3.2: Mean dry weights (g) of the three varieties at growth stages 2 (GS2), 3 (GS3), 4 (GS4), 5 (GS5) and at harvest with the SEM, n=3. Same letters indicate significant differences between compared pairs (both varieties and treatment), following two-way ANOVA ($p<0.05$) and Tukey's multiple comparison's test.

3.5.1 Gas-exchange measurements

Light response curves were obtained at GS1, GS2 and GS3 for the top and bottom layers of the canopy (Figure 3.9). At GS4, more detailed light response curves were obtained (top, middle, bottom of the canopy), at more PPFD points (Figure 3.10). Light response data was curve-fitted using two different light-response curve-fitting tools – one by Ye, (2007) for individual LRC curve-fitting whilst the modelling used the Mathematica command '**FindFit'** (with a minimum value of 0.05 for dark respiration) to calculate carbon gain. Table 3.3 show the Pmax values of GS1, GS2 and GS3, while Pmax, light compensation point, dark respiration and quantum yield are tabulated in Table 3.4.

For GS1, 2 and 3, Pmax did not differ significantly between varieties under the high and low N treatments. Similarly in GS4, there were no differences in Pmax observed between treatments at individual canopy levels for all the varieties. Expected differences were seen between the different levels of the canopy, where the highest Pmax values were observed at the top of the canopy and the lowest at the bottom of the canopy (data not shown). The A/Ci curve analysis revealed a reduction in the maximum carboxylation rate of Rubisco (Vc_{max}) and RuBP regeneration rate (J_{max}) in low N MR253 plants compared to high N plants, but this was not evident in the other varieties (Figure 3.11).

3.5.2 Canopy reconstructions and modelling

Figure 3.12 illustrates the final canopy reconstructions of the three rice varieties under the two treatments in GS5, while Figure 3.13 show a timecourse of canopy resconstructions, using a IR64 HN plant as an example. Leaf area index values (total LAI) and canopy extinction coefficient (k values), were obtained from ray tracing are shown in Figure 3.14a and Figure 3.14b, respectively while carbon

gain per unit leaf area as well as per unit ground area were calculated from modelled data is shown in Figure 3.14c. Canopy extinction coefficient was higher in the low N plants at the start, but levelled off at the end of the growth cycle. It can be seen that N treatment had more of an effect after 40 DAT, where high N plants had greater LAI relative to low N treatment plants. Carbon gain per unit ground area increased over the growth stages, but the opposite occurred in the carbon gain per unit leaf area over time for most of varieties under both N treatments. These differences can be attributed to the differences in LAI between the different canopies.

From canopy reconstructions, plant height and leaf angle inclinations as a function of depth, (Figure 3.15a and Figure 3.15b respectively) were calculated and averaged at each canopy depth, and were found to be different between the canopies. High N treated plants were generally taller than those in the low N treatment. IR64 plants in the low N treatment had lower inclination angles towards the top of the canopy (between 750 and 850 mm of plant height), indicating a more horizontal canopy. The Malaysian varieites exhibited a more vertical stature, with more vertical leaves at the top of the canopy, regardless of the N treatment. Interestingly, even though the low N plants were shorter, the leaves were observed to be much steeper than the high N plants.

Figure 3.16 illustrates the cumulative leaf area index (cLAI) and fractional interception (FI) across the five growth stages. A general sigmoidal response was observed for both parameters. In all varieties, high N treated plants showed a steeper rise in cLAI in the first three growth stages. At GS4 however, cumulative LAI increased more rapidly in lower N treated plants. At the final growth stage, mixed patterns were observed. Similar patterns were seen in FI, with tendency towards increased interception of light within the middle canopy regions. Total LAI (Figure 3.14a) is observed to follow a similar trend as well, where a higher LAI is seen in the earlier growth stages in high N treated plants.

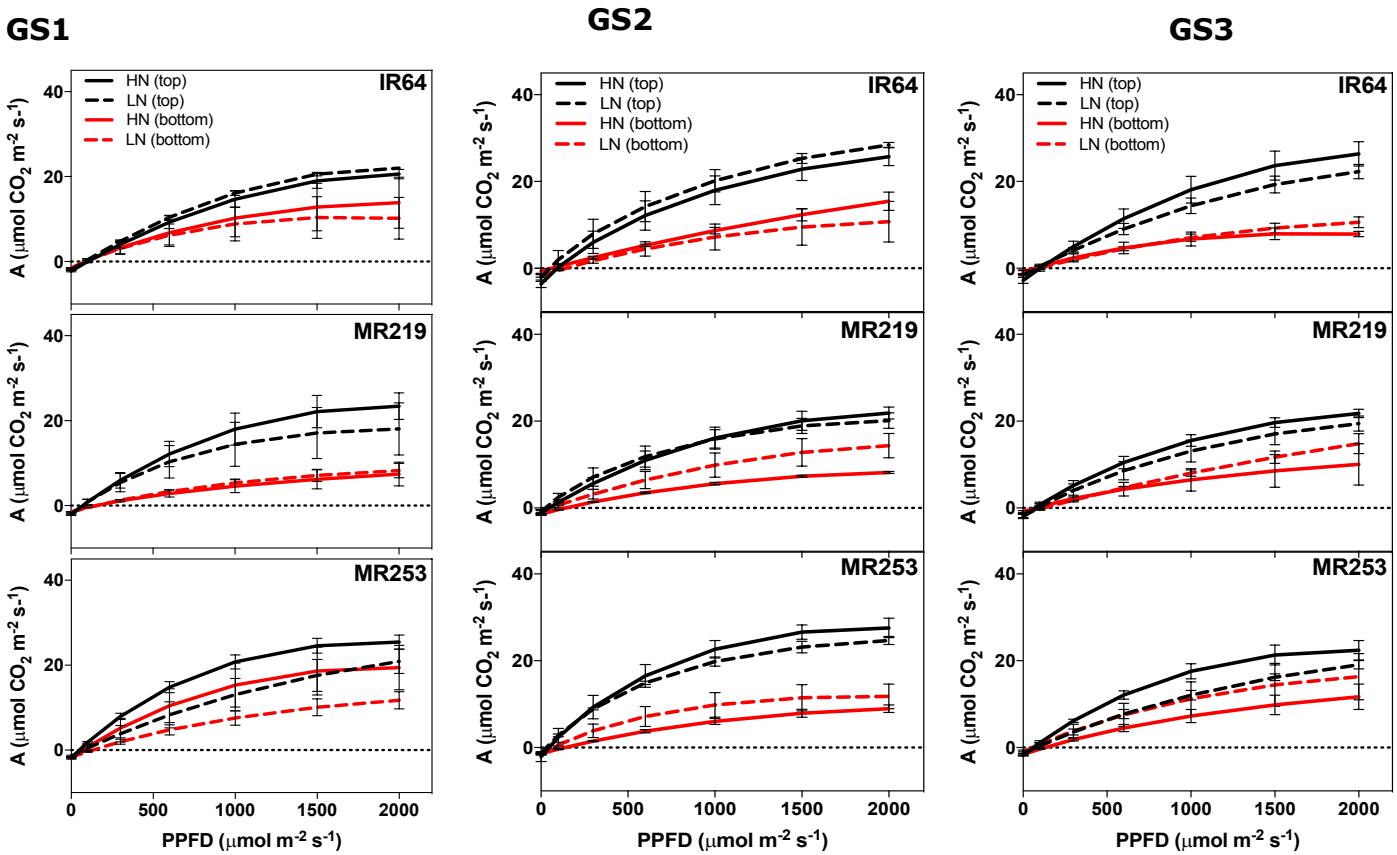


Figure 3.9: Light response curves of plants at growth stages 1 (GS1), 2 (GS2) and 3 (GS3), for the top and bottom levels in the canopy. Shown are the mean photosynthetic assimilation rates, A, (μmol CO_2 m^{-2} s^{-1}) at increasing photosynthetic photon flux densities (PPFD in μmol m^2 s^{-1}) and SEM bars, where n=3. Data has been fitted using a light response curve-fitting tool (Ye, 2007). HN – high nitrogen, LN – low nitrogen.

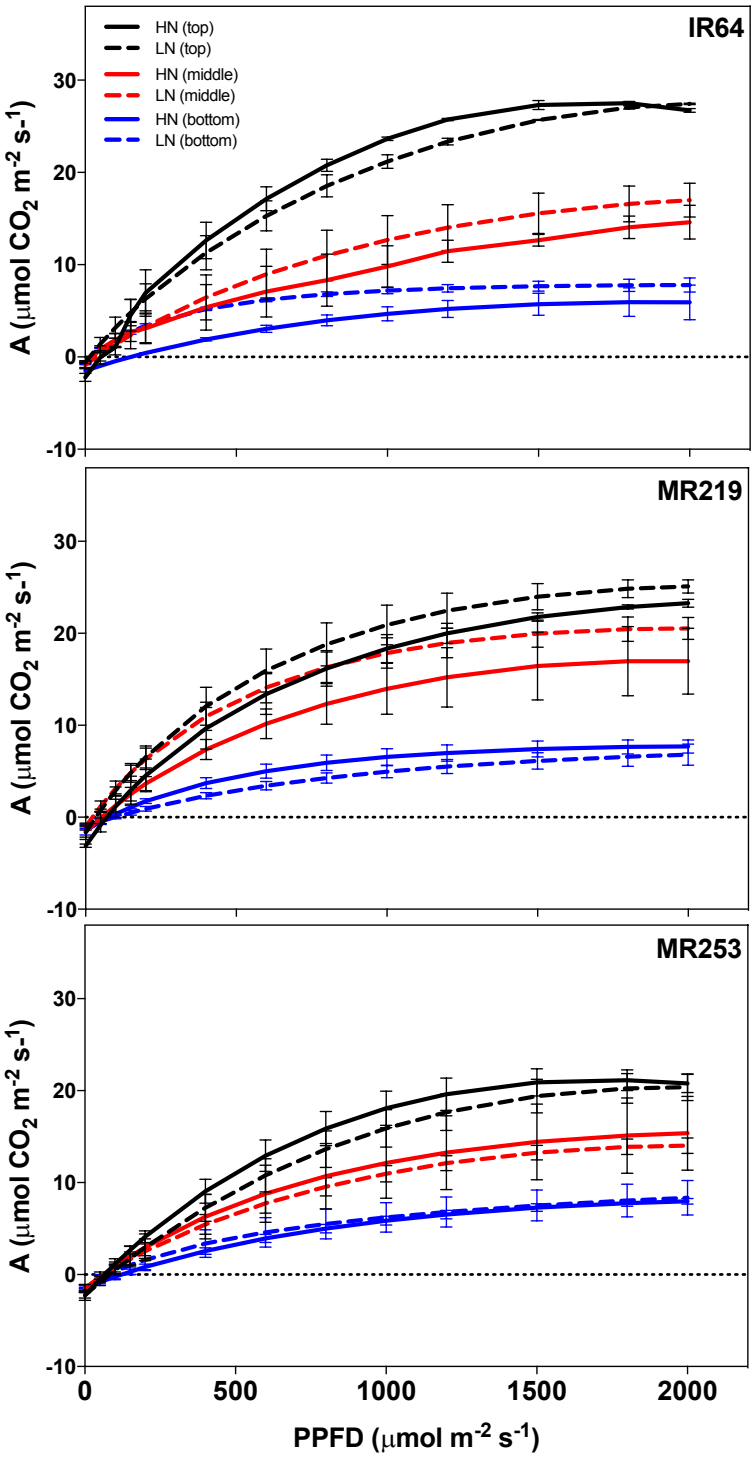


Figure 3.10: Detailed light response curves of plants at GS4 (65 DAT), for the top, middle and bottom levels of the rice canopy. Shown are the mean photosynthetic assimilation rates, A, (μmol CO_2 m^{-2} s^{-1}) at increasing photosynthetic photon flux densities (PPFD) and SEM bars, where n=3. Data has been fitted using a light response curve-fitting tool (Ye, 2007). HN – high nitrogen, LN – low nitrogen.

GS1

	High N				Low N			
Level in canopy	*Top*		*Bottom*		*Top*		*Bottom*	
Pmax	Mean	SEM	Mean	SEM	Mean	SEM	Mean	SEM
IR64	19.9	1.38	18.7	0.250	21.0	0.120	9.00a	5.31
MR219	22.7	3.22	7.25	0.950	22.8	0.300	5.03	2.29
MR253	24.5	1.65	18.0	5.85	20.3	2.61	9.47	2.64

GS2

	High N				Low N			
Level in canopy	*Top*		*Bottom*		*Top*		*Bottom*	
Pmax	Mean	SEM	Mean	SEM	Mean	SEM	Mean	SEM
IR64	25.3c	2.11	15.2	2.07	28.2ab	0.504	10.7	3.87
MR219	21.7	1.48	8.07	0.233	20.0	1.80	14.2	2.85
MR253	28.3ef	1.99	8.83e	0.829	24.2	0.664	14.8	0.600

GS3

	High N				Low N			
Level in canopy	*Top*		*Bottom*		*Top*		*Bottom*	
Pmax	Mean	SEM	Mean	SEM	Mean	SEM	Mean	SEM
IR64	26.2d	2.87	8.63cd	1.10	22.1	1.69	10.5b	1.21
MR219	21.7	0.987	9.65	4.95	19.3	1.83	14.5	2.23
MR253	22.4	2.29	11.5f	2.91	18.9	0.887	11.0	2.20

Table 3.3: The photosynthetic assimilation rates, P_{max}, (μmol CO_2 m^{-2} s^{-1}) for the rice varieties in both high and low nitrogen plots, at the top and bottom levels of the canopy, at growth stages 1 (GS1), 2 (GS2) and 3 (GS3). Shown are the means and their SEM, where n=3. Same letters indicate significant difference between the compared means ($p<0.05$) using a two-way ANOVA (comparing variety, treatment and level in canopy) and Tukey's multiple comparisons test.

Table 3.4: The photosynthetic assimilation rates, P_{max}, (μmol CO_2 m^{-2} s^{-1}), light compensation point (μmol photons m^{-2} s^{-1}), dark respiration, Rd, (μmol CO_2 m^{-2} s^{-1}) and maximum quantum yield (μmol CO_2 m^{-2} $s^{-}1$) for the rice varieties in both high and low nitrogen plots, at the top, middle and bottom levels of the canopy, at growth stage 4. Shown are the means and their SEM, where n=3. Same letters indicate significant difference between the compared means ($p<0.05$) using a two-way ANOVA (comparing variety, treatment and level in canopy) and Tukey's multiple comparisons test.

	High N						**Low N**					
Level in canopy	*Top*		*Middle*		*Bottom*		*Top*		*Middle*		*Bottom*	
P_{max} (μmol CO_2 m^{-2} s^{-1})	Mean	SEM	Mean	SEM	Mean	SEM	Mean	SEM	Mean	SEM	Mean	SEM
IR64	27.0*cd*	0.584	13.2*c*	1.55	3.83*d*	1.41	26.5*ab*	0.367	16.1*aj*	1.89	6.03*bj*	0.312
MR219	22.2*f*	0.742	15.2	4.25	4.93*f*	0.974	24.3*e*	0.500	18.8*k*	1.55	3.63*ek*	0.991
MR253	20.6*h*	1.38	13.3*m*	4.41	5.07*hm*	0.567	19.5*g*	1.47	12.1	0.895	5.90*g*	2.21

	High N						**Low N**					
Level in canopy	*Top*		*Middle*		*Bottom*		*Top*		*Middle*		*Bottom*	
Light compensation Point (μmol photons m^{-2} s^{-1})	Mean	SEM	Mean	SEM	Mean	SEM	Mean	SEM	Mean	SEM	Mean	SEM
IR64	58.3*a*	12.8	59.9*b*	45.4	150*abc*	0.00	18.4	6.70	57.9	26.5	23.6*cd*	5.50
MR219	85.5	32.6	54.6	21.0	74.6	11.9	27.3	11.3	25.0	11.1	97.2	27.4
MR253	64.0	5.90	71.3	27.7	121*d*	28.6	86.6	15.6	70.2	17.0	112	38.5

	High N						**Low N**					
Level in canopy	*Top*		*Middle*		*Bottom*		*Top*		*Middle*		*Bottom*	
Dark respiration (μmol CO_2 m^{-2} s^{-1})	Mean	SEM	Mean	SEM	Mean	SEM	Mean	SEM	Mean	SEM	Mean	SEM
IR64	2.53*ade*	0.120	0.767*a*	0.384	1.50	0.00	0.567*dfg*	0.133	0.867	0.285	0.700	0.115
MR219	3.10*bce*	0.208	1.60*b*	0.551	0.900*c*	0.00	1.63	0.801	1.03	0.371	1.00	0.265
MR253	2.23*g*	0.561	1.50	0.436	1.47	0.376	2.23*f*	0.338	1.47	0.296	1.43	0.0667

	High N						**Low N**					
Level in canopy	*Top*		*Middle*		*Bottom*		*Top*		*Middle*		*Bottom*	
Max Quantum yield (ϕCO_2)	Mean	SEM	Mean	SEM	Mean	SEM	Mean	SEM	Mean	SEM	Mean	SEM
IR64	0.0396*ab*	0.00581	0.0200*a*	0.00534	0.00783*b*	0.000271	0.0347	0.00696	0.0204	0.00716	0.0188	0.000526
MR219	0.0356*e*	0.00701	0.0251	0.00349	0.0142*e*	0.00268	0.00391*c*	0.00891	0.0355*d*	0.00474	0.00857*cd*	0.000510
MR253	0.0305*f*	0.00520	0.0213	0.00726	0.0104*f*	0.000768	0.0274	0.00649	0.0186	0.00433	0.0135	0.00501

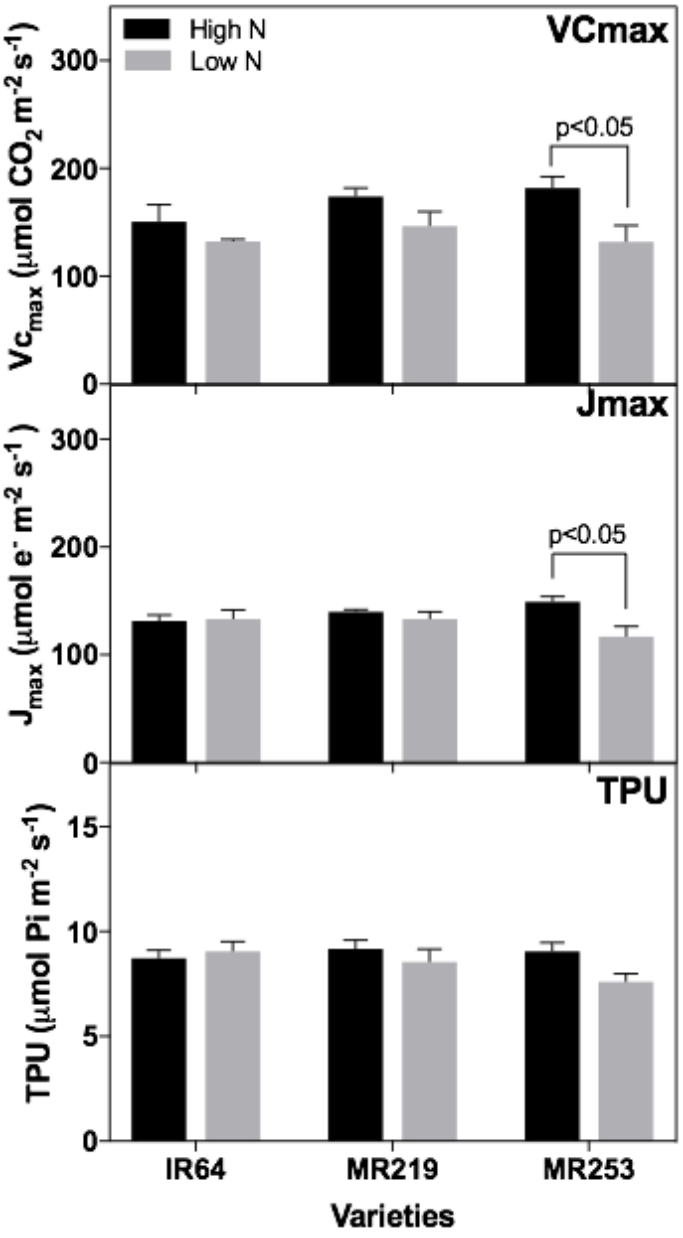


Figure 3.11: Maximum carboxylation rate of Rubisco (Vc_{max}), RuBP regeneration rate (J_{max}) and triosphosphate utilisation (TPU) of the rice varieties at 25°C, under the high and low N treatments, of the youngest fully extended leaf at growth stage 3. Values were calculated using the curve-fitting tool by Sharkey *et al*., (2007). Shown are the means and the SEM, n=3. For each bar, same letters indicate significant differences between comparisons following two-way ANOVA ($p<0.05$) and Tukey's multiple comparisons test.

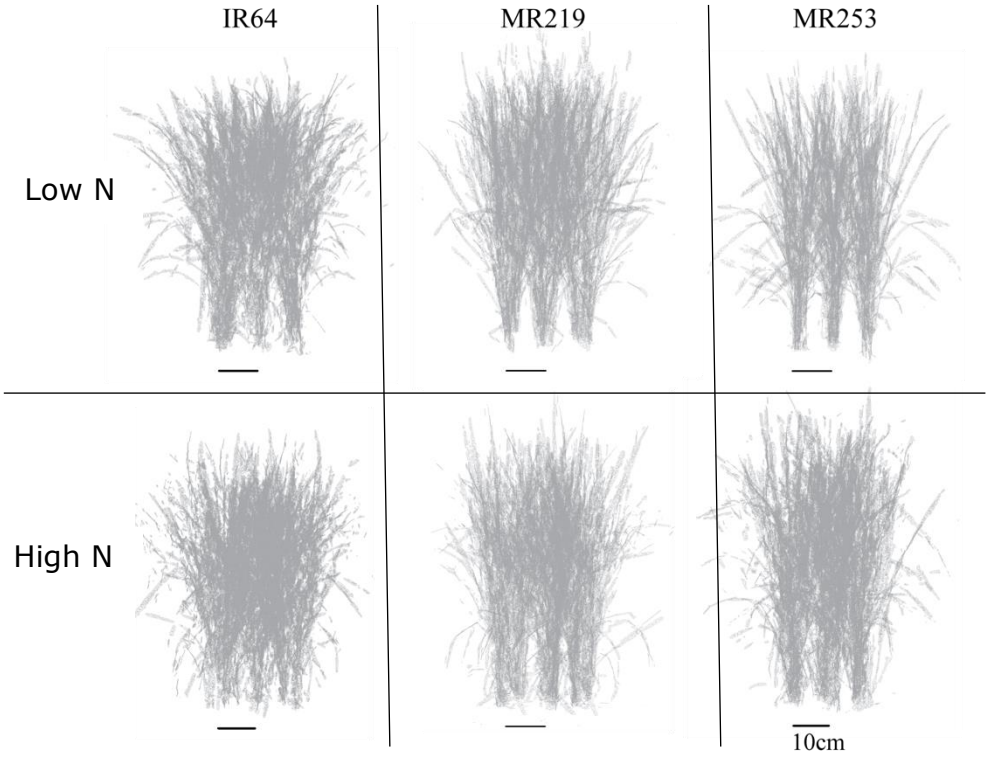


Figure 3.12: Representations of the whole canopy constructions at the final growth stage, GS5. Some visual differences in density and leaf angle can be seen between the varieties with only minor differences observed between N treatments. (Acknowledgement: Alexandra Burgess)

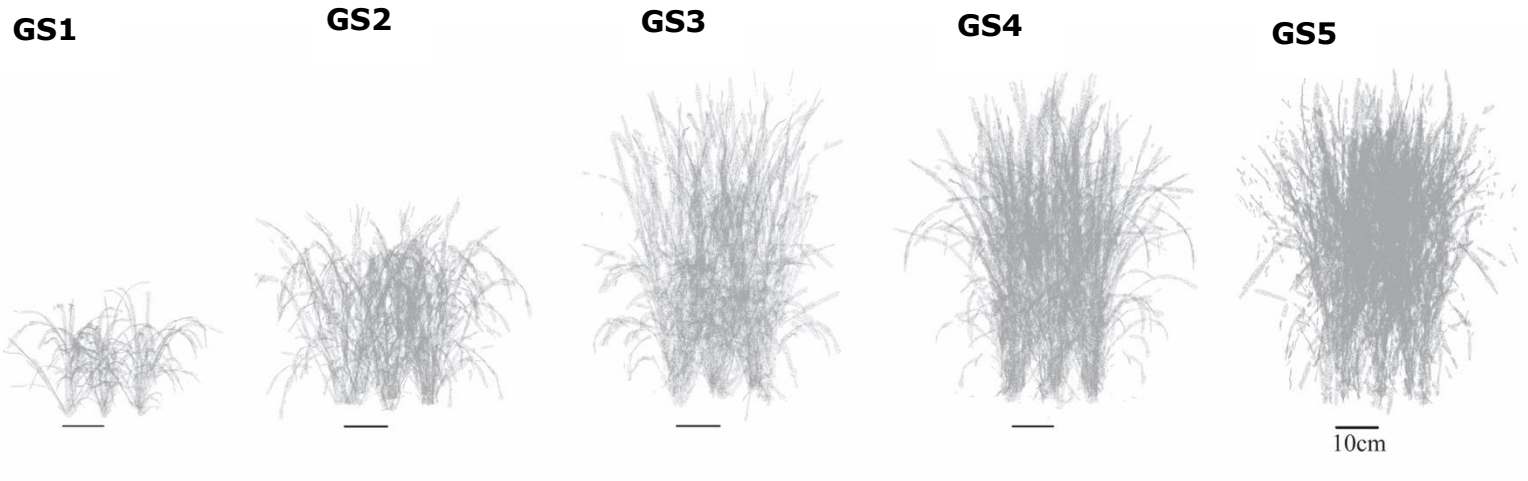


Figure 3.13: Representations of the whole canopy constructions at each growth stage (GS) for IR64 HN (high N). GS1 – 18 DAT, GS2 – 25 DAT, GS3 – 49 DAT, GS4 – 65 DAT, GS5 – 77 DAT. (Acknowledgement: Alexandra Burgess)

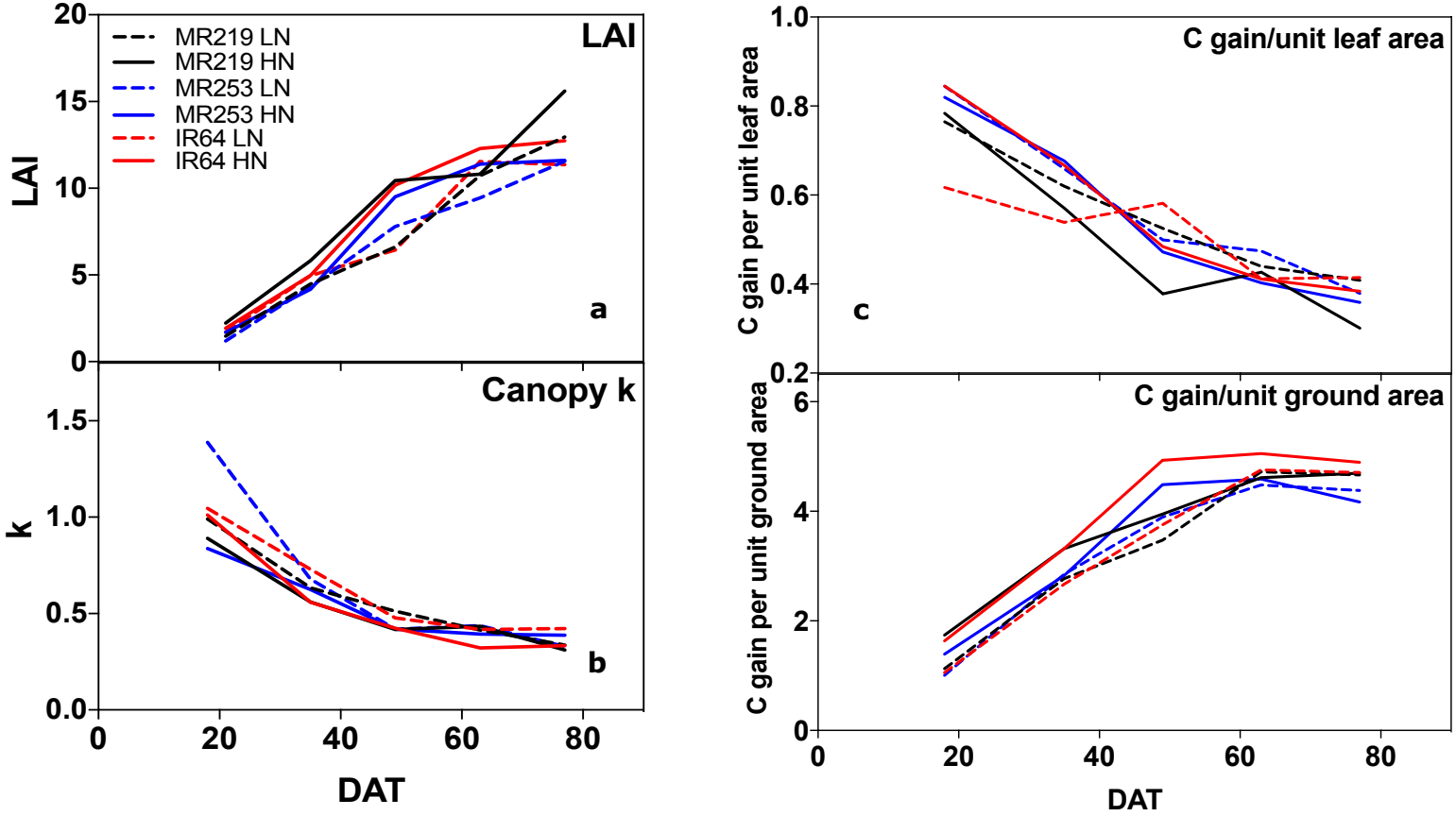


Figure 3.14: (**a**) Modelled Leaf area index, (**b**) canopy extinction coefficient, k, values and (**c**) Predicted carbon gain per unit leaf and ground area over the five growth stages. (Acknowledgement: Alexandra Burgess)

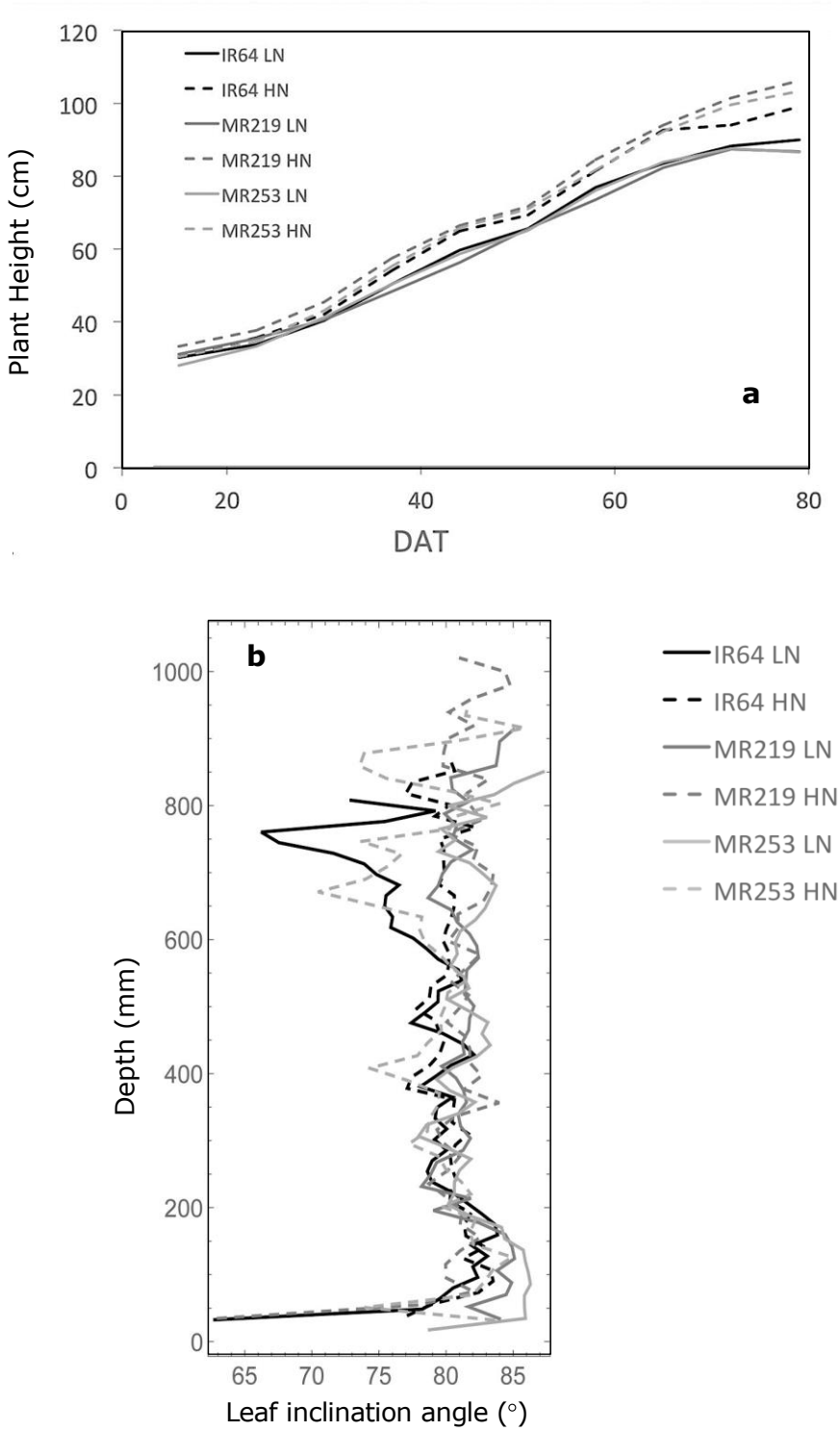


Figure 3.15: (**a**) Modelled plant height and (**b**) Leaf inclination angles (°) from the bottom to the top of the plant canopy (with increasing depth in the canopy) for all treatments. The mean inclination angle was calculated (horizontal subsection with respect to the vertical subsection). Here, an angle approaching 0 indicates a more horizontal leaf while an angle approaching 90 degrees indicates an increasingly vertical leaf (Burgess *et al*., 2017). Data processed in Mathematica. (Acknowledgement: Alexandra Burgess)

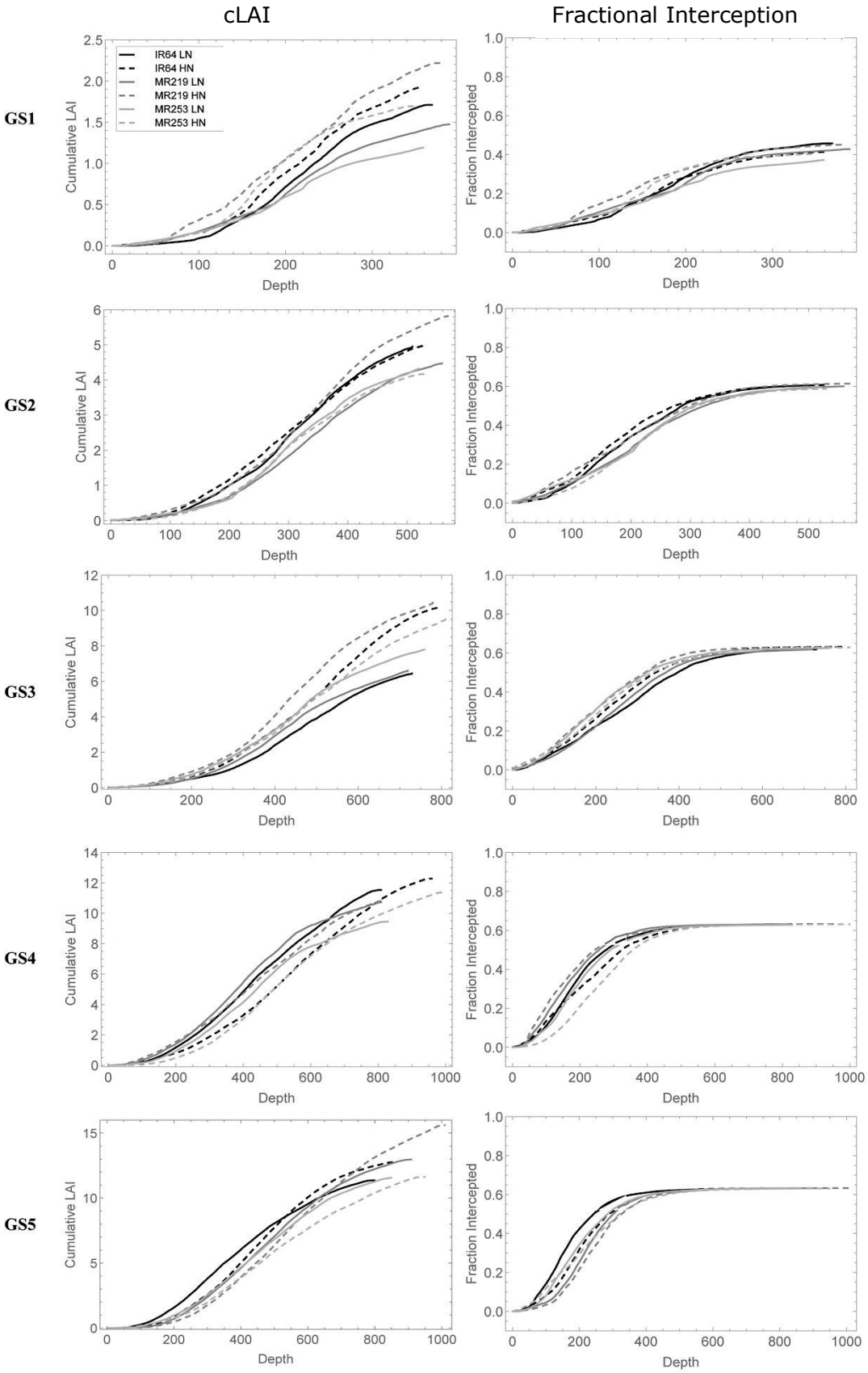


Figure 3.16: Modelled cumulative leaf area index (cLAI) (the area of leaf material per unit ground as a function of depth) and fractional interception (FI) with increasing depth (mm) for all growth stages. Data processed in Mathematica. (Acknowledgement: Alexandra Burgess)

3.6 **Discussion**

The arrangement of photosynthetic material (and surfaces) and the many layers of leaves of a plant affect how light is intercepted and how CO_2 is assimilated (Nobel *et al*., 1993; Burgess *et al*., 2017; Chang *et al*., 2019). Plants growing in a comparable light environment can exhibit complex spatial variations in the arrangement of these canopy components (Falster and Westoby, 2003), making it difficult to assess the productivity (and potential yield) of whole plant canopy. This complexity is further compounded in field conditions when growing conditions are less than optimal. As photosynthesis is closely linked to plant productivity and yield, a canopy that maximises light interception will intrinsically increase plant productivity and yield. Nitrogen is an essential macronutrient for plant growth and development, and therefore critical in determining canopy structure. As the structure of the canopy is directly linked to the light environment, assessing the architecture would shed light on how nitrogen affects whole canopy productivity.

In this study, the effects of two different nitrogen treatments on canopy architecture of two Malaysian and one high-yielding Philippine rice cultivars were examined across five growth stages using digital plant reconstruction coupled with gas exchange measurements. The resulting digital reconstructions were put through a forward ray tracer (Song *et al*., 2013) to model the 'behaviour' of light within the rice plant canopy, to accurately predict LAI, extinction coefficient and leaf inclination angles. Modelled data can be used in this way, as validated by previous studies in wheat and contrasting rice lines (Burgess *et al*., 2015; 2017). One of the key characteristics of using this image-based canopy reconstruction is that it is able to provide us more in-depth information about the canopy, that would otherwise be labour intensive to capture with rule-based approaches.

3.6.1 Nitrogen on the photosynthesis of a canopy

The majority lack of differences in P_{max} values, light compensation points, dark respiration and maximum quantum yield values ($p>0.05$) between high and low N treated plants was noted in all varieties. As indicated before, this could be due to the mild N treatment that was employed here as a result of residual nitrogen in the soil beds. Another possible reason would be the conservative characteristic of the Gramineae family where there is a tendency to prevent the dilution of canopy nitrogen (similar mechanism seen in extension rates of leaves on the main stem in Chapter 2, Figure 2.6) (Chen *et al*., 2003). It was expected that the lower regions of the canopy would exhibit a lowered photosynthetic capacity (and the corresponding parameters) as shown in Figure 3.9 and 3.10, due to the reduction of the amount of light received lower in the canopy.

Leaf nitrogen was similar between the high and low N treatment, which could have very likely contributed to the similar photosynthetic rates seen above. Interestingly, MR219 showed a little more susceptibility to a lowered N status, a possible implication as a result of lower stomatal density on the abaxial leaf surface as well as a very significantly thinner major vein thickness for leaves in the low N treatment. MR253 did not demonstrate the same responses (low N treated plants had similar characteristics as high N plants), which could explain why this particular variety is suited for more marginal growing conditions in Malaysia.

3.6.2 N status effects on rice canopy architecture

From this study we found that there was a larger accumulation of leaf area during the middle to late growth stages in most of the low N treated plants (seen in the differences in total LAI, Figure 3.14a). This delayed growth could have been because of relatively

high residual N in the soil beds in the Futurecrop glasshouse, where low N treated plants would have been able to utilize some of the available residual N, as the roots grew deeper into the soil bed.

The canopy light extinction coefficient, k value, is determined by the inclination angles of the leaves and solar elevation (called the zenith angle), which vary spatially and temporally. (Monsi and Saeki, 1953; Campbell, 1986; Zhang *et al*., 2014). The light extinction coefficient is assumed as a constant in many crop simulation models but vary vastly between the plants in different terrestrial ecosystems. For systems growing wheat, soybean and rice, a *k* value of 0.65, 0.45 and 0.5 respectively is normally used (Zhang *et al*., 2014). A low *k* value denotes a canopy with more upright leaves, where more solar radiation is able to pass through to the bottom layers of the plant canopy. It was observed here (Figure 4.13b) that k was lower in high N plants, permitting more light penetration into the canopy which in turn results in the accumulation of a higher LAI across the growing cycle. This contributes to a higher productivity long term. It is important to note however, that the higher k value and the low LAI in low N plants may not only be the result of lower overall productivity, but also due to a combination of that and photoprotective responses against high light. In instances of high light (which is present in tropical rice growing regions; see Section 1.5.5), plants growing in suboptimal conditions, while having a reduction in the number of photosynthetic apparatus, may also exhibit a reduction in canopy radiation use efficiency which is itself limited by factors such as photoinhibition (Murchie *et al*., 2009; Murchie *et al*., 2015). A higher extinction coefficient inherently indicates the presence of a more horizontal canopy. We found that in this study, low N plants had a higher k value. A more horizontal canopy for plant with lowered N status could be largely a strategy to enhance light capture on the youngest part of the canopy where the photosynthetic capacity is most likely the highest and concentrated.

Leaf inclination angles, LAI and the amount of light interception are closely linked. The theoretical implicit cost of higher leaf angles (i.e. a more erect canopy) is a decrease in the potential daily carbon gain through a decline in the total amount of light intercepted by the canopy (Falster and Westoby, 2003), i.e. light is intercepted over a smaller leaf surface area. In this study, higher leaf angles were present in plants under the high N treatment, in particular, the Malaysian varieties. This corroborates with lower carbon gain per unit leaf area in high N treatment relative to the low N treated plants. For the case of low N treated plants, when considering carbon gain per unit leaf area, the reduced LAI of the low N canopies enables higher light intensities over a greater surface area of the canopy which, when combined with similar photosynthetic parameters (for example, P_{max}), leads to a greater carbon gain. However, although the light levels are lower for the high N treatment, the greater LAI means that per unit ground area basis, carbon gain is higher. The carbon gain per unit leaf area in MR219 high N plants was particularly low in growth stage 4 and 5. Self-shading may have likely played a role in the high N treatment, which decreases the net amount of photosynthetic leaf area exposed to light, accounting for the lower carbon gain per unit leaf area observed in the middle growth stages.

One interesting thing that was observed was higher carbon gain per unit leaf area in the LN IR64 plants in the mid growth stages. This could be attributed to a possible growth 'advantage' over having a smaller canopy with lesser tillers (than HN IR64), where the certain plant positions inside the canopy are exposed to more light relative to the same positions within the HN canopies.

3.7 **Conclusion**

Using the methods employed here, we were able to explore, primarily, how the canopy behaves with respect to different nitrogen treatments. One of the key characteristics of using this image-based canopy reconstruction is that it is able to present us more in-depth information about the canopy, that would otherwise be labour intensive to capture with rule-based approaches.

We found that leaf photosynthetic capacity was generally less responsive than leaf area to N treatment (as the amount of N was sufficient) meaning that light capture and light distribution were more important in determining canopy photosynthesis and dry weights. We demonstrated that this method of reconstruction has helped us to identify and characterise unique canopy features (e.g. the vertical and horizontal distribution of leaf inclination angles) that would normally be difficult to quantify in the field. Such features include whole plant leaf inclination angles with respect to depth and cumulative leaf area index. Carbon gain estimations have also been possible using and these offer an insight to overall canopy productivity when coupled with gas exchange measurements. In this study, the reduction in leaf area accumulation during mild N deficiency occurred in the middle canopy regions and was associated with an improved canopy light distribution in the low N treatment resulting in a higher carbon gain per unit leaf area compared to high N. There is potential in improving yields further by improving the light distribution in high N treated plants.

Chapter 4:
Assessing the effects of mild to moderate nitrogen deficiency on plant development and canopy photosynthesis in field grown rice

Chapter 4

4.1 Introduction

Growing rice in the changing climate is increasing challenging. While a lot of research has been done involving single stress analyses in controlled or semi-controlled environments, it cannot be truly representative of how plants behave in field conditions. Out in the open, plants are exposed to a myriad of potential biotic and abiotic factors. For example, much can be said about the effects of a specific nutrient deficiency on a single plant, but often enough, the effects of single nutrient deficiencies are overshadowed by a combination of multiple stress factors. This type of interaction is described in the recent meta-analysis by Poorter *et al*., (2016) who use the apt phrase 'pampered inside, pestered outside'. In the instance of stress experiments using hydroponics, plants benefit from the homogeneity of the nutrient solution, rather than the uneven distribution of nutrients across the soil in the field (Poorter *et al*., 2016). Field studies are largely beneficial to fully characterise plant responses to stress as it helps us understand plant-environment interactions (Long *et al*., 2004; Ainsworth and Long, 2005; Long *et al*., 2005; Morgan *et al*., 2005; Long *et al*., 2006b; Ainsworth, 2008). The field environment presents fluctuating conditions which themselves are difficult to predict but can potentially affect yield and biomass substantially (Burgess *et al*., 2017). Signal transduction pathways are affected by changes in the physical environment and the plant's ability to respond and adapt to the changes would ultimately depend on plant fitness, and this varies on a genotypic level (Murchie and Niyogi, 2011; Townsend *et al*., 2017).

Yield gains in cereals post-Green Revolution have stagnated in major crops as shown in the maximisation of the harvest index and grain number (Parry *et al*., 2010; Reynolds *et al*., 2012). Improving the efficiency at which photosynthesis operates has been shown to

be an area of potential, to push the current limits of further yield increases (von Caemmerer *et al*., 2012; Ort *et al*., 2015).

4.1.1 Aims and objectives

The previous two chapters have described to a large degree how the growth and development of Malaysian rice cultivars are affected by varying nitrogen concentrations in a controlled environment with comparable fertiliser application to field fertiliser application (Chapter 2) and field-simulated setting (Chapter 3). How light behaves within the rice canopy, as examined in Chapter 3 using 3-dimensional canopy reconstructions have shed some light on the mechanisms that rice plants undertake to maximise productivity with respect to the changes in nitrogen nutrition. There is a need to corroborate this behaviour in field studies, where the presence of other biotic and abiotic factors (i.e. environmental pressures) could alter (both improve or exacerbate) the responses to nitrogen nutrition.

The following field trials aimed to investigate the physiological response of Malaysian rice cultivars to a lower soil N concentration, with a focus on canopy photosynthesis, architecture and changes in the light environment over the course of the growing season.

Two field studies over a period of 18 months were performed at the Crops for the Future Research Centre (CFFRC) in Semenyih, in the state of Selangor, two kilometres from The University of Nottingham, Malaysia Campus in Semenyih.

4.2 Field Trial 1

The objective of the first field trial was to screen the rice varieties for whole canopy level responses to growing conditions with reduced nitrogen fertilization. Interesting findings from this trial were further investigated in the second field trial in greater detail (differences between trials are stated in Section 4.3.3). The terms low N and nitrogen deficiency will be used interchangeably throughout the chapter.

4.2.1 Plant seeds and germination

Rice seeds were obtained from MARDI in Seberang Perai, Penang, in Peninsular Malaysia. The varieties obtained were MR219, MR220 and MR253. These varieties were chosen specifically for physiological evaluation – in particular to compare the fitness of the varieties under different nitrogen environments. According to the Malaysian Agricultural Research and Development Institute, MR219 is the most cultivated variety in Malaysia, and MR220 is the sister variety that is normally grown in place of MR219 in less optimal conditions. MR253 is a rice variety for marginal areas. The rice seeds were transported back to The University of Nottingham Malaysia Campus (UNMC) in Semenyih and stored in a cool and dry environment to prevent the growth of storage fungi such as Aspergillus and Penicillium.

The first trial began on 31st March 2016 and ended on 25th June 2016. Rice seeds were germinated in the nursery of the Field Research Centre (FRC) at Crops For the Future Research Centre (2°55’53.5”N, 101°52’38.7”E) in compost that contained N:P:K of 10:10:10. Figure 4.1a shows the germination tray modules that were used in the germination of the rice seeds. The trays were watered twice daily, morning and evening, and were placed in the nursery. To prevent exposure to harsh sunlight, trays were shielded by black plastic mesh-like tarp. Figure 4.1b shows week-old seedlings and

Figure 4.1c is a photograph of half of the prepared field prior to transplanting. The plantlets were transplanted 21 days after germination into the microplots that were dug to a depth of 5 cm to ensure uniformity. Figure 4.1d the rice micro-plots at leaf rank 9 development stage.

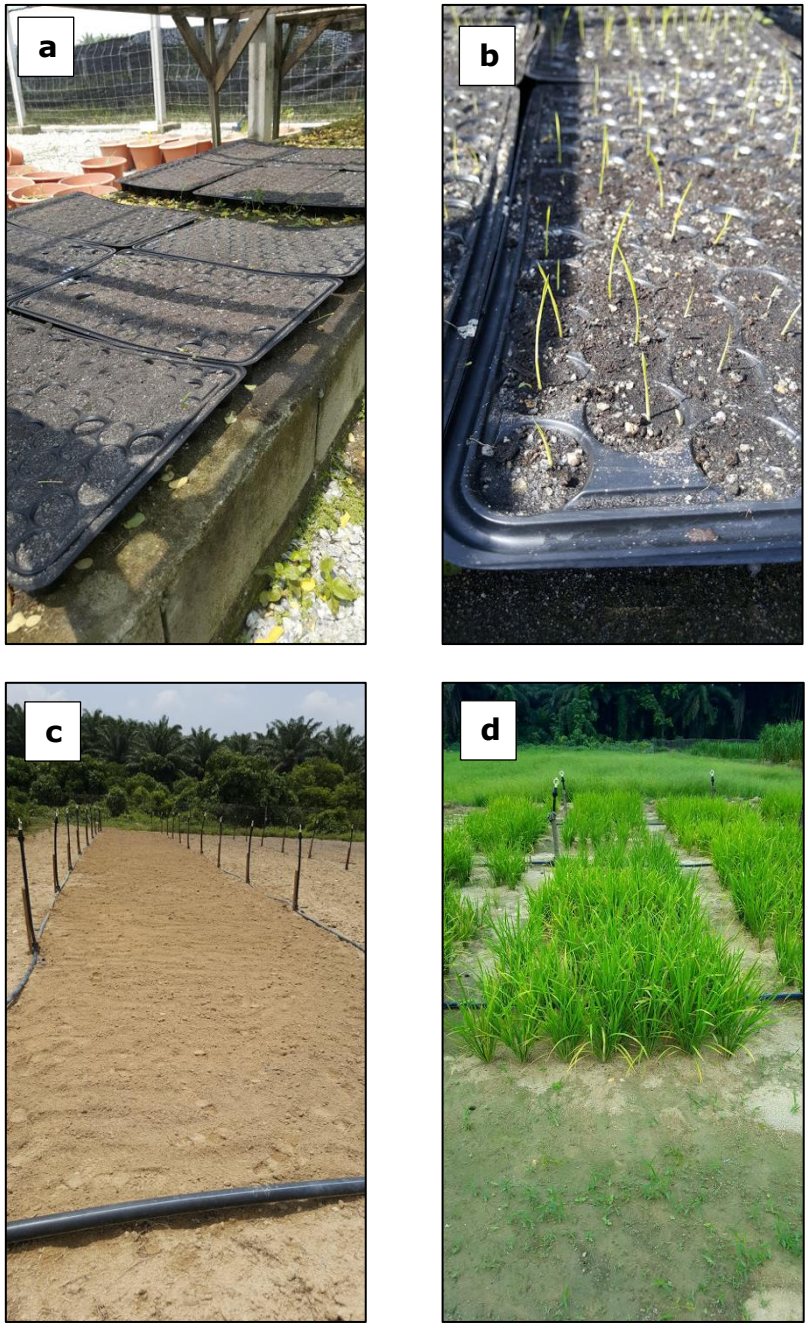


Figure 4.1: (**a**) Modules where seeds were germinated using compost. (**b**) Week-old seedlings with secondary leaf. (**c**) Prepared field with sprinklers for irrigation. (**d**) Rice plants at leaf 9.

4.2.2 Growth conditions and experimental design

Prior to the trial, a soil test was performed (by Applied Agricultural Resources SDN, BHD, Malaysia) to identify the concentrations of the different macro and micronutrients as well as the cation-exchange capacity (CEC) and pH. The results of the soil test are shown below in Table 4.1. For soil sampling, the entire experimental plot was divided into half through the middle (shown in Figure 4.2). The crosses in Figure 4.2 represent sampling points (red crosses – Plot 1, blue crosses – Plot 2). The soil from each sampled point was combined into one lot with the other three sampling points in each respective plot. The pH of the soil was adequate for rice growth and did not require a pH amendment.

Table 4.1: Soil analysis results for pH, N (%), K (m.e %), Na (m.e %), Fe (m.e %), P (ppm) and cation exchange capacity (m.e %). Soil was sampled from two plots.

	pH in water	N (%)	Total P (ppm)	C.E.C (m.e %)	K (m.e %)	Na (m.e %)	Fe (m.e %)
Plot 1	4.78	0.160	235	4.10	0.310	0.0200	10000
Plot 2	4.99	0.160	180	4.00	0.310	0.0200	8330

A split-plot that utilised a randomized block design within each plot was employed in the trials. For the first field trial, three replicates of each variety were arranged randomly in three by three for both the low N plot and control plot (Figure 4.2). Each three by three plot were subdivided into nine micro-plots. Each micro-plot contained 42 plants, arranged in a 6x7 configuration (Figure 4.3). The spacing between each plant was 20 centimetres, and 50 centimetres spacing was left between the micro-plots. A metre spacing separated the low N and control plots. A trench was dug around the plots to prevent the leaching of surface nutrients. The microplots were watered twice daily,

at 7 am and 7 pm using a sprinkler irrigation system (Figure 4.1c). Weeding was carried out frequently to reduce the competition for nutrients and routine checks on plant health were made to maintain the absence of pest and diseases.

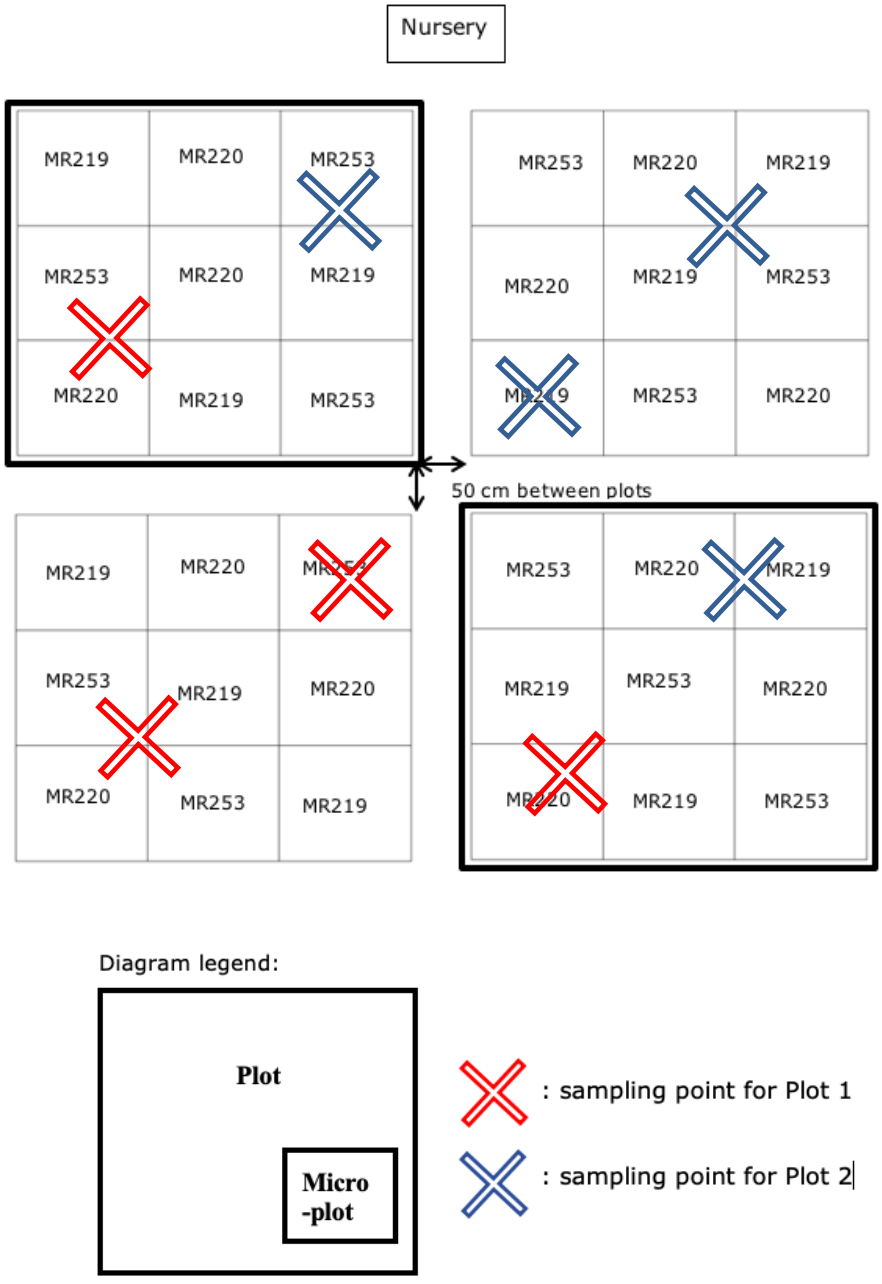


Figure 4.2: Split-plot layout of Field Trial 1. Bold boxes represent control plots, and the un-bolded boxes are low N plots. Soil was sampled from two plots at four points each, as indicated by crosses. Red crosses represent sampling points in Plot 1, and blue for points in Plot 2.

The fertilization regimes were calculated based on the recommendations from the International Rice Research Institute (IRRI; http://www.knowledgebank.irri.org/training/fact-sheets/nutrient-management/nitrogen-split-applications) and was adjusted to the area of the soil. The plots were fertilised three times during the growth season – prior to transplanting (T), at the start of the tillering phase (AT) and prior to panicle initiation (PI). NPK fertiliser was used prior to transplanting and was applied evenly to both plots. Subsequent fertilization required the application of the necessary macronutrient in their separate components – urea for nitrogen (N), triosphosphate (TSP) for phosphorus (P) and muriate of potash for potassium (K). Despite the different form of N (due to the availability of nutrient fertilisers on the field site), the amount of N supplied to the soil in the form of fertiliser is comparable to other chapters.

For a 7-8 t/ha yield of rice, NPK would need to be applied at a rate of 140 kg N/ha, 60 kg P/ha and 60 kg K/ha. Planting area (Figure 4.3) and fertiliser amounts (Table 4.2 and Table 4.3) are calculated below.

Total planting area:
4.6 meters x 4 meters = 18.4 m^2 = 0.00184 hectares

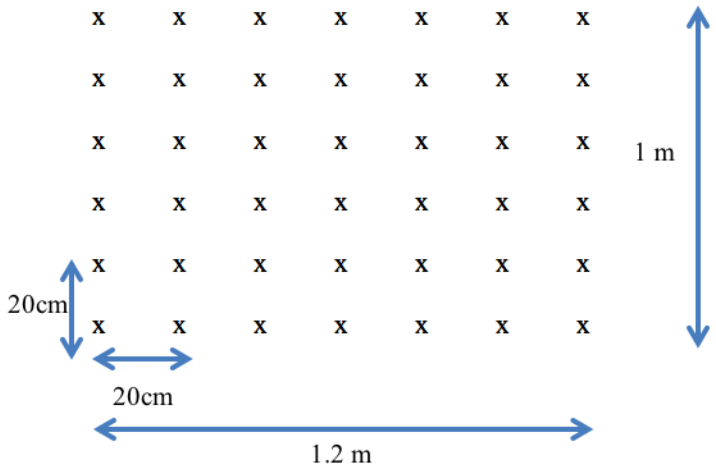


Figure 4.3: Dimensions of the 7 by 6 micro-plot, where x represents a single rice plant. The length and breadth of the micro-plot is one meter and 1.2 meters respectively while the spacing between plants is 20 centimetres.

Table 4.2: Control plot application at three application times. (T) is prior to transplanting, (AT) is at tillering and (PI) is panicle initiation.

*This is to scale down fertiliser application rate to obtain rate for the specific area of the plot (0.00184 hectares)

	N kg/ha	***Per plot (kg)**	**P kg/ha**	***Per plot (kg)**	**K kg/ha**	***Per plot (kg)**
(T)	30.0	0.0552	60.0	0.110	30.0	0.0552
(AT)	55.0	0.219				
(PI)	55.0	0.219			30.0	0.0552

Fertiliser application at (T), with 15:15:15 NPK:

= 0.0552 + 0.0552 + 0.0552 + additional 0.0552 of P (from triosphosphate-TSP)

= 0.1656 kg NPK + 0.0552 kg (TSP)

Fertiliser application at (AT), with 46% N in urea (46 kg N/100 kg urea):

= [55/46 x 100] x 0.00184

= 0.219 kg N

Fertiliser application at (PI), urea and K (muriate of potash-MOP):

= [55/46 x 100] x 0.00184 + 0.0552 kg K (MOP)

= 0.219 kg N + 0.0552 kg K

The low N plot did not receive any additional nitrogen after the initial fertilization prior to transplanting, as shown in Table 4.3.

Table 4.3: Lower-N plot application at three application times. (T) is prior to transplanting, (AT) is at tillering and (PI) is panicle initiation.

*This is to scale down fertiliser application rate to obtain rate for the specific area of the plot (0.00184 hectares)

	N kg/ha	***Per plot (kg)**	**P kg/ha**	***Per plot (kg)**	**K kg/ha**	***Per plot (kg)**
(T)	30.0	0.0552	60.0	0.110	30.0	0.0552
(AT)	x					
(PI)	x				30.0	0.0552

4.2.3 Plant physiology and gas exchange measurements

Plant height and primary tiller number

The first plant height measurement was recorded with a ruler a day after transplanting. It was noted that at this point of time, most plants were at the leaf 5 elongation stage. Height was measured from the bottom of the plant until the tip of the longest leaf on the top of the canopy. Primary tiller number was also noted weekly. Results were plotted against thermal time (thermal time in degree days = Mean daily temperature – base temperature of 10 degrees).

Light response curves

In the first trial, rapid light response measurements carried out using the LiCor-6400XT (Lincoln, Nebraska) infrared gas exchange analyser and were taken at two growth stages –at the active tillering phase and at flag leaf. To determine the leaf number, the newest completely elongated leaf was tagged each week. At the active tillering phase, rapid photosynthetic light response measurements were performed on leaf 9, a week after the second fertilization (AT). Active tillering light response measurements were only performed at one canopy level. Flag leaf light response measurements were carried out at two canopy levels – top and bottom, on primary tiller leaves. For the measurements on the top of the canopy, the flag leaf was used. For the bottom of the canopy, leaf 12 was used.

The PAR levels were as follows: 0, 200, 400, 800, 1200, 1500 and 1800 nm. Flow rate was set to 500 μmol s^{-1} and the chamber air temperature was set at 30°C. Reference CO_2 was maintained at 400 μl l^{-1} to simulate ambient CO_2 concentration. A stability period of between 2 and 3 minutes was programmed to allow for the leaf to adjust to the light level with 10% blue light. The part of the leaf in the cuvette was measured for leaf width from which the area was calculated. This is to correct for leaf area, as younger rice leaves do not generally fully cover the entire IRGA cuvette.

Light-adapted quantum yield of PSII

The quantum yield of PSII was recorded on leaf 9 and flag leaf, using a portable hand-held fluorometer FluorPen FP 100 (Photon Systems Instruments, Brno, Czech Republic). Measurements were taken on light-adapted plants, yielding Fq'/Fm' values.

Chlorophyll

Chlorophyll measurements were taken using the SPAD (Soil-Plant Analyses Development) 502 Plus Chlorophyll Meter (Spectrum Technologies, USA). Two measurements (two leaves – three points per leaf) were taken per microplot, totalling to six replicates per treatment per variety.

Canopy PAR and leaf area index

The PAR interception of the rice plant at two canopy levels were taken using the AccuPAR LP-80 Ceptometer (Decagon Devices, USA). Two measurements were obtained - one at the top of the canopy (unobstructed) and the other at the bottom of the microplot (same level as the soil). Measurements included both parallel and diagonal (to planting line) sampling techniques. The leaf area index (LAI) was calculated using the ceptometer and the values recorded. A total of five readings were taken per microplot, totalling to 15 replicates per treatment per variety. Care was taken to ensure that the light conditions remained uniform across measurements, especially on particularly cloudy and windy days where light levels fluctuated more frequently.

Statistics

Means and standard error of means were calculated in Microsoft Excel, and statistical analyses were carried out using GraphPad Prism. For most cases, a two-way ANOVA test and a post-hoc test followed using Tukey's multiple comparisons were used to analyse for statistical differences.

4.3 **Field Trial 2**

In the second field trial, more detailed measurements of plant phenology were made. This was to characterise the behaviour of light within the canopy and identify relationships at the individual plant level and varietal level.

4.3.1 **Plant seeds and germination**

The second trial began on the 31st of July 2017 and the final measurement done was on the 17th of November 2017. The marked-out plot was tilled and levelled two weeks before planting and the watering began the day after rotavation. The same varieties as the first field trial were grown – MR219, MR220 and MR253. Instead of germinating rice seeds in the nursery as in the first trial, seeds were directly sowed into the soil. The plot of land used was directly adjacent to the first trial at the Field Research Centre (FRC) at Crops For the Future Research Centre (2°55'53.5"N, 101°52'38.7"E), two miles from The University of Nottingham Malaysia campus.

For the second trial, rice seeds were sown using the direct seeding technique (IRRI;http://www.knowledgebank.irri.org/step-by-step-production/growth/planting/direct-seeding). This was recommended by the farm manager at the FRC, to limit labour requirements which would be needed for transplanted rice. Seeds were sown using the dibbling method after the application of fertiliser. A long wooden pole was used to dig holes into the soil and the rice seeds were dropped into the holes, which were subsequently covered with soil. To ensure that enough plants germinated, two to three seeds were sowed per hill, and the plots were thinned when the plants were bigger.

4.3.2 Growth conditions and experimental design

A split plot with a randomized block design for within the plots was utilised in the trials. Same as the first trial with some minor amendments, three repetitions of each variety were arranged randomly in a three by three plot for both the low N plot and control plot. Each three by three plot were subdivided into nine microplots (shown in Figure 4.4). Each microplot contained 56 rice plants, arranged in a 8 plants by 7 plants configuration. Between each plant in a microplot was a 20 cm spacing while between microplots was a spacing of 50 cm. A metre spacing separated the low N and control plots. The microplots were hand - watered twice daily, at 7 am and 7 pm. Weeding was carried out frequently to reduce the competition for nutrients, via spot weeding and herbicide applications.

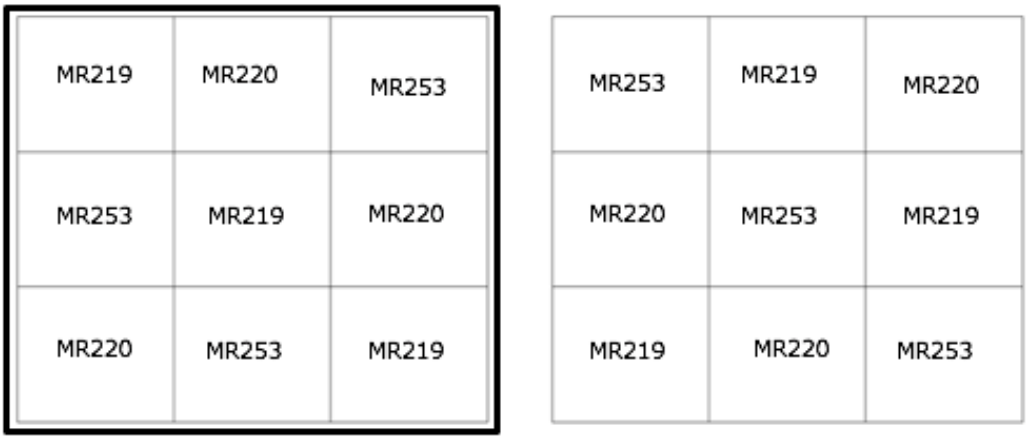


Figure 4.4: Split-plot layout of Field Trial 2. The bold box represents the control plot, and the non-bold box is the low N plot. In each plot, there are nine microplots. Within each microplot, a variety was grown (e.g. MR219) in a 8 by 7 configuration.

The fertilization requirements were similar to the first trial, but as the planting area differed slightly (due to the increase in number of plants) the amounts applied were calculated again. The plots were

fertilised three times during the growth season – prior to transplanting (T), at the start of the tillering phase (AT) and prior to panicle initiation (PI), as shown in Tables 4.4 and 4.5. NPK fertiliser was used prior to direct-seeding and was applied evenly to both plots. Subsequent fertilization required the application of the necessary macronutrient in their separate components – urea for nitrogen (N), triosphosphate for phosphorus (P) and muriate of potash for potassium (K), similar to Field Trial 1.

The calculations are shown below and are adjusted for planting area.

Total planting area (calculated from Figure 4.5):

4.6 meters x 4.6 meters = 21.16 m^2 = 0.002116 hectares

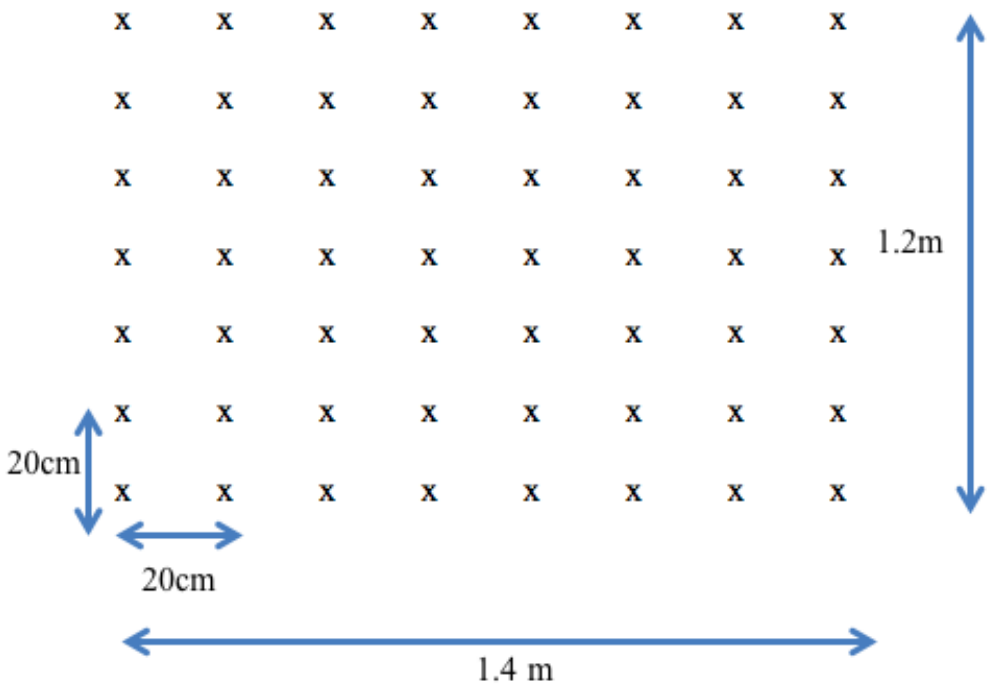


Figure 4.5: Dimensions of an 8 by 7 micro-plot in Field Trial 2, where x represents a single rice plant. The length and breadth of the micro-plot is 1.2 meters and 1.4 meters respectively while the spacing between plants is 20 centimetres.

Table 4.4: Control plot application at split application times. (T) is prior to transplanting, (AT) is at tillering and (PI) is panicle initiation.

	N kg/ha	***Per plot (kg)**	**P kg/ha**	***Per plot (kg)**	**K kg/ha**	***Per plot (kg)**
(T)	30.0	0.0638	60.0	0.127	30.0	0.0638
(AT)	55.0	0.2529				
(PI)	55.0	0.2529			30.0	0.0638

*This is to scale down fertiliser application rate to obtain rate for the specific area of the plot (0.002116 hectares)

Fertiliser application at (T), with 15:15:15 NPK:

= 0.06384 + 0.06384 + 0.06384 and 0.06384 of P (from triosphosphate – TSP)

= 0.19152 kg NPK + 0.06384 kg (TSP)

Fertiliser application at (AT), with 46% N in urea (46 kg N/100 kg urea):

= [55/46 x 100] x 0.002116

= 0.2529 kg N

Fertiliser application at (PI), urea and K (muriate of potash – MOP):

= [55/46 x 100] x 0.002116 + 0.06384 kg K (MOP)

= 0.2529 kg N + 0.06384 kg K

The low N plot did not receive any additional nitrogen after the initial fertilization prior to transplanting, as shown in Table 4.5.

Table 4.5: Nitrogen stress plot application at split application times. (T) is prior to transplanting, (AT) is at tillering and (PI) is panicle initiation.

	N kg/ha	***Per plot (kg)**	**P kg/ha**	***Per plot (kg)**	**K kg/ha**	***Per plot (kg)**
(T)	30.0	0.0638	60.0	0.127	30.0	0.0638
(AT)	x					
(PI)	x				30.0	0.0638

*This is to scale down fertiliser application rate to obtain rate for the specific area of the plot (0.002116 hectares)

4.3.3 Plant physiology and gas exchange measurements

This section is divided into two parts – the first is made up of Table 4.6, which shows a summary of the measurements that were identical or similar to those in Field Trial 1 (refer to Section 4.2.3 for detailed methodologies). The second part elaborates on the additional measurements made in Field Trial 2.

Table 4.6: List of parameters measured in Field Trial 2 that were similar to Field Trial 1, with minor changes.

Measurement	Field Trial 1	Field Trial 2
Plant height, leaf rank and tiller number	2 tagged plants per microplot (6 replicates per variety, per treatment)	2 tagged plants per microplot (6 replicates per variety, per treatment)
Chlorophyll (SPAD)		
Effective tillers (yield parameter)		
Canopy PAR interception and leaf area index (LAI)	5 readings for PAR (incoming) and 5 readings for PAR (transmitted) 5 LAI readings from ceptometer per microplot	5 readings for PAR (incoming) and 5 readings for PAR (transmitted) 5 LAI readings from ceptometer per microplot
Light response curve (to determine maximum assimilation rate, P_{max})	At active tillering: Leaf 9 At full flag leaf extension: Flag leaf (top of canopy) and Leaf 12 (bottom) 3 replicates per variety per treatment 7 PPFD points used: 0, 200, 400, 800, 1200, 1500, 1800	At active tillering: Leaf 9 3 replicates per variety per treatment 9 PPFD points used: 0, 50, 100, 200, 300, 400, 800, 1200, 1500

Dark-adapted quantum yield of PSII

The quantum yield of PSII (Qy) was recorded for two months in the second field trial, using a portable fluorometer FluorPen FP 100

(Photon System Instruments, Czech Republic). Measurements were taken on dark-adapted plants, yielding Fv/Fm values. Leaf clips that were provided with the fluorometer were used to dark-adapt the plants for 30 minutes. This allows the part of the leaf to remove the fast-relaxing form of NPQ (sometimes termed qE) which leaves the slowly relaxing form that is often assumed to be photoinhibitory damage to PSII (sometimes referred to as qI) before being subjected to a saturating pulse of light (Murchie and Lawson, 2013). One of the benefits to dark-adaptation is the true maximum value of fluorescence can be achieved, and is used particularly to assess plant responses to stress.

Crop health

The vigour of the microplots were assessed using the Trimble GreenSeeker handheld sensor (AgriOptics, New Zealand) by scanning the amount of light within specific wavelengths relevant for chlorophyll reflected back from each microplot. The NDVI (Normalised Difference Vegetation Index) reading on the display screen (between 0.00 and 0.99) is an indicator of the strength of the light reflected, where the closer the value to 0.99, the higher the NDVI value following the equation:

NDVI = (NIR-RED)/(NIR+RED)

Where NIR refers to the reflection in the near-infrared spectrum and RED refers to the reflection in the red range of the spectrum.

Leaf length, width and area

Leaf blade lengths (from the ligule to the tip of the fully expanded leaf blade) and widths (measured in the middle of the blade from one margin to the other) (Chatterjee *et al*., 2016) were measured and recorded using a ruler for both leaf 9 and flag leaf upon full elongation. In addition to this, rapid and non-destructive measurements of flag leaf area were obtained using the CI-203 handheld laser leaf area meter (CID Bio-Science). This measurement yielded leaf length,

width, as well as area. Measurements of six replicates per variety per treatment were obtained.

Leaf inclination angles

The angle between the leaf sheath and stem (Figure 4.6, ∠b) as well the angle between leaf blade and sheath (Figure 4.6, ∠c) of fully elongated leaf 9 were measured using a protractor, against a plain white background to ensure a more accurate reading. Leaf inclination angle (Figure 4.6, ∠a) was then calculated using the following equation:

$$\angle a = \angle b + (180^\circ - \angle c)$$

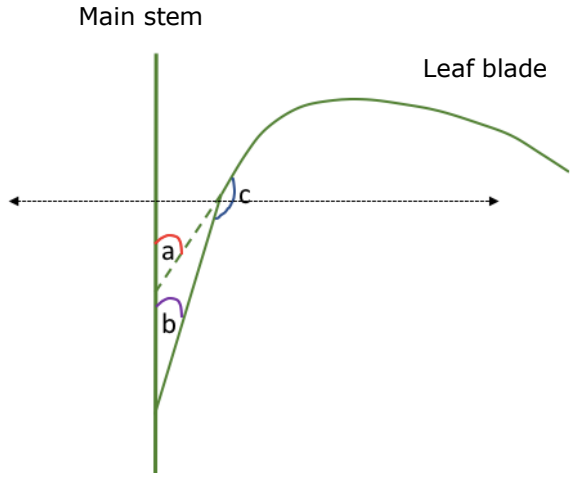


Figure 4.6: Leaf inclination measurement. Dotted line with arrows represents the plane, which is perpendicular to the main stem. ∠ a is the inclination angle of the leaf, which is calculated from measuring angles ∠ b and ∠ c, using the equation above.

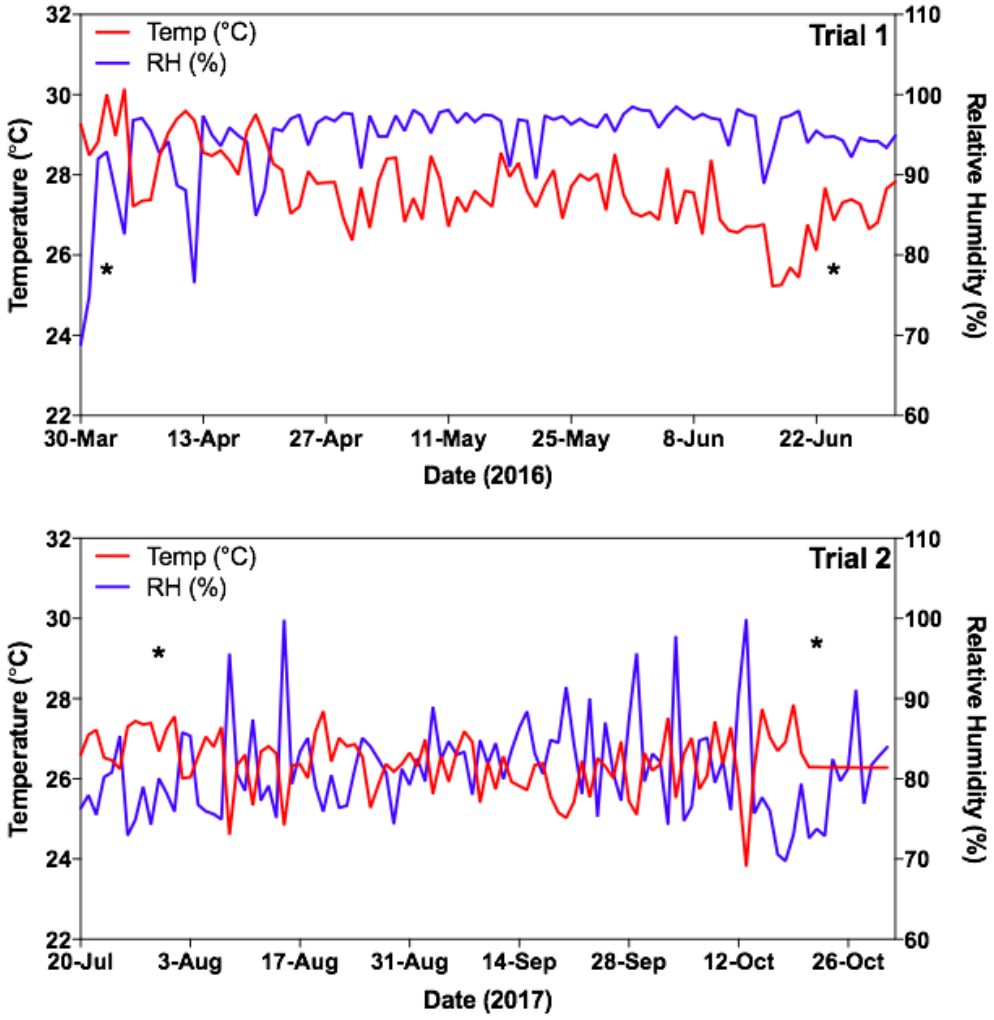
Statistics

Means and standard error of means were calculated in Microsoft Excel and GraphPad Prism, and statistical analyses were done using GraphPad Prism. For most cases, a two-way ANOVA test and a post-hoc test followed using Tukey's multiple comparisons were used to analyse for statistical differences.

4.4 **Results**

4.4.1 **Mean temperature and relative humidity**

Local data for daily temperature (°C) and relative humidity (%) were obtained from the weather station at CFFRC, Semenyih. Daily means over the two growth periods are shown in Figure 4.7. Figure 4.8 are the daily averages of solar radiation (MJ/m^2) for both of the trials. Solar radiation was variable across both seasons, accounting for the fluctuations in temperature and relative humidity observed.



	Trial 1		Trial 2	
	Mean	SD	Mean	SD
Temp (°C)	27.7	0.990	26.4	81.2
RH (%)	94.6	4.96	0.710	5.94

Figure 4.7: Daily mean temperature (°C) and relative humidity (%) across the two trials. The period between the black asterisks represent the time period for both trials. The table shows the mean temperatures and relative humidity (RH) during the trials and their standard deviation.

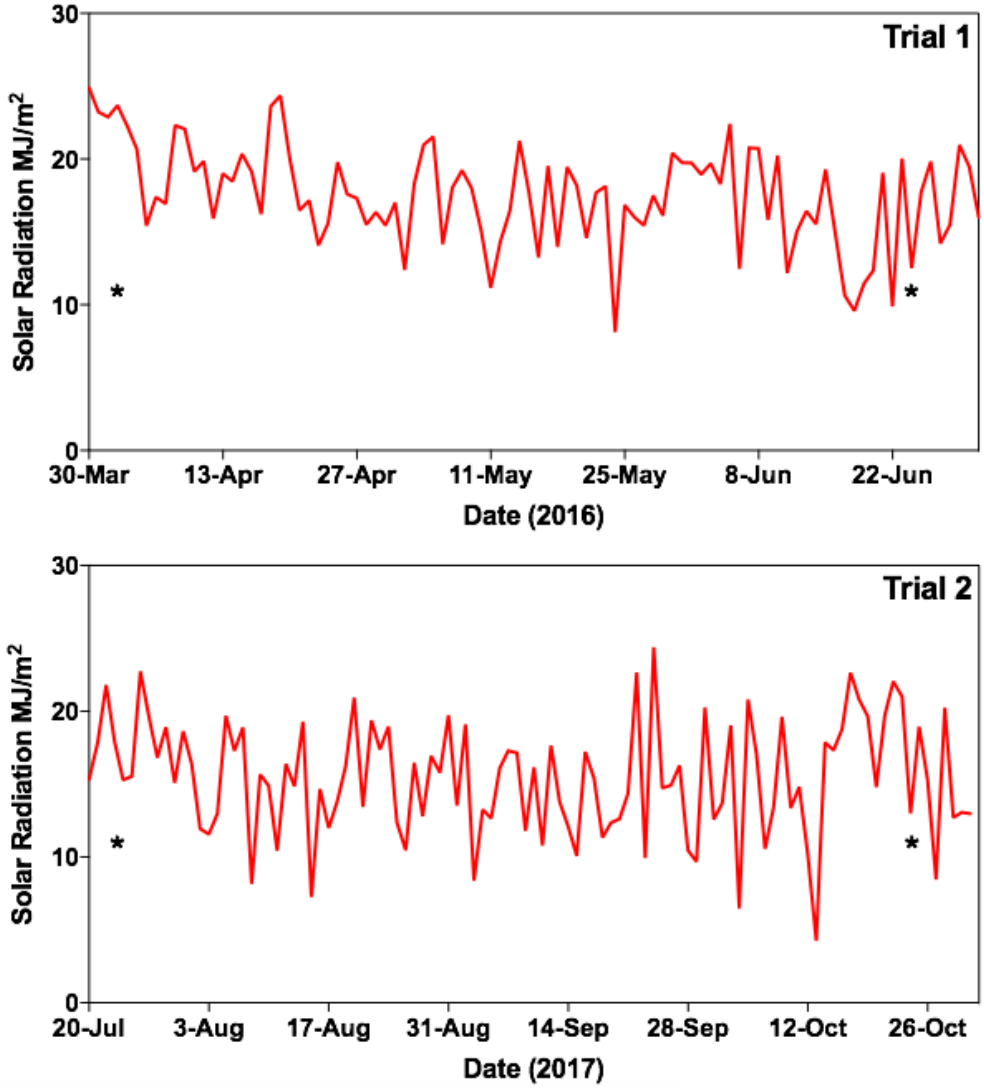


Figure 4.8: Daily mean solar radiation (MJ/m^2) across the two growth periods. The period between the black asterisks represent the time period for both trials.

4.4.2 Plant physiology measurements

Plant height, tiller dynamics and leaf position

Plant heights for control and low N plants from both field trials are shown in Figure 4.9a (Field Trial 1) and Figure 4.9b (Field Trial 2). Means (with SEM) are plotted against thermal time (°Cd). Plant height means were fitted using the Gaussian curve as it provided the best fit (R^2>0.9152). In the first trial, there were no significant differences between treatments in both trials with the exception of MR219, after 1400 °Cd. There were no genotypic differences between the controls and low N plants of the MR219 and MR220 varieties. However, these two were significantly different from MR253, as MR253 plants were generally shorter under both control and low N treatments. In the second field trial, the plant heights were similarly unaffected.

Differences between overall plant heights against thermal time were insignificant, despite the reduction in nitrogen fertilization in the low N plot. However, this maintenance of height is not reflected in the number of tillers on the main stem or the rate of tiller emergence with thermal time, as shown in Figure 4.10, together with the means of leaf position on the main stem from Field Trial 2. Unlike plant height, there were pronounced differences between the number of primary tillers and also the rate of tiller emergence between treatments. For all varieties under low N treatments, there was a significant reduction in the number of tillers produced ($p<0.05$), and more so in the MR219 variety ($p<0.001$). The 25% reduction in tiller number (with respect to control plants) in MR219 low N plants is coupled with longer a thermal time taken to reach T_{n+1}, where n is the number of tillers on the main stem. This visible decrease in rate of primary tiller emergence occurred after 500 °Cd. This is after the second round of fertilization, at active tillering. It was also noted that the decrease in the emergence rate occurred later in the first trial, which could have been the difference between direct sowing and transplanting, or the effect of temperature on tiller emergence.

Table 4.7 is a summary of final plant heights and tiller number for plants in Field Trial 2. MR219 appears to be the variety most susceptible to N-deficiency amongst the three Malaysian varieties. The number of leaves on the main stem decreased on average by one between control and low N MR219 plants ($p<0.05$). This is substantiated by the significantly longer phyllochron ($p<0.05$) in low N plants. Leaf number on the main stem and the phyllochron (°Cd) for both trials are shown in Table 4.8. The phyllochron is the time interval between leaf tip appearance and is significantly correlated with temperature. The phyllochron was estimated by obtaining the inverse of the linear regression (1/slope) of leaf position with respect to the main stem.

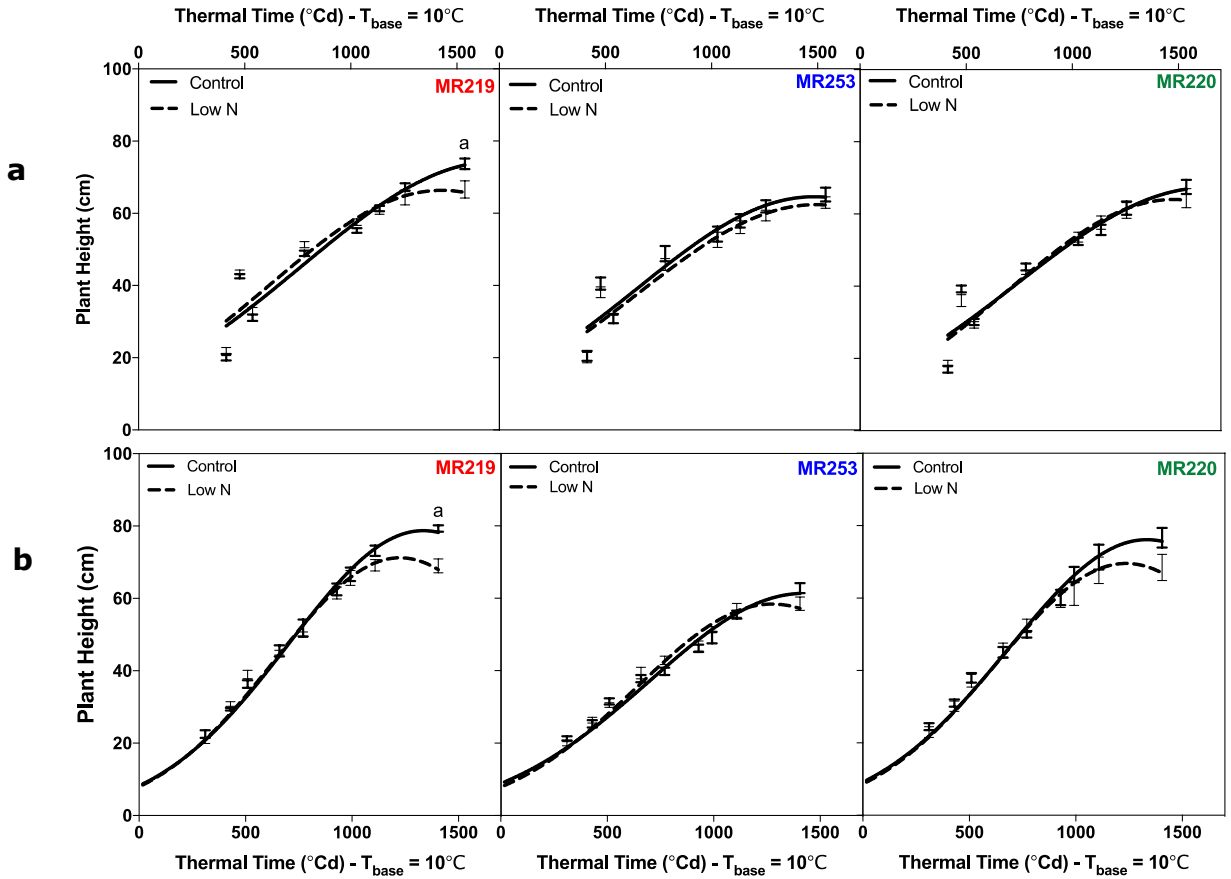


Figure 4.9: Plant heights (cm) for all plants in both control and low N treatments in Field Trial 1 (**a**) and Field Trial 2 (**b**). Shown are the means (and SEM) plotted against thermal time (°Cd). Data was curve-fitted using a least squares Gaussian equation, n=6.

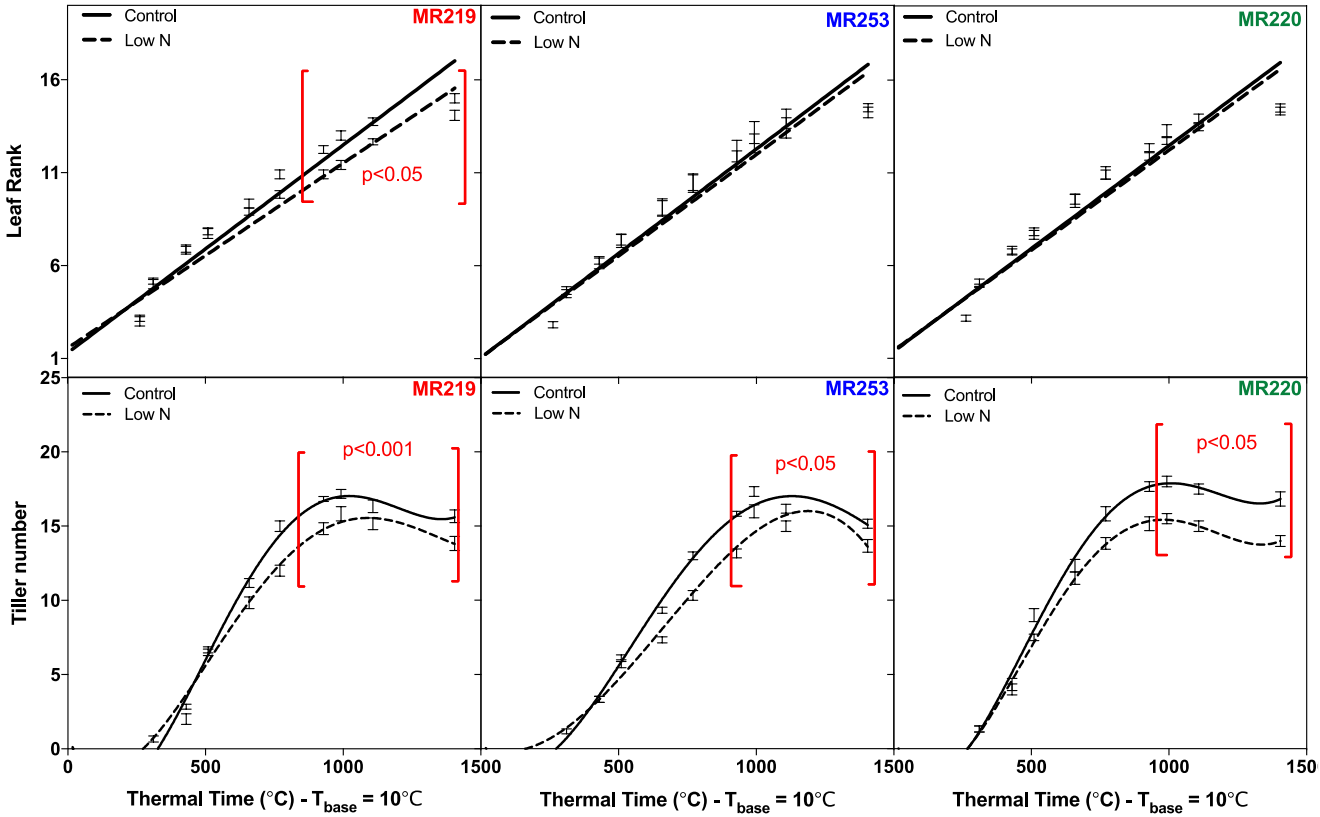


Figure 4.10: Leaf position (rank) and tiller numbers from Field Trial 2. Shown are the means and SEM, plotted against thermal time (°Cd), n=6. Data was fitted using a least squares non-linear regression (centered fourth order polynomial). Brackets represent significant differences between control and low N, following a two-way ANOVA and Tukey's multiple comparisons test.

Table 4.7: Growth characteristics prior to flowering at 1405 degree days (°Cd) for Field Trial 2. Included are the means and the standard deviations. Same letters represent significant differences ($p<0.05$) between compared pairs (plant height and tiller number analysed separately), from two-way ANOVA and Tukey's multiple comparisons test, n=6.

Trial 2	**Plant Height (cm)**				**No. of primary tillers/hill***			
	Control		**Low N**		**Control**		**Low N**	
	Mean	SEM	Mean	SEM	Mean	SEM	Mean	SEM
MR219	79.3ae	0.882	69.0ce	1.93	17.2g	0.307	14.8g	0.401
MR253	62.8ab	1.42	58.5cd	1.88	17.3	0.333	16.0	0.447
MR220	76.7bf	2.70	68.5df	3.61	18.0h	0.365	15.5h	0.342

* where a hill is made up of one plant

Table 4.8: Number of leaves on the main stem and estimated phyllochron (°Cd) for both field trials. Included are the means and the standard error of means. Same letters represent significant differences ($p<0.05$) between compared pairs within each trial (trials analysed separately), from two-way ANOVA and Tukey's multiple comparisons test, n=6.

Trial 1	**No. of leaves on main stem**				**Estimated phyllochron (°Cd)**			
	Control		**Low N**		**Control**		**Low N**	
	Mean	SEM	Mean	SEM	Mean	SEM	Mean	SEM
MR219	15.0	0.632	14.5	0.548	88.1*a*	1.58	93.2*a*	1.71
MR253	15.0	0.632	14.2	0.753	85.8*b*	1.34	91.8*b*	2.26
MR220	15.2	0.408	14.3	0.516	86.8	0.852	90.6	1.05

Trial 2	**No. of leaves on main stem**				**Estimated phyllochron (°Cd)**			
	Control		**Low N**		**Control**		**Low N**	
	Mean	SEM	Mean	SEM	Mean	SEM	Mean	SEM
MR219	15.0*a*	0.258	14.1*a*	0.271	89.5*b*	1.28	101*bc*	1.47
MR253	14.5	0.548	14.3	0.689	89.4	2.77	91.9*c*	2.82
MR220	14.5	0.548	14.3	0.516	90.4	1.79	92.7	1.06

Chlorophyll

Mean SPAD values and standard error of means for the screen for two growth stages (maximum tillering, at 21 DAT and heading, at 65 DAT) in Field Trial 1 are tabulated in Table 4.9. There were no significant treatment differences ($p>0.05$) found in all three varieties. The only decrease in greenness (as an index of chlorophyll content) was between growth stages, for all varieties under both treatments as well, where values fell significantly ($p<0.05$), by at least 10%.

In the second field trial, eight readings were taken between the period of 5th leaf rank and 70 days after sowing, and these are shown in Figure 4.11. There is a fairly similar trend in which the SPAD values follow – a steady initial increase in chlorophyll until 30 DAS, followed by a decrease of between 5 to 15% until 47 DAS. Subsequent readings after 47 DAS generally showed higher values of greenness in the measured leaves for all plants under both treatments. However, unlike the first trial, there were no varietal differences between deficient plants ($p>0.05$) found at any point of measurement at all. In control plants, varietal significant differences ($p<0.05$) were only found between MR219 and MR253 at 61 DAS. Within the varieties, deficiency was only a factor for MR220 at 68 DAS ($p<0.05$). There is variation in the chlorophyll content in rice leaves, but this variation seems more temporally driven than as a result of nitrogen deficiency.

Table 4.9: Mean SPAD values for the three rice varieties in control and low N conditions at two growth stages (maximum tillering - 21 DAT, heading – 65 DAT) in Field Trial 1. Also included are the SEM, n=12. Same letters represent significant differences ($p<0.05$) between compared means following a two-way ANOVA and Tukey's multiple comparisons test.

Growth Stage:	**Maximum Tillering**				**Heading**			
	Control		**Low N**		**Control**		**Low N**	
	Mean	SEM	Mean	SEM	Mean	SEM	Mean	SEM
MR219	43.4*b*	0.500	43.7*ae*	0.550	36.8*b*	0.650	35.8*e*	0.700
MR253	44.2*c*	0.810	46.0*af*	0.560	39.4*c*	0.770	39.5*f*	0.780
MR220	43.2*d*	0.400	44.7*g*	0.700	38.3*d*	1.50	37.1*g*	1.44

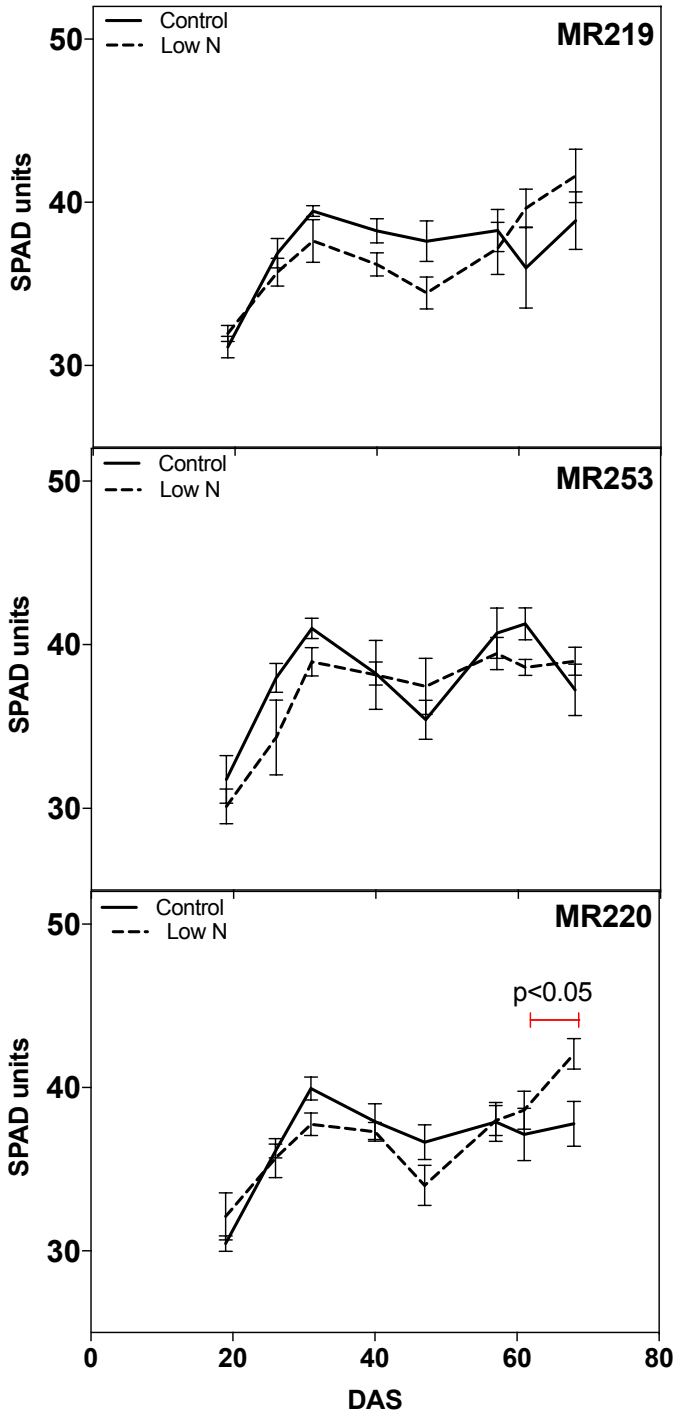


Figure 4.11: Mean SPAD values for the three rice varieties in control and low N conditions in Field Trial 2. Shown are the means and the standard errors of the means (SEM), n=6. For some cases, the error bars are too small to be visible. The red bar indicates a significant difference following two-way ANOVA ($p>0.05$) and Tukey's multiple comparisons test.

Leaf Area Index

As seen in Figure 4.12a, there was a general increase in the LAI in both control and deficient plants in all varieties. There were generally more significant differences ($p<0.05$) between varieties at specific measurement points. LAI was considerably higher in MR219 than MR253 at 48 DAT ($p<0.05$) in both control and deficient plants, but older plants the differences were negligible. Treatment differences was only apparent in older plants in MR219 ($p<0.0001$). LAI for MR220 and MR253 control and low N plants were not significantly different ($p>0.05$).

In the second field trial, LAI was monitored from the start of tillering (leaf 5/6 rank) to heading (emergence of the tip of the panicle from the flag leaf sheath), between 26 DAS and 68 DAS (means and SEM are shown in Figure 4.12b). Generally, LAI increased rapidly during the active tillering stage, dropped marginally prior to panicle initiation and increased again until heading. For the MR219 variety, two-way ANOVA revealed differences between the control and low N plants that were highly significant ($p<0.0001$) after 40 DAS. MR253 plants generally had lower LAI, but there were no differences between deficient and control ($p>0.05$). The LAI of MR219's sister variety, MR220, was markedly higher ($p<0.0001$) at 40 DAS in deficient plants but dropped significantly at 47 DAS before increasing at a similar rate as the control plants. This indicates that radiation interception was affected by the lower N-status of the plants.

Leaf area index was compared at heading (48 DAT in field trial 1 and 68 DAS in field trial 2), and this is illustrated in Figure 4.13. There is a stark difference ($p<0.05$) in LAI between the trails for all varieties under both treatments, apart from low N MR219 rice plants. The differences range from a 9% decrease (between deficient MR253 plants) to a 40% difference (between control MR219 plants).

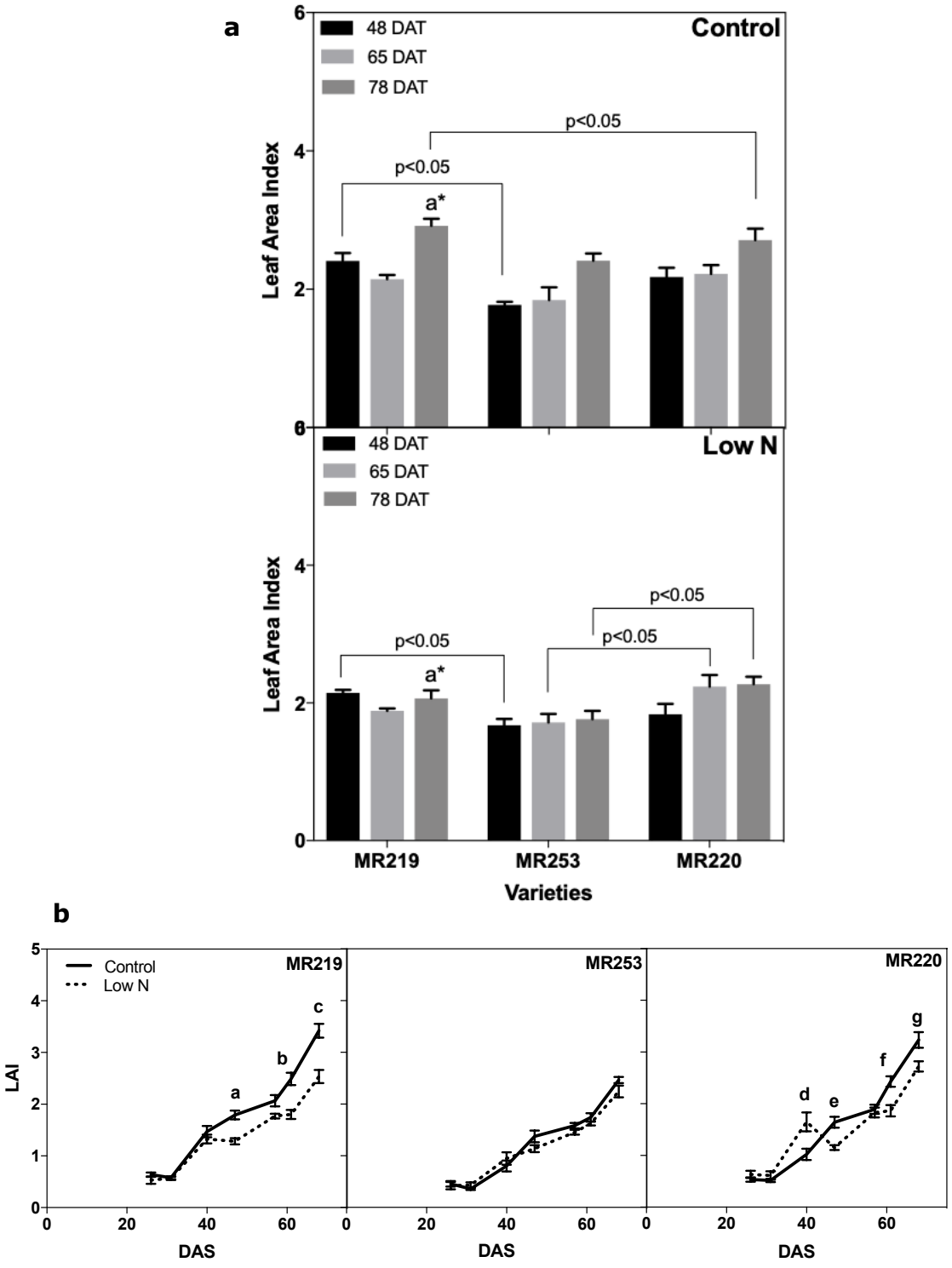


Figure 4.12: (**a**) LAI for 48, 65 and 78 DAT in Field Trial 1. (**b**) LAI for plants in Field Trial 2 until heading. Shown are the means and SEM, n=15. For some cases, the error bars are too small to be visible. The letters indicate a significant difference ($p<0.05$) between compared pairs, following two-way ANOVA and Tukey's multiple comparison's test. The asterisks denote high significance ($p<0.0001$).

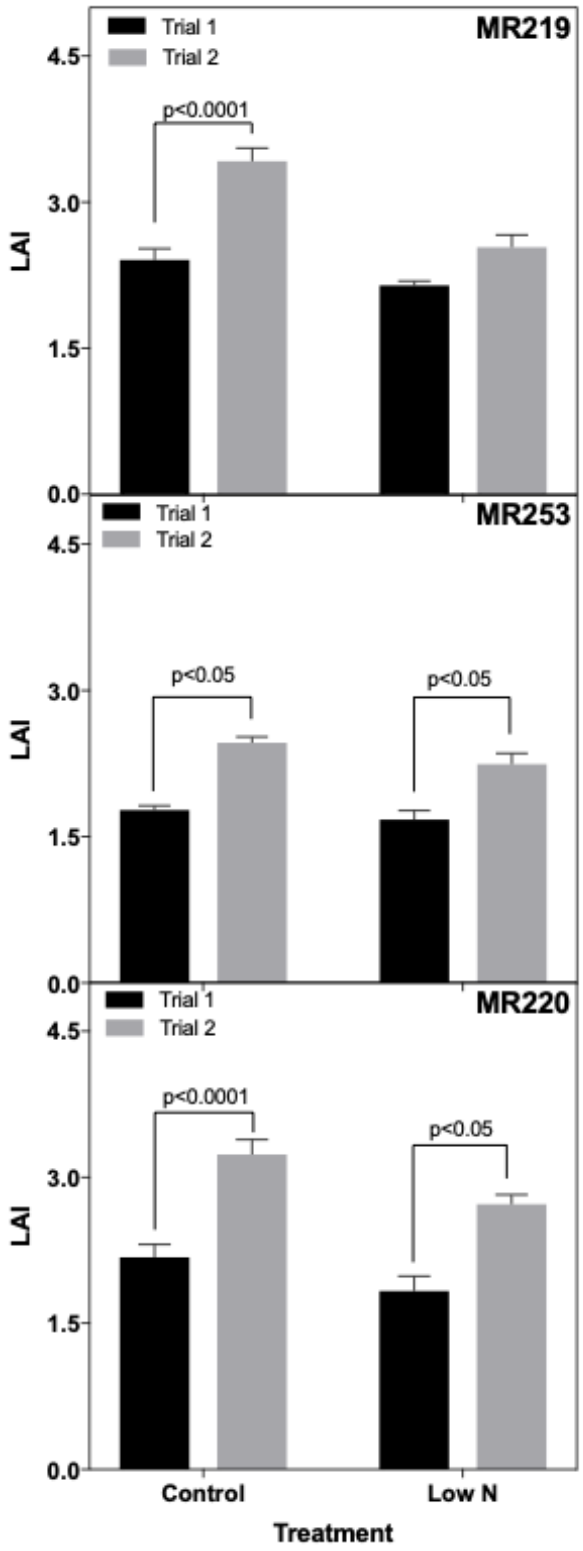


Figure 4.13: Comparison of LAI between both field trials at heading. Shown are the means and SEM, n=15. For some cases, the error bars are too small to be visible. The bars indicate a significant difference ($p<0.05$) between compared pairs following two-way ANOVA and Tukey's multiple comparison's test.

4.4.3 Leaf and canopy morphology dynamics

In field trial 2, more in-depth measurements were obtained to examine the effects of nitrogen deficiency on leaf and canopy traits. Below are trend and comparisons obtained from Field Trial 2.

Leaf lengths and widths

The lengths of leaf 9 and flag leaf, once fully extended, were measured and the means and SEM are shown in Figure 4.14. Flag leaves were found to be shorter than leaf 9 – ranging from 23 cm in MR253 (control) to 31.8 cm in MR219 (control). Control plants of the MR253 variety were visibly shorter than deficient plants, but the differences were not statistically significant ($p>0.05$). MR219 and MR220 plants in both treatments did not have significant varietal differences ($p>0.05$), but generally did with MR253 plants ($p<0.05$). In leaf 9, varietal differences were more apparent than treatment differences. It is clear in this study that MR253 rice plants had shorter leaves than the other two Malaysian varieties. Only MR219 showed a statistically significant difference ($p<0.05$) in leaf 9 lengths.

Leaf width measurements were also taken from a fully elongated leaf 9 and flag leaf. The data shown in Figure 4.15 are means with their SEM. Contrary to leaf lengths, leaf widths were found to be longer in flag leaves, suggesting an inverse relationship with length. Flag leaves of MR219 and MR220 were at least 25% wider than leaf 9, both in deficient and in control conditions. Once again, the visible difference in flag leaf widths between MR253 control and deficient plants was not found to be statistically significant ($p>0.05$). Only MR219 showed significant differences ($p<0.05$) in leaf 9 width.

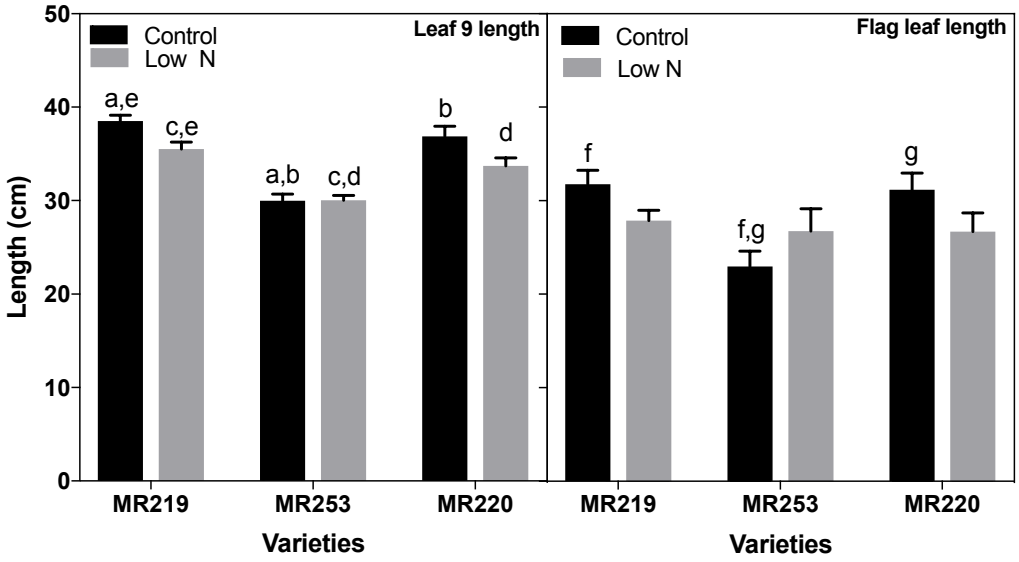


Figure 4.14: Mean leaf 9 and flag leaf lengths (cm) for the three rice varieties in control and low N conditions in Field Trial 2. Shown are the means and the standard errors of the means (SEM), n=6. Same letters indicate significant differences between compared pairs (analysed separately), following a two-way ANOVA ($p<0.05$) and Tukey's multiple comparison's test.

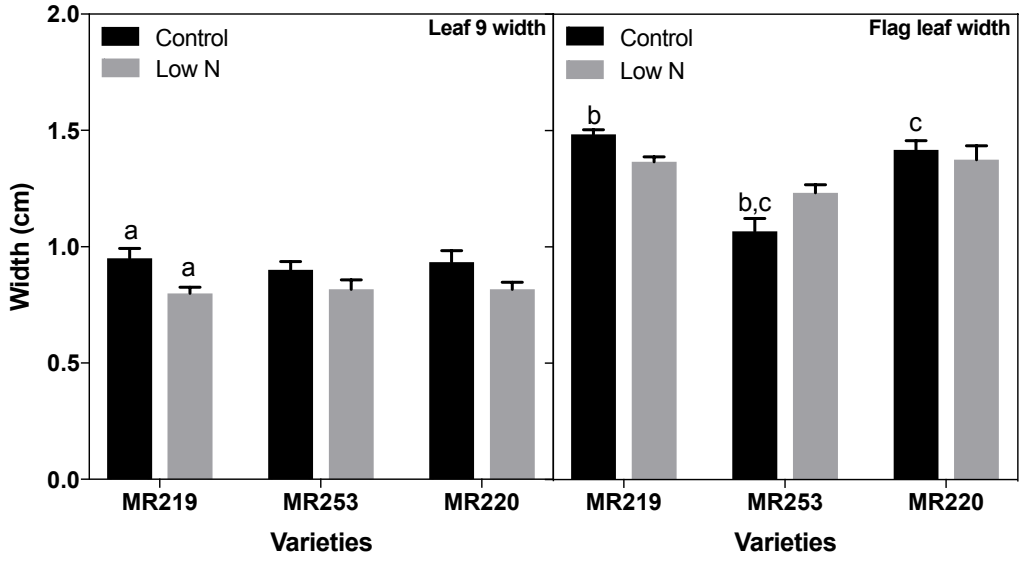


Figure 4.15: Mean leaf 9 and flag leaf widths (cm) for the three rice varieties in control and low N conditions. Shown are the means and the standard errors of the means (SEM), n=6. Same letters indicate significant differences between compared pairs (analysed separately), following a two-way ANOVA ($p<0.05$) and Tukey's multiple comparison's test.

Leaf inclination angle

Leaf 9 angles (∠ *a* on Figure 4.6) between the leaf and sheath, as well as between the sheath and stem were recorded at 11 am on the same day as gas exchange measurements. Leaf inclination angles were calculated from these measured angles, and the means and SEM are shown in Figure 4.16. Generally, the angles of the leaf blade with respect to the main stem were between 26.2° (MR253) and 38.3° (MR220). Leaves were more horizontal in low N MR220 plants ($p<0.05$), as shown in the higher inclination angles as compared to control plants. Angles were similar within varieties in both treatments for MR219. Control MR253 leaves were more visibly erect than MR253 low N leaves.

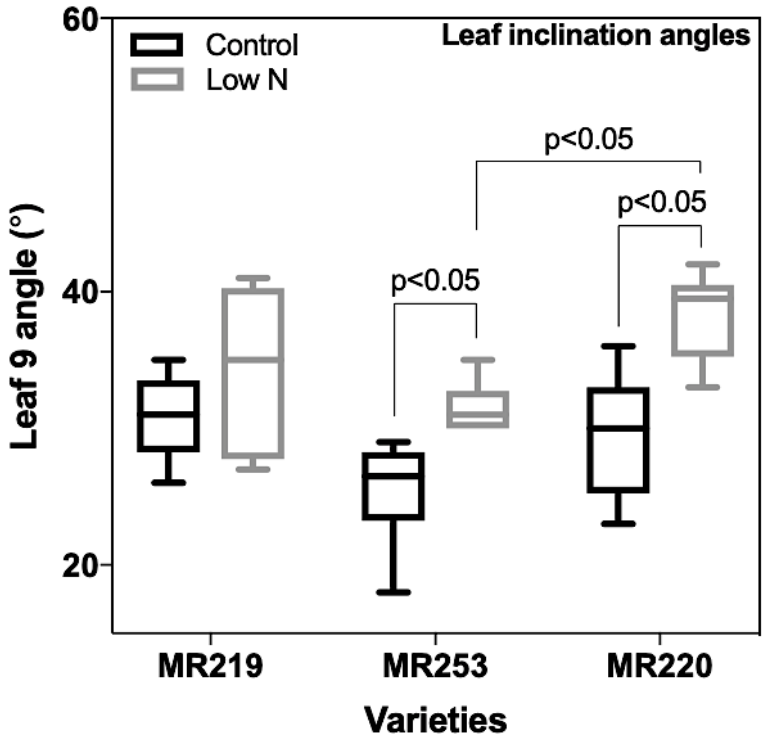


Figure 4.16: Minimum and maximum values of leaf 9 inclination (°). Bars indicate significant differences between compared pairs, following a two-way ANOVA and Tukey's multiple comparisons test (n=6).

Leaf area and NDVI

Prior to flowering, flag leaf area was measured using a portable leaf area meter. The mean areas and SEM are shown in Figure 4.17a. Visible differences between MR219 control and N-deficient plants were statistically significant ($p<0.05$). Interestingly, MR253 control plants had distinctly smaller flag leaf area ($p<0.0001$) as compared to the N-deficient plants. Figure 4.17b are the normalized difference vegetation index (NDVI) means and SEM. This index has been used to predict the N-status of crops in agriculture. Here, treatment effects were much more apparent, apart from MR253. NDVI values were exceptionally lower in N-deficient plants as compared to control plants.

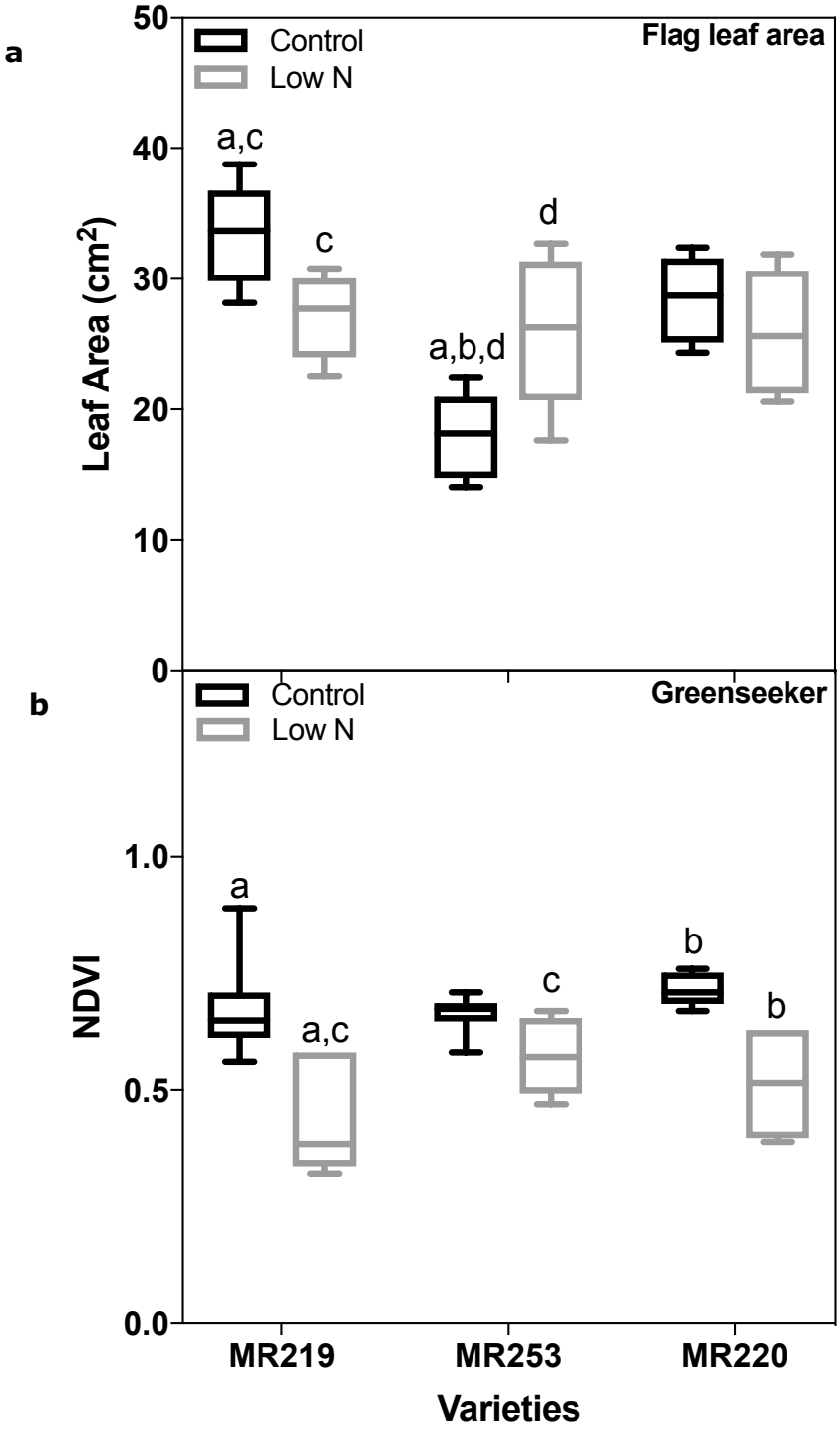


Figure 4.17: (**a**) Box and whiskers plot with minimum and maximum values of leaf area (cm^2) and (**b**) normalized difference vegetation index (NDVI). Same letters indicate significant differences ($p<0.05$) between compared pairs. following a two-way ANOVA and Tukey's multiple comparisons test (n=6).

Canopy light interception

The behaviour of light was predicted by calculating the percentage of light intercepted. Shown in Figure 4.18 are the means calculated from incoming PAR at the top of the canopy (PAR_i) and the transmitted PAR at the bottom of the canopy (PAR_b) as shown in the equation below:

Light intercepted (%) = $[(PAR_i - PAR_b)/ PAR_i] \times 100$

Shown are the means, and the letters represent significant differences ($p<0.05$) from two-way ANOVAs. It was found that control plants intercepted more light than low N MR219 and MR220 plants ($p<0.05$). In contrast, MR253 intercepted a similar percentage of light regardless of treatment and the significant reduction in leaf inclination. More light was able to reach the bottom of the canopy in deficient plants, with the sister varieties MR219 and MR220 showing marked differences ($p<0.05$) between control and low N plots.

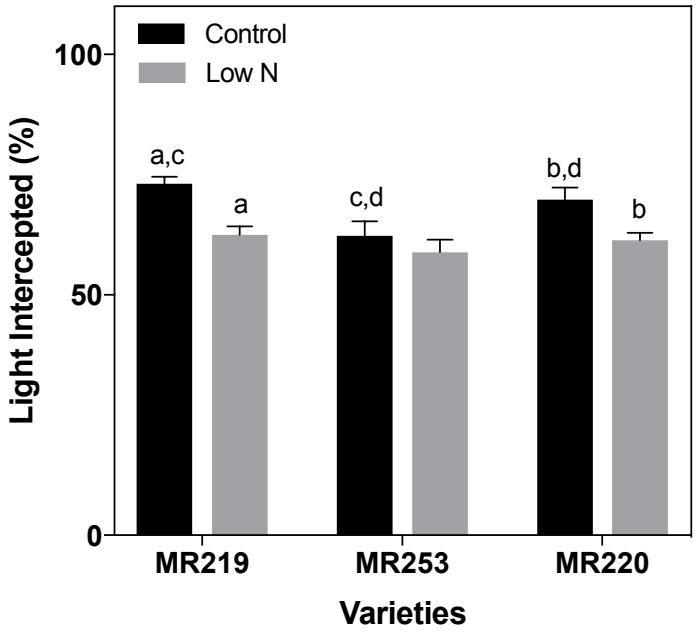


Figure 4.18: Light intercepted (%) by canopy in control and stressed plants. Shown are the means and SEM. Same letters indicate significant differences ($p<0.05$) between compared pairs, from a two-way ANOVA and Tukey's multiple comparisons test (n=6).

4.4.4 Gas exchange measurements

P_{max} and stomatal conductance

Shown in Figure 4.19 are the mean photosynthetic assimilation rates with increasing PPFD at the top and bottom of the plant canopy in the three varieties under the two treatments. Data was curve-fitted using a light response curve-fitting tool (Ye, 2007), and R^2>0.98 for all the fitted data. The maximum assimilation rates (P_{max}) were obtained from the fitted curve and this is presented in Figure 4.20. P_{max} values recorded were relatively high, even though gas exchange was carried out in ambient CO_2 concentrations. The sister varieties exhibit similar P_{max} between control and deficient plots, and the only significant variation found was between control and low N MR253 plants ($p<0.05$) following a two-way ANOVA with multiple comparisons. Stomatal conductance (g_S) for Field Trial 1 is shown in Figure 4.21. Similar to P_{max}, the values recorded for g_S was relatively high even though the measurements were carried out at 400 ppm of CO_2, particularly at higher PPFD. The variation in g_S between the top and bottom of the canopy is less pronounced than P_{max}. Low N MR253 plants were found to exhibit lower g_S than control plants, similar to the variation in P_{max}.

In Field Trial 2 however, there were visible decreases in P_{max} in low N MR253 and MR220 plants, and MR219 control plants exhibiting a surprisingly lower assimilation rate than low N plants (Figure 4.22 and Figure 4.23). However, two-way ANOVAs revealed that there were no significant differences found between treatments and varieties ($p>0.05$) in all plants.

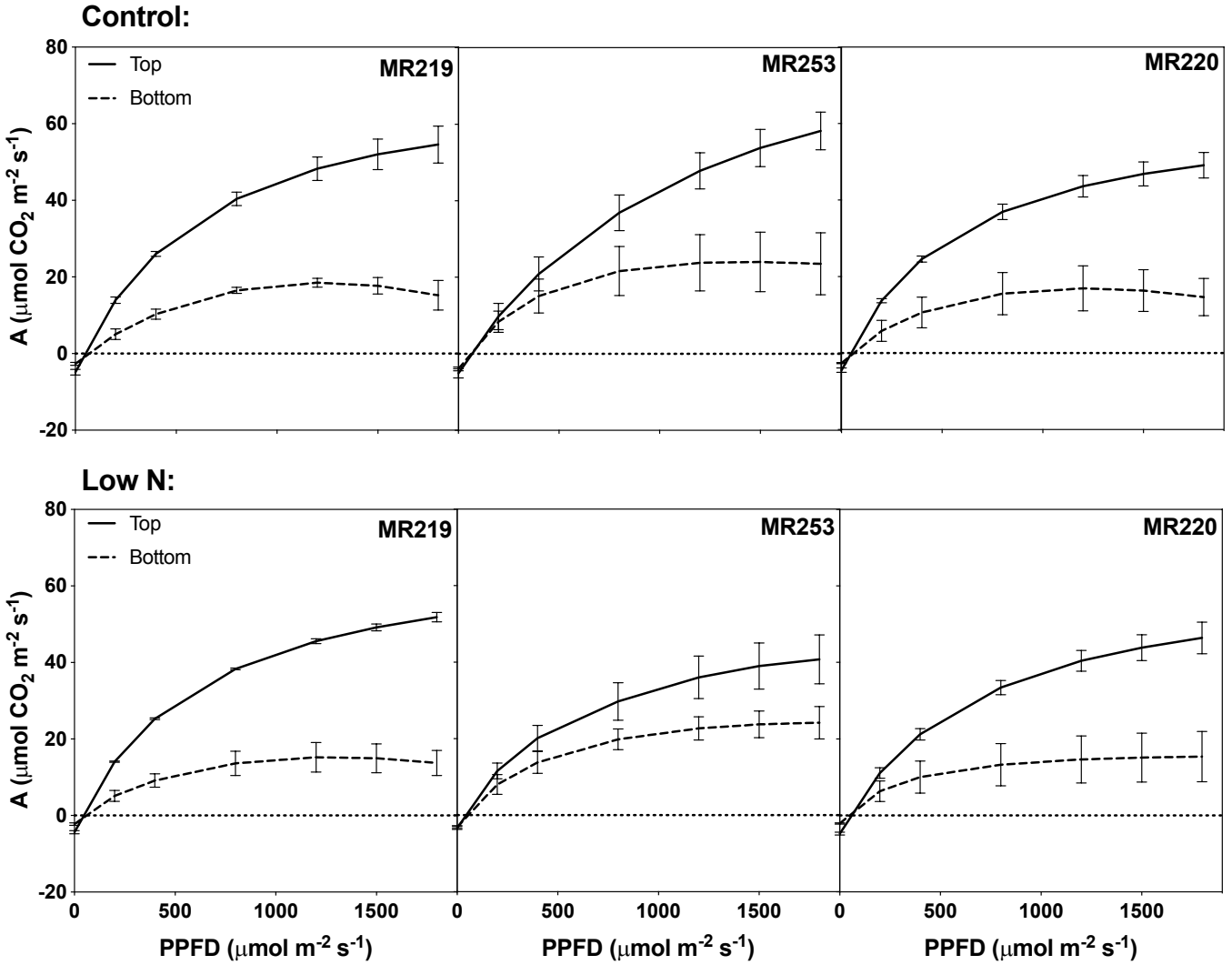


Figure 4.19: Light response curves for top and bottom of the canopy in control and low N plants in Field Trial 1. Shown are the mean photosynthetic assimilation rates (μmol CO_2 m^{-2} s^{-1}) at increasing photosynthetic photon flux densities (PPFD in μmol m^2 s^{-1}) and SEM bars (n=3). Data has been fitted using a light response curve-fitting tool (Ye, 2007).

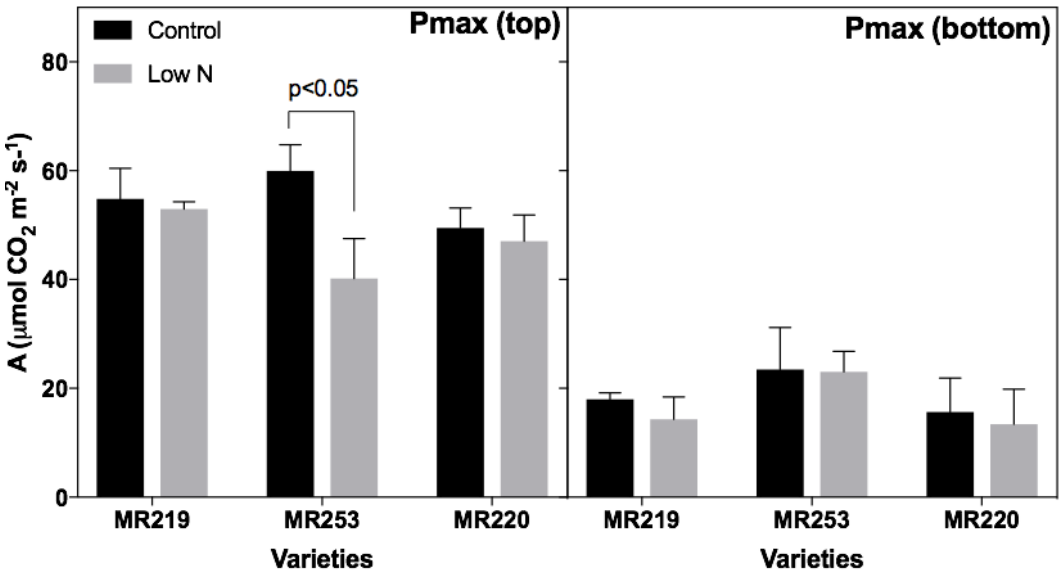


Figure 4.20: Mean and SEM of photosynthetic assimilation rates, P_{max} (μmol CO_2 m^{-2} s^{-1}) at the top and bottom canopy levels, in saturated light conditions obtained from curve-fitted data in Field Trial 1 (Ye, 2007). The bar denotes significant difference, following a two-way ANOVA and Tukey's multiple comparisons test (n=3).

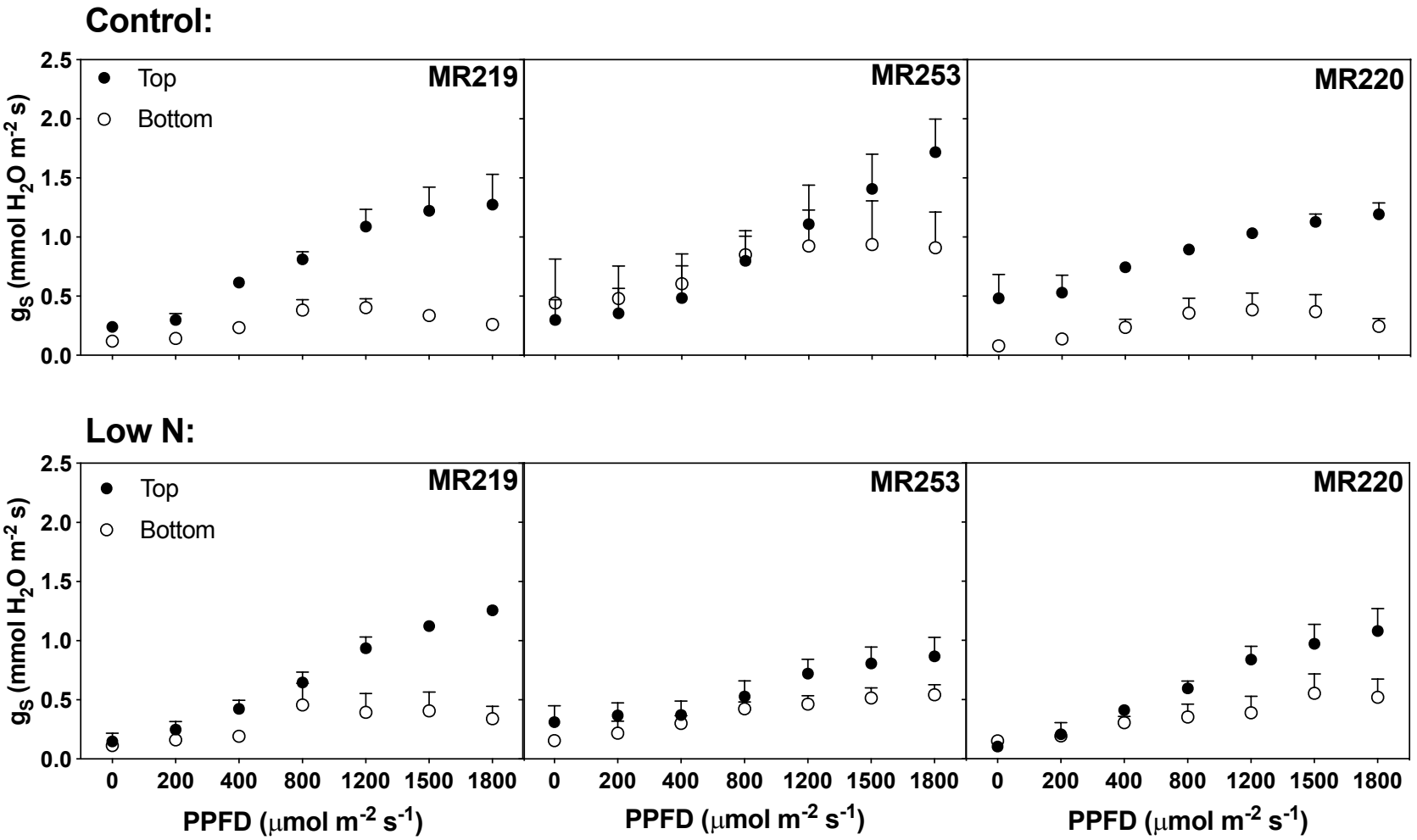


Figure 4.21: Mean stomatal conductance, g_S (μmol CO_2 m^{-2} s^{-1}), at the top and bottom of the plant canopy in Field Trial 1, at increasing photosynthetic photon flux densities (PPFD in μmol m^2 s^{-1}) and SEM bars (n=3).

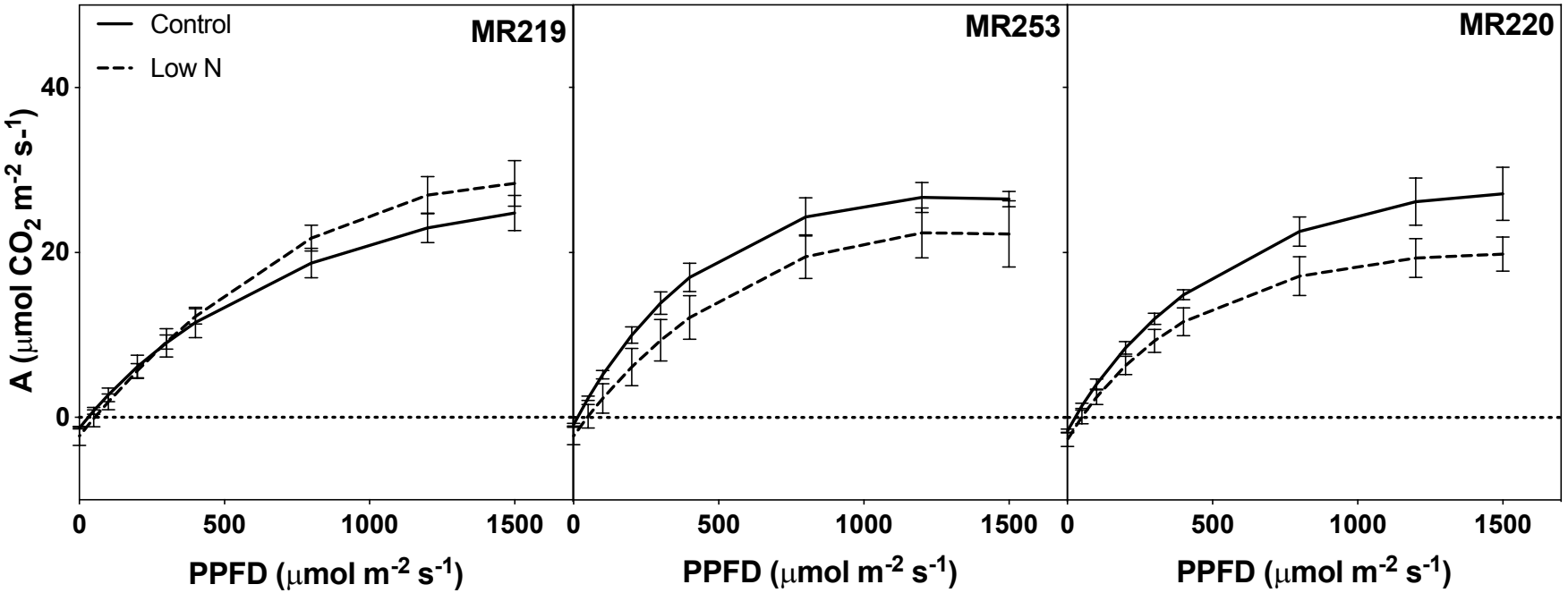


Figure 4.22: Light response curves for leaf 9 in control and low N plants in Field Trial 2. Shown are the mean photosynthetic assimilation rates (μmol CO_2 m^{-2} s^{-1}) at increasing photosynthetic photon flux densities (PPFD μmol m^2 s^{-1}) and SEM bars (n=3). Data has been fitted using a light response curve-fitting tool (Ye, 2007).

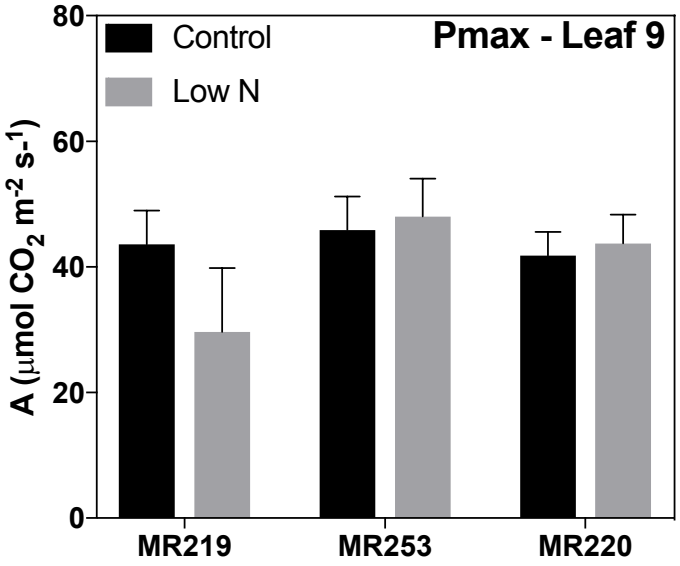


Figure 4.23: Mean and SEM of photosynthetic assimilation rates, P_{max} (μmol CO_2 m^{-2} s^{-1}), in saturated light conditions obtained from curve fitted data in Field Trial 2. No significant differences were found from a two-way ANOVA and Tukey's multiple comparisons test (n=3).

Light-adapted (Fv'/Fm') and dark-adapted (Fv/Fm) Qy

Figure 4.24 shows the quantum efficiencies of Photosystem II in all varieties in the light-adapted state in Field Trial 1. Data was taken at three points in the reproductive phase – at heading (panicle exsertion) (48 DAT), flowering (65 DAT) and prior to grain filling (78 DAT). Significant differences were only observed at 78 DAT, between all control and low N plants, apart from MR220. In low N MR219 plants, there was a significant decline in Fv'/Fm' in low N plants. Conversely, there is a significant increase in Fv'/Fm' in low N MR253 plants, demonstrating that a higher percentage of incoming light is being proportioned to photochemistry or heat dissipation, instead of the expected non-photochemical quenching.

Figure 4.25 shows the maximum quantum yield (Fv/Fm) of Photosystem II of dark-adapted rice plants under both treatments during the vegetative stage, up until heading in Field Trial 2. The y-axis is the ratio Fv/Fm. Fv/Fm was found to vary across the growth period and did not have a distinctive pattern apart from the drop-in

value between 30 DAS and 40 DAS in most plants. Fv/Fm values ranged from between 0.45 to 0.84, indicating that photoinhibition may have been dependent on prevailing light conditions.

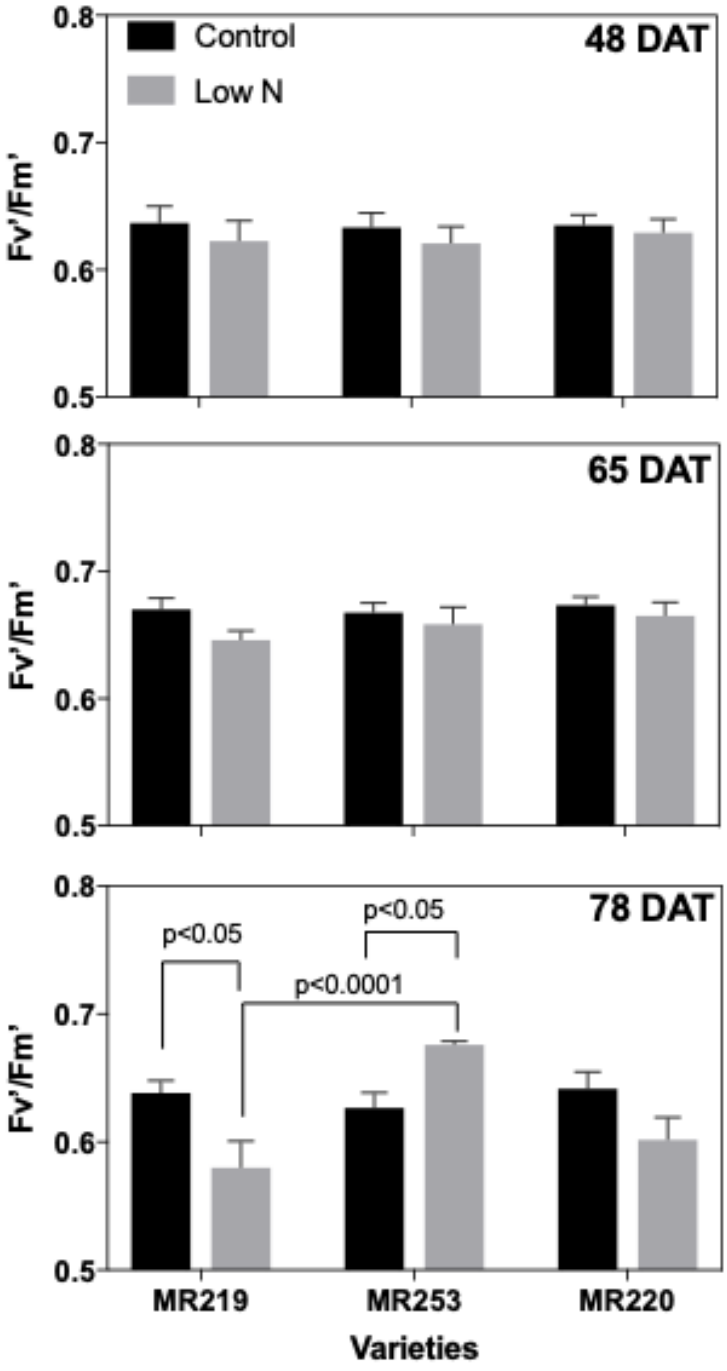


Figure 4.24: Light-adapted Fv'/Fm' in plants in Field Trial 1 at 48, 65 and 78 DAT. Shown are the means and SEM, n=3. Bars indicate level of significant differences between compared pairs from a two-way ANOVA and Tukey's multiple comparisons test.

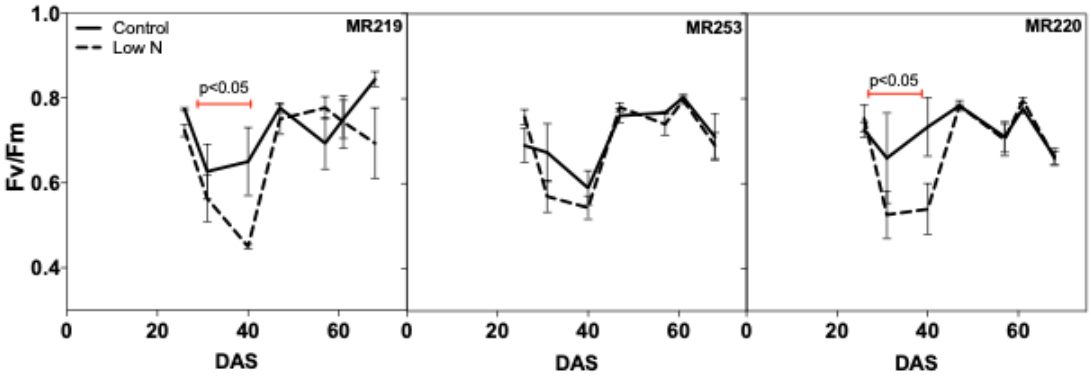


Figure 4.25: Maximum efficiency of Photosystem II in dark-adapted state or Fv/Fm values in Field Trial 2. Shown are means and SEM. Letters indicate significant differences ($p<0.05$) and asterisks indicate highly significant differences ($p<0.0001$) from a two-way ANOVA and Tukey's multiple comparisons test (n=6).

4.4.5 Yield parameter

The number of effective tillers is used as a function of yield in this study, and they were obtained at the grain-filling growth stage (110 DAS). The mean number of effective tillers from both trials are in Table 4.10, with the standard error of means. Key differences were found between control and low N plants in all varieties. MR253 generally had a lower number of tillers and was found to vary significantly from MR220 between the control plots in Field Trial 1.

Table 4.10: Number of effective tillers from both field trials. Shown are means and standard error of means. Letters indicate significant differences ($p<0.05$) from a two-way ANOVA and Tukey's multiple comparisons test (n=6).

	Trial 1				**Trial 2**			
	Control		**Low N**		**Control**		**Low N**	
	Mean	SEM	Mean	SEM	Mean	SEM	Mean	SEM
MR219	14.2*a*	0.601	11.5*a*	0.428	15.3*e*	0.211	13.0*e*	0.258
MR253	12.3*bd*	0.422	10.3*b*	0.715	14.3*f*	0.333	12.5*f*	0.922
MR220	14.7*cd*	0.422	12.0*c*	0.577	15.8*g*	0.307	12.8*g*	0.601

4.4.6 Correlation matrices

Figures 4.26 (control plants) and 4.27 (low N plants) are the correlation matrices for the growth and yield parameters in Field Trial 2. The correlation matrices revealed allometric relationships between growth parameters in both control and low N treatments. There was a general negative correlation between plant height and the number of tillers, while there was a positive correlation between the number of tillers and the number of effective tillers in both of the treatments. One interesting key difference between the treatments was that flag leaf lengths and plant heights were highly correlated in control plants, but this was not seen in low N plants.

Table 4.11: Pearson's correlation matrix with correlation coefficients for growth parameters against the yield parameter, for control plants in Field Trial 2 for control plants. PH – plant height; MS leaves – number of leaves on main stem; TN – tiller number; FLL – flag leaf length; FLW – flag leaf width; FLArea – flag leaf area; L9L – leaf 9 length; L9W – leaf 9 width; Cumul LAI – cumulative leaf area index; Eff. Tillers – number of effective tillers. Squares highlighted in pink represent significant correlation ($p<0.05$) and squares highlighted in brown represent highly significant correlation ($p<0.0001$).

	PH	**MS leaves**	**TN**	**FLL**	**FLW**	**FLArea**	**L9L**	**L9W**	**Eff. Tillers**
PH									
MS leaves	0.089								
TN	-0.237	-0.019							
FLL	0.787	0.189	-0.151						
FLW	0.481	-0.100	0.382	0.528					
FLArea	0.708	0.058	0.098	0.773	0.715				
L9L	0.816	0.169	0.143	0.678	0.670	0.809			
L9W	0.198	0.162	0.083	0.170	0.374	0.270	0.460		
Eff. Tillers	0.492	0.107	0.397	0.573	0.597	0.601	0.619	0.323	

Table 4.12: Pearson's correlation matrix with correlation coefficients for growth parameters against the yield parameter, for control plants in Field Trial 2 for low N plants. PH – plant height; MS leaves – number of leaves on main stem; TN – tiller number; FLL – flag leaf length; FLW – flag leaf width; FLArea – flag leaf area; L9L – leaf 9 length; L9W – leaf 9 width; Cumul LAI – cumulative leaf area index; Eff. Tillers – number of effective tillers. Squares highlighted represent significant correlation ($p<0.05$).

	PH	**MS leaves**	**TN**	**FLL**	**FLW**	**FLArea**	**L9L**	**L9W**	**Eff. Tillers**
PH									
MS leaves	0.185								
TN	-0.653	-0.304							
FLL	0.165	-0.220	0.040						
FLW	0.303	0.264	-0.160	-0.004					
FLArea	-0.166	-0.187	0.247	0.593	-0.018				
L9L	0.322	-0.152	-0.013	0.508	0.499	0.086			
L9W	-0.179	-0.387	0.151	0.171	-0.110	0.196	0.315		
Eff. Tillers	-0.262	-0.525	0.507	0.493	-0.110	0.684	0.278	0.418	

4.5 **Discussion**

Nitrogen limitation to plants in field conditions is not an uncommon occurrence. While most modern rice varieties have been selected for their high-yielding and short maturation traits, a major challenge continues to persist. As the cost of manufacturing nitrogenous fertiliser continues to rise, efforts have been channelled into identifying ways to increase yield without increasing fertiliser input per unit leaf area.

Nitrogen deficiency is easily one of the most common stress in rice fields. While severe deficiency is uncommon, mild to moderate N-deficiency is almost always present to a certain degree. In this period of mild to moderate stress, plants adapt and acclimate to survive. However, accounting for this type of mild to moderate stress is time-consuming and resource heavy, as such, it is mostly overlooked or ignored. There is potential to drive the limits of yield potential by understanding plant adaptation at both the physiological and genetic levels.

4.5.1 **Changes in rice phenology in low N rice**

Plant exhibit elaborate responses to changes in nitrogen supply at the phenological level. These changes involve a complex interplay of intercellular and intracellular signalling as well as gene regulation. The association of yield to plant phenology has been well documented, and its sensitivity to the external environment allows for reliable assessments of the changing climate on yield when used as a proxy in growth simulation models. However, the non-linear responses of yield to the changing climate makes it challenging and more often than not, it is not easily framed using a regression-based simulation. Any deviation or departure from the observed would require recalibration using empirical data. In this study, the ability to tolerate mild to moderate N-deficiency was variety specific but non-linear, as shown by the isometric changes in phenology.

The appearance of leaves on the main stem (leaf rank or leaf position) is linear against thermal time (data fitted using a linear regression R^2=0.9526). The inverse of this linear relationship will yield an estimation of the phyllochron, which is the amount of time the plant takes between the appearance of successive leaf tips (Haun, 1973; Kirby, 1995; Sié *et al*., 1998; Krishnan *et al*., 2011). The phyllochron has been found to be linked with temperature (Bartholomew and Williams, 2008), nitrogen status (Khan *et al*., 2019), planting density (Martínez-Eixarch *et al*., 2013) in rice and other grasses. In stressed growing conditions, the phyllochron can be affected by a wide variety of overlapping stress factors, which could be challenging to diagnose. It is vital to determine the limiting factor in order to address the stress correctly. The phyllochron usually ranges between 3 to 8 days, or 75 to 200 degrees days (°Cd) at 20 °C (Counce *et al*., 2000) and increases with developmental stage advancement (Itoh and Sano, 2006). Cumulative phyllochron is the total time it takes from the emergence of the first true leaf to the full elongation of the flag leaf.

In the case of this study, the principal difference was that the phyllochron (°Cd) was significantly shorter in all plants in the first field trial ($p<0.05$) apart from N-deficient MR253 plants. This difference ranged between 0.25 – 0.6 days. The mean temperature for the growing season in the first trial was 1.2 °C higher than the second trial (Figure 4.7), indicating a juxtaposition of higher temperatures with the shorter phyllochron. Rice phenology is highly sensitive to temperature, and at mild to moderate nitrogen stress, this sensitivity is further exacerbated. Rice is generally cultivated twice a year in Malaysia – at April-May for early rice, and July-August for the second growing season. The early rice season is characterised by lower amounts of rainfall and warmer temperatures and vice versa for the wet season rice in the second half of the year, which possibly accounts for the difference between the mean temperature in both trials.

Itoh and Sano (2006) has suggested however, that the phyllochron in rice might actually be controlled internally instead of the external environment. In their study, the rates of change with temperature did not follow a distinct pattern and were even variable within the same genotype. This is possibly an explanation for the insignificant change in phyllochron in MR253 deficient plants between trials. This uncoupling with thermal time could be a result of the lowered N-status of the plant. This corroborates with the significantly lower number of tillers produced, and eventually the lower number of effective tillers during the reproductive stage.

At leaf level, differences in leaf lengths and width of leaf 9 and flag leaf were accounted for. Generally, leaf 9 was longer than flag leaf in plants under both treatments. Leaf width was the opposite – flag leaves were found to be wider at the widest part of the leaf than leaf 9. Positive correlations were found between flag leaf lengths, flag leaf area and effective tiller number in both treatments (Figures 4.25 and 4.26). Interestingly, the flag leaves of MR253 control plants were found to be smaller than MR219 and MR220, but showed no varietal differences within the low N treated plants. Genetic variation within rice populations in leaf size is common, but it has been proven that the flag leaf of a plant is a major source of photoassimilates during the reproductive stage of the rice plant. As such, changes in the dimensions and characteristics of the flag leaf would have a substantial impact on grain yield (Jennings and Beachell, 1964; Bing *et al*., 2006; Zhang *et al.,* 2007).

Leaves are the main sites of photosynthesis and generally increase in size up until the last three to five leaves on the main stem (Tivet *et al*., 2001). A reduction of leaf expansion in low N conditions have been found to be a consequence of a reduction of cytokinin in leaf sheath.

4.5.2 Nitrogen-mediated tillering

Tillering is considered a key agronomic trait in shoot architecture and yield, as the right balance of resources will produce effective panicles from the emerged tillers. One of the most common methods of increasing tillering in cereals is increasing the nitrogen input into the system. Managing planting density is also an effective way of promoting optimum and productive tillering (Fagade *et al*., 1971; Lin *et al*., 2009; Huang *et al*., 2013; Mathan *et al*., 2016; Tian *et al* 2017), but with increasingly limited growing area and expensive hybrid seeds, this would have to be in line with other management practices to ensure the maintenance of yield. As such, it has been common practice to increase the N load into the soil for the purpose of producing enough effective tillers during the reproductive stage. During the active tillering stage of development in rice, fertiliser is normally applied to support tiller production as tillering is highly dependent on the N-status of the plant (Wang *et al*., 2017). Fertiliser is also applied prior to panicle initiation to support the elongating panicle and the subsequent reproductive stage.

Modern elite rice varieties generally produce between 15 to 25 tillers in total and this includes primary, secondary and tertiary tillers (Pawar *et al*., 2016). Not all of the tillers produced during the vegetative stage of growth would yield panicles, and this would normally be dependent on environmental conditions. There is much potential in using tillering as a target in yield improvements as its plasticity in early development allows direct manipulation of canopy architecture (Hussein *et al*., 2014).

The reduction in the rate of tillering as early as 500 °Cd was apparent in all N-deficient plants in all three varieties. This reduction in tillering in early development is in response to the maintenance of the growth rate of leaves on the main stem, as shown by the lack of a significant difference in the rate of leaf appearance between control and deficient plants. In control plots, tillering continued at a rate

higher than deficient plots after the application of the second round of fertiliser. Endogenously, tiller bud outgrowth is regulated by a molecular crosstalk between genes and the phytohormones cytokinin, auxin and strigolactone (Azizi *et al*., 2015; Li *et al*., 2016). Nitrogen promotes higher cytokinin levels in tiller buds, which in turn activates tiller bud (axillary bud) outgrowth. The signalling network and metabolism of this phytohormone is closely linked to the status of nitrogen (Kiba *et al*., 2010; Krouk *et al*., 2011; Kamada-Nobusada *et al*., 2013; Azizi *et al*., 2015). Increased nitrogen supply to the plant has been found to increase the concentrations of cytokinin in other members of the Gramineae family; maize (Takei *et al*., 2001) and wheat (Garnica *et al*., 2010).

The development of tillers is made up of a highly complex system involving the signalling between genes, hormones and the external environment. The management and transport of nitrogen in rice is coordinated by nitrate transporters, but only a few have been characterised. A recent study by Wang *et al*., (2018) discovered that overexpression of the rice nitrate transporter OsNPF7.2 resulted in the upregulation of cytokinin-response regulators in the transduction pathway (Zurcher and Muller, 2016). The increased expression of this nitrate transporter subsequently boosted nitrate assimilation into the plants and increased accumulation of cytokinin in the axillary bud. Li *et al*., (2016) identified OsmiR393 (microRNA393), a microRNA that decreases the transduction of the auxin signal in tiller buds in rice. The authors found that OsmiR393 expression was upregulated in the presence of nitrogen fertiliser, accumulating in the axillary bud and consequently downregulating the auxin signal. Overexpression resulted in an increase tiller number, and they found that increasing N supply to knockdown mutants (producing very few tillers) did not result in any addition to overall tiller number.

The complexity at which nitrogen signalling exists within the rice plant is brought about by the involvement of many molecular

players and transduction pathways, with many of them having overlapping functions.

Plant height is also controlled by a network of genes, quantitative trait loci (QTL) and phytohormones. The gene, MONOCULMN1 (MOC1), was recently first discovered as a key regulator of lateral branching in tillering. While MOC1 primarily regulates the formation of tiller branches, it also has been found to have a negative effect on plant height (Li *et al*., 2003). This was seen in the second field trial, where tiller number negatively correlated with plant height in low N plants (-0.653, $p<0.05$). One particular group of phytohormones mediating plant height in rice is gibberellins (GA) (Wang and Li, 2005). In the presence of a higher amount of nitrogen, GA has been found to be upregulated (Jang *et al*., 2008), confirming that the growth and development of the plant is dependent on the metabolism of nitrogen.

4.5.3 Relationship between photosynthesis and canopy responses to low N

At the canopy level, leaf area index is also closely linked to tillering rate - where when LAI increases, the relative rate of tillering would start to decline. Peng *et al*., (2002) found that the relative tillering rate decreased exponentially as LAI increased.

Leaf area index is defined as the total one-sided area of leaf per unit ground surface area and is dimensionless. LAI changes over the duration of plant growth, and increases rapidly when the growth conditions are favourable. Maximum LAI is normally achieved at the end of the heading stage, right before flowering. Leaf and tiller senescence during maturation would cause LAI to decline in rice and other cereal crops. LAI is affected by a variety of factors, ranging from nutrient deficiency to planting density (Fagade and Datta, 1971; Peng *et al*., 1995b). LAI has been used in many systems to characterise the behaviour of light within plant canopies, and the

attenuation of light in the canopy depends heavily on the morphology and phenology of the plant (Murchie *et al*., 1999; Horton, 2000; Falster and Westoby, 2003; Peng and Ismail, 2004). There is a fine line between achieving optimal leaf density for light interception and excessive canopy expansion that could potentially self-shade its leaves. This already delicate balance can be easily disrupted by a change in the external environment.

At molecular level, plant stress can significantly reduce the ability of the plant to achieve optimal leaf (and tiller) density, as described in the sub-section above. In the case of this study, this variation at leaf level conferred a canopy level response for the Malaysian rice varieties in both field trials, but to different extents. In the first trial, the significant difference in LAI between control and N-deficient plants was found in the MR219 and MR253 varieties, but only at the end of the vegetative stage, at 78 days after transplanting. There were more varietal differences than between treatments, as shown in Figure 4.13a. MR253 exhibited a lower LAI than the other two varieties and this was also reflected in Field Trial 2 (Figure 4.13b). Interestingly, MR253 low N plants had very similar LAI over the growing period as the control plants in Field Trial 2. Conversely, there was a substantial difference in LAI between control and low N plants in the sister varieties, from as early as the active tillering stage.

At first glance, MR219 and MR220 seemed to be more negatively affected by the N-status of the plant, while MR253 was much less susceptible to a lower soil N. This general reduction in LAI across both field trials for MR219 and MR220 could be a compensation approach to reduce possible dilution of leaf nitrogen per unit leaf area (Evans 1989; Hikosaka 2004, 2010). Nitrogen dilution per unit leaf area can result in a reduction in the photosynthetic capacity of the plant. To confirm this, photosynthetic light response measurements were made to obtain the maximum photosynthetic rate (P_{max}) under saturating light, of each variety under both treatments. The P_{max} for these two varieties were not different in Field Trial 1 (Figure 4.20),

which corroborated with the lack of a difference in LAI between low N and control plants in the same field trial. Interestingly, in Field Trial 2, P_{max} values of MR219 and MR220, while visibly different, were not found to be significantly different in control and low N plants (Figure 4.23). It is clear from here that these two varieties prioritised the maintenance of photosynthetic capacity and remain relatively productive (Chen *et al*., 2003), and this was reflected by a reduction in the leaf area index of the rice plant. MR219 plants displayed identical rates of photosynthesis from 0 to 500 PPFD (shown in the initial apart of the slope in Figure 4.19).

MR253 behaved quite contrarily in both trials. While there were no differences in LAI between control and low N plants in Field Trial 1, there was a significant reduction in P_{max} in the top of the canopy, but not at the bottom of the canopy (Figure 4.20). Lower leaves in the plant canopy have lowered N-status, but this is sufficient to prevent leaf senescence while still contributing to the accumulation of photoassimilates albeit with a much reduced P_{max}. Stomatal conductance was also lower in low N MR253 plants (Figure 4.21), indicating that this drop in photosynthesis could be a result of a reduced amount of photosynthetic machinery (stomatal limitation) and intermediates in the cells of the leaves. On the other hand, Fv'/Fm' was found to be significantly higher in low N MR253 plants then the control plants. Fv'/Fm' is the maximum efficiency of Photosystem II in light conditions, if all PSII centres were open. The lower Fv'/Fm' in control plants indicate a higher level of non-photochemical quenching, while still maintaining a high P_{max}. In sufficient-N conditions, plants would generally exhibit a higher Fv'/Fm', reflecting lower NPQ (Murchie and Harbinson, 2014). Stressed plants normally exhibit higher NPQ levels; as a photoprotective response to remove the excess excitation energy in light harvesting complexes in the photosynthetic machinery. This excess energy, if not quenched, can potentially trigger the formation of free radicals which are damaging to the plant (Demmig-Adams and Adams, 2006; Murchie and Lawson, 2013; Murchie *et al*., 2015). In

this study, there is a distinct reversal of this phenomenon – low N MR253 exhibited a lower P_{max}, and lower NPQ, suggesting that a larger proportion of the excess excitation energy could have been re-emitted as heat.

Conversely, this reduction in P_{max} was not reflected in Field Trial 2, even though no differences in LAI were observed like in Field Trial 1. Light saturated photosynthesis is generally positively correlated with the N-status of the plant (Peng *et al*., 1995a,b). In this study however, the reduction in nitrogen supply to the low N plots did not confer a reduction in P_{max}. This dissociation was found in all varieties. P_{max} is affected by a number of factors, and at the whole-plant level, plant architecture and light distribution are two key factors. In-depth measurements of the behaviour of light within the canopy revealed that low N MR253 plants had a higher extinction coefficient (Figure 4.18a), as compared to control plants ($p<0.05$), indicating the presence of a more horizontal canopy. Measurements of leaf 9 angles with respect to the main stem also revealed that low N MR253 plants had less erect leaves than the controls ($p<0.05$), which corroborates with the higher *k* value. Despite these differences in architecture, low N MR253 plants still intercepted a similar amount of light (Figure 4.18b) as the control plot, which accounts for the similar P_{max}. Additionally, SPAD values (Figure 4.12) and dark-adapted Qy (Figure 4.25) measurements did not reveal significant differences in greenness and Fv/Fm between control and low N MR253 plants.

The changes in plant architecture here could have been a canopy level response to redistribute nitrogen to the younger leaves to maintain optimum growth and photosynthesis rates, in less nitrogen-optimal conditions. One thing to consider here is that while the top layer of the canopy is exhibiting optimal P_{max}, it might not be the same way in the lower canopy layers. It is therefore important to study photosynthesis at different canopy layers and whole-plant photosynthesis (measuring canopy gas exchange using canopy photosynthesis and transpiration systems, see Song and Zhu, 2018

for review) instead of just single leaf as this will give a better indication of health and productivity in mild to moderate nitrogen stress. In the case of this study, the possible redistribution of nitrogen to younger leaves could accelerate leaf senescence in the lower parts of the canopy, or even tiller senescence, which leads to a decline in effective tillers (Makino *et al*., 1983; Makino *et al*., 1984). While P_{max} and LAI were sustained in low N plants of the MR253 variety, this was not sufficient in producing a similar number of effective tillers when comparing with the control plot (Table 4.10). This is perhaps the reason behind the decline in P_{max} for low N plants in Field Trial 1, when P_{max} was measured during the reproductive stage, instead of the vegetative stage in Field Trial 2. Here, it is observed that the N-deficient plant loses the ability to maintain high levels of photosynthesis in later stages of development. It can be concluded here that while there was some form of acclimation to the lowered N-status initially, the persistent shortage of nitrogen supply eventually led to a decline in P_{max} in later stages.

Net leaf photosynthesis saturates at higher irradiances for leaves with higher nitrogen content (Lemaire and Gastal, 1997; Li *et al*., 2009; Sun *et al*., 2016). The allocation of nitrogen to leaves is dependent on the stage of development and the light environment. Leaves receiving more irradiance would naturally have a higher nitrogen content, in order to maximise photosynthetic productivity (Niinemets, 1998; Hikosaka *et al*., 2005). It was evident from this study that redistribution of nitrogen to photosynthetically active organs was favoured to ensure relative productivity, in plants growing in low N plots.

4.6 **Conclusion**

There were varietal trade-offs between canopy architecture and photosynthesis observed in this study. The mechanisms the Malaysian rice varieties employed here underpin the developmental and phenotypic plasticity of plants, where individuals within a species exhibit various degrees of the fundamental basis of stress response (Schmitt *et al*., 2003; Kroon *et al*., 2005).

MR253 behaved differently from the other two Malaysian varieties. The initially low susceptibility of this variety to a lower N-status has most likely made it a good candidate for cultivation in areas with poor soil nutrition and possibly other abiotic stress. The inherently erect canopy with a short stature allowed a more homogenous penetration of light during the vegetative stage. However, the plant was unable to maintain a higher P_{max} due to structural and physiological limitations from a presumed shortage of nitrogen further on in development. This may have resulted in a decline in the reproductive tillers.

The traits and behaviour in response to the lowered nitrogen status in Malaysian varieties have been characterised in this study. The integration of these photosynthetic and morphological changes with their corresponding genetic basis will further our understanding of plants response and adaptation to less than optimal conditions.

Chapter 5:
General Discussion

Chapter 5

5.1 Introduction

Since the Green Revolution in the 1960s, there have been a plethora of new technologies and theoretical breakthroughs that have helped us close yield gaps by improving crop management strategies and developing high-yielding lines. As it currently stands however, the current rate of food production is not sufficient to satisfy the future demand of a growing population of at least 60 million by 2050 (Wiebe *et al*., 2015; Reynolds *et al*., 2018). With a changing climate and more erratic weather patterns, it is becoming more challenging to realize higher yields in increasingly tougher growing environments. To push past yield barriers put up by the changing environment, there is an inherent need to improve plant productivity. Research in the recent years have offered many new options, with engineering optimal plant canopies being one of the most promising techniques. It has been predicted that an increase in the rate of plant photosynthesis in cereal crops is required to increase yield (Hubbart *et al*., 2007). Coupled with observational data, we would be able to accurately assess canopy behaviour of rice plants growing in different nitrogen concentrations, as shown in this study.

5.2 Experimental Overview

Malaysian rice varieties were grown in three different environments, to investigate leaf and canopy level responses to different nitrogen concentrations. For the first time, Malaysian rice canopies were modelled using 3-dimensional image-based reconstructions, to predict photosynthesis and carbon gain.

5.2.1 Summary of findings of individual rice varieties

In Chapter 2, Malaysian varieties MR219 and MR253 as well as the IRRI variety IR64 were grown under full nutrient complement (100%

N), 50% N as well as 25% N. Here, key leaf developmental features were quantified to monitor the effect of a reduction in nitrogen nutrition. These growth room trials gave some initial insight into how each variety grew and what physiological mechanisms were employed to deal with a reduction in nitrogen available for growth. Chapter 3 examined the same three rice varieties in simulated field conditions, employing novel reconstruction techniques to extract unique canopy properties and model canopy photosynthesis under high and low nitrogen treatments. The final chapter, Chapter 4, investigated the development of the two Malaysian varieties (MR219 and MR253) as well as MR220, which is the sister variety of MR219. These varieties were grown under reduced nitrogen fertilization in field conditions in Malaysia, and their gas exchange and canopy development monitored.

MR253

This variety was, out of all the ones that were grown, the most compact plant. Plant height differences were seen between the effects of HN (high nitrogen) and LN (low nitrogen) treatments between the plants growing in the different environments (i.e. simulated field setting – glasshouse and actual field settings). Interestingly, the differences in plant height were seen in the glasshouse trial and not the field trials. Nevertheless, tiller number remained unchanged in both despite the differences in N nutrition in all trials with the exception of 100% N and 25% N treatments in the controlled environment trial. Here, the substantial reduction in the concentration of N reduced the number of tillers by almost half. Similarly, the number of stomata and lengths remained unchanged with the exception of the 25% N treatment in the controlled environment trial. SPAD values were affected by the changes in N nutrition, but this was more attributed to the differences of chlorophyll utilisation at the various growth stages.

In gas exchange measurements, P_{max} in the controlled environment trials declined with decreasing nitrogen concentrations. MR253 had the highest NPQ values in most of the N deficient plants in the controlled environment trials, indicating a potentially useful trait for resilience in harsher growing environments. This photoprotective mechanism protects a vulnerable plant from photoinhibition in high light conditions which are common in Malaysia. This increase in NPQ however, has been shown to be at the expense of (trade-off) CO_2 assimilation (Hubbart *et al*., 2018), as shown in the pronounced decrease in A/Ci in Chapter 2. In addition to this, while MR253 grows well in more marginal environments than the other Malaysian cultivars as shown in this study (relative to MR219 and MR220), this variety has been shown to not have as high a yield potential as the sister varieties (Salmah, 2014), averaging only about 4.5 to 6.8 tonnes per hectare. Interestingly, LN MR253 plants in Chapter 3 maintained high carbon gain per unit leaf area, as a result of the maintenance of relatively similar P_{max} throughout the growth stages. As MR253 is a relatively new variety (released in 2010, by MARDI) more in-depth analysis needs to be conducted to characterise canopy productivity to maximise yield.

MR219 and MR220

Compared to MR253, MR219 was more affected by changes in the N status, both morphologically and in terms of gas exchange properties. This variety exhibited the largest differences in leaf nitrogen (chlorophyll from SPAD values and % leaf N) between HN and LN plants in both field and simulated field settings. In terms of leaf size and anatomy, MR219 LN plants grew thinner leaves (as seen in the reduction of the thickness of both the major and minor veins). In Chapter 3, it was found that LN M219 plants had higher stomatal number on the abaxial leaf surface, indicating a possible N-deficiency response to increase the amount of gas exchange apparatus to maintain high P_{max} as demonstrated by the similar P_{max} between HN and LN MR219 plants.

MR220 was examined to investigate any potential physiological and biochemical differences from its sister variety, MR219 (both are hybrids of MR151 and MR137). This variety has been used to grow in regions where MR219 was unable to reach desirable yields (as a result of disease resistance). In this study, MR220 was only grown in the field trials, but any similarities in characteristics in plant physiology and photosynthesis with MR219 may shed some light on how its canopy behaves spatially and temporally. From the plant development analyses in Chapter 4, it is clear that there are some similarities, particularly in the final plant heights and the effective tiller numbers.

IR64

In a previous study by Burgess *et al*., (2017), the IR64 canopy was similarly studied, which lends itself as a basis for comparison to the current work. IR64 is a high-yielding indica variety with a similar maturation period as compared to the Malaysian varieties (Mackill and Khush, 2018).

Overall, IR64 grew a much larger canopy, with the highest number of tillers. It is particularly more sensitive to changes in N nutrition, as seen in the early vegetative plant development in Chapter 2. In the low N plants, we see a redistribution of N through a significant decrease in the number of tillers between the 100% N and lower N plants in the controlled environment trial, as well as the simulated field experiment. As nitrogen affects tillering in rice plants (Wang *et al*., 2017), one would expect this to occur to a plant that produces many tillers. In Chapter 2, the decrease in N was substantial enough to cause a negative response in photosynthetic parameters. There was at least a 50% reduction in the photosynthetic capacity between the 100% N and 25% N plants. This shows a lowered resilience in IR64 to a drastic drop in N status. The reduction in N in

Chapter 3 was not as substantial, and while it did have an effect on the number of tillers, P_{max} was preserved.

In the same chapter, IR64 HN plants consistent had the highest carbon gain per unit ground area, as well as the highest k values. There is much to be improved about the stature of the IR64 plant, as a less upright plant reduces the amount of light that is able to penetrate the canopy. Most of the photons get absorbed only by the upper layers of the canopy. There is still some opportunity to increase the penetration of light into the canopy of IR64 plants, and potentially further increase plant productivity through the increase of the carbon gain per unit leaf and ground area.

5.2.2 Wider impact of findings on breeding and farming practices

Malaysia's dependency on rice will continue to grow in the coming decades. A lot of work between the 1960s and 2000s has been carried out by MARDI (Omar *et al*., 2019) to further the yield gains by breeding for high-yielding elite varieties that are also able to withstand harsher conditions. Many rice growing locations in Malaysia such as Serdang and Batu Hitam are poor in fertile soils and require a substantial nutrient amendment to support the growth during the growing seasons (http://eapvp.org/files/report/docs/malaysia/04-4%20Country%20Report_Malaysia1.pdf). This study highly recommends considering canopy level improvements in photosynthesis to develop rice varieties that are sturdy and more resilient to stressful environments.

Particular attention should be placed on improvements on canopy architecture, as seen in Chapter 3 where even though N levels were not particularly deficient (due to the residual N present in the soil), there were differences in canopy morphology and associated parameters (i.e. leaf area index, carbon gain per unit ground area and leaf inclination angles). The Malaysian variety MR253 shows some promise, despite the lower yields of 6-8 t/ha (Ramli, 2017) compared to MR219 with an average of 10 t/ha, of resilience in lower N conditions. Changes in canopy architecture while maintaining relatively similar photosynthetic rates under lower N fertilization rates (as seen in the field-simulated trial) in the Malaysian varieties indicates an avenue for exploration for 'reengineering and re-optimization' of current rice canopies for the ideal architectural ideotype. An ideal canopy is selected for and bred based on the elimination of less ideal characteristics and/or for its high-yielding characteristics (Donald, 1968; Sharma *et al*., 2013). This ideal canopy would operate a high level of photosynthesis (at the canopy

level) whilst making minimum demand on resources (in the case of this study, a lower demand on N fertilization) per unit of dry matter production.

Malaysia's efforts on increasing rice yield has largely focused on breeding for pest and disease resistance (e.g. rice blast resistance, Miah *et al*., 2017), yield potential and tolerance to abiotic stress (e.g. submergence tolerance, Oladosu *et al*., 2020) as well as hybrid rice. A majority of MARDI's breeding efforts has been placed on increasing yield potential by selecting for agronomic traits such as the number of productive tillers and the total number of spikelets per panicle (Othman *et al*., 1986; Chandra *et al*., 2009) as well as rice nutritional and physicochemical quality (e.g. grain appearance, moisture content and amylose content) (Elixon *et al*., 2016; Neoh and Lum, 2018). There is scope for actualizing a rice ideotype that addresses yield potential (through optimum canopy architecture) as the production objective. The Malaysian varieties examined in this study, particularly MR219, was bred for high yield potential. From the results in this study, a potential capacity for improving the current varieties (for an increase in yield potential) has emerged, as it has been shown that the yield potential barrier (as described in Chapter 1) could be overcome by engineering canopies that optimizes radiation capture.

With the in-depth quantitative information from the 3-dimensional characterisation of the plant canopy and mathematical modelling (e.g. leaf curvature and light extinction coefficient) and traditional breeding techniques (e.g. the selection for higher leaf angles and related agronomic traits), feasible plant ideotypes can be derived. The results of this study recommend directing efforts to the evaluating canopy architecture in field grown rice (using the same canopy modelling techniques in Chapter 3, and the nitrogen application rates in Chapter 4).

5.2.3 Future work

Cereal breeding crosses parental lines with traits of interest to accumulate alleles that are associated with higher yields (Reynolds and Langridge, 2016; Reynold *et al*., 2018). Plant canopy architecture has been recognized as one of the most important targets for selection for increased light use efficiency, which in turn lends a hand in increasing yield potential (Peng, 2000; Murchie *et al*., 2009; Chang *et al*., 2019).

Although measurements at leaf level provide accurate and relatively high reproducible methods to screen for plant productivity, these are in isolation from whole canopy behaviour and can easily be misrepresentative (Furbank *et al*., 2019). As shown in the work here, gas exchange measurements at leaf level alone cannot and do not scale up to canopy level observations. Combined with empirical data of plant development and gas exchange, image-based phenotyping carried out on simulated field conditions can offer new insights and knowledge on the relationship between phenotype and genotype (Furbank, 2009b; Furbank and Tester, 2011; Rahman *et al*., 2015; Furbank *et al*. 2019).

The canopy modelling work in Chapter 3 coupled with the empirical data (both in controlled and field environment) have demonstrated the potential of 3-dimensional image-based reconstructions to accurately predict photosynthetic capacity and carbon gain in Southeast Asian rice varieties. Several opportunities (listed below) for further research can strengthen the results in this study as well as shed more light on canopy responses to interactions of different phenotypes with environmental pressures in field conditions. These opportunities are summarised below:

1. Validation of the physiological and canopy reconstructions in field-grown rice in Malaysia using the same method proposed in this study.
2. Examine the interaction of temperature, rainfall and nitrogen status on canopy photosynthesis in field grown rice. This study would offer more insight on how the rice plant canopy behaves during different growing seasons, so as to maximise grain yield potential through improved photosynthesis.
3. On a wider scope, to combine reconstruction work with canopy vertical nitrogen distribution for increased canopy radiation use efficiency

5.3 **Final conclusions**

The trials above indicate that the Malaysian and IRRI varieties exhibit contrasting N uptake and growth responses. These varieties have been bred for their niche (to suit their growing environments), but using image-based reconstruction approaches in this study has shown that these rice varieties have not been fully optimized for maximum productivity and can still be fine-tuned to maximise yield through improving light capture within the plant canopy. In the changing climate, the increasing cost of inputs and resources as well as the degradation of arable land, rice plants (and other cereals) will require a continuous re-evaluation for maximum yield with increasing environmental and biotic pressures.

References

Acevedo-Siaca, L. G., Coe, R., Wang, Y., Kromdijk, J., Quick, W. P., & Long, S. P. (2020). Variation in photosynthetic induction between rice accessions and its potential for improving productivity. *New Phytologist*.

Ainsworth, E. A., & Long, S. P. (2005). What have we learned from 15 years of free-air CO_2 enrichment (FACE)? A meta-analytic review of the responses of photosynthesis, canopy properties and plant production to rising CO_2. *New phytologist*, *165*(2), 351-372.

Ainsworth, E. A. (2008). Rice production in a changing climate: a meta-analysis of responses to elevated carbon dioxide and elevated ozone concentration. *Global Change Biology*. *14*(7), 1642-1650.

Alam, M. M., Siwar, C., Molla, R. I., Talib, B., & bin Toriman, M. E. (2012). Paddy farmers' adaptation practices to climatic vulnerabilities in Malaysia. *Mitigation and Adaptation Strategies for Global Change*, *17*(4), 415-423.

Anderson, J. M., Chow, W. S., & Park, Y. I. (1995). The grand design of photosynthesis: acclimation of the photosynthetic apparatus to environmental cues. *Photosynthesis Research*, *46*(1-2), 129-139.

Argenta, G., Silva, P. R. F. D., & Sangoi, L. (2004). Leaf relative chlorophyll content as an indicator parameter to predict nitrogen fertilization in maize. *Ciência Rural*, *34*(5), 1379-1387.

Asseng, S., Kassie, B. T., Labra, M. H., Amador, C., & Calderini, D. F. (2017). Simulating the impact of source-sink manipulations in wheat. *Field Crops Research*, *202*, 47-56.

Athanasiou, K., Dyson, B. C., Webster, R. E., & Johnson, G. N. (2010). Dynamic acclimation of photosynthesis increases plant fitness in changing environments. *Plant Physiology*, *152*(1), 366-373.

Azizi, P., Rafii, M. Y., Maziah, M., Abdullah, S. N. A., Hanafi, M. M., Latif, M. A., Rashid, A. A., & Sahebi, M. (2015). Understanding the shoot apical meristem regulation: a study of the phytohormones, auxin and cytokinin, in rice. *Mechanisms of development*, *135*, 1-15.

Bainbridge, G., Madgwick, P., Parmar, S., Mitchell, R., Paul, M., Pitts, J., Keys, A.J., Parry, M. A. (1995). Engineering Rubisco to change its catalytic properties. *Journal of Experimental Botany*, *46*(special issue), 1269-1276.

Baker, N. R. (2008). Chlorophyll fluorescence: a probe of photosynthesis in vivo. *Annual Review of Plant Biology*, *59*, 89-113.

Bakker, J. C. (1991). Effects of humidity on stomatal density and its relation to leaf conductance. *Scientia Horticulturae*, *48*(3-4), 205-212.

Barber, J. (2017). A mechanism for water splitting and oxygen production in photosynthesis. *Nature plants*, *3*(4), 1-5.).

Bartholomew, P. W., & Williams, R. D. (2006). Effects of exposure to below-freezing temperatures, soil moisture content and nitrogen application on phyllochron in cool-season grasses. *Grass and Forage Science*, *61*(2), 146-153.

Belgio, E., Kapitonova, E., Chmeliov, J., Duffy, C. D., Ungerer, P., Valkunas, L., & Ruban, A. V. (2014). Economic photoprotection in photosystem II that retains a complete light-harvesting system with slow energy traps. *Nature Communications*, *5*(1), 1-8.

Bing, Y., Wei-Ya, X., Li-Jun, L., & Yong-Zhong, X. (2006). QTL analysis for flag leaf characteristics and their relationships with yield and yield traits in rice. *Acta Genetica Sinica*, *33*(9), 824-832.

Boese, S. R., & Huner, N. P. (1990). Effect of growth temperature and temperature shifts on spinach leaf morphology and photosynthesis. *Plant Physiology*, *94*(4), 1830-1836.

Buchanan, B. B. (2016). The carbon (formerly dark) reactions of photosynthesis. *Photosynthesis research*, *128*(2), 215-217.

Bunce, J. (2018). Three methods of estimating mesophyll conductance agree regarding its CO2 sensitivity in the RubisCO-limited Ci range. *Plants*, *7*(3), 62.

Burgess, A. J., Retkute, R., Pound, M. P., Foulkes, J., Preston, S. P., Jensen, O. E., Pridmore, T. P., & Murchie, E. H. (2015). High-resolution three-dimensional structural data quantify the impact of photoinhibition on long-term carbon gain in wheat canopies in the field. *Plant Physiology*, *169*(2), 1192-1204.

Burgess, A. J., Retkute, R., Herman, T., & Murchie, E. H. (2017). Exploring relationships between canopy architecture, light distribution, and photosynthesis in contrasting rice genotypes using 3D canopy reconstruction. *Frontiers in plant science*, *8*, 734.

Burundukova, O. L., Zhuravlev, Y. N., Solopov, N. V., & P'yankov, V. I. (2003). A method for calculating the volume and surface area in rice mesophyll cells. *Russian Journal of Plant Physiology*, *50*(1), 133-139.

Callaway, E. (2014). Domestication: The birth of rice. *Nature*. *514*(7524), S58-S59.

Campbell, G. S. (1986). Extinction coefficients for radiation in plant canopies calculated using an ellipsoidal inclination angle distribution. *Agricultural and forest meteorology*, *36*(4), 317-321.

Carmo-Silva, E., Scales, J. C., Madgwick, P. J., & Parry, M. A. (2015). Optimizing Rubisco and its regulation for greater resource use efficiency. *Plant, Cell & Environment*, *38*(9), 1817-1832.

Cegelski, L., & Schaefer, J. (2006). NMR determination of photorespiration in intact leaves using in vivo $^{13}CO_2$ labeling. *Journal of Magnetic Resonance*, 178(*1*), 1-10.

Challinor, A. J., Wheeler, T. R., Craufurd, P. Q., & Slingo, J. M. (2005). Simulation of the impact of high temperature stress on annual crop yields. *Agricultural and Forest Meteorology*, *135*(1-4), 180-189.

Chandra, B. S., Reddy, T. D., Ansari, N. A., & Kumar, S. S. (2009). Correlation and path analysis for yield and yield components in rice (*Oryza sativa* L.). *Agricultural Science Digest*, *29*(1), 45-47.

Chang, T. G., Zhao, H., Wang, N., Song, Q. F., Xiao, Y., Qu, M., & Zhu, X. G. (2019). A three-dimensional canopy photosynthesis model in rice with a complete description of the canopy architecture, leaf physiology, and mechanical properties. *Journal of experimental botany*, *70*(9), 2479-2490.

Chatterjee, J., Dionora, J., Elmido-Mabilangan, A., Wanchana, S., Thakur, V., Bandyopadhyay, A., Darshan, S. B., & Quick, W. P. (2016). The evolutionary basis of naturally diverse rice leaves anatomy. *PloS one*, *11*(10), e0164532.

Choudhury, A. T. M. A., & Kennedy, I. R. (2005). Nitrogen fertilizer losses from rice soils and control of environmental pollution problems. *Communications in soil science and plant analysis*, *36*(11-12), 1625-1639.

Choudhury, F. K., Rivero, R. M., Blumwald, E., & Mittler, R. (2017). Reactive oxygen species, abiotic stress and stress combination. *The Plant Journal*, *90*(5), 856-867.

Cha-um, S., Supaibulwatana, K., & Kirdmanee, C. (2007). Glycinebetaine accumulation, physiological characterizations and growth efficiency in salt-tolerant and salt-sensitive lines of indica rice (*Oryza sativa* L. ssp. indica) in response to salt stress. *Journal of Agronomy and Crop Science*, *193*(3), 157-166.

Chen, Y., Murchie, E. H., Hubbart, S., Horton, P., & Peng, S. (2003). Effects of season-dependent irradiance levels and nitrogen-

deficiency on photosynthesis and photoinhibition in field-grown rice (*Oryza sativa*). *Physiologia plantarum, 117*(3), 343-351.

Chen, Y., Wang, M., & Ouwerkerk, P. B. (2012). Molecular and environmental factors determining grain quality in rice. *Food and Energy Security*, *1*(2), 111-132.

Christin, P. A., & Osborne, C. P. (2013). The recurrent assembly of C4 photosynthesis, an evolutionary tale. *Photosynthesis research*, *117*(1-3), 163-175.

Counce, P. A., Keisling, T. C., & Mitchell, A. J. (2000). A uniform, objective, and adaptive system for expressing rice development. *Crop Science*, *40*(2), 436-443.

Danila, F. R., Quick, W. P., White, R. G., Furbank, R. T., & von Caemmerer, S. (2016). The metabolite pathway between bundle sheath and mesophyll: quantification of plasmodesmata in leaves of C3 and C4 monocots. *The Plant Cell*, *28*(6), 1461-1471.

Dau, H. (1994). Molecular mechanisms and quantitative models of variable photosystem II fluorescence. *Photochemistry and photobiology*, *60*(1), 1-23.

Davis, P. A., & Hangarter, R. P. (2012). Chloroplast movement provides photoprotection to plants by redistributing PSII damage within leaves. *Photosynthesis research, 112*(3), 153-161.

De Kroon, H., Huber, H., Stuefer, J. F., & Van Groenendael, J. M. (2005). A modular concept of phenotypic plasticity in plants. *New phytologist*, *166*(1), 73-82.

Demao, J., & Xia, L. (2001). Cultivar differences in photosynthetic tolerance to photooxidation and shading in rice (*Oryza sativa* L.). *Photosynthetica*, *39*(2), 167-175.

Demmig-Adams, B. (1990). Carotenoids and photoprotection in plants: a role for the xanthophyll zeaxanthin. *Biochimica et Biophysica Acta (BBA)-Bioenergetics*, *1020*(1), 1-24.
Demmig-Adams, B., & Adams Iii, W. W. (1992). Photoprotection and other responses of plants to high light stress. *Annual review of plant biology*, *43*(1), 599-626.

Demmig-Adams, B., & Adams, W. W. (2006). Photoprotection in an ecological context: the remarkable complexity of thermal energy dissipation. *New Phytologist*, *172*(1), 11-21.

Dermody, O., Long, S. P., McConnaughay, K., & DeLUCIA, E. H. (2008). How do elevated CO_2 and O_3 affect the interception and utilization of radiation by a soybean canopy?. *Global Change Biology*, *14*(3), 556-564.

Ding, F., Wang, M., Zhang, S., & Ai, X. (2016). Changes in SBPase activity influence photosynthetic capacity, growth, and tolerance to chilling stress in transgenic tomato plants. *Scientific reports*, *6*(1), 1-14.

Ding, F., Wang, M., & Zhang, S. (2017). Overexpression of a Calvin cycle enzyme SBPase improves tolerance to chilling-induced oxidative stress in tomato plants. *Scientia horticulturae*, *214*, 27-33.

Driever, S. M., Simkin, A. J., Alotaibi, S., Fisk, S. J., Madgwick, P. J., Sparks, C. A., Jones, H.D., Lawson, T., Parry, M.A., & Raines, C. A. (2017). Increased SBPase activity improves photosynthesis and grain yield in wheat grown in greenhouse conditions. *Philosophical Transactions of the Royal Society B: Biological Sciences*, *372*(1730), 20160384.

Dobermann, A. (2000). *Rice: Nutrient disorders & nutrient management*. International Rice Research Institute.

Donald, C. M. The breeding of crop ideotype. *Euphytica* 17, 385–403 (1968).

Elixon, S., Asfaliza, R., Othman, O., Norsuha, M. S., Maisarah, M. S., Allicia, J., & Shahida, H. (2017). Evaluation on yield, yield component and physico-chemicals of advanced rice lines. *J. Trop. Agric. and Fd. Sc*, *45*(2), 131-143.

Equiza, M. A., & Tognetti, J. A. (2002). Morphological plasticity of spring and winter wheats in response to changing temperatures. *Functional Plant Biology*, *29*(12), 1427-1436.

Evans, J. R. (1989). Photosynthesis and nitrogen relationships in leaves of C3 plants. *Oecologia*, *78*(1), 9-19.

Evans, J. R., Kaldenhoff, R., Genty, B., & Terashima, I. (2009). Resistances along the CO_2 diffusion pathway inside leaves. *Journal of experimental botany*, *60*(8), 2235-2248.

Evans, J. R. (2013). Improving photosynthesis. *Plant physiology*. *162*(4), 1780-1793.

Evans, J. R., & Santiago, L. S. (2014). PrometheusWiki gold leaf protocol: gas exchange using Li-COR 6400. *Functional Plant Biology*, *41*(3), 223-226.

Evans, L. T., & Dunstone, R. L. (1970). Some physiological aspects of evolution in wheat. *Australian Journal of Biological Sciences*, *23*(4), 725-742.

Evans, L. T., & Fischer, R. A. (1999). Yield potential: its definition, measurement, and significance. *Crop Science*, *39*(6), 1544-1551.

Fagade, S. O., & De Datta, S. K. (1971). Leaf Area Index, Tillering Capacity, and Grain Yield of Tropical Rice as Affected by Plant Density and Nitrogen Level 1. *Agronomy journal*, *63*(3), 503-506.

Fageria, N. K. (2007). Yield physiology of rice. *Journal of Plant Nutrition*, *30*(6), 843-879.

Falster, D. S., & Westoby, M. (2003). Leaf size and angle vary widely across species: what consequences for light interception? *New Phytologist*, *158*(3), 509-525.

Food and Agriculture Organization of the United Nations. (2012). FAOSTAT Database. Rome, Italy: FAO. Retrieved January 28, 2015 from http://www.fao.org/faostat/en/#data/QC

Food and Agriculture Organization of the United Nations. (2012). FAOSTAT Database. Rome, Italy: FAO. Retrieved June 13, 2019 from http://www.fao.org/faostat/en/#data/QC

Food and Agriculture Organization of the United Nations. (2012). FAOSTAT Database. Rome, Italy: FAO. Retrieved May 8, 2020 from http://www.fao.org/faostat/en/#data/QC

Farquhar, G. D., & Von Caemmerer, S. (1982). Modelling of photosynthetic response to environmental conditions. *Physiological plant ecology II*, *12*(1), 549-587.

Farquhar, G. D., & Sharkey, T. D. (1982). Stomatal conductance and photosynthesis. *Annual review of plant physiology*, *33*(1), 317-345.

Fatah, F. A., & Cramon-Taubadel, S. V. (2017). Profitability and Competitiveness of Rice Farming in Malaysia: A Policy Analysis Matrix. *Asian Journal of Agriculture and Development*, *14*(1362-2017-3060), 31-48.

Feng, L., Han, Y., Liu, G., An, B., Yang, J., Yang, G., Li, Y., & Zhu, Y. (2007a). Overexpression of sedoheptulose-1, 7-bisphosphatase enhances photosynthesis and growth under salt stress in transgenic rice plants. *Functional Plant Biology*, *34*(9), 822-834.

Feng, L., Wang, K., Li, Y., Tan, Y., Kong, J., Li, H., Li, Y., & Zhu, Y. (2007b). Overexpression of SBPase enhances photosynthesis against high temperature stress in transgenic rice plants. *Plant cell reports*, *26*(9), 1635-1646.

Feng, L., Li, H., Jiao, J., Li, D., Zhou, L., Wan, J., & Li, Y. (2009). Reduction in SBPase activity by antisense RNA in transgenic rice plants: effect on photosynthesis, growth, and biomass allocation at different nitrogen levels. *Journal of Plant Biology*, *52*(5), 382-394.

Fitzgerald M. A., & Resurreccion, A. P. (2009). Maintaining the yield of edible rice in a warming world. *Functional Plant Biology*, *36*(12), 1037- 1045.

Flexas, J., Ribas-Carbó, M., Diaz-Espejo, A., Galmés, J., & Medrano, H. (2008). Mesophyll conductance to CO_2: current knowledge and future prospects. *Plant, cell & environment*, *31*(5), 602-621.

Food and Agriculture Organization of the United Nations. (2015). FAOSTAT Database. Rome, Italy: FAO. Retrieved June 30, 2015 from http://www.fao.org/faostat/en/#data/QC

Furbank. R. T., von Caemmerer, S., Sheehy, J., Edwards, G. (2009a). C4 rice: a challenge for plant phenomics. *Functional Plant Biology, 36*(11), 845–856.

Furbank, R. T. (2009b). Plant phenomics: from gene to form and function. *Functional Plant Biology*, *36*(10), 5-6.

Furbank, R. T., Quick, W. P., & Sirault, X. R. (2015). Improving photosynthesis and yield potential in cereal crops by targeted genetic manipulation: prospects, progress and challenges. *Field Crops Research*, *182*, 19-29.

Furbank, R. T., & Tester, M. (2011). Phenomics–technologies to relieve the phenotyping bottleneck. *Trends in plant science*, *16*(12), 635-644.

Furukawa, Y., & Ponce, J. (2010). Dense 3d motion capture from synchronized video streams. In *Image and Geometry Processing for 3-D Cinematography* (pp. 193-211). Springer, Berlin, Heidelberg.

Galmés, J., Capó-Bauçà, S., Niinemets, Ü., & Iñiguez, C. (2019). Potential improvement of photosynthetic CO2 assimilation in crops by exploiting the natural variation in the temperature response of Rubisco catalytic traits. *Current opinion in plant biology*, *49*, 60-67.

Garnica, M., Houdusse, F., Zamarreño, A. M., & Garcia-Mina, J. M. (2010). The signal effect of nitrate supply enhances active forms of cytokinins and indole acetic content and reduces abscisic acid in wheat plants grown with ammonium. *Journal of plant physiology*, *167*(15), 1264-1272.

Gifford, R. M., & Evans, L. T. (1981). Photosynthesis, carbon partitioning, and yield. *Annual Review of Plant Physiology*, *32*(1), 485-509.

Gilland, B. (2006). Population, nutrition and agriculture. *Population and Environment*, *28*(1), 1-16.

Giuliani, R., Koteyeva, N., Voznesenskaya, E., Evans, M. A., Cousins, A. B., & Edwards, G. E. (2013). Coordination of leaf

photosynthesis, transpiration, and structural traits in rice and wild relatives (genus *Oryza*). *Plant physiology*, *162*(3), 1632-1651.

Givnish, T. J. (1988). Adaptation to sun and shade: a whole-plant perspective. *Functional Plant Biology*, *15*(2), 63-92.

Good, A. G., Shrawat, A. K., & Muench, D. G. (2004). Can less yield more? Is reducing nutrient input into the environment compatible with maintaining crop production? *TRENDS in Plant Science, 9*(12), 597-605.

GRiSP (Global Rice Science Partnership) (2013). *Rice almanac, 4th edition*. Los Baños, Philippines. International Rice Research Institute. 283 p.

Hall, A. E. (2001). Heat stress and its impact. *Plant Stress. Ed A Blum. http://www. plantstress. com/Articles/heat_i/heat_i. htm*.

Hatch, M. D. (1987). C4 photosynthesis: a unique blend of modified biochemistry, anatomy and ultrastructure. *Biochimica et Biophysica Acta (BBA)-Reviews on Bioenergetics*, *895*(2), 81-106.

Hatch, M. D., & Slack, C. R. (1966). Photosynthesis in sugarcane leaves: a new carboxylation reaction and the pathway of sugar formation. *Journal of Biochemistry, 101*, 103–111

Hatfield, J. L., & Prueger, J. H. (2015). Temperature extremes: effect on plant growth and development. *Weather and Climate Extremes*, *10*, 4-10.

Haun, J. R. (1973). Visual quantification of wheat development 1. *Agronomy Journal*, *65*(1), 116-119.
Hedden, P. (2003). Constructing dwarf rice. *Nature biotechnology*, *21*(8), 873.

Herman, T., Murchie, E. H., & Warsi, A. A. (2015). Rice Production and Climate Change: A Case Study of Malaysian Rice. *Pertanika Journal of Tropical Agricultural Science*, *38*(3), 321-328.

Hikosaka, K. (2004). Interspecific difference in the photosynthesis–nitrogen relationship: patterns, physiological causes, and ecological importance. *Journal of Plant Research*, *117*(6), 481-494.

Hikosaka, K., Ishikawa, K., Borjigidai, A., Muller, O., & Onoda, Y. (2005). Temperature acclimation of photosynthesis: mechanisms involved in the changes in temperature dependence of photosynthetic rate. *Journal of experimental botany*, *57*(2), 291-302.

Hikosaka, K. (2010). Mechanisms underlying interspecific variation in photosynthetic capacity across wild plant species. *Plant Biotechnology*, *27*(3), 223-229.

Hirel, B., Chardon, F., & Durand, J. (2007). The contribution of molecular physiology to the improvement of nitrogen use efficiency in crops. *Journal of Crop Science and Biotechnology*, *10*, 129-136.

Horton, P., Ruban, A. V., & Walters, R. G. (1996). Regulation of light harvesting in green plants. *Annual review of plant biology*, *47*(1), 655-684.

Horton, P. (2000). Prospects for crop improvement through the genetic manipulation of photosynthesis: morphological and biochemical aspects of light capture. *Journal of Experimental Botany*, *51*(suppl_1), 475-485.

Horton, P., & Murchie, E. H. (2000). C4 photosynthesis in rice: some lessons from studies of C3 photosynthesis in field-grown rice. In *Studies in Plant Science* (Vol. 7, pp. 127-144). Elsevier.

Horton, P., Murchie, E. H., Ruban, A. V., & Walters, R. G. (2001). Increasing rice photosynthesis by manipulation of the acclimation and adaptation to light. In *Novartis Foundation symposium* (pp. 117-129). Chichester; New York; John Wiley; 1999.

Horton, P., & Ruban, A. (2005). Molecular design of the photosystem II light-harvesting antenna: photosynthesis and photoprotection. *Journal of Experimental Botany, 56*(411), 365-373.

Huang, L. F., Zheng, J. H., Zhang, Y. Y., Hu, W. H., Mao, W. H., Zhou, Y. H., & Yu, J. Q. (2006). Diurnal variations in gas exchange, chlorophyll fluorescence quenching and light allocation in soybean leaves: the cause for midday depression in CO_2 assimilation. *Scientia horticulturae*, *110*(2), 214-218.

Huang, M., Yang, C., Ji, Q., Jiang, L., Tan, J., & Li, Y. (2013). Tillering responses of rice to plant density and nitrogen rate in a subtropical environment of southern China. *Field Crops Research*, *149*, 187-192.

Huang, X., Kurata, N., Wang, Z. X., Wang, A., Zhao, Q., Zhao, Y., Liu, K., Lu, H., Li, W., Guo, Y., & Lu, Y. (2012). A map of rice genome variation reveals the origin of cultivated rice. *Nature*, *490*(7421), 497-501.

Hubbart, S., Peng, S., Horton, P., Chen, Y., & Murchie, E. H. (2007). Trends in leaf photosynthesis in historical rice varieties developed in the Philippines since 1966. *Journal of Experimental Botany*, *58*(12), 3429-3438.

Hubbart, S., Bird, S., Lake, J. A., & Murchie, E. H. (2013). Does growth under elevated CO_2 moderate photoacclimation in rice?. *Physiologia plantarum*, *148*(2), 297-306.

Hubbart, S., Smillie, I. R., Heatley, M., Swarup, R., Foo, C. C., Zhao, L., & Murchie, E. H. (2018). Enhanced thylakoid photoprotection can increase yield and canopy radiation use efficiency in rice. *Communications Biology*, *1*(1), 22.

Hussien, A., Tavakol, E., Horner, D. S., Muńoz-Amatriaín, M., Muehlbauer, G. J., & Rossini, L. (2014). Genetics of tillering in rice and barley. *The plant genome*, *7*(1).

Inada, K., & Nishiyama, F. (1987). Growth responses of sun and shade plants in simulated vegetation shade and neutral shade. *Japanese Journal of Crop Science*, *56*(1), 99-108.

IRRI (2002) *Standard Evaluation System for Rice*. International Rice Research Institute, Manila.

IRRI (International Rice Research Institute). (2012). *Rice and climate change: Hot topic*. International Rice Research Institute.

Iseki, K., Homma, K., Irie, T., Endo, T., & Shiraiwa, T. (2013). The long-term changes in midday photoinhibition in rice (*Oryza sativa* L.) Growing under fluctuating Soil Water Conditions. *Plant Production Science, 16*(4), 287-294.

Itoh, Y., & Sano, Y. (2006). Phyllochron dynamics under controlled environments in rice (*Oryza sativa* L.). *Euphytica*, *150*(1-2), 87-95.

Jagadish, S. V. K., Craufurd, P. Q., & Wheeler, T. R. (2007). High temperature stress and spikelet fertility in rice (*Oryza sativa* L.). *Journal of experimental botany*, *58*(7), 1627-1635.

Jang, S. W., Hamayun, M., Sohn, W. Y., Kang, S. M., Choi, K. I., Shin, D. H., & Lee, I. J. (2008). Growth and gibberellins levels of two rice cultivars as influenced by different nitrogen containing compounds. *Journal of Crop Science and Biotechnology*, *11*(4), 223-226.

Jennings, P. R., & Beachell, H. M. (1964). Breeding rice for nitrogen responsiveness. In *Proc. Symp. Mineral Nutrition of Rice Plant* (pp. 449-457).

Jones, H. G. (1998). Stomatal control of photosynthesis and transpiration. *Journal of experimental botany*, 387-398.Kamada-Nobusada, T., Makita, N., Kojima, M., & Sakakibara, H. (2013).

Nitrogen-dependent regulation of de novo cytokinin biosynthesis in rice: the role of glutamine metabolism as an additional signal. *Plant and Cell Physiology*, *54*(11), 1881-1893.

Kambezidis, H. D., Kaskaoutis, D. G., Kharol, S. K., Moorthy, K. K., Satheesh, S. K., Kalapureddy, M. C. R., Badarinath, K. V. S., Sharma, A. R., & Wild, M. (2012). Multi-decadal variation of the net

downward shortwave radiation over south Asia: The solar dimming effect. *Atmospheric Environment*, *50*, 360-372.

Kant, S., Bi, Y. M., & Rothstein, S. J. (2011). Understanding plant response to nitrogen limitation for the improvement of crop nitrogen use efficiency. *Journal of Experimental Botany, 62*(4), 1499-1509.

Keren, N., & Krieger-Liszkay, A. (2011). Photoinhibition: molecular mechanisms and physiological significance. *Plant Physiology, 142*(1), 1-5.

Khan, A., Muhammad, A., Khan, A. A., Anwar, S., & Hollington, P. A. (2019). Nitrogen affects leaf expansion and elongation rates during early growth stages of wheat. *Int. J. Agric. Biol.*, *21*(6), 1117-1122.

Khush GS, Virk PS. (2005). *IR varieties and their impact*. Los Baños (Philippines): International Rice Research Institute. 163 p.

Khush, G.S. (2005). New technologies for rice production. In: Toriyama K, Heong KL, Hardy B, (Eds.). *Rice is life: scientific perspectives for the 21st century*. Proceedings of the World Rice Research Conference held in Tokyo and Tsukuba, Japan, 4-7 Nov. 2004.

Kiba, T., Kudo, T., Kojima, M., & Sakakibara, H. (2010). Hormonal control of nitrogen acquisition: roles of auxin, abscisic acid, and cytokinin. *Journal of experimental botany*, *62*(4), 1399-1409.

Kirby, E. J. M. (1995). Factors affecting rate of leaf emergence in barley and wheat. *Crop Science*, *35*(1), 11-19.

Kinsman, E. A., & Pyke, K. A. (1998). Bundle sheath cells and cell-specific plastid development in Arabidopsis leaves. *Development*, *125*(10), 1815-1822.

Kortschak, H. P., Hartt, C. E., & Burr, G. O. (1965). Carbon dioxide fixation in sugarcane leaves. *Plant Physiology*, *40*(2), 209.

Kramer, D. M., Avenson, T. J., & Edwards, G. E. (2004). Dynamic flexibility in the light reactions of photosynthesis governed by both electron and proton transfer reactions. *Trends in plant science*, *9*(7), 349-357.

Krishnan, P., Ramakrishnan, B., Reddy, K. R., & Reddy, V. R. (2011). High-temperature effects on rice growth, yield, and grain quality. *Advances in Agronomy*, *111*, 87-206.

Kromdijk, J., Głowacka, K., Leonelli, L., Gabilly, S. T., Iwai, M., Niyogi, K. K., & Long, S. P. (2016). Improving photosynthesis and crop productivity by accelerating recovery from photoprotection. *Science*, *354*(6314), 857-861.

Krouk, G., Ruffel, S., Gutiérrez, R. A., Gojon, A., Crawford, N. M., Coruzzi, G. M., & Lacombe, B. (2011). A framework integrating plant growth with hormones and nutrients. *Trends in plant science*, *16*(4), 178-182.

Kumagai, E., Araki, T., & Kubota, F. (2009). Characteristics of gas exchange and chlorophyll fluorescence during senescence of flag leaf in different rice (Oryza sativa L.) cultivars grown under nitrogen-deficient condition. *Plant production science*, *12*(3), 285-292.

Kumagai, E., Hamaoka, N., Araki, T., & Ueno, O. (2014). Dorsoventral asymmetry of photosynthesis and photoinhibition in flag leaves of two rice cultivars that differ in nitrogen response and leaf angle. *Physiologia plantarum*, *151*(4), 533-543.

Kumar, P. A., Parry, M. A., Mitchell, R. A., Ahmad, A., & Abrol, Y. P. (2002). Photosynthesis and nitrogen-use efficiency. In *Photosynthetic nitrogen assimilation and associated carbon and respiratory metabolism, 12,* 23-34

Kyle, D. J., Ohad, I., Guy, R., & Arntzen, C. J. (1984). Selective thylakoid protein damage and repair during photoinhibition. *Advances in photosynthesis research, 3,* 67-70

Lake, J. A., Quick, W. P., Beerling, D. J., & Woodward, F. I. (2001). Plant development: signals from mature to new leaves. *Nature*, *411*(6834), 154.

Langdale, J. A. (2011). C4 cycles: past, present, and future research on C4 photosynthesis. *The Plant Cell*, *23*(11), 3879-3892.

Lawson, T., Bryant, B., Lefebvre, S., Lloyd, J. C., & Raines, C. A. (2006). Decreased SBPase activity alters growth and development in transgenic tobacco plants. *Plant, cell & environment*, *29*(1), 48-58.

Lefebvre, S., Lawson, T., Fryer, M., Zakhleniuk, O. V., Lloyd, J. C., & Raines, C. A. (2005). Increased sedoheptulose-1, 7-bisphosphatase activity in transgenic tobacco plants stimulates photosynthesis and growth from an early stage in development. *Plant Physiology*, *138*(1), 451-460.

Lemaire, G., & Gastal, F. (1997). N uptake and distribution in plant canopies. In *Diagnosis of the nitrogen status in crops* (pp. 3-43). Springer, Berlin, Heidelberg.

Li, X., Qian, Q., Fu, Z., Wang, Y., Xiong, G., Zeng, D Wang, X., Liu, X., Teng, S., Hiroshi, F. and Yuan, M. (2003). Control of tillering in rice. *Nature*, *422*(6932), 618.

Li, X., Xia, K., Liang, Z., Chen, K., Gao, C., & Zhang, M. (2016). MicroRNA393 is involved in nitrogen-promoted rice tillering through regulation of auxin signal transduction in axillary buds. *Scientific reports*, *6*, 32158.

Li, X., Wu, L., Geng, X., Xia, X., Wang, X., Xu, Z., & Xu, Q. (2018). Deciphering the Environmental Impacts on Rice Quality for Different Rice Cultivated Areas. *Rice*, *11*(1), 7.

Li, Y., Gao, Y., Xu, X., Shen, Q., & Guo, S. (2009). Light-saturated photosynthetic rate in high-nitrogen rice (*Oryza sativa* L.) leaves is related to chloroplastic CO_2 concentration. *Journal of Experimental Botany*, *60*(8), 2351-2360.

Lin, X. Q., Zhu, D. F., Chen, H. Z., Cheng, S. H., & Uphoff, N. (2009). Effect of plant density and nitrogen fertilizer rates on grain yield and nitrogen uptake of hybrid rice (*Oryza sativa* L.). *Journal of Agricultural Biotechnology and Sustainable Development*, *1*(2), 44-53.

Liu, Z., Sun, N., Yang, S., Zhao, Y., Wang, X., Hao, X., & Qiao, Z. (2013). Evolutionary transition from C3 to C4 photosynthesis and the route to C4 rice. *Biologia*, *68*(4), 577-586.

Lloyd, J., Grace, J., Miranda, A. C., Meir, P., Wong, S. C., Miranda, H. S., Wright, I. R., Gash, J. H. C., & McIntyre, J. (1995). A simple calibrated model of Amazon rainforest productivity based on leaf biochemical properties. *Plant, Cell & Environment*, *18*(10), 1129-1145.

Long, S. P., Ainsworth, E. A., Leakey, A. D., & Morgan, P. B. (2005). Global food insecurity. Treatment of major food crops with elevated carbon dioxide or ozone under large-scale fully open-air conditions suggests recent models may have overestimated future yields. *Philosophical Transactions of the Royal Society B: Biological Sciences*, *360*(1463), 2011-2020.

Long, S. P., Ainsworth, E. A., Rogers, A., & Ort, D. R. (2004). Rising atmospheric carbon dioxide: plants FACE the future. *Annual Review of Plant Biology*, *55*, 591-628.

Long, S. P., Ainsworth, E. A., Leakey, A. D., Nösberger, J., & Ort, D. R. (2006a). Food for thought: lower-than-expected crop yield stimulation with rising CO_2 concentrations. *Science*, *312*(5782), 1918-1921.

Long, S. P., Zhu, X. G., Naidu, S. L., & Ort, D. R. (2006b). Can improvement in photosynthesis increase crop yields? *Plant, Cell & Environment*, *29*(3), 315-330.

Long, S. P., Marshall-Colon, A., & Zhu, X. G. (2015). Meeting the global food demand of the future by engineering crop photosynthesis and yield potential. *Cell*, *161*(1), 56-66.

Mackill, D. J., & Khush, G. S. (2018). IR64: a high-quality and high-yielding mega variety. *Rice*, *11*(1), 18.

Maclean, J. L., Dawe, D. C., Hardy, B., & Hettel, G. P. (2002). *Rice almanac.* International Rice Research Institute, West Africa Rice Development Association. International Center for Tropical Agriculture, Food and Agriculture Organization. CAB International, Wallingford, UK.

Mae, T. (1997). Physiological nitrogen efficiency in rice: nitrogen utilization, photosynthesis, and yield potential. *Plant nutrition for sustainable food production and environment, 196*(2), 201-210

Mae, T., & Ohira, K. (1981). The remobilization of nitrogen related to leaf growth and senescence in rice plants (*Oryza sativa* L.). *Plant and Cell Physiology*, *22*(6), 1067-1074.

Mahmod, I. F., Barakbah, S. S., Osman, N., & Omar, O. (2014). Physiological response of local rice varieties to aerobic condition. *International Journal Agriculture Biology*, *16*(4), 738-744.

Makino, A., Mae, T., & Ohira, K. (1983). Photosynthesis and ribulose 1, 5-bisphosphate carboxylase in rice leaves: changes in photosynthesis and enzymes involved in carbon assimilation from leaf development through senescence. *Plant Physiology*, *73*(4), 1002-1007.

Makino, A., Mae, T., & Ohira, K. (1984). Relation between nitrogen and ribulose-1, 5-bisphosphate carboxylase in rice leaves from emergence through senescence. *Plant and Cell Physiology*, *25*(3), 429-437.

Makino, A., Mae, T., & Ohira, K. (1985). Photosynthesis and ribulose-1, 5-bisphosphate carboxylase/oxygenase in rice leaves from emergence through senescence. Quantitative analysis by carboxylation/oxygenation and regeneration of ribulose 1, 5-bisphosphate. *Planta*, *166*(3), 414-420.

Makino, A., Sato, T., Nakano, H., & Mae, T. (1997). Leaf photosynthesis, plant growth and nitrogen allocation in rice under different irradiances. *Planta*, *203*(3), 390-398.

Makino, A. (2003). Rubisco and nitrogen relationships in rice: leaf photosynthesis and plant growth. *Soil Science and Plant Nutrition*, *49*(3), 319-327.

Makino, A. (2011). Photosynthesis, grain yield, and nitrogen utilization in rice and wheat. *Plant physiology*, *155*(1), 125-129.

Malnoë, A. (2018). Photoinhibition or photoprotection of photosynthesis? Update on the (newly termed) sustained quenching component qH. *Environmental and Experimental Botany*, *154*, 123-133.

Mantilla-Perez, M. B., & Salas Fernandez, M. G. (2017). Differential manipulation of leaf angle throughout the canopy: current status and prospects. *Journal of Experimental Botany*, *68*(21-22), 5699-5717.

Martinez-eixarch, M., ZHU, D. F., del Mar Catala-forner, M., Eva, P. M., & TOMÁS-NAVARRO, N. (2013). Water, nitrogen and plant density affect the response of leaf appearance of direct seeded rice to thermal time. *Rice Science*, *20*(1), 52-60.

Maruyama, A., Kuwagata, T., & Ohba, K. (2007). Dependence of solar radiation transport in rice canopies on developmental stage. *Japan Agricultural Research Quarterly: JARQ*, *41*(1), 39-45.

Masud, M. M., Rahman, M. S., Al-Amin, A. Q., Kari, F., & Leal Filho, W. (2014). Impact of climate change: an empirical investigation of Malaysian rice production. *Mitigation and adaptation strategies for global change*, *19*(4), 431-444.

Mathan, J., Bhattacharya, J., & Ranjan, A. (2016). Enhancing crop yield by optimizing plant developmental features. *Development*, *143*(18), 3283-3294.

Maxwell, K., & Johnson, G. N. (2000). Chlorophyll fluorescence—a practical guide. *Journal of experimental botany*, *51*(345), 659-668.
Mittler, R. (2006). Abiotic stress, the field environment and stress combination. *Trends in Plant Science*, *11*(1), 15-19

Miah, G., Rafii, M. Y., Ismail, M. R., Puteh, A. B., Rahim, H. A., & Latif, M. A. (2017). Marker-assisted introgression of broad-spectrum blast resistance genes into the cultivated MR219 rice variety. *Journal of the science of food and agriculture*, *97*(9), 2810-2818.

McCree, K. J. (1981). Photosynthetically active radiation. In *Physiological plant ecology I* (pp. 41-55). Springer, Berlin, Heidelberg.

Moldenhauer, K., Slaton, N., (2001). Rice growth and development. In: Slaton, N.A. (Ed.), Rice Production Handbook. Misc. Publ. 192. Coop. Ext. Service, University of Arkansas, Little Rock, pp. 7–14

Moldenhauer, K. A., Gibbons, J. H., Smith, C. W., & Dilday, R. H. (2003). *Rice morphology and development* (pp. 103-127). Rice: Origin,

Monsi, M., & Saeki, T. (2005). On the factor light in plant communities and its importance for matter production. *Annals of botany*, *95*(3), 549.

Monteith, J. L. (1972). Solar radiation and productivity in tropical ecosystems. *Journal of applied ecology*, *9*(3), 747-766.

Monteith, J. L. (1977). Climate and the Efficiency of Crop Production in Britain. *Philosophical Transactions of the Royal Society of London Series B*, *281*, 277-294.

Morgan, P. B., Bollero, G. A., Nelson, R. L., Dohleman, F. G., & Long, S. P. (2005). Smaller than predicted increase in aboveground net primary production and yield of field-grown soybean under fully open-air [CO2] elevation. *Global Change Biology*, *11*(10), 1856-1865.

Murata, N., Takahashi, S., Nishiyama, Y., & Allakhverdiev, S. I. (2007). Photoinhibition of photosystem II under environmental stress. *Biochimica et Biophysica Acta (BBA)-Bioenergetics*, *1767*(6), 414-421.

Murchie, E. H., & Horton, P. (1997). Acclimation of photosynthesis to irradiance and spectral quality in British plant species: chlorophyll content, photosynthetic capacity and habitat preference. *Plant, Cell & Environment*, *20*(4), 438-448.

Murchie, E. H., Chen, Y. Z., Hubbart, S., Peng, S., & Horton, P. (1999). Interactions between senescence and leaf orientation determine in situ patterns of photosynthesis and photoinhibition in field-grown rice. *Plant Physiology*, *119*(2), 553-564.

Murchie, E. H., Hubbart, S., Chen, Y., Peng, S., & Horton, P. (2002). Acclimation of rice photosynthesis to irradiance under field conditions. *Plant Physiology*, *130*(4), 1999-2010.

Murchie, E. H., Pinto, M., & Horton, P. (2009). Agriculture and the new challenges for photosynthesis research. *New Phytologist*, 181(3), 532-552.

Murchie, E. H., & Niyogi, K. K. (2011). Manipulation of photoprotection to improve plant photosynthesis. *Plant physiology*, *155*(1), 86-92.

Murchie, E. H., & Lawson, T. (2013). Chlorophyll fluorescence analysis: a guide to good practice and understanding some new applications. *Journal of experimental botany*, *64*(13), 3983-3998.

Murchie, E. H., & Harbinson, J. (2014). Non-photochemical fluorescence quenching across scales: from chloroplasts to plants to communities. In *Non-Photochemical Quenching and Energy Dissipation in Plants, Algae and Cyanobacteria, 40*, 553-582.

Murchie, E. H., Ali, A., & Herman, T. (2015). Photoprotection as a trait for rice yield improvement: Status and prospects. *Rice*, *8*(1), 31.

Murchie, E. H. (2017). Safety conscious or living dangerously: what is the 'right' level of plant photoprotection for fitness and productivity?. *Plant, Cell and Environment*, *40*(8), 1239-1242.

Nagai, T., & Makino, A. (2009). Differences between rice and wheat in temperature responses of photosynthesis and plant growth. *Plant and Cell Physiology*, *50*(4), 744-755.

Najim, M. M. M., Lee, T. S., Haque, M. A., & Esham, M. (2007). Sustainability of rice production: A Malaysian perspective. *The Journal of Agricultural Sciences*, *3*(1), 1-12.

Nehe, A. S., Misra, S., Murchie, E. H., Chinnathambi, K., & Foulkes, M. J. (2018). Genetic variation in N-use efficiency and associated traits in Indian wheat cultivars. *Field crops research*, *225*, 152-162.

Neoh, W. T., & Lum, M. S. (2018). Nutritional Quality of Rice Variety in Sabah, Malaysia.

Nguyen, H. T., Babu, R. C., & Blum, A. (1997). Breeding for drought resistance in rice: physiology and molecular genetics considerations. *Crop Science*, *37*(5), 1426-1434.

Nguyen, N. V. (2002). Global climate changes and rice food security. *Rome: FAO*.

Niinemets, Ü., & Tenhunen, J. D. (1997). A model separating leaf structural and physiological effects on carbon gain along light gradients for the shade-tolerant species Acer saccharum. *Plant, Cell & Environment*, *20*(7), 845-866.

Niinemets, Ü. (1998). Adjustment of foliage structure and function to a canopy light gradient in two co-existing deciduous trees. Variability in leaf inclination angles in relation to petiole morphology. *Trees*, *12*(7), 446-451.

Niinemets, Ü., & Anten, N. P. (2009). Packing the photosynthetic machinery: from leaf to canopy. In *Photosynthesis in silico* (pp. 363-399). Springer, Dordrecht.

Nobel, P. S., Forseth, I. N., & Long, S. P. (1993). Canopy structure and light interception. In *Photosynthesis and Production in a Changing Environment* (pp. 79-90). Springer, Dordrecht.

Nobel, P. S. (2009). Physiochemical and environmental plant physiology – Academic Press.

Omar S. C., Shaharudin A., Tumin S. A. (2019) *The status of the paddy and rice industry in Malaysia*. Khazanah Research Institute. Kedah, Malaysia.

Ort, D. R., Zhu, X., & Melis, A. (2011). Optimizing antenna size to maximize photosynthetic efficiency. *Plant physiology*, *155*(1), 79-85.

Ort, D. R., Merchant, S. S., Alric, J., Barkan, A., Blankenship, R. E., Bock, R., Croce, R., Hanson, M. R., Hibberd, M. J., Long, S. P., Moore,T.A., Moroney, J., Niyogi, K. K., Parry, M. A. J., Peralta-Yahya, P. P., Prince, R. C., Redding, K.E., Spalding, M. H., van Wijk, K. J., Vermaas, W. F. J., von Caemmerer, S., Weber, A. P. M., Yeates, T. O., Yuan, J. S and Xin, G. Z. (2015). Redesigning photosynthesis to sustainably meet global food and bioenergy demand. *Proceedings of the national academy of sciences*, *112*(28), 8529-8536.

Oladosu, Y., Rafii, M. Y., Arolu, F., Chukwu, S. C., Muhammad, I., Kareem, I., ... & Arolu, I. W. (2020). Submergence Tolerance in Rice: Review of Mechanism, Breeding and, Future Prospects. *Sustainability*, *12*(4), 1632.

Othman, O., Alias, I. and Hadzim, K. (1986). Rice varietal improvement in peninsular Malaysia. MARDI Report. p. 1 – 18. Serdang: MARDI

Ouyang, W., Struik, P. C., Yin, X., & Yang, J. (2017). Stomatal conductance, mesophyll conductance, and transpiration efficiency in relation to leaf anatomy in rice and wheat genotypes under drought. *Journal of Experimental Botany*, *68*(18), 5191-5205.

Parry, M. A. J., Andralojc, P. J., Mitchell, R. A., Madgwick, P. J., & Keys, A. J. (2003). Manipulation of Rubisco: the amount, activity, function and regulation. *Journal of Experimental Botany*, 54(386), 1321-1333.

Parry, M. A., Reynolds, M., Salvucci, M. E., Raines, C., Andralojc, P. J., Zhu, X. G., Price, G. D., Condon, A. G., & Furbank, R. T. (2011). Raising yield potential of wheat. II. Increasing photosynthetic capacity and efficiency. *Journal of Experimental Botany, 62*(2), 453-467.

Patindol, J. A., Siebenmorgen, T. J., & Wang, Y. J. (2015). Impact of environmental factors on rice starch structure: a review. *Starch-Stärke*, *67*(1-2), 42-54.

Pawar, S. Y., Radhakrishnan, V. V., & Mohanan, K. V. (2016). The Importance of Optimum Tillering in Rice-An overview. *South Indian Journal of Biological Sciences*, *2*(1), 125-127.

Peet, M. M., & Kramer, P. J. (1980). Effects of decreasing source/sink ratio in soybeans on photosynthesis, photorespiration, transpiration and yield. *Plant, Cell & Environment*, *3*(3), 201-206.

Peng, S., Laza, M. R. C., Garcia, F. V., & Cassman, K. G. (1995a). Chlorophyll meter estimates leaf area-based nitrogen concentration of rice. *Communications in Soil Science and Plant Analysis*, *26*(5-6), 927-935.

Peng, S., Cassman, K. G., & Kropff, M. J. (1995b). Relationship between leaf photosynthesis and nitrogen content of field-grown rice in tropics. *Crop science*, *35*(6), 1627-1630.

Peng, S., (2000). Single leaf and canopy photosynthesis. In: Sheehy, J.E., Mitchell, P.L., Hardy, B. (Eds.), Redesigning Rice Photosynthesis to Increase Yield. International Rice Research Institute/Elsevier, Makati City, Philippines/Amsterdam, The Netherlands, pp. 213–228.

Peng, S., & Ismail, A. M. (2004). Physiological basis of yield and environmental adaptation in rice. *Physiology and biotechnology integration for plant breeding. Marcel Dekker, New York*, 83-140.

Peng. S. B., Huang, J. L., Sheehy, J.E., Laza, R. C., Visperas, R, M., Zhong, X. H., Centeno, G.S., Khush, G. S., Cassman, K. G. (2004). Rice yields decline with higher night temperature from global warming. *PNAS, 101*(27), 9971-9975.

Peng, S., Khush, G. S., Virk, P., Tang, Q., & Zou, Y. (2008). Progress in ideotype breeding to increase rice yield potential. *Field Crops Research*, *108*(1), 32-38.

Peng, X., & Zhang, S. W. (2002). Research on Rice Growth Status Based on NDVI and LAI [J]. *Northeast Surveying and Mapping*, *4*, 4.

Pfundel E. (1998). Estimating the contribution of photosystem I to total leaf chlorophyll fluorescence. *Photosynthetic Research, 56*, 185–95.

Pilbeam, D. J. (2015). Breeding crops for improved mineral nutrition under climate change conditions. *Journal of experimental botany*, *66*(12), 3511-3521.

Pons, T. L., Flexas, J., Von Caemmerer, S., Evans, J. R., Genty, B., Ribas-Carbo, M., & Brugnoli, E. (2009). Estimating mesophyll conductance to CO2: methodology, potential errors, and recommendations. *Journal of Experimental Botany*, *60*(8), 2217-2234.

Poorter, H., Fiorani, F., Pieruschka, R., Wojciechowski, T., Putten, W. H., Kleyer, M., Schurr, U., & Postma, J. (2016). Pampered inside, pestered outside? Differences and similarities between plants

growing in controlled conditions and in the field. *New Phytologist*, *212*(4), 838-855.

Pound, M. P., French, A. P., Murchie, E. H., & Pridmore, T. P. (2014). Automated recovery of three-dimensional models of plant shoots from multiple color images. *Plant physiology*, *166*(4), 1688-1698.

Prasad, P. V. V., Boote, K. J., & Allen, L. H. (2006a). Adverse high temperature effects on pollen viability, seed-set, seed yield and harvest index of grain-sorghum [Sorghum bicolor (L.) Moench] are more severe at elevated carbon dioxide due to higher tissue temperatures. *Agricultural and forest meteorology*, *139*(3), 237-251.

Prasad, P. V. V., Boote, K. J., Allen, L. H., Sheehy, J. E., & Thomas, J. M. G. (2006b). Species, ecotype and cultivar differences in spikelet fertility and harvest index of rice in response to high temperature stress. *Field crops research*, *95*(2), 398-411.

Quero, G., Bonnecarrère, V., Fernández, S., Silva, P., Simondi, S., & Borsani, O. (2019). Light-use efficiency and energy partitioning in rice is cultivar dependent. *Photosynthesis research*, *140*(1), 51-63.

Rabu, M. R., & Shah, M. D. M. (2013). Food and livelihood security of the Malaysian paddy farmers. *Economic and Technology Management Review*, *8*, 59-69.

Rahman, H., Ramanathan, V., Jagadeeshselvam, N., Ramasamy, S., Rajendran, S., Ramachandran, M., Sudheer, P.D., Chauhan, S., Natesan, S. & Muthurajan, R. (2015). Phenomics: technologies and applications in plant and agriculture. In *PlantOmics: The Omics of Plant Science* (pp. 385-411). Springer, New Delhi.

Raines, C. A. (2003). The Calvin cycle revisited. *Photosynthesis research*, *75*(1), 1-10.

Raines, C. A. (2011). Increasing photosynthetic carbon assimilation in C3 plants to improve crop yield: current and future strategies. *Plant physiology*, *155*(1), 36-42.

Redfern, S. K., Azzu, N., & Binamira, J. S. (2012). Rice in Southeast Asia: facing risks and vulnerabilities to respond to climate change. *Building resilience for adaptation to climate change in the agricultural sector*, *23*, 295.

Retkute, R., Smith-Unna, S. E., Smith, R. W., Burgess, A. J., Jensen, O. E., Johnson, G. N., Preston, S. P., & Murchie, E. H. (2015). Exploiting heterogeneous environments: does photosynthetic acclimation optimize carbon gain in fluctuating light?. *Journal of experimental botany*, *66*(9), 2437-2447.

Reynolds M.P., van Ginkel M., & Ribaut J. M. (2000) Avenues for genetic modification of radiation use efficiency in wheat. *Journal of Experimental Botany*, *51*, 459–473.

Reynolds, M. P., Pellegrineschi, A., & Skovmand, B. (2005). Sink-limitation to yield and biomass: a summary of some investigations in spring wheat. *Annals of Applied Biology*, *146*(1), 39-49.

Reynolds, M., Foulkes, M. J., Slafer, G., Berry, P., Parry, M. A. J., Snape, J. W., Angus, W. J. (2009). Raising yield potential in wheat. *Journal of Experimental Botany*, *60*, 1899–1918.

Reynolds, M., Foulkes J., Furbank R., Griffiths S., King J., Murchie E., Parry M., & Slafer, G. (2012). Achieving yield gains in wheat. *Plant Cell and Environment, 35*(10), 1799-1823.

Reynolds, M., & Langridge, P. (2016). Physiological breeding. *Current Opinion in Plant Biology*, *31*, 162-171.

Reynolds, M., Kropff, M., Crossa, J., Koo, J., Kruseman, G., Molero Milan, A., Rutkoski, J., Schulthess, U., Sonder, K., Tonnang, H., Vadez, V. (2018). Role of modelling in international crop research: overview and some case studies. *Agronomy*, *8*(12), 291.

Ramli, A., (2017). Rice varietal development for food sovereignty: a case of MARDI accessed 8 May 2020 http://ap.fftc.agnet.org/ap_db.php?id=736&print=1

Richards, R. A. (2000). Selectable traits to increase crop photosynthesis and yield of grain crops. *Journal of Experimental Botany,* 51, 447–458.

Rizhsky, L., Liang, H., & Mittler, R. (2002). The combined effect of drought stress and heat shock on gene expression in tobacco. *Plant Physiology*, *130*(3), 1143-1151.

Rizhsky, L., Liang, H., Shuman, J., Shulaev, V., Davletova, S., Mittler, R. (2004). When defense pathways collide. The response of Arabidopsis to a combination of drought and heat stress. *Plant physiology*, *134*(4), 1683-1696.

Running, S. W., & Coughlan, J. C. (1988). A general model of forest ecosystem processes for regional applications I. Hydrologic balance, canopy gas exchange and primary production processes. *Ecological modelling*, *42*(2), 125-154.

Sack, L., & Scoffoni, C. (2013). Leaf venation: structure, function, development, evolution, ecology and applications in the past, present and future. *New Phytologist*, *198*(4), 983-1000.

Sage, R. F. (1990). A model describing the regulation of Rubisco, electron transport and triose phosphate use, in response to light intensity and CO_2 in C3 plants. *Plant Physiology*, *94*, 1728-1734.

Sage, R. F., Christin, P. A., & Edwards, E. J. (2011). The C4 plant lineages of planet Earth. *Journal of Experimental botany*, *62*(9), 3155-3169.

Sage, R. F., Sage, T. L., & Kocacinar, F. (2012). Photorespiration and the evolution of C4 photosynthesis. *Annual review of plant biology*, *63*, 19-47.

Sage, T. L., & Sage, R. F. (2009). The functional anatomy of rice leaves: implications for refixation of photorespiratory CO_2 and efforts to engineer C4 photosynthesis into rice. *Plant and Cell Physiology*, *50*(4), 756-772.

Sakaguchi, J., & Fukuda, H. (2008). Cell differentiation in the longitudinal veins and formation of commissural veins in rice (Oryza sativa) and maize (*Zea mays*). *Journal of plant research*, *121*(6), 593-602.

Salmah, T. (2014) Effect of weedy rice on the yield of cultivated rice (*Oryza sativa*) in greenhouse and field environment. Universiti Sains Malaysia.

Sampson, J. (1961). A method of replicating dry or moist surfaces for examination by light microscopy. *Nature*, *191*(4791), 932-933.

Schmitt J, Stinchcombe JR, Heschel MS, Huber H. (2003). The adaptive evolution of plasticity: Phytochrome-mediated shade avoidance responses. *Integrative and Comparative Biology, 43*, 459–469.

Seneweera, S., Arun-Chinnappa, K. S., & Hirotsu, N. (2018). Scope, Options and Approaches to Climate Change: Increase Crop Yield Potential Through the Understanding of Genetic Control of Plant Responses to Increased Carbon Dioxide. *Food Security and Climate Change*, 119-130.

Sharma, D., Sanghera, G. S., Sahu, P., Sahu, P., Parikh, M., Sharma, B., Bandarkar, S., Chaudhari, P., & Jena, B. K. (2013). Tailoring rice plants for sustainable yield through ideotype breeding and physiological interventions. *Afr J Agric Res*, *8*(40), 5004-5019.

Shamshiri, R. R., Ibrahim, B., Ahmad, D., Man, H. C., & Wayayok, A. (2018). An overview of the system of rice intensification for paddy fields of Malaysia. *Indian J. Sci. Technol*, *11*, 18.
Shamsudin, M. N. (2014). Rice Farms Efficiency and Factors Affecting the Efficiency in MADA Malaysia. *Journal of Applied Sciences*, *14*(18), 2177-2182.

Sharkey, T. D., Bernacchi, C. J., Farquhar, G. D., & Singsaas, E. L. (2007). Fitting photosynthetic carbon dioxide response curves for C_3 leaves. *Plant, cell & environment*, *30*(9), 1035-1040.

Shearman, V. J., Sylvester-Bradley, R., Scott, R. K., & Foulkes, M. J. (2005). Physiological processes associated with wheat yield progress in the UK. *Crop Science*, *45*(1), 175-185.

Sharkey, T. D. (2019). Is triose phosphate utilization important for understanding photosynthesis?. *Journal of experimental botany*, *70*(20), 5521-5525.

Sheehy, J. E. (2000). Limits to yield for C3 and C4 rice: an agronomist's view. *Studies in Plant Science*, *7*, 39-52.

Sheehy, J. E., Mitchell, P. L., & Hardy, B. (Eds.). (2007). *Charting new pathways to C4 rice*. International Rice Research Institute, Los Baños, Philippines.

Sheehy, J. E., & Mitchell, P. L. (2011). Rice and global food security: the race between scientific discovery and catastrophe. *ACCESS NOT EXCESS—the search for better nutrition,* 81-90.

Sheehy, J. E., & Mitchell, P. L. (2013). *Designing Rice for the 21st Century: The Three Laws of Maximum Yield*. Discussion Paper Series 48, International Rice Research Institute, Los Baños, Philippines.

Sheehy, J. E., & Mitchell, P. L. (2015). Calculating maximum theoretical yield in rice. *Field Crops Research*, *182*, 68-75.

Shrestha, S., Brueck, H., & Asch, F. (2012). Chlorophyll index, photochemical reflectance index and chlorophyll fluorescence measurements of rice leaves supplied with different N levels. *Journal of Photochemistry and Photobiology B: Biology*, *113*, 7-13.

Sié, M., Dingkuhn, M., Wopereis, M. C. S., & Miezan, K. M. (1998). Rice crop duration and leaf appearance rate in a variable thermal environment.: I. Development of an empirically based model. *Field Crops Research*, *57*(1), 1-13.

Siebenkäs, A., Schumacher, J., & Roscher, C. (2015). Phenotypic plasticity to light and nutrient availability alters functional trait ranking across eight perennial grassland species. *AoB Plants*, *7*.

Sinclair, T. R., Murphy, C. E., & Knoerr, K. R. (1976). Development and evaluation of simplified models for simulating canopy photosynthesis and transpiration. *Journal of Applied Ecology*, 813-829.

Sinclair, T. R., & Horie, T. (1989). Leaf nitrogen, photosynthesis, and crop radiation use efficiency: a review. *Crop science*, *29*(1), 90-98.

Sinclair, T.R., and Muchow, R.C., (1999). Radiation use efficiency. *Advance Agronomy*, 65, 215-265.

Siwar, C., Alam, M. M., Murad, M. W., & Al-Amin, A. Q. (2009). Impacts of climate change on agricultural sustainability and poverty in Malaysia. In *Proceedings of the 10th International Business Research Conference, Dubai, UAE* (pp. 1-15).

Siwar, C., Ahmed, F., & Begum, R. A. (2013). Climate change, agriculture and food security issues: Malaysian perspective. *Journal of Food, Agriculture and Environment*, *11*(2), 1118-1123.

Siwar, C., Idris, N. D. M., Yasar, M., & Morshed, G. (2014). Issues and challenges facing rice production and food security in the granary areas in the East Coast Economic Region (ECER), Malaysia. *Research Journal of Applied Sciences, Engineering and Technology*, *7*(4), 711-722.

Smil, V., (2005). Feeding the world: How much more rice do we need? In: Toriyama K, Heong KL, Hardy B, (Eds.). Rice is life: scientific perspectives for the 21st century. Proceedings of the World Rice Research Conference held in Tokyo and Tsukuba, Japan, 4-7 Nov. 2004.

Smillie, I. R. A., Pyke, K. A., & Murchie, E. H. (2012). Variation in vein density and mesophyll cell architecture in a rice deletion mutant population. *Journal of experimental botany*, *63*(12), 4563-4570.

Smith, C. W., & Dilday, R. H. (Eds.). (2003). *Rice: origin, history, technology, and production* (Vol. 3). John Wiley & Sons.

Solargis. Solargis Database. Bratislava, Slovakia. Retrieved February 23, 2015 from https://solargis.com/maps-and-gis-data/overview.

Song, Q., Zhang, G., & Zhu, X. G. (2013). Optimal crop canopy architecture to maximise canopy photosynthetic CO_2 uptake under elevated CO_2–a theoretical study using a mechanistic model of canopy photosynthesis. *Functional Plant Biology*, *40*(2), 108-124.

Song, Q., & Zhu, X. G. (2018). Measuring canopy gas exchange using CAnopy Photosynthesis and Transpiration Systems (CAPTS). In *Photosynthesis* (pp. 69-81). Humana Press, New York, NY.

Sun, J., Ye, M., Peng, S., & Li, Y. (2016). Nitrogen can improve the rapid response of photosynthesis to changing irradiance in rice (*Oryza sativa* L.) plants. *Scientific reports*, *6*, 31305.

Sun, X., Guo, J., Guo, S., Guo, H., & Hu, S. (2019). Divergent responses of leaf N: P: K stoichiometry to nitrogen fertilization in rice and weeds. *Weed Science*, *67*(3), 339-345.

Sustainable rice production for food security. Proceedings of the 20th Session of the International Rice Commission. Bangkok, Thailand, 23–26 July 2002 (available at: http://www.fao.org/DOCREP/006/Y4751E/ y4751e03.htm).

Suzuki, Y., Ohkubo, M., Hatakeyama, H., Ohashi, K., Yoshizawa, R., Kojima, S., Hayakawa, T., Yamaya, T., Mae, T., Makino, A. (2007). Increased Rubisco content in transgenic rice transformed with the 'sense' rbcS gene. *Plant and cell physiology. 48*(4): 626-637.

Sylvester-Bradley, R., & Kindred, D. R. (2009). Analysing nitrogen responses of cereals to prioritize routes to the improvement of nitrogen use efficiency. *Journal of experimental botany*, *60*(7), 1939-1951.

Taiz, L., & Zeiger, E. (2010). Plant physiology 5th Ed. *Sunderland, MA: Sinauer Associates*.

Takahashi, F., & Shinozaki, K. (2019). Long-distance signaling in plant stress response. *Current opinion in plant biology*, *47*, 106-111.

Takahashi, S., & Murata, N. (2008). How do environmental stresses accelerate photoinhibition?. *Trends in plant science*, *13*(4), 178-182.

Takei, K., Sakakibara, H., Taniguchi, M., & Sugiyama, T. (2001). Nitrogen-dependent accumulation of cytokinins in root and the translocation to leaf: Implication of cytokinin species that induces gene expression of maize response regulator. *Plant and Cell Physiology*, *42*(1), 85-93.

Terashima, I., Hanba, Y. T., Tholen, D., & Niinemets, Ü. (2011). Leaf functional anatomy in relation to photosynthesis. *Plant Physiology*, *155*(1), 108-116.

Tholen, D., & Zhu, X. G. (2011). The mechanistic basis of internal conductance: a theoretical analysis of mesophyll cell photosynthesis and CO_2 diffusion. *Plant Physiology*, *156*(1), 90-105.

Tholen, D., Boom, C., & Zhu, X. G. (2012). Opinion: prospects for improving photosynthesis by altering leaf anatomy. *Plant science*, *197*, 92-101.

Tian, G., Gao, L., Kong, Y., Hu, X., Xie, K., Zhang, R., Ling, N., Shen, Q., & Guo, S. (2017). Improving rice population productivity

by reducing nitrogen rate and increasing plant density. *PloS one*, *12*(8), e0182310.

Tivet, F., DA Silveira Pinheiro, B., De Raïssac, M., & Dingkuhn, M. (2001). Leaf blade dimensions of rice (*Oryza sativa* L. and *Oryza glaberrima* Steud.). Relationships between tillers and the main stem. *Annals of botany*, *88*(3), 507-511.

Townsend, A. J., Retkute, R., Chinnathambi, K., Randall, J. W., Carmo-Silva, E., & Murchie, E. H. (2017). Suboptimal acclimation of photosynthesis to light in wheat canopies. *Plant physiology*, *176*(2), 1213.

Turner, N. C., O'Toole, J. C., Cruz, R. T., Namuco, O. S., & Ahmad, S. (1986). Responses of seven diverse rice cultivars to water deficits I. Stress development, canopy temperature, leaf rolling and growth. *Field Crops Research*, *13*, 257-271.

Uddling, J., Gelang-Alfredsson, J., Piikki, K., & Pleijel, H. (2007). Evaluating the relationship between leaf chlorophyll concentration and SPAD-502 chlorophyll meter readings. *Photosynthesis research*, *91*(1), 37-46.

Ueno, O., Kawano, Y., Wakayama, M., & Takeda, T. (2006). Leaf vascular systems in C3 and C4 grasses: a two-dimensional analysis. *Annals of Botany*, *97*(4), 611-621.

United Nations, Department of Economic and Social Affairs, Population Division (2019). *World Population Prospects 2019: Ten Key Findings*.

Vaghefi, N., Shamsudin, M. N., Makmom, A., & Bagheri, M. (2011). The economic impacts of climate change on the rice production in Malaysia. *International Journal of Agricultural Research*, *6*(1), 67-74.

Vaghefi, N., Shamsudin, M. N., Radam, A., & Rahim, K. A. (2013). Impact of climate change on rice yield in the main rice growing areas of Peninsular Malaysia. *Research Journal of Environmental Sciences*, *7*(2), 59.

Vaghefi, N., Siwar, C., & Aziz, S. A. A. G. (2015). A Framework for Green Growth and Socio-Economic Development in Malaysia. *Current World Environment*, *10*(1), 29.

Vaz, J., & Sharma, P. K. (2011). Relationship between xanthophyll cycle and non-photochemical quenching in rice (*Oryza sativa* L.) plants in response to light stress. *Indian Journal of Experimental Biology, 48*, 60-67.

Vicente, R., Morcuende, R., & Babiano, J. (2011). Differences in rubisco and chlorophyll content among tissues and growth stages in

two tomato (Lycopersicon esculentum Mill.) varieties. *Agronomy Research*, *9*, 501-507.

Vicente, R., Pérez, P., Martínez-Carrasco, R., Gutiérrez, E., & Morcuende, R. (2015). Nitrate supply and plant development influence nitrogen uptake and allocation under elevated CO_2 in durum wheat grown hydroponically. *Acta Physiologiae Plantarum*, *37*(6), 114.

Vogelmann, T. C. (1989). Penetration of light into plants. *Photochemistry and Photobiology*, *50*(6), 895-902.

von Caemmerer, S. (2000). *Biochemical models of leaf photosynthesis* (No. 2). Csiro publishing.

von Caemmerer, S. (2003). C4 photosynthesis in a single C3 cell is theoretically inefficient but may ameliorate internal CO2 diffusion limitations of C3 leaves. *Plant, Cell & Environment*, *26*(8), 1191-1197.

von Caemmerer, S., Farquhar, G., & Berry, J. (2009). Biochemical model of C3 photosynthesis. In *Photosynthesis in silico* (pp. 209-230). Springer Netherlands.

von Caemmerer, S., Quick, W. P., & Furbank, R. T. (2012). The development of C4 rice: current progress and future challenges. *Science*, *336*(6089), 1671-1672.

von Caemmerer, S. (2013). Steady-state models of photosynthesis. *Plant, cell & environment*, *36*(9), 1617-1630.

Vos, J., & Van der Putten, P. E. L. (1998). Effect of nitrogen supply on leaf growth, leaf nitrogen economy and photosynthetic capacity in potato. *Field Crops Research*, *59*(1), 63-72.

Walsh, B. (2009). America's food crisis and how to fix it. Retrieved November 8, 2011, from http:// www.time.com/time/health/article/0,8599,1917458,00.html.

Walters, R. G. (2005). Towards an understanding of photosynthetic acclimation. *Journal of experimental botany*, *56*(411), 435-447.

Wang, J., Lu, K., Nie, H., Zeng, Q., Wu, B., Qian, J., & Fang, Z. (2018). Rice nitrate transporter OsNPF7. 2 positively regulates tiller number and grain yield. *Rice*, *11*(1), 12.

Wang, Y., & Li, J. (2005). The plant architecture of rice (*Oryza sativa*). *Plant molecular biology*, *59*(1), 75-84.

Wang, Y., Lu, J., Ren, T., Hussain, S., Guo, C., Wang, S., Cong, R., Li, X. (2017). Effects of nitrogen and tiller type on grain yield and physiological responses in rice. *AoB Plants*, *9*(2).

Wang, Q. A., Lu, C. M., & Zhang, Q. D. (2005). Midday photoinhibition of two newly developed super-rice hybrids. *Photosynthetica*, *43*(2), 277-281.

Wassmann, R., Jagadish, S. V. K., Heuer, S., Ismail, A., Redona, E., Serraj, R., Singh, R. K., Howell, G., & Sumfleth, K. (2009). Climate change affecting rice production: the physiological and agronomic basis for possible adaptation strategies. *Advances in agronomy*, *101*, 59-122.

Weyers, J. D., & Johansen, L. G. (1985). Accurate estimation of stomatal aperture from silicone rubber impressions. *New phytologist*, *101*(1), 109-115.

Wiebe, K., Lotze-Campen, H., Sands, R., Tabeau, A., van der Mensbrugghe, D., Biewald, A., Bodirsky, B., Islam, S., Kavallari, A., Mason-D'Croz, D., Müller, C. (2015). Climate change impacts on agriculture in 2050 under a range of plausible socioeconomic and emissions scenarios. *Environmental Research Letters*, *10*(8), 085010.

Wild, M., Ohmura, A., Gilgen, H., & Rosenfeld, D. (2004). On the consistency of trends in radiation and temperature records and implications for the global hydrological cycle. *Geophysical Research Letters*, *31*(11).

Wu, C., (2011). VisualSFM: A Visual Structure from Motion System. http:// ccwu.me/vsfm/ (June 11, 2014)

Xu, G., Fan, X., & Miller, A. J. (2012). Plant nitrogen assimilation and use efficiency. *Annual review of plant biology*, *63*, 153-182.

Xu, Z. Z., Zhou, G. S., & Shimizu, H. (2009). Effects of soil drought with nocturnal warming on leaf stomatal traits and mesophyll cell ultrastructure of a perennial grass. *Crop Science*, *49*(5), 1843-1851.

Yamamoto, Y., Aminaka, R., Yoshioka, M., Khatoon, M., Komayama, K., Takenaka, D., Yamashita, A., Nijo, N., Inagawa, K., Morita, N., Sasaki, T., & Yamamoto, Y. (2008). Quality control of photosystem II: impact of light and heat stresses. *Photosynthesis Research*, *98*(1-3), 589-608.

Yamori, W., & von Caemmerer, S. (2009). Effect of Rubisco activase deficiency on the temperature response of CO_2 assimilation rate and Rubisco activation state: insights from transgenic tobacco with reduced amounts of Rubisco activase. *Plant physiology*, *151*(4), 2073-2082.

Yamori, W., Kondo, E., Sugiura, D., Terashima, I., Suzuki, Y., & Makino, A. (2016). Enhanced leaf photosynthesis as a target to increase grain yield: insights from transgenic rice lines with variable

Rieske FeS protein content in the cytochrome *b6/f* complex. *Plant, cell & environment*, *39*(1), 80-87.

Ye, J., & Pan, L. (2016). *Concepts and realities of family farming in Asia and the Pacific* (No. 139). Working paper.

Ye, Z. P., & Yu, Q. (2007). Comparison of a new model of light response of photosynthesis with traditional models. *Journal-Shenyang Agricultural University*, *38*(6), 771.

Yin, Y., Li, S., Liao, W., Lu, Q., Wen, X., & Lu, C. (2010). Photosystem II photochemistry, photoinhibition, and the xanthophyll cycle in heat-stressed rice leaves. *Journal of plant physiology*, *167*(12), 959-966.

Yoon, D. K., Ishiyama, K., Suganami, M., Tazoe, Y., Watanabe, M., Imaruoka, S., Ogura, M., Ishida, H., Suzuki, Y., Obara, M., & Mae, T. (2020). Transgenic rice overproducing Rubisco exhibits increased yields with improved nitrogen-use efficiency in an experimental paddy field. *Nature Food*, *1*(2), 134-139.

Yoshida, S. (1981). *Fundamentals of rice crop science*. International Rice Research Institute.

Zhen, S., & Bugbee, B. (2020). Far-red photons have equivalent efficiency to traditional photosynthetic photons: Implications for redefining photosynthetically active radiation. *Plant, Cell & Environment*.

Zhang, C. J., Chu, H. J., Chen, G. X., Shi, D. W., Zuo, M., Wang, J., Lu, C. G., & Chen, L. (2007). Photosynthetic and biochemical activities in flag leaves of a newly developed superhigh-yield hybrid rice (*Oryza sativa*) and its parents during the reproductive stage. *Journal of plant research*, *120*(2), 209-217.

Zhang, L., Paakkarinen, V., van Wijk, K. J., & Aro, E. M. (2000). Biogenesis of the chloroplast-encoded D1 protein: regulation of translation elongation, insertion, and assembly into photosystem II. *The Plant Cell Online*, *12*(9), 1769-1781.

Zhang, L., Hu, Z., Fan, J., Zhou, D., & Tang, F. (2014). A meta-analysis of the canopy light extinction coefficient in terrestrial ecosystems. *Frontiers of earth science*, *8*(4), 599-609.

Zhou, Y., Lam, H. M., & Zhang, J. (2007). Inhibition of photosynthesis and energy dissipation induced by water and high light stresses in rice. *Journal of Experimental Botany*, *58*(5), 1207-1217.

Zhu, K., Yuan, F. H., Guan, X., Wu, J. B., & Wang, A. Z. (2019). Measuring and calculating methods of plant mesophyll conductance: A review. *Ying yong sheng tai xue bao= The journal of applied ecology*, *30*(5), 1772-1782.

Zhu, L., Bloomfield, K. J., Hocart, C. H., Egerton, J. J., O'Sullivan, O. S., Penillard, A., Weerasinghe, L. K., & Atkin, O. K. (2018). Plasticity of photosynthetic heat tolerance in plants adapted to thermally contrasting biomes. *Plant, cell & environment*, *41*(6), 1251-1262.

Zhu, X. G., Portis, A. R., & Long, S. P. (2004). Would transformation of C3 crop plants with foreign Rubisco increase productivity? A computational analysis extrapolating from kinetic properties to canopy photosynthesis. *Plant Cell and Environment, 27*(2), 155-165.

Zhu, X. G., Long, S. P., & Ort, D. R. (2008). What is the maximum efficiency with which photosynthesis can convert solar energy into biomass?. *Current opinion in biotechnology*, *19*(2), 153-159.

Zhu, X. G., Long, S. P., & Ort, D. R. (2010). Improving Photosynthetic Efficiency for Greater Yield. *Annual Review of Plant Biology. 61*: 235-261.

Zhu, X. G., Song, Q., & Ort, D. R. (2012). Elements of a dynamic systems model of canopy photosynthesis. *Current opinion in plant biology*, *15*(3), 237-244.

Zivcak, M., Brestic, M., Kunderlikova, K., Sytar, O., & Allakhverdiev, S. I. (2015). Repetitive light pulse-induced photoinhibition of photosystem I severely affects CO_2 assimilation and photoprotection in wheat leaves. *Photosynthesis research*, *126*(2-3), 449-463.

Zivcak, M., Olsovska, K., & Brestic, M. (2017). Photosynthetic Responses Under Harmful and Changing Environment: Practical Aspects in Crop Research. In *Photosynthesis: Structures, Mechanisms, and Applications* (pp. 203-248). Springer, Cham.

Zürcher, E., & Müller, B. (2016). Cytokinin synthesis, signalling, and function—advances and new insights. *International review of cell and molecular biology*, *324*, 1-38.